https://theses.gla.ac.uk/

Theses Digitisation:

https://www.gla.ac.uk/myglasgow/research/enlighten/theses/digitisation/

This is a digitised version of the original print thesis.

Copyright and moral rights for this work are retained by the author

A copy can be downloaded for personal non-commercial research or study, without prior permission or charge

This work cannot be reproduced or quoted extensively from without first obtaining permission in writing from the author

The content must not be changed in any way or sold commercially in any format or medium without the formal permission of the author

When referring to this work, full bibliographic details including the author, title, awarding institution and date of the thesis must be given

Enlighten: Theses
https://theses.gla.ac.uk/
research-enlighten@glasgow.ac.uk

DEVELOPMENT AND APPLICATION OF NEW METHODS FOR INVESTIGATING PYROLYSIS PRODUCTS FROM SELECTED PIGMENTS AND PIGMENTED POLYMER SYSTEMS

By

Gordon John Seeley

A Thesis Submitted for the Degree of Doctor of Philosophy

Supervisor: Dr I.C. McNeill
University of Glasgow

Faculty of Science
Chemistry Department
University of Glasgow
1997

ProQuest Number: 10992173

All rights reserved

INFORMATION TO ALL USERS
The quality of this reproduction is dependent upon the quality of the copy submitted.

In the unlikely event that the author did not send a complete manuscript
and there are missing pages, these will be noted. Also, if material had to be removed,
a note will indicate the deletion.

ProQuest 10992173

Published by ProQuest LLC (2018). Copyright of the Dissertation is held by the Author.

All rights reserved.
This work is protected against unauthorized copying under Title 17, United States Code
Microform Edition © ProQuest LLC.

ProQuest LLC.
789 East Eisenhower Parkway
P.O. Box 1346
Ann Arbor, MI 48106 – 1346

Thesis
10669
Copy 1

GLASGOW
UNIVERSITY
LIBRARY

To Jim Seeley.

ACKNOWLEDGEMENTS

The work presented in this thesis was performed in the Department of Physical Chemistry at the University of Glasgow between October 1990 and December 1993.

Dr. I.C. McNeill provided valuable access to his experience, along with guidance and advice for which I express my sincere gratitude.

I also wish to thank members of staff in the Chemistry Department for their assistance. In particular, I am grateful for the assistance provided by Dr. W.J. Cole, G. McCormack and T. Richie for analytical work and advice. I also express my appreciation for the time and expertise W. McCormack contributed to the project. I also thank J. Gorman and the other members of the Polymer Research Group, especially M. Mohammed, who offered assistance and were a pleasure to work with.

I am also indebted to my family who never failed to provide the support I needed to bring this project to a conclusion.

Finally, I also thank Sandoz and Dr. Kaul for providing the funding and materials for this study.

CONTENTS

SUMMARY		x
CHAPTER 1	INTRODUCTION	
1.1	**Background**	**1**
1.2	**Polymer Degradation vs Fire Safety**	**2**
1.2.1	Introduction to Polymer Degradation	2
1.2.2	Introduction to Fire Safety Science	4
1.3	**The Burning Cycles**	**5**
1.3.1	Required Degradation Environments	6
1.4	**Materials Under Study**	**7**
CHAPTER 2	TECHNIQUES EMPLOYED FOR THERMAL DEGRADATION AND PRODUCT ANALYSIS	
2.1	**Introduction**	**9**
2.2	**Thermal Degradation Techniques**	**10**
2.2.1	Thermogravimetric Analysis	10
2.2.2	Thermal Volatilisation Analysis	10
2.2.2.1	Limitations of the TVA Environment	10
2.2.3	Degradation Under Static Nitrogen	11
2.2.3.1	Usage	11
2.2.3.2	Limitations	12
2.2.4	Flow Apparatus	13
2.2.4.1	Product Trapping	14
2.2.4.2	Product Analysis	14
2.2.5	Degradation Under Flaming Conditions	14
2.2.5.1	Traditional Approaches	15
2.2.5.2	Power Calculation	17
2.2.5.3	Heater Construction	19
2.2.5.4	Test Characteristics	20
2.2.5.4.1	Radiant Heat Flux Meter	20
2.2.5.4.2	Radiant Heat Flux Measurements	22
2.2.5.5	Enclosure For Flaming Apparatus	27
2.2.5.6	Supplying Power to the Enclosure	27
2.2.5.7	Pilot	27
2.2.5.8	Final Local Sample Environment	29
2.2.5.9	Overall System and Operation	30
2.2.5.10	Oxygen Depletion	33
2.3	**Methods of Analysis**	**35**
2.3.1	Sub-Ambient Thermal Volatilisation Analysis (SATVA)	35
2.3.1.1	Pump System	35

2.3.1.2	Mass Spectrometry	36
2.3.1.3	Operation	36
2.3.2	Infrared Spectroscopy	37
2.3.3	Gas Chromatography	38
2.3.3.1	Conditions	39
2.3.4	Simultaneous Gas Chromatography-Mass Spectrometry	41
CHAPTER 3	**POLYPROPYLENE AND POLYESTER DEGRADATION**	**43**
3.1	**Polymers in this Chapter**	**43**
3.2	**Introduction to Polypropylene**	**43**
3.3	**Introduction to PET PBT copolymer**	**44**
3.4	**Thermal Degradation of Polypropylene FBF**	**45**
3.4.1	Thermogravimetric Analysis	45
3.4.2	Product Analysis - Dynamic Nitrogen	46
3.4.3	Product Analysis - Dynamic Air	47
3.4.4	Product Analysis - Flaming Conditions	48
3.5	**Thermal Degradation of Polypropylene Wax**	**53**
3.5.1	Thermogravimetric Analysis	53
3.5.2	Product Analysis - Dynamic Nitrogen	54
3.5.3	Product Analysis - Dynamic Air	54
3.5.4	Product Analysis - Flaming Conditions	55
3.6	**Thermal Degradation of Polyester DNOP 43**	**60**
3.6.1	Thermogravimetric Analysis	60
3.6.2	Product Analysis - Dynamic Nitrogen	61
3.6.3	Product Analysis - Dynamic Air	62
3.6.4	Product Analysis - Flaming Conditions	64
3.7	**Major Product Summaries and Mechanisms**	**67**
3.7.1	**Polypropylene FBF and Polypropylene Wax**	**67**
3.7.1.1	Dynamic Nitrogen	67
3.7.1.2	Dynamic Air	68
3.7.1.3	Flaming Conditions	70
3.7.2	**Polyester DNOP 43**	**71**
3.7.2.1	Dynamic Nitrogen	71
3.7.2.2	Dynamic Air	73
3.7.2.3	Flaming Conditions	75
CHAPTER 4	**ORGANIC AZO- AND DISAZO COLOURANTS**	**90**
4.1	**Introduction to Azo Dyes**	**90**
4.2	**Chemistry of Azo Dyes**	**90**
4.2.1	Azo-Hydrazone Tautomerism	91
4.3	**Organic Azo Dyes under Study**	92
4.4	**Thermal Degradation of Sandorin Rouge**	93
4.4.1	Thermogravimetric Analysis	93
4.4.2	Product Analysis — Static Nitrogen	94

4.4.3	Product Analysis — Dynamic Nitrogen	96
4.4.4	Product Analysis — Dynamic Air	98
4.4.5	Product Analysis - Flaming Conditions	100
4.5	**Degradation of Sandorin Scarlet 4RF**	**106**
4.5.1	Thermogravimetric Analysis	106
4.5.2	Product Analysis — Dynamic Nitrogen	107
4.5.3	Product Analysis — Dynamic Air	109
4.5.4	Product Analysis — Flaming Conditions	110
4.6	**Degradation of Graphtol Fast Red 2GLD**	**112**
4.6.1	Thermogravimetric Analysis	112
4.6.2	Product Analysis — Dynamic Nitrogen	113
4.6.3	Product Analysis — Dynamic Air	116
4.6.4	Product Analysis — Flaming Conditions	118
4.7	**Major Product Summaries and Mechanisms**	**126**
4.7.1	**Sandorin Red BN**	126
4.7.1.1	Static and Dynamic Nitrogen	126
4.7.1.2	Dynamic Air	128
4.7.1.3	Flaming Conditions	129
4.7.2	**Sandorin Scarlet 4RF**	130
4.7.2.1	Dynamic Nitrogen	130
4.7.2.2	Dynamic Air	132
4.7.2.3	Flaming Conditions	132
4.7.3	**Graphtol Fast Red 2GLD**	133
4.7.3.1	Dynamic Nitrogen	133
4.7.3.2	Dynamic Air	134
4.7.3.3	Flaming Conditions	135
CHAPTER 5	**REMAINING ORGANIC COLOURANTS**	**168**
5.1	**Introduction**	168
5.2	**Chemistry**	168
5.3	**Structures**	169
5.4	**Thermal Degradation of Estofil Blue S-RLS**	170
5.4.1	Thermogravimetric Analysis	170
5.4.2	Product Analysis — Dynamic Nitrogen	171
5.4.3	Product Analysis — Dynamic Air	174
5.4.5	Product Analysis — Flaming Conditions	175
5.5	**Thermal Degradation of Sandorin Violet BL**	178
5.5.1	Thermogravimetric Analysis	178
5.5.2	Product Analysis — Dynamic Nitrogen	179
5.5.3	Product Analysis — Dynamic Air	181
5.5.4	Product Analysis — Flaming Conditions	182
5.6	**Major Product Summaries and Mechanisms**	186
5.6.1	**Estofil Blue S-RLS**	186
5.6.1.1	Dynamic Nitrogen	186
5.6.1.2	Dynamic Air	188
5.6.1.3	Flaming Conditions	189
5.6.2	**Sandorin Violet BL**	189
5.6.2.1	Dynamic Nitrogen	189

5.6.2.2	Dynamic Air	191
5.6.2.3	Flaming Conditions	192
CHAPTER 6	**CO-ORDINATED DISAZO INORGANIC COLOURANTS**	**210**
6.1	**Introduction**	**210**
6.2	**Chemistry**	**210**
6.3	**Structures**	**211**
6.4	**Thermal Degradation of Savinyl Yellow 2RLS**	**213**
6.4.1	Thermogravimetric Analysis	213
6.4.2	Product Analysis — Static Nitrogen	214
6.4.3	Product Analysis — Dynamic Nitrogen	215
6.4.4	Product Analysis — Dynamic Air	219
6.4.5	Product Analysis — Flaming Conditions	222
6.5	**Thermal Degradation of Savinyl Orange RLSE**	**223**
6.5.1	Thermogravimetric Analysis	223
6.5.2	Product Analysis — Static Nitrogen	225
6.5.2.1	330°C Products	225
6.5.2.2	500°C Products	225
6.5.3	Product Analysis — Dynamic Nitrogen	227
6.5.4	Product Analysis — Dynamic Air	228
6.5.5	Product Analysis — Flaming Conditions	229
6.6	**Thermal Degradation of Savinyl Black RLS**	**232**
6.6.1	Thermogravimetric Analysis	232
6.6.2	Product Analysis — Dynamic Nitrogen	233
6.6.3	Product Analysis — Dynamic Air	235
6.6.4	Product Analysis — Flaming Conditions	237
6.7	**Major Product Summaries and Mechanisms**	**239**
6.7.1	**Savinyl Yellow 2RLS**	**239**
6.7.1.1	Static and Dynamic Nitrogen	239
6.7.1.2	Dynamic Air	241
6.7.1.3	Flaming Conditions	241
6.7.2	**Savinyl Orange RLSE**	**242**
6.7.2.1	Static and Dynamic Nitrogen	242
6.7.2.2	Dynamic Air	244
6.7.2.3	Flaming Conditions	245
6.7.3	**Savinyl Black RLS**	**246**
6.7.3.1	Dynamic Nitrogen	246
6.7.3.2	Dynamic Air	247
6.7.3.3	Flaming Conditions	248
CHAPTER 7	**REMAINING METAL CONTAINING COLOURANTS**	**273**
7.1	**Introduction to Dyes in this section**	273
7.2	**Chemistry of the Dyes**	273
7.3	**Structures**	274

7.4	**Thermal Degradation of Graphtol Fire Red 3RL**	275
7.4.1	Thermogravimetric Analysis	275
7.4.2	Product Analysis - Dynamic Nitrogen	276
7.4.3	Product Analysis - Dynamic Air	278
7.4.4	Product Analysis -Flaming Conditions	279
7.5	**Thermal Degradation of Sandorin Red Violet 3RL**	**281**
7.5.1	Thermogravimetric Analysis	281
7.5.2	Product Analysis — Dynamic Nitrogen	281
7.5.3	Product Analysis — Dynamic Air	285
7.5.4	Product Analysis -Flaming Conditions	286
7.6	**Major Product Summaries and Mechanisms**	**290**
7.6.1	**Graphtol Fire Red 3RL**	**290**
7.6.1.1	Dynamic Nitrogen	290
7.6.1.2	Dynamic Air	292
7.6.1.3	Flaming Conditions	294
7.6.2	**Sandorin Red Violet 3RL**	**294**
7.6.2.1	Dynamic Nitrogen	295
7.6.2.2	Dynamic Air	297
7.6.2.3	Flaming Conditions	298

CHAPTER 8	PIGMENTED POLYMER SYSTEMS	**314**
8.1	**Introduction**	**314**
8.2	**Polypropylene System**	**314**
8.3	**Polybutyleneterephthalate System**	**314**
8.4	**Thermal Degradation of Sanylene Red BN**	**315**
8.4.1	Thermogravimetric Analysis	315
8.4.2	Product Analysis — Static Nitrogen	316
8.4.3	Product Analysis — Dynamic Nitrogen	318
8.4.4	Product Analysis — Dynamic Air	322
8.4.5	Product Analysis — Flaming Conditions	324
8.5	**Thermal Degradation of Estofil Blue MP8**	**328**
8.5.1	Thermogravimetric Analysis	328
8.5.2	Product Analysis — Dynamic Nitrogen	329
8.5.3	Product Analysis — Dynamic Air	331
8.5.4	Product Analysis — Flaming Conditions	332
8.6	**Major Product Summaries and Mechanisms**	**334**
8.6.1	**Sanylene Red BN**	**334**
8.6.1.1	Static and Dynamic Nitrogen	334
8.6.1.2	Dynamic Air	336
8.6.1.3	Flaming Conditions	337
8.6.2	**Estofil Blue MP8**	**338**
8.6.2.1	Dynamic Nitrogen	338
8.6.2.2	Dynamic Air	340
8.6.2.3	Flaming Conditions	341

CHAPTER 9	CONCLUSIONS	355
9.1	**General Findings**	355
9.2	**Effects of colourants on the polymer systems**	356
9.3	**Toxicity of products**	356
9.4	**Achievements**	357
9.5	**Areas for further study**	357

	BIBLIOGRAPHY	359

INDEX OF TABLES

Table 2.1	Heat flux meter calibration data	22
Table 2.2	Properties of common GC carrier gases	39
Table 3.1	Key temperatures from thermogravimetry of Polypropylene FBF	45
Table 3.2	SATVA peak assignments from Figure 3.4	47
Table 3.3	SATVA peak assignments from Figure 3.5	48
Table 3.4	GC-MS peak assignments from Figure 3.6	48
Table 3.5	Observations from Polypropylene FBF under flaming conditions	49
Table 3.6	SATVA peak assignments from Figure 3.7	50
Table 3.7	GC-MS peak assignments from Figure 3.8	50
Table 3.8	Key temperatures from thermogravimetry of Polypropylene Wax	53
Table 3.9	Residue percentages from air degradation of Polypropylene Wax	54
Table 3.10	SATVA peak assignments from Figure 3.11	55
Table 3.11	Observations from Polypropylene FBF under flaming conditions	56
Table 3.12	SATVA peak assignments from Figure 3.12	57
Table 3.13	GC-MS peak assignments from Figure 3.13	57
Table 3.14	Key temperatures from thermogravimetry of Polyester DNOP 43	60
Table 3.15	Residue percentages from nitrogen degradation of DNOP 43	61
Table 3.16	SATVA peak assignments from Figure 3.15	62
Table 3.17	SATVA peak assignments from Figure 3.16	62
Table 3.18	GC-MS peak assignments from Figure 3.17	63
Table 3.19	Observations from DNOP 43 under flaming conditions	64
Table 3.20	SATVA peak assignments from Figure 3.18	65
Table 3.21	GC-MS peak assignments from Figure 3.19	66
Table 4.1	Key temperatures from thermogravimetry of Sandorin Red	93
Table 4.2	SATVA peak assignments from Figure 4.5	95
Table 4.3	GC-MS peak assignments from Figure 4.8	96
Table 4.4	Residue percentages from nitrogen degradation of Sandorin Red	97
Table 4.5	SATVA peak assignments from Figure 4.9	98

Table 4.6	GC-MS peak assignments from Figure 4.11	98
Table 4.7	Residue percentages from air degradation of Sandorin Red	98
Table 4.8	SATVA peak assignments from Figure 4.12	99
Table 4.9	GC-MS peak assignments from Figure 4.13	99
Table 4.10	Observations from Sandorin Red under flaming conditions	100
Table 4.11	SATVA peak assignments from Figure 4.14	101
Table 4.12	GC-MS peak assignments from Figure 4.18	101
Table 4.13	GC-MS peak assignments from Figure 4.19	102
Table 4.14	GC-MS peak assignments from Figure 4.20	104
Table 4.15	Key temperatures from thermogravimetry of Sandorin Scarlet 4RF	106
Table 4.16	Residue percentages from nitrogen degradation of Sandorin Scarlet 4RF	107
Table 4.17	SATVA peak assignments from Figure 4.22	107
Table 4.18	GC-MS peak assignments from Figure 4.23	108
Table 4.19	Residue percentages from air degradation of Sandorin Scarlet 4RF	109
Table 4.20	SATVA peak assignments from Figure 4.25	110
Table 4.21	Observations from Sandorin Scarlet under flaming conditions	110
Table 4.22	SATVA peak assignments from Figure 4.27	111
Table 4.23	GC-MS peak assignments from Figure 4.29	111
Table 4.24	Key temperatures from thermogravimetry of Graphtol Fast Red 2GLD	112
Table 4.25	Residue percentages from nitrogen degradation of Graphtol Fast Red	113
Table 4.26	GC-MS peak assignments from Figure 4.32	114
Table 4.27	GC-MS peak assignments from Figure 4.33	114
Table 4.28	Residue percentages from air degradation of Graphtol Fast Red	116
Table 4.29	GC-MS peak assignments from Figure 4.35	117
Table 4.30	Observations from Graphtol Fast Red under flaming conditions	118
Table 4.31	SATVA peak assignments from Figure 4.36	119
Table 4.32	GC-MS peak assignments from Figure 4.37	119
Table 4.33	GC-MS peak assignments from Figure 4.38	121
Table 5.1	Key temperatures from thermogravimetry of Estofil Blue S-RLS	170
Table 5.2	Residue percentages from nitrogen degradation of Estofil Blue S-RLS	171
Table 5.3	SATVA peak assignments from Figure 5.5	172
Table 5.4	GC-MS peak assignments from Figure 5.6	172
Table 5.5	GC-MS peak assignments from Figure 5.7	173
Table 5.6	GC-MS peak assignments from Figure 5.8	174
Table 5.7	Residue percentages from air degradation of Estofil Blue S-RLS	174
Table 5.8	SATVA peak assignments from Figure 5.9	175
Table 5.9	GC-MS peak assignments from Figure 5.10	175
Table 5.10	Observations from Estofil Blue under flaming conditions	176
Table 5.11	SATVA peak assignments from Figure 5.11	177
Table 5.12	GC-MS peak assignments from Figure 5.13	177
Table 5.13	Key temperatures from thermogravimetry of Sandorin Violet BL	178
Table 5.14	Residue percentages from nitrogen degradation of Sandorin Violet BL	180
Table 5.15	SATVA peak assignments from Figure 5.15	180

Table 5.16	GC-MS peak assignments from Figure 5.17	181
Table 5.17	SATVA peak assignments from Figure 5.18	182
Table 5.18	GC-MS peak assignments from Figure 5.20	182
Table 5.19	Observations from Sandorin Violet under flaming conditions	183
Table 5.20	SATVA peak assignments from Figure 5.21	184
Table 6.1	SATVA peak assignments from Figure 6.6	215
Table 6.2	GC-MS peak assignments from Figure 6.7	218
Table 6.3	Residue percentages from nitrogen degradation of Savinyl Yellow 2RLS	215
Table 6.4	SATVA peak assignments from Figure 6.8	216
Table 6.5	GC-MS peak assignments from Figure 6.9	217
Table 6.6	GC-MS peak assignments from Figure 6.10	218
Table 6.7	Residue percentages from air degradation of Savinyl Yellow 2RLS	219
Table 6.8	SATVA peak assignments from Figure 6.11	220
Table 6.9	GC-MS peak assignments from Figure 6.12	221
Table 6.10	Observations from Savinyl Yellow under flaming conditions	222
Table 6.11	SATVA peak assignments from Figure 6.13	223
Table 6.12	Key temperatures from thermogravimetry of Savinyl Orange RLSE	223
Table 6.13	SATVA peak assignments from Figure 6.15	225
Table 6.14	SATVA peak assignments from Figure 6.16	226
Table 6.15	GC-MS peak assignments from Figure 6.17	226
Table 6.16	Residue percentages from nitrogen degradation of Savinyl Orange RLSE	227
Table 6.17	SATVA peak assignments from Figure 6.18	227
Table 6.18	GC-MS peak assignments from Figure 6.19	228
Table 6.19	SATVA peak assignments from Figure 6.20	229
Table 6.20	GC-MS peak assignments from Figure 6.21	229
Table 6.21	Observations from Savinyl Orange under flaming conditions	230
Table 6.22	SATVA peak assignments from Figure 6.22	231
Table 6.23	GC-MS peak assignments from Figure 6.24	231
Table 6.24	GC-MS peak assignments from Figure 6.25	232
Table 6.25	SATVA peak assignments from Figure 6.27	234
Table 6.26	GC-MS peak assignments from Figure 6.28	234
Table 6.27	SATVA peak assignments from Figure 6.29	236
Table 6.28	GC-MS peak assignments from Figure 6.30	236
Table 6.29	Observations from Savinyl Black under flaming conditions	237
Table 6.30	SATVA peak assignments from Savinyl Black under flaming conditions	238
Table 6.31	GC-MS peak assignments from Figure 6.31	238
Table 7.1	Key temperatures from thermogravimetry of Graphtol Fire Red	275
Table 7.2	SATVA peak assignments from Figure 7.4	276
Table 7.3	GC-MS peak assignments from Figure 7.5	277
Table 7.4	SATVA peak assignments from Figure 7.6	278
Table 7.5	GC-MS peak assignments from Figure 7.7	278
Table 7.6	Observations from Graphtol Fire Red under flaming conditions	279
Table 7.7	SATVA peak assignments from Figure 7.8	280
Table 7.8	Key temperatures from thermogravimetry of Sandorin Red Violet	281

Table 7.9	Residue percentages from nitrogen degradation of Sandorin Red Violet	282
Table 7.10	SATVA peak assignments from Figure 7.10	283
Table 7.11	GC-MS peak assignments from Figure 7.11	283
Table 7.12	GC-MS peak assignments from Figure 7.12	284
Table 7.13	Residue percentages from air degradation of Sandorin Red Violet	285
Table 7.14	SATVA peak assignments from Figure 7.13	286
Table 7.15	GC-MS peak assignments from Figure 7.15	286
Table 7.16	Observations from Sandorin Red Violet under flaming conditions	286
Table 7.17	SATVA peak assignments from Figure 7.16	287
Table 7.18	GC-MS peak assignments from Figure 7.17	288
Table 7.19	GC-MS peak assignments from Figure 7.18	289
Table 8.1	Key temperatures from thermogravimetry of Sanylene Red BN	315
Table 8.2	SATVA peak assignments from Figure 8.2	317
Table 8.3	GC-MS peak assignments from Figure 8.3	317
Table 8.4	Residue percentages from nitrogen degradation of Sanylene Red BN	319
Table 8.5	SATVA peak assignments from Figure 8.4	319
Table 8.6	GC-MS peak assignments from Figure 8.5	320
Table 8.7	Residue percentages from air degradation of Sanylene Red BN	322
Table 8.8	SATVA peak assignments from Figure 8.6	322
Table 8.9	GC-MS peak assignments from Figure 8.7	323
Table 8.10	Observations from Sanylene Red under flaming conditions	324
Table 8.11	SATVA peak assignments from Figure 8.8	325
Table 8.12	GC-MS peak assignments from Figure 8.9	326
Table 8.13	Key temperatures from thermogravimetry of Estofil Blue MP8	328
Table 8.14	Residue percentages from nitrogen degradation of Estofil Blue MP8	329
Table 8.15	SATVA peak assignments from Figure 8.11	330
Table 8.16	GC-MS peak assignments from Figure 8.12	330
Table 8.17	Residue percentages from air degradation of Estofil Blue MP8	331
Table 8.18	SATVA peak assignments from Figure 8.13	332
Table 8.19	Observations from Estofil Blue under flaming conditions	332
Table 8.20	SATVA results from Estofil Blue under flaming conditions	333
Table 8.21	GC-MS peak assignments from Figure 8.14	333

SUMMARY

The main objective of this study was to develop a method to determine the products likely to be evolved under a fire situation from a series of pigments, polymers and pigmented polymer systems. This allows some assessment of the hazards presented by the materials should the fire situation arise.

Chapter 1 describes how this study relates to the work of the polymer degradation chemist and the fire safety engineer. The most applicable fire model is also described. Some basic information on the materials studied is also summarised. The materials degraded are described in more detail in the relevant chapters.

The concepts employed in the design of the degradation apparatus is described in the first part of Chapter 2. The remainder of this chapter describes the analysis procedures used throughout the studies in the following chapters.

The remaining chapters all follow a standard format. Firstly, the materials to be degraded are categorised and described. The degradation of the materials is then described, with studies in inert atmosphere being followed by degradation in air and then flaming conditions. The final sections in each chapter outline any conclusions which may be drawn as to the mechanism of degradation for each of the materials. The increasing complexity of the degradation mechanism when air was introduced resulted in increased difficulties drawing conclusions under these conditions.

Chapter 3 describes the thermal degradation of the uncoloured polymer samples. The offers little more information than the literature provides, but is included for comparison with the coloured systems in Chapter 8.

Organic disazo and azo samples are studied in Chapter 4. These three samples all possessed structural similarities. Chapter 5 details the degradation of an anthraquinone and a triphendioxazine colourant. Chapters 6 and 7 describe the structures and thermal degradation of some metal containing colourants.

Chapter 8 contains the degradation study of the polymers described in chapter 3 when colourants are present at around 25%. The polypropylene sample is degraded with a disazo colourant studied in chapter 4, and the polyester with the anthraquinone from Chapter 5.

Overall, the methods developed proved satisfactory. Products were analysed under conditions ranging from inert atmosphere to flaming conditions. Ignition occurred with samples where a reasonable stream of flammable volatiles could be expected. Equally predictable was the lack of ignition in the chlorinated samples. Varying char forming behaviour was also observed.

CHAPTER 1

INTRODUCTION

1.1 BACKGROUND

Thermal degradation is of importance in both the manufacture and application of natural and synthetic materials[1]. In manufacturing there are considerations of the abilities of the materials to withstand the synthesis or processing conditions. Similarly, the final application for the product must be within the temperatures dictated by the thermal stability.

There are also situations outwith the normal usage of the materials to be considered. These include the disposal of excess or redundant material, or the possibility of accidental exposure to fire. These factors are of particular importance when large amounts of material are involved. The fire situation is of significance when large amounts of a particular component is on one site, in say a storage area or while awaiting further processing.

This study had two major objectives. The first was to gain some insight into the thermal degradation pathways for a series of polymers, pigments, and pigmented polymer systems. The second was to develop a method for analysing the products under the fire situation. It will be seen that there are no universally applicable approaches for these studies[2,3,4]. Methods were developed and applied to attain these two objectives for the materials under study. The positive and negative attributes of these methods are discussed in this and the following chapters. The remaining six

chapters contain the results obtained using these methods to study the samples supplied by the sponsor.

1.2 POLYMER DEGRADATION VS FIRE SAFETY

The two main objectives for this study overlap two well defined disciplines, namely thermal polymer degradation and fire safety engineering. The first of these fields covers the products from polymeric materials under heating and the mechanisms for the formation of the products. Fire safety engineering tend to focus on the larger scale properties of materials when they become the fuel for fire[5]. The principles behind these approaches are outlined in the following two sections.

1.2.1 Introduction to Polymer Degradation

There are various processes which cause polymeric materials to degrade. These can cause the polymer to develop undesirable characteristics. Deterioration through weathering is typically due to exposure to ultraviolet and visible radiation, often combined with oxidation of the radiated material[6]. This study, however, was of the thermal degradation of a series of samples.

Thermal degradation is of relevance at a number of stages in the polymers life cycle. Firstly, there is any heat applied under processing conditions. Clearly for a material to be of use, processing must have a limited impact on the chemistry, and therefore properties, of the material. The second area for consideration is the loss of useful properties during the intended use for the polymer. This is normally only a problem for polymers which are to be used at elevated temperatures. The third place where thermal degradation is of interest is in the fire situation. It is possible with many materials to

control how they behave when exposed to extremely elevated temperatures, thereby reducing the contribution of the polymer to the fire hazard[7]. This is the main area of interest in this study, where temperatures of up to 1000°C are considered.

One final application for the study of thermal degradation is for the recycling of the polymeric materials. Heating may be used to reduce some polymers back to monomer for recycling purposes, or to produce a fuel oil mixture from the polymer[8].

It is apparent that some thermal properties may only be enhanced at the cost of others. By way of example, recycling involves the generation of monomer and other volatile products under heating. This decomposition is generally undesirable in the other three circumstances described above. Ease of monomer production may cause problems under processing conditions, and depolymerisation will certainly effect the properties of the material. Many thermal degradation products flammable, thereby producing a fire hazard.

The chemist studying polymer degradation will normally work with small samples. This will help to prevent side reactions, allowing the initiation stages of the degradation to be determined. This is a key step to finding ways of controlling the degradation. There are many techniques available for this study, but the nature of the materials prohibits the development of a universal method. An example of this effect is to consider high vacuum thermal degradation methods against studies at atmospheric pressure[9]. In the first case, the volatile components leave the hot zone rapidly to prevent additional contribution to the reaction. However, volatile stabilising additives may also be drawn from the system, preventing them from displaying any potential contribution to the

process. Clearly these advantages and disadvantages are reversed when performing a study at atmospheric pressure.

It is apparent from these considerations that degradation methods must be chosen carefully for the system under study.

1.2.2 Introduction to Fire Safety Science

Fire safety engineering tends to involve the study of thermal degradation of the finished products rather than analysing small samples of the raw (but potentially treated) product. The interest in the polymeric material is therefore less chemically biased, but targeted towards the physical responses in the fire situation.

There are many tests and standards to which polymeric materials must comply, in order to be used in certain applications[10,11]. One important aspect of testing is whether or not a sample can be ignited, or will continue to burn. The study of this apparently simple property has resulted in a range of tests. One of the most significant is the determination of the Limiting Oxygen Index (LOI). Here, for *ASTM D 2863-77*, the test material is mounted vertically in a tube, and ignited at the top. The oxygen content of the atmosphere flowing along the tube is lowered to the minimum level that supports combustion. This oxygen content is expressed as a percentage, and is the value quoted as the LOI. This, like all other tests, has some weaknesses. Perhaps the most significant is the unrealistically low level of radiant heat compared with most real fire situations. Lighting the sample from below would provide more heat to the unburnt sample, but describes a quite different fire situation. It is apparent that which end is ignited will affect volatile production and char formation. Evidence of melt dripping would only be provided when the sample is ignited from below.

The samples studied here could not be vertically mounted as they were in powder form. Processing was not considered as altering the thermal history of the materials would have been undesirable. One sample form which was applicable to this study was that adopted for Cone Calorimeter or the study of Critical Mass Flux at Firepoint[12]. The basic design of the apparatus for these methods is further described in the following chapter.

It follows from the num,ber of fire models that there is no universal one. The best compromise is to consider the potential hazards for the product, and apply tests accordingly. The methods adopted in this study will be explained and justified in Chapter 2.

1.3 The Burning Cycle

The primary requirements were to assess the products which were likely to be evolved under the fire situation and gain some mechanistic information of the decomposition pathways. To do this it is necessary to consider what basic processes occur during the burning process[9]. The candle model can be adopted when flaming occurs, and is shown in Figure 1.1:

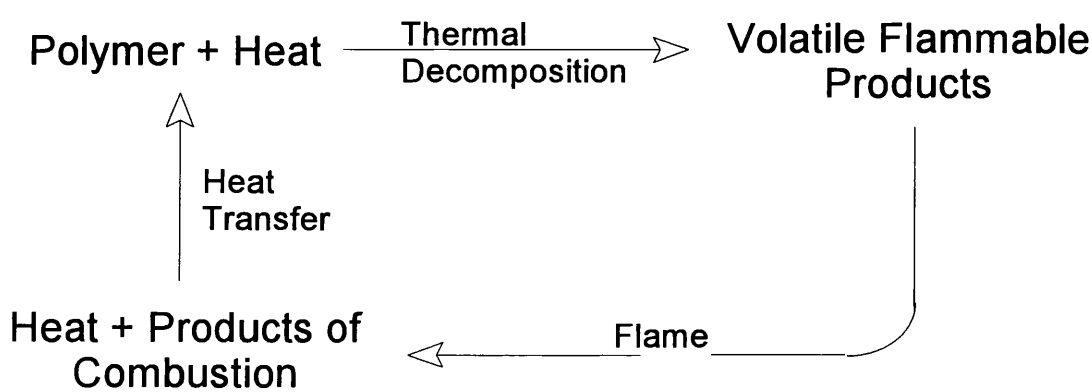

Figure 1.1: The Burning Cycle

1.3.1 Required Degradation Environments

Studies carried out under inert atmosphere could reveal the fuel, as well as the non-flammable products. The degree of stability of the test material (which in this study included colourants as well as polymers) could also be considered at this stage.

The products of combustion are very dependent on the conditions of the burning. The effects of background temperature and oxygen levels are variables which means that studies under flaming conditions alone cannot produce a universally applicable set of product analyses.

The following conditions were used in order to take account of these factors:

1. Firstly the fuel components and thermal stability had to be determined through studies under inert atmosphere. Materials identified at this stage may or may not be further degraded in the burning process.
2. Samples may be oxidised prior to ignition, or fail to ignite. It was therefore deemed important that the sample should be degraded under an air flow, but with no source of ignition, and the products analysed.
3. Finally, the samples were to be exposed to conditions as similar to the fire situation as was possible, and all the products gathered for analysis.

Analysis of the products from the degradations under the above conditions resulted in three main product groups:

1 Fuel.

2 Products from oxidation without flame.

3 Products from a "standardised" fire situation.

1.4 Materials under Study

All the materials studied were supplied by Sandoz. Most of the samples studied were colourants[14-17]. Some of these were also studied as dispersions through polymeric material. The colourants were insoluble, and so are better described as pigments rather than dyes. The pigmented polymer systems were colour concentrates. This means that a high loading of pigment was present in the polymer, which could then be added to an uncoloured batch to provide the required colour.

At the start of each chapter a detailed description is given of the materials studied in the sections which follow. This information is summarised here.

Chapter 3 covers the degradation of the unpigmented polymer samples. Polypropylene and polypropylene wax were the carrier for one of the pigments, and a poly(ethylene terephthalate)/ poly(butylene terephthalate) copolymer was used for another.

Organic disazo colourants were studied in chapter 4. This class of colourant is of the most commercial significance. The first of these, Sandorin Red BN, was also studied further in chapter 8. The remaining all organic colourants are studied in chapter 5. The pigments studied were based upon an anthraquinone and a triphendioxazine structure. The anthraquinone was also studied in chapter 8. Chapter 6 describes the thermal degradation of three metal complex azo dyes. All three contain two azo groups. It is unclear if these are pigments or dyes. This point is elaborated upon in section 6.1. The degradation of the remaining metal-containing colourants are described in chapter 7. Categorisation of these colourants proved difficult. One may be described as an azo dye, and the other was structurally similar to phthalogen dyes. Chapter 8 contains the

results and analyses from the degradation of the polymers described in chapter 3 when colourants were added.

Mechanistic suggestions based on the major products of thermal degradation are given at the end of each chapter. It will be apparent when reading these sections that formation of many of the products may be readily explained, while the rationalisation of others is highly speculative.

CHAPTER 2

TECHNIQUES EMPLOYED FOR THERMAL DEGRADATION AND PRODUCT ANALYSIS

2.1 INTRODUCTION

The polymer degrading chemist favours methods which lead to minimal side reactions, in order to facilitate the elucidation of the mechanism for the decomposition[4,18]. Such methods were desirable for the initial stages of these studies to ascertain the fuel for the studies under flaming conditions.

This chapter details why new methods had to be developed and previous approaches modified for the samples under study. The reasoning behind each method will be explained and any limitations highlighted. It should be realised that there will always have to be compromises taken, as is illustrated by the diverse array of methods used by researchers today.

Product analysis was performed through a range of techniques, with Subambient Thermal Volatilisation Analysis (SATVA) taken as the starting point[19,20]. This allowed the separation of the more volatile products which were then studied through traditional methods such as MS, IR, GC and GC-MS[21-22,28,30-37]. These procedures are also briefly detailed in this section.

2.2 THERMAL DEGRADATION TECHNIQUES

2.2.1 Thermogravimetric Analysis

Thermogravimetric Analysis (TG) was used to provide information on the thermal stability of the samples[23]. The weight loss of the sample can be obtained either over time with isothermal heating, or with programmed heating as was used for these studies.

The thermobalance used was a Du Pont 951 Thermogravimetric Analyser coupled with a Du Pont 990 Thermal Analyser. A platinum boat was used to hold samples of around 5 mg in size.

2.2.2 Thermal Volatilisation Analysis

Thermal Volatilisation Analysis (TVA) was developed by McNeill[18-20]. This extensively published method was available in the laboratory, so was considered a suitable starting point for these studies. The environment surrounding the sample is illustrated in Figure 2.1.

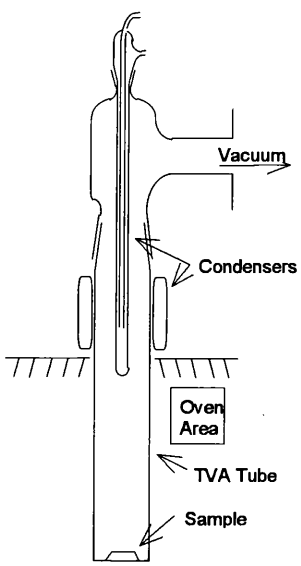

Figure 2.1: TVA degradation environment

The sample environment is evacuated throughout the degradation by continuous pumping. The oven, a Perkin Elmer F11 GC unit, is normally programmed at a rate of 10°Cmin^{-1} to a maximum of 500°C.

2.2.2.1 Limitations of the TVA Environment

Some of the pigments under study were found to sublime under TVA conditions, rendering vacuum methods with

programmed heating unsuitable. A "break-seal" tube could be used, but this would encourage side reactions — for example the HCl in some samples would certainly react with the other materials present in the enclosure. Clearly there are two directions in which the difficulties may be addressed.

A: Flash Heating

This was not regarded as a good model for the fire situation. This method of degradation did become available, however, in the form of the Pyroprobe, and is detailed in the analysis section.

B: Non-Vacuum Approach

The sample volatility was such that degradation occurred without the evaporation of the sample when the pressure was atmospheric. In consequence, the TVA apparatus was modified to allow the degradations to occur under static nitrogen at atmospheric pressure.

2.2.3 Degradation Under Static Nitrogen

A simple modification was made to the TVA environment to maintain an atmospheric pressure of nitrogen in the degradation region. This apparatus is illustrated in Figure 2.2.

2.2.3.1 Usage

The whole volume as illustrated was filled with nitrogen to atmospheric pressure, then isolated with a tap from the vacuum line. The liquid N_2 trap was then put in place. The trap had the purpose of:

a: Maintaining the pressure at 1 atm

b: Removing the volatile products reducing further side reactions.

The heating program was as used for conventional a TVA experiment. On completion, the apparatus was pumped out into the SATVA trap for analysis of the volatile materials. The cold ring fraction gathered around the water-filled condensers as in conventional TVA.

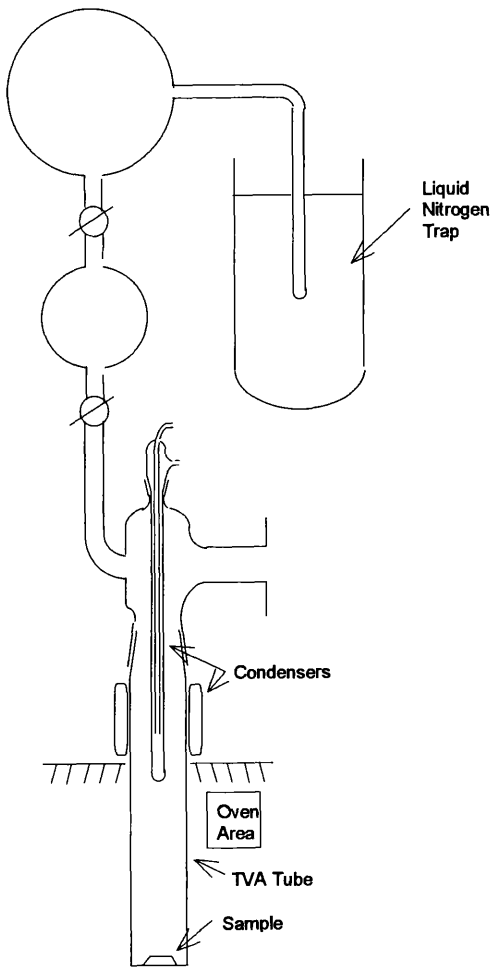

Figure 2.2 Apparatus for Degradation under Static Nitrogen

2.2.3.2 Limitations

The volatility problem had been solved, but not without a cost. The main problem remaining was that there will almost certainly be an increase in the susceptibility of the system to side reactions. The products may have a significant residence time not only in the hot zone, but within the sample matrix itself. This effect is exacerbated by the lack of incentive for the products to travel into the cold trap, although something of a weak flow may well be expected.

Another difference from TVA was that the onset of the degradation, or at least evolution of volatiles, could not be monitored here. Thermogravimetric Analysis was consequently the only guide to the thermal stability.

Most importantly, this approach would be of no use for studying the products of degradation under air, as any oxygen depletion problem would be exaggerated further by the action of the trap.

2.2.4 Flow Apparatus

This is illustrated in Figure 2.3.

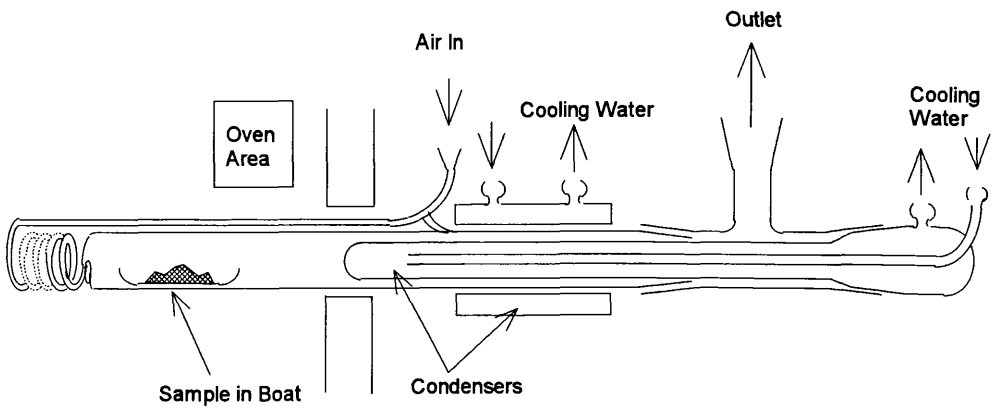

Figure 2.3: Apparatus for Degradation under Flow Conditions

The degradation tube was made from silica glass, and was hence capable of working at temperatures in excess of 1000°C. The path of the incoming gas was lengthened in the hot zone by being passed through a coiled tube. This was done in order to reduce any variance between the sample and the oven heating rates. The maximum was held for 10 minutes to offset this delay.

The oven used was a NEF 2—1 60A Air Exchange Furnace, with a maximum working temperature of 1100°C. The temperature was programmable, and the now standard rate of 10°Cmin^{-1} was used. The method provided no indication of the temperature for the onset of degradation as there was no real-time indicators of the degradation, such as weight loss. The maximum temperature to be attained was determined separately through thermogravimetric analysis.

As well as being suitable for analysis under dynamic air, this approach was also suited to study under inert atmosphere. As a result, this method was used in place of the Static Nitrogen Apparatus for subsequent analyses, the earlier work being repeated on this system.

2.2.4.1 Product Trapping

The flow from the outlet was carried out through a spiral trap. This was surrounded with a dry-ice/acetone jacket. Oxygen condensation was therefore avoided, although it did mean that the more volatile materials were not condensed. Inert atmosphere studies could be carried out under helium flow, allowing the use of a liquid nitrogen trap. Volatile materials could be detected if the vent were coupled to an FT-IR spectrometer, probably requiring a high path reflectance cell to obtain reasonable absorbance. Unfortunately this was not available during these studies.

2.2.4.2 Product Analysis

On completion of the degradation the inlet was stoppered, high vacuum applied and the volatile products drawn into the SATVA system for study. The SATVA process is described in section 2.3.1. Alternatively, the trap jacket was replaced with liquid nitrogen to facilitate the transport of the products to an alternative SATVA line, for, say, the use of on-line mass spectrometry. The volatile products were then separated for identification.

2.2.5 Degradation Under Flaming Conditions

All that remained now was to develop a method for degradation studies under flaming conditions. On failure to uncover any work done in this direction by polymer degrading

chemists, the obvious choice was to turn to considering the fruits of the fire safety engineer[10-13]. This revealed an array of alternative methods, comparable in diversity with the procedures used from the chemistry perspective. This was due to the many different aspects of fire response covered.

2.2.5.1 Traditional Approaches

Many of these approaches could be disregarded as they required strips of material, such as the Limiting Oxygen Index (LOI) test. Much work has been done with this most standard of tests. It has well documented limitations, emphasising the intractability of the problem of finding a universal method.

The samples will only burn through flame (where applicable) on the initiation of the burning cycle. This requires that sufficient fuel is evolved to provide an ignitable fuel/air mix[13]. This rate of evolution is known as the critical mass flux at firepoint. The system Drysdale et al worked on for measuring this quantity, displays much in common with the requirements of this work. The apparatus is shown schematically in Figure 2.4.

A conical heater is used to provide even heating over the sample surface. It also allows the flame to go up the middle. The typical sample diameter is 5 cm in this apparatus. Replacement of the moveable sample mount illustrated with a fixed one is of use for studies such as time to ignition at a particular radiant heat flux (RHF). This self explanatory quantity is the heater output, and is normally measured in kWm^{-2}.

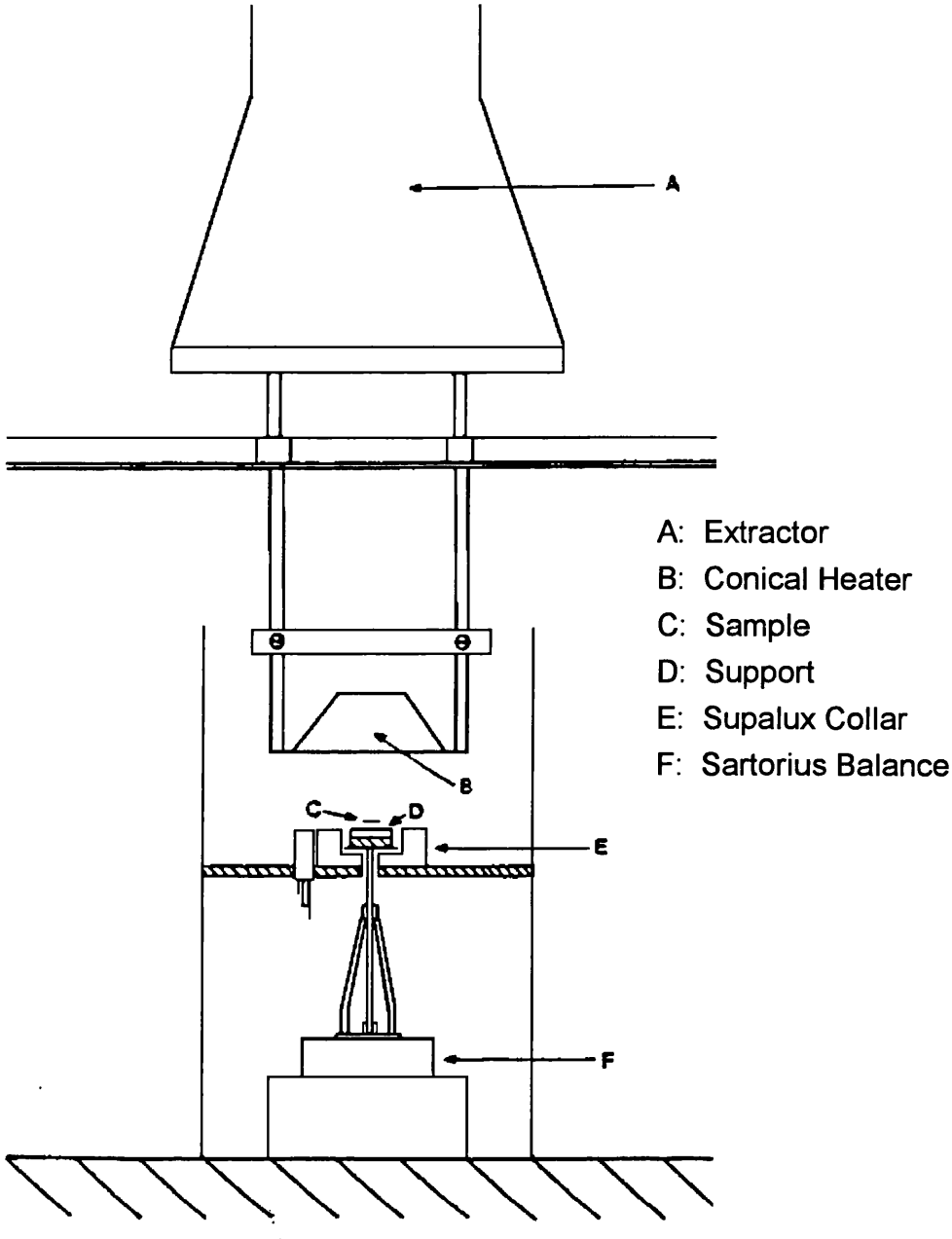

Figure 2.4: Critical mass flux at firepoint apparatus

It was clear that a miniaturisation of this apparatus was desirable. This way the normal size of laboratory samples could be studied, and the whole apparatus contained in manageably proportioned glassware.

Certain features had to be preserved. Most important was the radiant heat flux. Smaller samples should require a lower RHF to provide the critical mass flux in a short time,

due to reduced heat losses through the bulk of the sample. However, there were other changes which could prove significant to the heater power requirement.

The sample would now be of a reduced diameter. Some work on the effect of sample size had been executed in Edinburgh. This showed that the diameter of the sample did not greatly affect the fire response characteristics measurements, until the test diameter was below 1 cm. The size and material of the mount around the sample did make a difference. Air currents induced by the heater will clearly be inhibited by a larger mount. In our apparatus space was limited, so there would be no overlap of the support. It was predicted that the containment would also encourage the formation of an air flow through the centre of the heater and back down the cooler walls.

It was not feasible to calculate the power needed accurately, so a heater was constructed to match the RHF of the bare heater used by Drysdale et al. A 40 kWm^{-2} RHF was the target.

2.2.5.2 Power Calculation

The distance between the sample and the conical heter is shown schematically below.

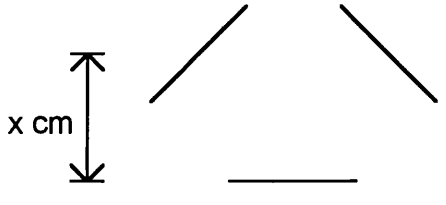

The initial calculation for the power required a major assumption. This was that the heater could be considered as a point source, thereby radiating uniformly in all directions. The arrangement may be described schematically.

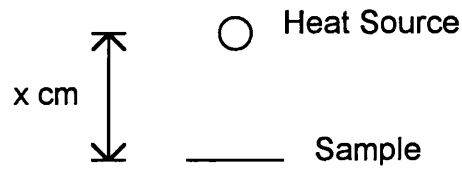

The sample approximates to being on the surface of a sphere of x cm radius,

i.e., the area of sphere, $A = {}^{4}/_{3}\pi r^3$

The distance between the centre of the heater and the sample was expected to be ~3-4 cm.

i.e., area of sphere, A = 113 to 268 cm^2

i.e., A = 0.0113 to 0.0268 m^2

so if 1 m^2 requires 40 kW (see section 2.2.5.1)

then 0.0113 m^2 requires 40 x 0.0113 kW = 452 W

and 0.0268 m^2 requires 40 x 0.0268 kW = 1,072 W

Consequently, if the sample were at 3 cm from the heater, then the power requirement would be half of that at 4 cm. The shorter distance was favoured, in order to keep the design of the apparatus more manageable.

It should be kept in mind that these figures were calculated only as a rough guide, as the effects on the power requirement of scaling down the apparatus could not be accurately predicted. It was apparent that if the maximum power available could match the figure calculated above, then a suitable RHF may be attained through reducing the potential of the supply to the heater. Any extra output demands ought to be covered by the fact that the heater would not be a point source, but a cone deflecting heat down upon the sample.

2.2.5.3 Heater Construction

The heater had to be of under 8 cm diameter in order for it to fit in the available housing (see Figure 2.11). An alternative surround could have been made, but the one to hand happened to be of convenient size, and suitable volume. The size constraints did, however, lead to practical problems in the construction.

The difficulty was based upon the length of element required. An element wire of a high resistance would be easier to wind, as it would be shorter. The problem with such a filament is the tendency for it to fuse when under load. This meant that a longer heavier element, consequently of lower resistance, was required. The difficulty now was to be fitting enough element into the heater to reduce the current drawn.

This was accomplished by arranging ten ceramic posts of 4 mm diameter in the shape of a cone. Each individual peg was wound with ~8 turns of the wire. The wound posts were then set into a ceramic ring of 7 cm external diameter.

The resultant resistance was 8 Ω. Using the relationship

$$P = V^2/R$$

where

V = Potential (Volts)

R = Resistance (Ohms)

P = Power (Watts), it was found that the required potential would be 56.6 V. The relationship

$$P = IV$$

where I = current in amperes, it was calculated that the resultant current would be slightly in excess of 7 A.

The final dimensions are given in Figure 2.11.

2.2.5.4 Test Characteristics

2.2.5.4.1 Radiant Heat Flux Meter

The radiant heat flux meter operates using the thermocouple principle[24]. The apparatus is as illustrated in Figure 2.5.

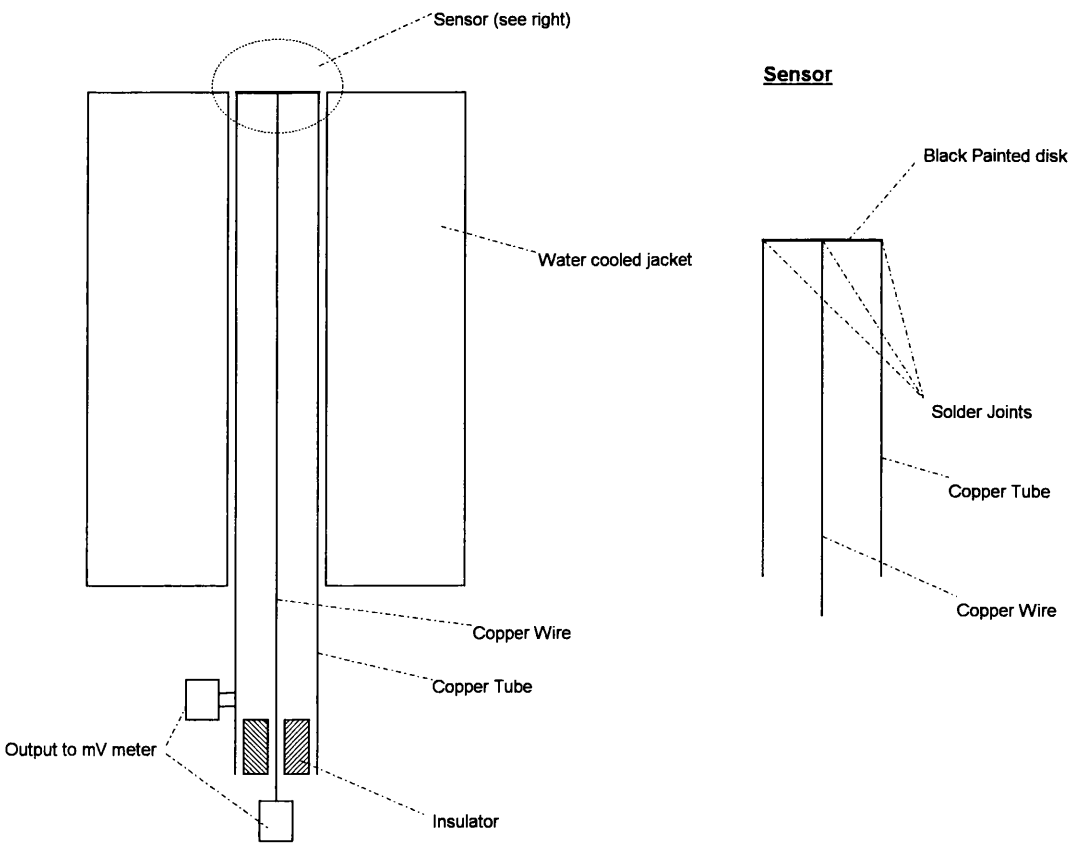

Figure 2.5: Radiant Heat Flux Meter

The disk is of constantan to provide the hot and cold junctions with the copper, as is required by the thermocouple principle. The hot junction is the contact with the copper wire and the cold junction the contact with the copper tube.

Calibration was performed by measuring the millivoltage output for the meter to be used and a reference meter at five different heights from a heat source. The heater used for this purpose was a cone heater of the type used in the flammability tests for critical mass flux at firepoint. This was maintained at a constant 760°C. The reference meter had previously been calibrated, and was reported as providing an output of

$$0.08480 \text{ mV/kWm}^{-2}$$

This calibration constant, k, relates the meter output to the radiant heat flux by the following equation:

$$\text{Radiant Heat Flux} = V/k \qquad \text{Equation 2.1}$$

where V = Meter output in millivolts

k = constant for meter in mV/kWm^{-2}

The calibrated RHF meter and the one for these studies were positioned at a series of distances from the 760°C conical heater. The mV response from each heater was measured. The constant from the previously calibrated heater was used to calculate the final column in Table 2.1.

Table 2.1: Calibration Data

Height	Calib/mV	Tested/mV	Heat flux(kWm^{-2})
infinite	0.000	0.000	0.00
1	0.805	0.302	9.49
2	1.250	0.467	14.74
3	1.870	0.695	22.05
4	2.190	0.825	25.83
5	2.590	0.942	30.54

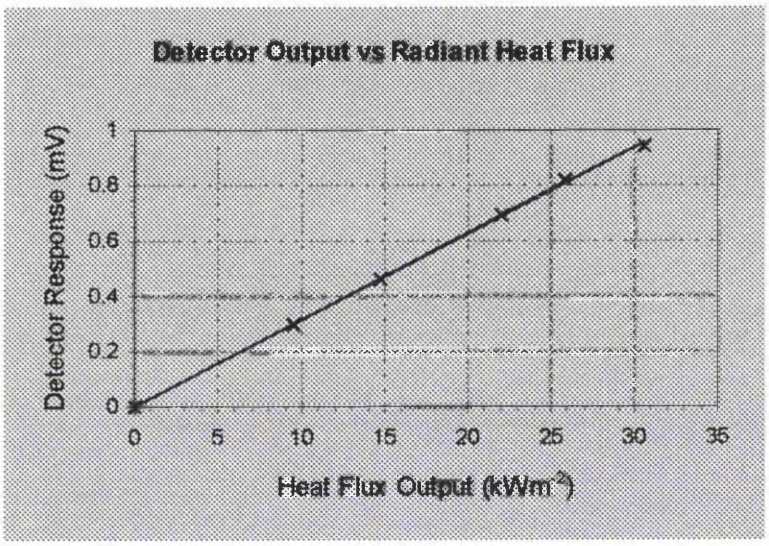

These values are plotted graphically on the left.

The best fit line was calculated through the least squares method. This was found to be,

gradient = 0.03140 mV/kWm^{-2}.

This constant was then used in Equation 2.1 to determine the radiant heat flux, RHF, for the heater used for the flaming studies presented here.

2.2.5.4.2 Radiant Heat Flux Measurements

This was measured over a range of different distances and voltages to the heater. The distance, d, was as illustrated in Figure 2.6.

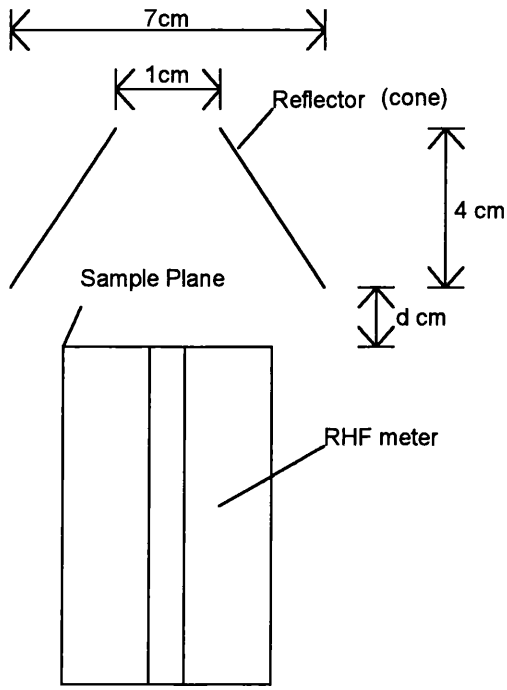

Figure 2.6: Distance d between heater and meter

Power to the heater was supplied by a "Variac" unit. The voltage was measured with a separate meter as the scale provided on the supply offered a low degree of precision. The results obtained from the apparatus in Figure 2.6 are illustrated graphically in Figure 2.7. The data obtained were used to assess the voltage required for the studies, as well as confirming the sample-heater distance used.

The first graph, RHF vs Time, demonstrates the warm-up characteristics. The supply voltage was 60.8 V and d was 16 mm. It can be seen that the output was around 50% after 1 min. The maximum of 29.6 kWm^{-2} was reached after 7 min. The second graph, RHF vs d, illustrates the effect of varying the sample-heater distance. The supply voltage was constant at 60.8V. The heater was allowed time to stabilise output before the readings were taken. It can be seen that small inaccuracies in d in the sample position would only result in a change of around 2-3 kWm^{-2} in the RHF. The lower two graphs are of RHF vs voltage. The distance, d, was 16 mm for both sets of results. The power output has clearly increased with the ageing of the heater,

i.e. RHF (60.8V) = 29.6 kWm^{-2} on unused heater

and RHF (60.0V) = 38.8 kWm^{-2} after 3 months.

The increase in output through use is hard to explain. A decrease in the resistance would have increased the power. A build-up of carbon or a metalic oxide film on the heater could have caused this.

All of the degradation studies were performed at as near to 60 V as possible. This was because this ageing effect had not been noticed during the course of the studies. Also, it was not practical to test the heater between each experiment to keep the RHF constant. The "Variac" used was difficult to set precisely, which is why much of the data presented here was at 60.8 V rather than 60.0 V. The manifestation of the increase in output can be seen through examination of the degradation observations.

Air flow over the sample is known to influence the RHF it experiences, as was indicated in 2.2.5.1. RHF vs time was tested with the apparatus in Figure 2.6 placed in a fume hood. It should be noted that the measurements were taken after 3 months of usage, which is why the outputs are higher than for the similar graph in figure 2.7. The maximum outputs were:

RHF (d = 16 mm, V = 60.0V) = 36.4 kWm^{-2} with hood off

RHF (d = 16 mm, V = 60.0V) = 38.8 kWm^{-2} with hood on.

This highlights the point that the environment around the heater influences the convective cooling experienced by the sample. This indicates that the RHF

measurements here are not an absolute guide. Unfortunately, the size of the meter prohibited locating it within the apparatus.

The calculations given in 2.2.5.2 were for a heater capable of producing an RHF of up to 40 kWm^{-2}. In practice the output ranged from 29.6-38.8 kWm^{-2} for the majority of the studies. This proved adequate for providing the fuel evolution rates (critical mass flux) to obtain ignition. The distance of 16 mm was chosen for these measurements as this was the closest that the sample plane could be practically set from the heater.

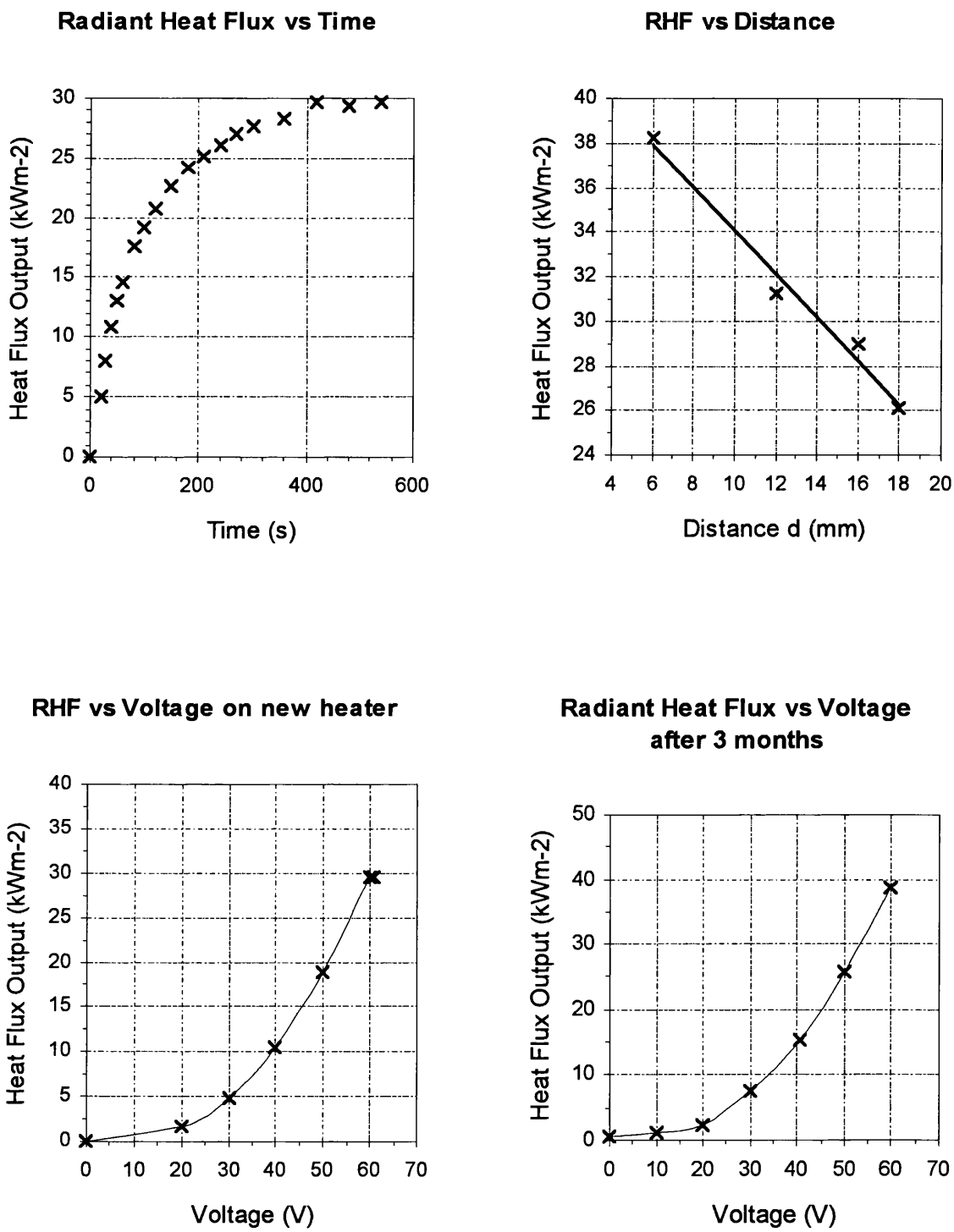

Figure 2.7: Heater Output Characteristics

2.2.5.5 Enclosure For Flaming Apparatus

Glass was considered the ideal material for containing this degradation environment. This allowed ease of cleaning, and observations to be made during the studies. It also meant that "Quickfit" connectors could be used to seal the required fittings to the body of the vessel. The alternative would have been to use heated stainless steel[25]. This would have been more diificult to construct. Limitations to the size of the apparatus were imposed by the abilities of the glass-blowing department. Further details, such as the dimensions, are given in Figures 2.11 and 2.12.

2.2.5.6 Supplying Power to the Enclosure

The electrical connections to the heater had to allow a vacuum-tight seal. The glass-blowers were able to fit a pair of tungsten wires to one B19 cone, as illustrated in Figure 2.8.

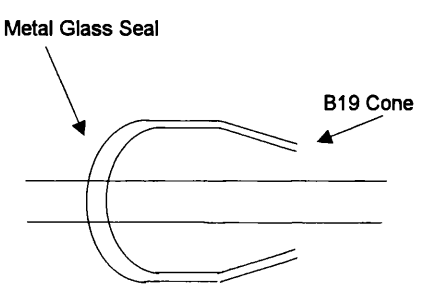

Figure 2.8: Heater power supply

The links to the tungsten were achieved with the connectors from inside a "chocolate-block" terminal. The coupling to the heater was completed with copper multicore wire covered with ceramic spines for thermally stable insulation. These cables were regularly cleaned to avoid contamination during the degradation studies.

2.2.5.7 Pilot

The alternatives were either to use a spark or a flame to initiate the burning cycle. The latter was disregarded for three reasons

a: Source of more products

b: Uncontrollable heat source

c: Safety (extinguishing would cause explosion hazard)

This was reason enough to justify a spark pilot. This has one major disadvantage as it is not as rich a source of radicals as the flame, rendering it a less efficient pilot.

The spark gap was around 2 mm to allow car components to be used.

The circuit diagram is shown in Figure 2.9.

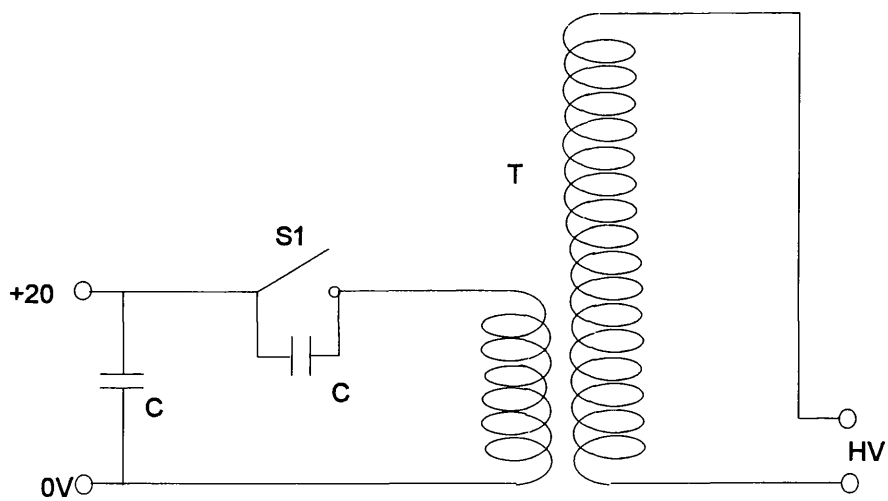

Figure 2.9: Spark Circuit Diagram

The DC input was provided by a bench power supply. The transformer, T, was the coil from a car. This was a cheap and convenient method of obtaining the high potential required.

The spark itself was introduced into the overall vessel through a metal/glass seal, as shown in Figure 2.10.

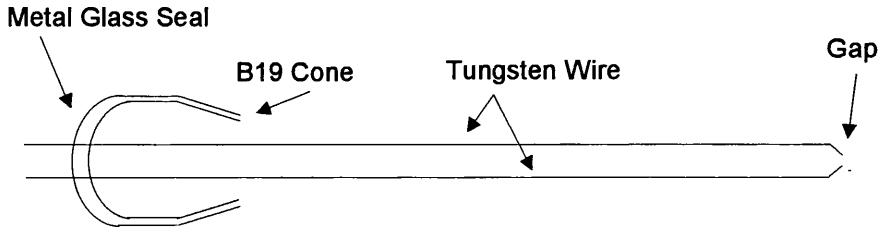

Figure 2.10: Spark Source

2.2.5.8 Final Local Sample Environment

The arrangement surrounding the sample is shown in the Figure 2.11.

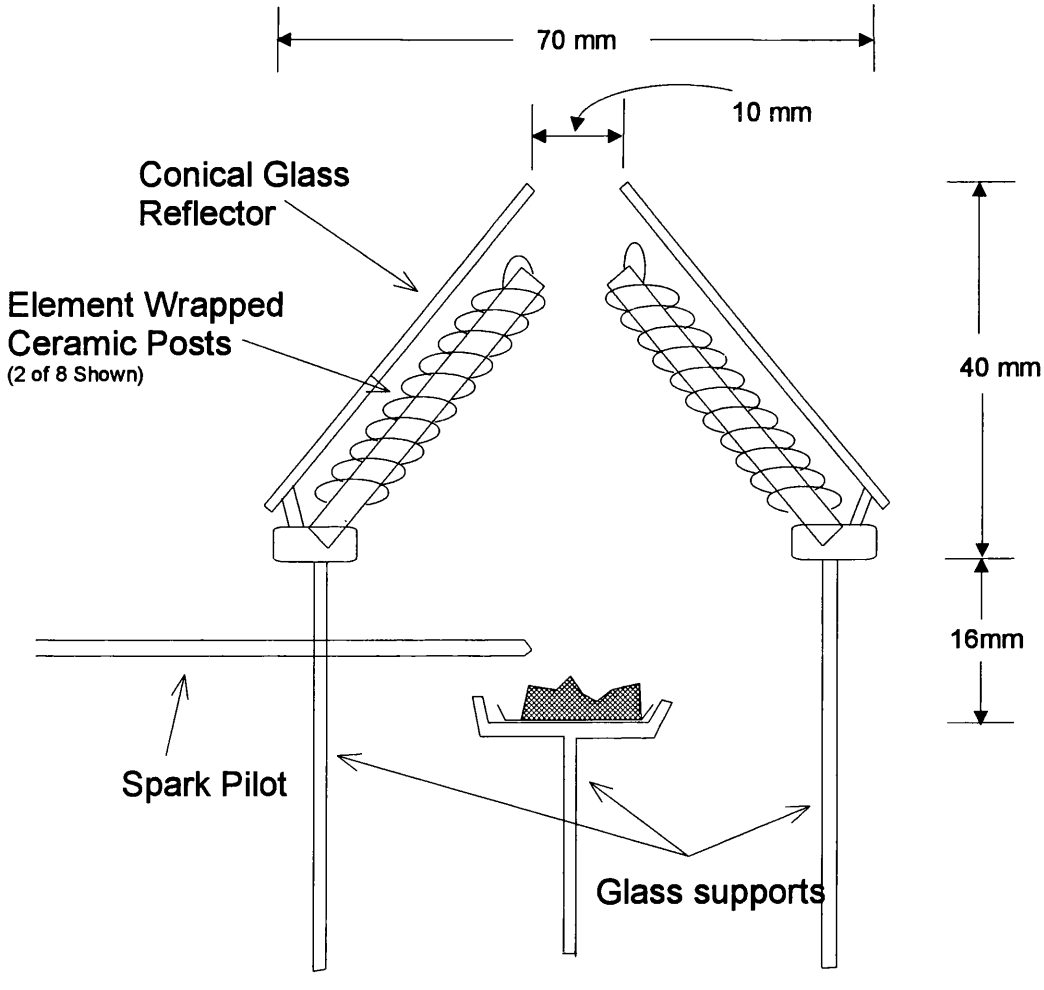

Figure 2.11: Sample degradation environment

The sample was placed either on a metal planchet, or latterly on a glass substitute. No difference in the behaviour of the samples was observed.

One other consideration was the warm-up time of the heater. Detailed information on this is presented in section 2.2.5.4.2. Exposure to the heat on warm up may lead to increased surface oxidation, and the possibility of the slow evolution of the fuel materials. In the latter case, the critical mass flux for fire point of the sample may not be reached. A "blocker" was used to allow the heater to warm up before the sample was heated. This took the form of a disc of glass of ~22 mm diameter which was placed between the sample and the heater. This could be turned to the side by rotation of the B21 joint from which it was attached to the walls of the containing vessel. The small size of the blocker was a product of the limited space available. It was apparent that it could not protect the sample indefinitely. By way of standardisation, it was only kept in place for one minute from switch on. It can be seen from the heater response graphs that around half power had been attained by this time. The observations made for the polypropylene studies confirm the effectiveness of the blocker, where ignition occurred within seconds of the sample being exposed.

2.2.5.9 Overall System and Operation

The complete apparatus is illustrated in Figure 2.12. The arrangement beyond the degradation region is identical to that for the air/nitrogen flow apparatus. The trap was surrounded with a dry ice/acetone jacket during the degradation. It was noted previously that this meant some products would not be condensed. However, the time of degradation was much shorter under these conditions. This allowed an IR cell, as shown in Figure 2.13, to be placed over the vent. Although this was of little use for

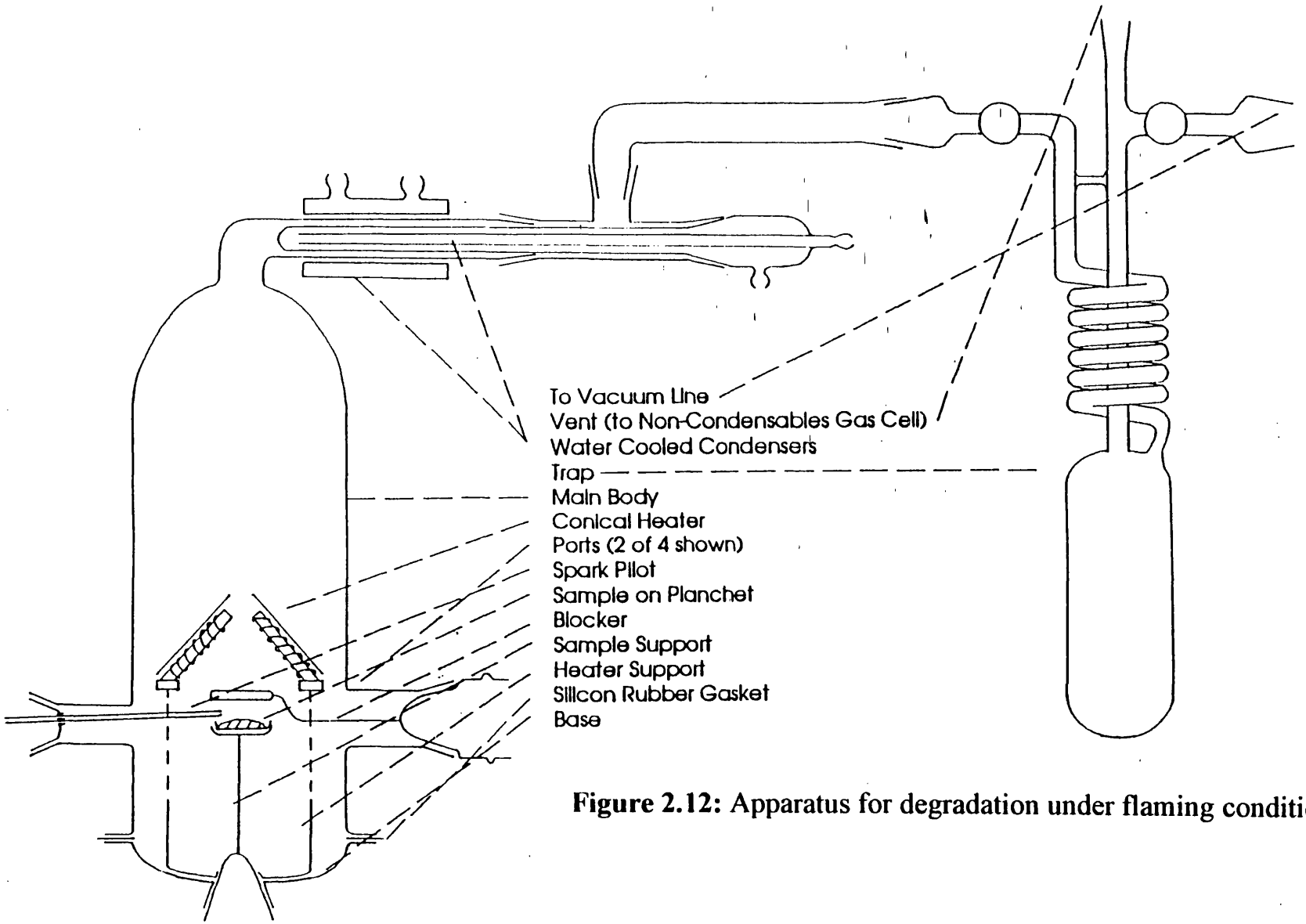

Figure 2.12: Apparatus for degradation under flaming conditions

quantitative study, it did provide some indication of the non-condensables produced. The inlet to the apparatus was stoppered on completion of the degradation, and analysis carried out as per the dynamic air/ nitrogen apparatus.

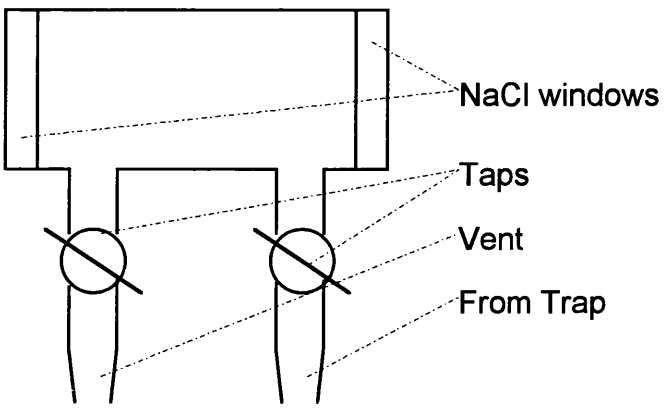

Figure 2.13: IR Cell for Non-Condensables

Condenser tubing was wrapped around the glass shell of the degradation area. This had a dual purpose. The first and most important was to protect the glass from stresses induced by the heat from the ~0.5 kW heater. The second aim was to reduce the side reactions by condensing products onto the glass shell. This transpired due to ring currents as illustrated in the Figure 2.14. These products are known as the cold ring fraction (CRF).

This resulted in much of the CRF being deposited on the walls of the degradation vessel rather than being carried through to the condenser area as in the non-flaming flow apparatus. These materials were extracted by washing the walls with a solvent, in particular methylenechloride or acetone. The later was found to be the most effective in the majority of cases.

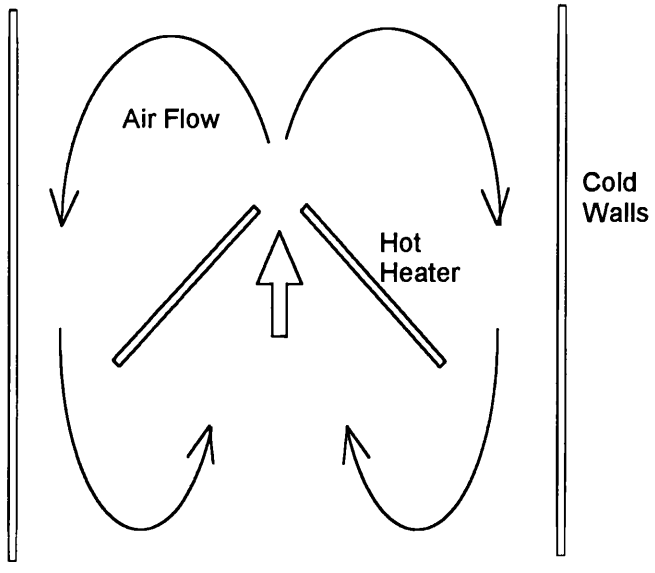

Figure 2.14: Air Currents

2.2.5.10 Oxygen Depletion

The characteristics for oxygen depletion were considered. The total volume of the vessel before the vent to the condensers was around 2 litres. Calculation of the number of moles of oxygen present should consider the expansion of the air on warm-up. Using Charles' Law to calculate the volume lost relative to STP conditions, the graph below for moles O_2 relative to temperature was obtained.

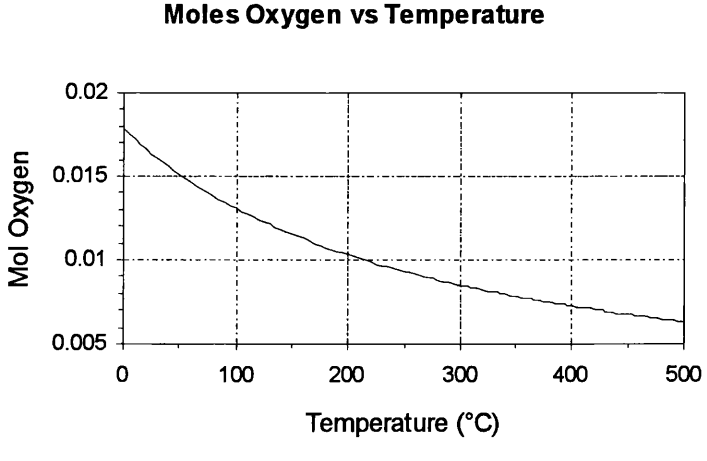

It would be difficult to determine the exact number of moles of oxygen present in the apparatus, as it is not practicable to measure

the wide-ranging temperatures around the enclosure. A reasonable rough estimate may be to say that the degree of expansion is equivalent to no more than 100°C. This would give 0.0140 mol of O_2, as opposed to the 0.0175 mol at STP.

This can then be related to the oxygen requirements of the samples. This is not as straightforward a calculation as it may at first appear. A first approximation would be to allow for complete oxidation. Problems then arise in not knowing the effect of dropping oxygen levels on the rate of the oxidation of the sample, or indeed for sustaining the flame when present. A second important factor is the extent of protective residue formation.

This should not be greatly affected by oxygen depletion as the oxidation of the bulk will normally be a minor factor. The fuel evolution will not be greatly influenced by the quantity of oxygen present. This means that the fuel contribution can be measured as the mass lost from the starting sample weight. Furthermore, the remaining weight will be predominately due to carbon.

It was apparent that oxygen depletion will have arisen during some of the degradation studies presented in the following chapters. The extent of this effect must have varied from sample to sample. Some of the samples formed a large amount of involatile residue, thereby providing less fuel and requiring less oxygen. Some burned very aggressively, meaning that even a large excess of oxygen would not prevent a localised depletion around the sample. The depletion effect would have been of the greatest significance where the sample burned smoothly with only a small residue. An example of this final case was the polymeric samples as described in Chapter 3.

2.3 METHODS OF ANALYSIS

2.3.1 Subambient Thermal Volatilisation Analysis (SATVA)

Subambient Thermal Volatilisation Analysis (SATVA) was the main starting point for the analysis of the degradation products[18-20]. This technique provided some separation of the products which were mobile under high vacuum. In particular, this approach excels in the identification of the gaseous products, leaving the liquids isolated for analysis through other methods. A representation of the apparatus is given in Figure 2.15.

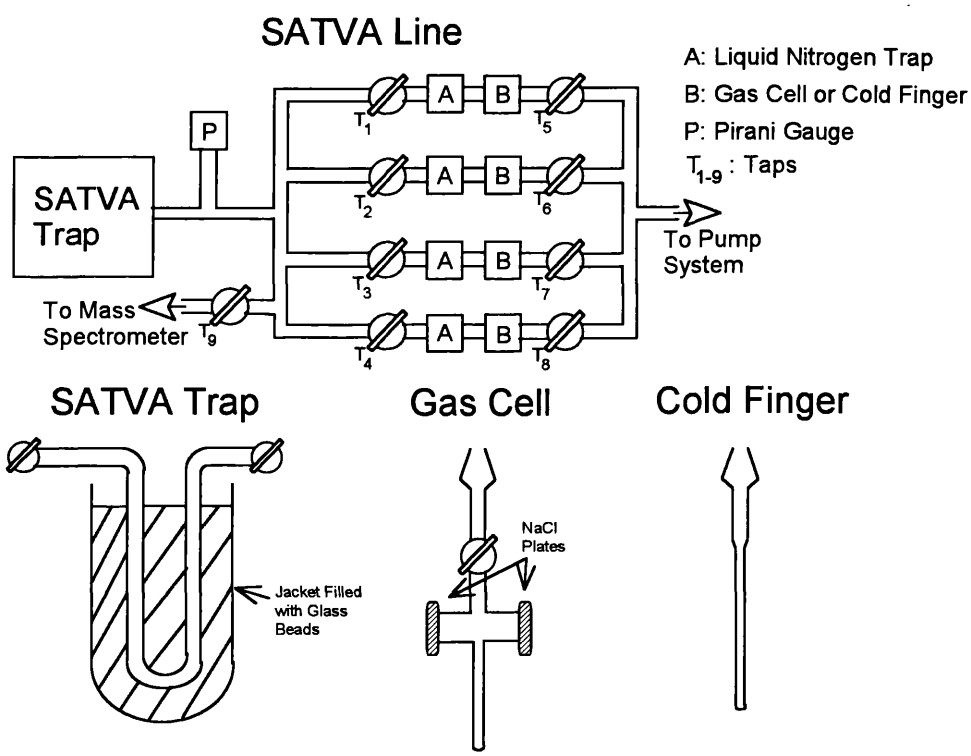

Figure 2.15: SATVA Apparatus

2.3.1.1 Pump System

The system was continuously evacuated using a two stage pump system. A rotary pump provided the backing vacuum. This reduced the overall pressure to around

10^{-2} mm Hg. The vacuum was further improved with a silicone oil filled diffusion pump. Pirani gauge[26,27] readings indicated the vacuum to be of around 10^{-4} mm Hg behind the diffusion pump. It should be noted that this pressure is close to the lower limit for the Pirani principle, but does represent a realistic figure.

Liquid nitrogen traps were placed between the two pumps, and ahead of the glass vacuum line. These both assisted the vacuum and reduced contamination from the pump oil. Examination of the results chapters show that there was still some contamination of the product fractions. Fortunately silicon-based materials from the diffusion pump could be easily disregarded as the samples under study contained no silicon. There were, however, unexpected aliphatic hydrocarbons found in some of the analyses. The rotary pump is one probable source of these.

2.3.1.2 Mass Spectrometry

One of the SATVA lines in the laboratory was fitted with a Leda-Mass Quadrupole Mass Spectrometer[28]. This gas sampling device had a mass range of 1 to 300 amu. The mass range practically detected was limited to around 100 amu, due to a sharp fall off in response with higher masses. Electron Impact ionisation was used at an energy of 70 eV. The unit itself was maintained at a constant 80°C.

2.3.1.3 Operation

Normally three gas cells and one cold finger were attached at positions B on Figure 2.17. The SATVA trap with the bead jacket was frozen with liquid nitrogen. The mobile degradation products were then distilled into it under high vacuum.

The whole line was then evacuated by opening taps T_{1-8}, the mass spectrometer area having a separate pump system. The liquid nitrogen was then put into place at positions A and taps T_{2-4} closed. At this point the liquid nitrogen jacket around the SATVA trap was removed. The trap then took around 50 minutes to warm to 0°C. During this time the pressure on the Pirani gauge was recorded on a computer. A BBC Master computer was interfaced to one of the SATVA lines used, and an IBM compatible PC on the line coupled to the quadrupole MS.

Tap T_9 could be opened when a Pirani response was detected, allowing a mass spectrum to be obtained. The amount of material entering the analyser could be controlled by a bleed valve. The separately eluting products could be directed into different limbs by taps T_{1-4}. It was found that only the gases and very volatile liquids could be isolated by volatility under vacuum alone, so the remaining liquids were gathered together into the fourth limb of the line. All the taps were closed after the Pirani response fell to zero, and the now separated products were distilled into the gas cells and the cold finger for further analysis.

2.3.2 Infrared Spectroscopy (IR)

The infrared spectroscopic analyses performed in the first eighteen months of the project were carried out over four different machines[21,22]. The Polymer Laboratory was equipped with a Perkin Elmer PE734 spectrometer. This was adequate when sufficient sample was available. Weaker spectra, such as those obtained when studying small gas peaks from the SATVA line, required higher sensitivity with some form of manipulation. This was originally done using a Philips PU 9800 FT-IR Spectrometer and a Perkin-Elmer Infrared Data Station 983 with PE 3600 data system, available in

the departmental Spectroscopy Services Laboratory. The latter spectrometer was also capable of scanning down to 200 cm^{-1} which was used in some cases for the study of the metallic residues. Regrettably these results were not very satisfactory. During the final 12 months of the project, a Nicolet Magna 550 FT-IR spectrometer with Omnic software was used throughout.

The range used was 4000-625 cm^{-1} for the gas cells from the SATVA apparatus, as these had NaCl windows through which the beam passed. In some cases, the CRF was also studied by casting a film onto a NaCl plate. This method was unsatisfactory due to the number of materials present in these fractions, which meant that some kind of separation was required.

Identifications from the IR spectra were accomplished through a two stage process. Firstly, comparison with correlation charts of absorption wavenumber against particular functional groups were used to provided a rough guide to the product classification[22,29]. Secondly, reference spectra were compared, which normally confirmed the identification unambiguously[31,31].

2.3.3 Gas Chromatography

Most of the gas chromatography of liquid fractions was initially carried out on the Shimadzu GC14A instrument within the Polymer Laboratory[32,33]. The recorder used was a Shimadzu C-6A Chromatopac. The oven itself was a two column device, and was fitted for use with packed columns. Detection was through a Thermal Conductivity Detector (TCD). The Chromatopac permitted its signal to be integrated, allowing some determination of the relative quantities of the components present. It

would have been necessary to prepare reference solutions for these to be calculated with any accuracy, due to the varying detector response for different materials. This process was hindered by the poor availability of reference compounds, and the number of products involved.

Capillary column studies were performed on a Hewlett-Packard 5880A Gas Chromatograph. This was used where higher resolution was required to separate more complicated samples, and for examining the less volatile CRF fractions.

2.3.3.1 Conditions

The carrier gas employed was helium. This was chosen as it gives the greatest sensitivity with a TCD. Helium has a relatively high thermal conductivity, as can be seen in the table below:

Table 2.2: Properties of common GC carrier gases.

Gas	Mol. wt, g	Viscosity $\mu P, \eta x10^6$	Thermal Conductivity cal/sec. cm (°C/cm)$x10^{-6}$
CO_2	44.01	189	49
Ar	39.95	269	50
O_2	32.00	256	77
N_2	28.01	219	73
He	4.00	228	388
H_2	2.02	108	490

The effect on the detector response with respect to changes in the gas composition and operating temperatures was studied by Schmauch and Dinerstein[34]. This work rationalised the two main factors which effects detector response:

1. The thermal conductivity differences between the carrier gas and the gases under study.
2. The operating conditions within the cell.

The table above clearly shows that the helium and the hydrogen have a much higher thermal conductivity than the others. This has a twofold effect on increasing the sensitivity of the detector. The first benefit is from the increase in the thermal conductivity difference. The typical products under study will have a much lower thermal conductivity. The second advantage is that a higher bridge current may be used in the TCD. This also leads to an increase in the detector response. Helium was used in preference to Hydrogen on grounds of safety. The fact that the more dense higher molecular weight carriers give better separation due to reduced component diffusion was not a consideration here, as resolution was not a problem.

Two packed analysis columns were used for the study of the liquid products volatile under vacuum. Both were $^1/_8$" internal diameter 2 metre packed columns. The support for each was Chromasorb Whp. The stationary phases were OV-1 and OV-17, both at a 10% loading. The former is a non-polar column, which proved suitable for most of the work. OV-17 is a slightly polar medium, which was fitted in case any problems of co-elution arose on the OV-1. The high loading (10%) was chosen as the liquids under study frequently had a high number of volatile components. The molecular weight range under study was not such as to cause bleed problems with high temperature at this loading. The two columns were also sufficiently similar to reduce the effect of baseline drift associated with the use of a two column TCD apparatus.

The liquid fractions produced by degradation of the polymer containing samples typically contained many more products than those of the pure pigment alone. This resulted in a GC trace of many peaks, which could not be reasonably resolved through the use of packed columns alone. There were two main capillary columns used for the

separation of these mixtures. The first was the thin film column, which was used for most of the analyses. This was a 25 m x 0.32 mm ID CP-Sil5 CB 0.12 μm film thickness column from Chromatopac. An alternative of 1.2 μm film thickness was also used for the study of liquids of higher volatility — the liquid fractions from the polymer containing samples.

The temperatures quoted here represent only a rough guide, with any variations being only minor. The injection port and the detector were maintained at a minimum of 10°C above the maximum column temperature. This ensured that the sample was volatilised immediately onto the top of the column. This also has the result of reducing the effect of the accelerating carrier, as the temperature rises, on the baseline from the TCD.

The temperature program itself was dependent on the liquid under study. Typically, 50°C was the starting temperature, although 80°C was sometimes used when there were no early peaks. The lower temperature was then maintained for 1 minute, then the temperature raised at a rate of 10°C/min until the upper temperature was reached. This was then held isothermally for 5 minutes. The machine was set to a typical upper limit of 220°C with the liquid fractions, although it was normally not necessary to go this high. The columns had been conditioned to 250°C.

2.3.4 Simultaneous Gas Chromatography-Mass Spectrometry

It was considered impracticable to carry out identification of the liquids through the use of reference compounds, due to the many and varied products associated with thermal degradation of colourants and polymers. As a result, gas chromatography-mass spectrometry (GC-MS) was employed. This procedure was hampered by the

limited availability of time on such a machine. The departmental facility offered limited sensitivity and chromatographic separation, resulting in much overlap of peaks. It was therefore not well suited to the study of weaker samples, or those which involved the polymeric materials where there are many products present. The main alternative to this was to use the SERC service based in Swansea. This had the disadvantage of being over-subscribed, resulting in only a limited number of samples being analysed there. The third alternative, which became available late into the project, was to use a HP GC-MS machine which belonged to W.J. Cole's laboratory within the Chemistry Department. Clearly, there was a limit to how many samples could be studied in this manner.

All the columns used for the GC-MS analyses were non-polar or very slightly polar, *i.e.* equivalent to an OV-1 stationary phase. The chromatographs presented in the following chapters were total ion current (TIC) readings from the GC-MS analyses[28].

In some cases, when there were no reference available, it was necessary to study the fragmentation patterns to determine the structure of a degradation products[35]. Most mass spectra were interpreted through comparison with reference spectra[36,37].

CHAPTER 3

POLYPROPYLENE AND POLYESTER DEGRADATION

3.1 POLYMERS CONSIDERED IN THIS CHAPTER

The first polymer degraded was polypropylene. This was supplied in two forms, polypropylene wax and polypropylene FBF. Only limited information on these polymers was made available. The first of these was a low molecular weight polypropylene. The second appeared to be a stabilised polypropylene. No information was supplied on the nature of any additives present, the method of initiation of polymerisation or the stereochemistry of the polymer.

The second polymer was a polyester. The name provided was "Polyester — Copolymerisat DNOP 43". This has been referred to as Polyester DNOP 43 throughout this chapter. Again, little information was available on this sample, other than that it was a copolymer containing terephthalate and butylene sections.

3.2 INTRODUCTION TO POLYPROPYLENE

Since commercial introduction in 1957, polypropylene has become a widely used polymer[38], with extensively documented and well understood properties. It is for this reason that little space will be used reiterating this information.

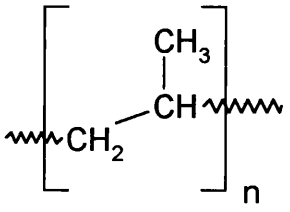

Figure 3.1: Polypropylene structure

The repeat structure of polypropylene is illustrated in Figure 3.1. It can be seen that this is a polymer of a monosubstituted olefin. This means that alternative conformations are available, as the methylated carbon on the backbone is effectively a chiral centre. The orientation of the methyl group may be random to provide the atactic structure. If the methyl groups are in a repeated conformation, then there are two stereoregular possibilities. When they are all arranged in the same conformation the isotactic structure arises, and when they alternate it is called the syndiotactic structure.

Regrettably no information was provided on either the tacticity or the method of initiation or polymerisation for this sample. It will be seen in the following sections that the Polypropylene FBF sample had some kind of stabiliser added, the nature of which was not revealed.

3.3 INTRODUCTION TO PET PBT COPOLYMERS

Poly(ethylene terephthalate) (PET) was first produced commercially in 1944[38]. It is also a widely used polymer. A common form is in thin films, where it is used as a support for magnetic tape and computer disks. PET is also blown for drinks bottles. The tensile strength of PET film is about 25,000 psi, which is two to three times greater than that for cellophane or cellulose acetate film. The tensile strength is around double that of aluminium and equal to mild steel when considering the area of the specimen at break point.

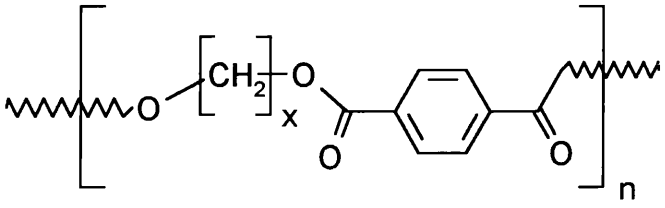

x = 2 for PET : x = 4 for PBT

Figure 3.2: Structure of PET and PBT

Polymers and copolymers of poly(butylene terephthalate) (PBT) are of relatively limited use. The structures of PET and PBT are illustrated in Figure 3.2.

3.4 THERMAL DEGRADATION OF POLYPROPYLENE FBF

Much work has already been done on the degradation of polypropylene[39-44]. However, it was deemed necessary to study this system for two reasons. Firstly, this was a commercial sample which presumably contained additives, the nature of which was unknown. There were some unusual products found in the degradation product analysis. Inorganic additives may not have been detectable. The second reason for studying the thermal degradation of this sample was that new methods were in use. The information obtained here would be relevant to the studies of the coloured systems in chapter 8.

3.4.1 Thermogravimetric Analysis

The TG traces obtained for dynamic nitrogen and air are shown in Figure 3.3, and are summarised in the following table:

Table 3.1: Key temperatures from thermogravimetry of Polypropylene FBF

Conditions	T_{thresh}(°C)	T_{end}(°C)	%Residue
Dynamic Nitrogen	275	465	1
Dynamic Air	220	360	1

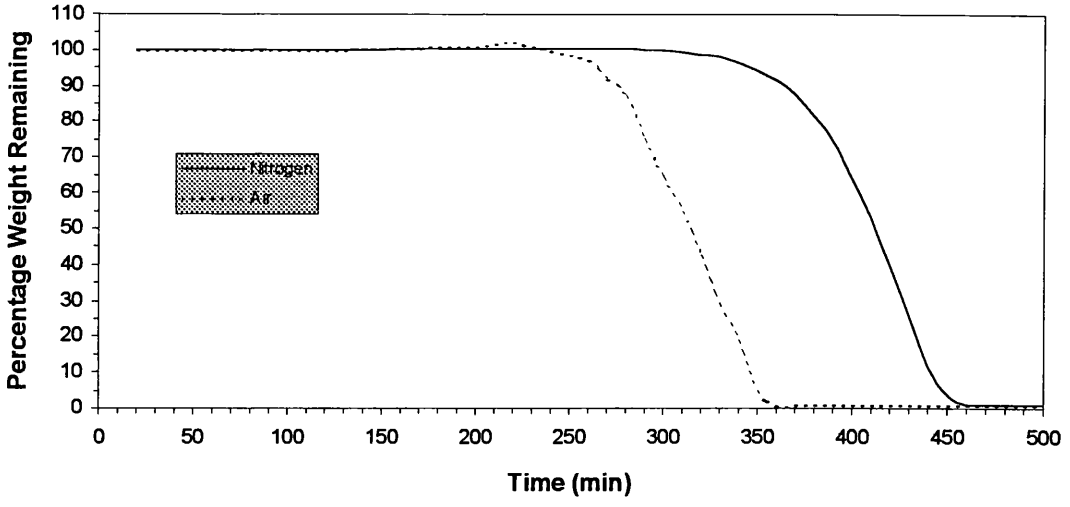

Figure 3.3: Thermogravimetrc Analysis traces from Polypropylene FBF

It may be seen from the traces that the degradation under air gives a similar shaped TG trace to the degradation under nitrogen, but at a temperature of around 100°C earlier. There was also a slight weight gain observed under dynamic air before the onset of the weight loss. This is to be expected for polypropylene, and is commented on in the mechanisms section.

3.4.2 Product Analysis — Dynamic Nitrogen

These studies were carried out with a heating rate of 10°C/min up to 500°C. An initial analysis was executed to 470°C, but this left a small amount of residue. No residue was found with 500°C as the maximum temperature.

A typical SATVA trace for the volatilisation of condensable degradation products is shown in Figure 3.4. The on-line mass spectrometer provided good data for product analysis. The mass spectrum obtained at 7 minutes into the SATVA separation was attributed to the volatilisation of ethane. This was determined through peaks at m/e = 28, 27, 26, 29 and 30. The m/e = 28 peak was considerably stronger than the other four. The weakness of this SATVA peak does not mean that this was a minor

degradation product, but may be due to the temperature of the product trapping. The trap during the degradation was a dry-ice/ acetone trap, kept cool by regularly adding liquid nitrogen. The peak at 10 minutes was due to the volatilisation of propene. This was seen through mass spectrometer peaks at m/e = 41, 39, 42, 27, 40 and 26 in decreasing intensity. When 15 minutes had elapsed the mass spectrum was consistent with the presence of 2-methylpropene. The spectrum was more ambiguous when the maximum of the second peak was reached at 20 minutes, due to other products associated with peak 3 at 30 minutes. These products appeared to be the predicted hydrocarbons. The methylpropene MS peaks were at m/e = 41, 39, 56 and 55. Liquid fraction analysis was not performed here. Some data were obtained through TVA and static nitrogen studies. These results only duplicate other well documented polypropylene studies, so are not discussed at length here. They are, however, are considered briefly in the mechanisms section.

Table 3.2: SATVA peak assignments from Figure 3.4

Peak	Assignment
1	Propene preceded by a small amount of ethane
2	2-methylpropene
Peaks 3 and 4	Other aliphatic hydrocarbons

3.4.3 Product Analysis — Dynamic Air

These studies were carried out with a heating rate of 10°C/min up to 360°C. No residue remained. A typical SATVA trace for the volatilisation of the condensable degradation products is illustrated in Figure 3.5. Infrared analysis provided information for identifying the components forming the SATVA gas peaks. Peak 1 at 10 minutes was attributed to CO_2. The IR spectrum was weak, but had definite absorptions at 2300 and 720 cm^{-1}. Peak 2 at 12 minutes was due to the evolution of formaldehyde.

This was inferred through IR absorptions at 1745, 1770, 1730 and around 2720 to 2960 cm^{-1}. These identifications for peaks 1 and 2 were confirmed by mass spectrometry. The mass spectrum of the products evolved at 21 minutes into the SATVA separation indicates the volatilisation of acetone. This was deduced from the peaks at m/e = 43, 27, 28, 26 and 58. The IR analysis of all products from 15 minutes onwards was dominated by water absorptions. These findings are summarised in the following table:

Table 3.3: SATVA peak assignments from Figure 3.5

Peak	Assignment
1	CO_2
2	Formaldehyde
Remaining peaks	Some acetone, but mainly water. See below for GC-MS of ether extract.

The TIC trace from the GC separation of the liquid fraction is shown in Figure 3.6. The MS traces for similar aliphatic hydrocarbons look very much alike. The selected identifications given below serve to give an idea of the products present.

Table 3.4: GC-MS peak assignments from Figure 3.6

Retention Time	Product	Retention Time	Product
1:05	Solvent (diethylether)	7:28	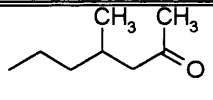 or alternative methylations
4:22	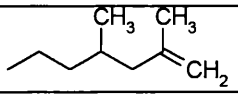	24:34	Silicone contaminant

3.4.4 Product Analysis — Flaming Conditions

The following observations were made during the degradation under flaming conditions:

Table 3.5: Observations from Polypropylene FBF under flaming conditions.

Sample Size:	167.4 mg
Residue:	47.4 mg (28.3%)
Time (min)	**Observations:**
2:15	Ignition
3:00	Flaming had ceased
Comments:	Some liquid remained, but failed to ignite

The SATVA trace for the volatilisation of the condensable degradation products is presented in Figure 3.7. The trapping during the degradation must have been colder than the usual -77°C as a peak can be seen at 5 minutes, indicating a trapped product of greater volatility than CO_2. It will be seen in this and the following chapters that the products produced under flaming conditions are dominated by CO_2 and water. This typically resulted in a two peak SATVA trace. There were only a few exceptions, such as this particular study, when more than two peaks were present in the SATVA trace. FT-IR analysis was used for peak identification. Peak 1 at 5 minutes was due to the evolution of ethylene and acetylene. The ethylene was identified by IR absorptions at 2900 to 3150 cm^{-1} and around 950, 1445 and 1890 cm^{-1}. The absorptions for acetylene were weaker, and seen at 730, 3312 and 3265 cm^{-1}. The spectrum was too weak to see the predicted additional bands at 1350 and 1305 cm^{-1}. The main gas peak at 15 minutes was predominately due to CO_2, as was seen through the FT-IR absorptions at 2360, 2342 and 720 cm^{-1}. The products forming peak 3 at 22 minutes were not unambiguously identified. The spectrum was confused by the presence of other products, including water and CO_2. There was some evidence of —CH_2 or —CH_3 symmetric and asymmetric stretching at 2800 to 3000 cm^{-1}. There was also a strong absorption at 1733 cm^{-1}, perhaps indicating an aldehyde or a diketone carbonyl. A reasonable match was dimethyl-1,2-diketone. Clearly the product

cannot be identified unambiguously. These findings are summarised in the following table:

Table 3.6: SATVA peak assignments from Figure 3.7

Peak	Assignment
1	Ethylene and acetylene
2	CO_2
3	Not unambiguously identified
4	Mainly water. See below for GC-MS of ether extract.

The liquid dominated liquid fraction had diethylether added to make an extract for GC-MS analysis. The TIC trace for the GC separation is presented in Figure 3.8. The peak assignments are listed in the following table:

Table 3.7: GC-MS peak assignments from Figure 3.8

Retention Time	Product	Retention Time	Product
0.59	Ethyl acetate	1.61	Isomers of 2,3,3-trimethyl-1,4-pentadiene, including substituted cyclohexenes
0.73	Benzene	1.82	2,6-dimethyl-3-heptene matched best, although not perfectly
0.78	Possibly 2-pentanone	2.05	(1 alpha.,2 beta.,4 beta.,) 1,2,4-trimethylcyclohexane. fitted best. Alternative substitutions cannot be disregarded
0.99	Possibly (E)-3-penten-2-one	2.13	Possibly 2-methyl-2-hepten-4-one
1.03	Unidentified aliphatic hydrocarbon	2.22	Possibly 2,4-dimethyl-1-heptene
1.26	Toluene	2.28	Unidentified aliphatic hydrocarbon
1.31	Possibly 2-methyl-3-hexyne, or a methylated diene of MW 96	2.33	Ethyl benzene, o- or p-xylene all possible
1.37	Unidentified aliphatic hydrocarbon	2.41	Trimethylcyclohexane. Unclear which isomer
1.44	Possibly 3-hexen-2-one	2.47	Ethyl benzene, o- or p-xylene all possible

Table 3.7 (continued)

Retention Time	Product	Retention Time	Product
2.65	3,3,5-trimethyl cyclohexene most likely. Isomers such as 2,4-dimethyl-2,4-heptadiene also possible (although less likely)	3.51	Possibly similar to (Z)-5-undecen-1-ol
2.73	Benzocyclobutane or styrene	3.69	Probably 4-methyl-2-heptanone
2.80	3,3,5-trimethyl cyclohexene most likely. Isomers such as 2,4-dimethyl-2,4-heptadiene also possible (although less likely). Very similar spectrum to 2.65	3.81	Benzaldehyde
2.84	Another of the xylene type spectra	4.28	Good match for 1,2,4-trimethylbenzene, isomers of 1-ethyl-?-methyl-benzene, or methylethylbenzene
2.99	3,3,5-trimethylcyclohexanone fits reasonably well		
3.16	Not unlike 3-methyl-(E)-2-pentene	4.46	Any one of the trimethyl-benzene isomers possible. (ethyl-methyl-benzene less likely)
3.26	Unsure. Spectrum similar to 2,3,4,5-tetramethyl-1,4-hexadiene 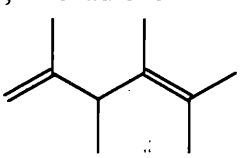	4.79	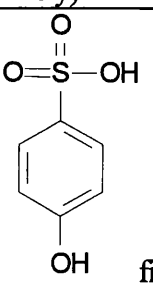 fits well. 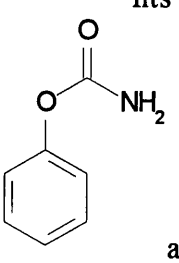 also possible

Table 3.7 (continued)

Retention Time	Product	Retention Time	Product
4.88	No database matches	10.62	A siloxane. Probably decamethylcyclopentasilo xane
4.99	Weak spectrum. Similar to 2-propenyl-benzene or ethenyl-methyl-benzene	12.00	Spectrum too weak to identify. No molecular ion
5.04	Weak spectrum. Possibly trimethyl-benzene, ethyl-methyl-benzene, or 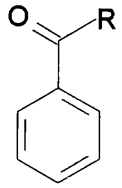 perhaps	14.22	Spectrum too weak to identify. No molecular ion
5.12	Weak. Not unlike 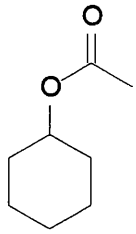	14.44	Spectrum too weak to identify. No molecular ion
5.52	Unidentified alkene	14.62	Spectrum too weak to identify. No molecular ion
6.05	Contaminant (a silicone)	14.71	Spectrum too weak to identify. No molecular ion
7.22	2-pentyl-phenol or 3,5-dimethylpyridine fit reasonably. Not certain	NOTE:	The last four spectra were of similar substituted cyclic alkenes
9.73	Naphthalene or azulene	15.48	A siloxane. Probably dodecamethylcyclohexa-siloxane
9.80	Not identified. Probably an aliphatic hydrocarbon	16.06	Spectrum too weak to identify. No molecular ion. An alkene perhaps

3.5 THERMAL DEGRADATION OF POLYPROPYLENE WAX

This sample was not studied in great detail. The main objective was to see if there were any unusual features regarding product composition or polymer stability.

3.5.1 Thermogravimetric Analysis

The TG traces obtained for dynamic nitrogen and air are shown in Figure 3.9, and are summarised in the following table:

Table 3.8: Key temperatures from thermogravimetry of Polypropylene Wax

Conditions	T_{thresh}(°C)	T_{end}(°C)	%Residue
Dynamic Nitrogen	200	430	3
Dynamic Air	170	460	1

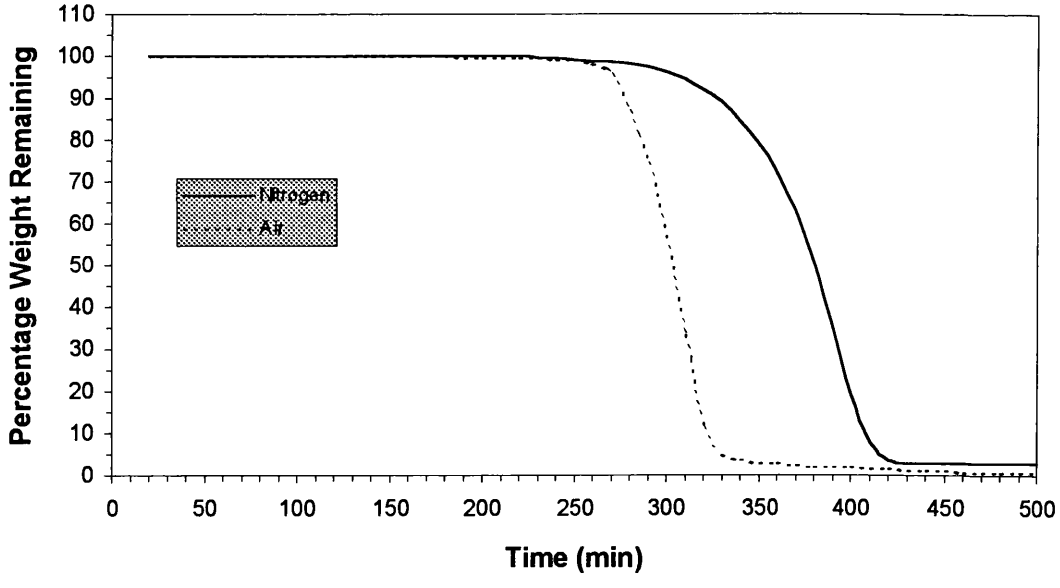

Figure 3.9: Thermogravimetric Analysis traces from Polypropylene Wax

The plot for degradation under dynamic air shows a reduced rate of weight loss immediately after T_{thresh}. This is probably due to oxidation of the sample, as was suggested for the Polypropylene FBF. It can also be seen that this sample displays

poorer stability, which is more probably due to a lack of stabiliser than the lower molecular weight.

3.5.2 Product Analysis — Dynamic Nitrogen

A temperature programme of 10°C/min up to 500°C was used. No residue remained. The resulting SATVA trace for the volatilisation of the condensable degradation products is presented in Figure 3.10. On one previous degradation there was an additional peak at 10 minutes. This peak was too small for a definite identification, but it may be supposed that it was due to propene by comparison with the degradation of polypropylene FBF. The products forming the peak at 20 minutes, which was a shoulder of the large liquid peak, were analysed by infrared spectroscopy. It appeared that 2-methylalk-1-enes of indeterminable length were present. The SATVA trace is clearly very similar to that obtained for the degradation of polypropylene FBF. Consequently this study was not carried any further.

3.5.3 Product Analysis — Dynamic Air

These studies were carried out with a temperature programme of 10°C/min up to 350°C. The residue remaining is compared with that from TG analysis below:

Table 3.9: Residue percentages from air degradation of Polypropylene Wax

	Weight Remaining	
Temperature	**Thermogravimetry**	**Flow tube**
350°C	3%	7%

This figures compare favourably, allowing for the errors experienced in the TG analyses. It has been suggested in Chapter 4 that the greater bulk of sample found in the flow tube apparatus leads to a larger residue than TG predicts. This sample, like

the other polymeric cases, was something of an exception as thermally stable residue formation was not favoured.

A sample SATVA trace for the volatilisation of the condensable degradation products is shown in Figure 3.11. Both infrared spectroscopy and mass spectrometry were used to identify the gaseous products. Peak 1 at 14 minutes was due to the evolution of CO_2. This was concluded by the IR absorptions at 2320, 720 and around 3610 and 3715 cm^{-1}. The second peak at 17 minutes was due to formaldehyde, as was seen through the absorptions at around 1745 cm^{-1} and around 2700 to 3000 cm^{-1}. Identification of the remaining gases was complicated as they did not separate cleanly from the liquid fraction of peak 3. The IR spectrum displayed characteristics consistent with acetone and some acetaldehyde or propionaldehyde. The predicted acetone absorptions at 1738, 2367, 1215 and 2970 cm^{-1} were all present. A small amount of acetaldehyde was also suggested by the absorptions at 1120, 1100, around 1400, 2700 to 2850 cm^{-1} and broadening of the acetone carbonyl band up over 1760 cm^{-1}. The CO_2, formaldehyde and acetone were all confirmed by mass spectrometry. These findings are summarised in the following table:

Table 3.10: SATVA peak assignments from Figure 3.11

Peak	Assignment
1	CO_2
2	Formaldehyde
Remainder	Mostly unstudied, but included acetone and acetaldehyde or propionaldehyde

3.5.4 Product Analysis — Flaming Conditions

The apparatus was arranged as described in Chapter 2. The observations made during the degradation are summarised in the following tables:

Table 3.11: Observations from Polypropylene FBF under flaming conditions

First Run	
Sample Size:	99.8 mg
Time (min)	**Observations:**
1:10	Sample melted into a single drop.
~3:00	The drop had spread out and was bubbling.
3:30	Ignition. Extinguished by 3:50.
4:30	Stopped.
Comments:	The planchet was sloping slightly, which meant that some of the melt dripped off during the burning stage.

Second Run	
Sample Size:	96.0 mg
Time (min)	**Observations:**
1:05	Sample melted.
2:30	Smoking started.
2:50	Ignition.
3:15	Extinguished. The melt continued to bubble for a few seconds.
5:00	Stopped.
Comments:	This time, the sample was not bubbling at the moment of ignition. The observation at 3:15 implies oxygen depletion.

The SATVA trace obtained for the volatilisation of the condensable degradation products are presented in Figure 3.12. Non-condensable trapping was used. This fraction was studied by FT-IR spectroscopy. Carbon monoxide was confirmed through absorptions at 2170 and 2116 cm^{-1}. It is clear that the SATVA trace is heavily overloaded. The thermocouple trace shows that the warming rate of the trap was reduced by the latent heat of sublimation or vaporisation of the gaseous products.

The products volatilised for the first 15 minutes of the SATVA separation were collected together for analysis by FT-IR spectroscopy. The spectrum was dominated by CO_2, as was seen through absorptions saturating at 670 and 2300 to 2400 cm^{-1}, along with the additional absorptions at 3728, 3706, 3625 and 2300 cm^{-1}. There was also formaldehyde present. This was seen through the distinctive absorptions at 2700

to 3000 cm^{-1} and at around 1745 cm^{-1}. The IR spectrum for the products present at the second half of the gas peak showed only the same products, with an increased amount of formaldehyde. The products forming the small peak before the main gas peak were not identified. On a repeat study of this degradation acetone and small traces of ethylene were also detected. The latter product may have produced the small peak at 5 minutes. The acetone was seen through IR absorptions at 1355, 1739, 1217 and 1970 cm^{-1}. The ethylene was suggested through a small absorption at 949 cm^{-1}. The other absorptions were masked by absorptions due to the other products present. These observations are summarised in the following table:

Table 3.12: SATVA peak assignments from Figure 3.12

Peak	Assignment
Non-condensables	CO
1	Mainly CO_2 with some formaldehyde, acetone and a little ethylene also detected.
2	Mainly water. See below for GC-MS of ether extract.

The products forming the second large peak were collected in a cold finger. This fraction had the appearance of being mainly water, with small droplets of non-aqueous material also present. This was typical for the liquid fraction obtained for degradation under flaming conditions. Diethylether was used to form an extract for GC-MS analysis. This provided the TIC trace shown in Figure 3.13. The peak assignments are presented in the following table:

Table 3.13: GC-MS peak assignments from Figure 3.13

Retention Time	Product	Retention Time	Product
1.73	Small O-containing hydrocarbon, like 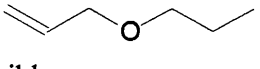 Possibly some 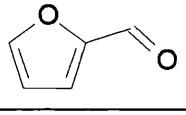 co-eluting	1.85	Silicone contaminant

Table 3.13 (continued)

Retention Time	Product	Retention Time	Product
2.05	Silicone contaminant	2.77	Styrene, or the usual bicyclo alternative
2.15	Probably 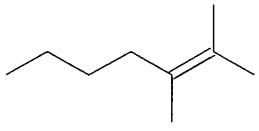	2.82	Looks like 3,3,5-trimethylcyclohexene again
2.25	2,4-dimethyl-1-heptene, 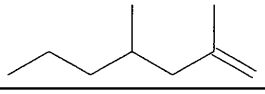	2.86	Xylene
2.34	Xylene	3.02	Probably 2,4,6-trimethyl-3-heptene 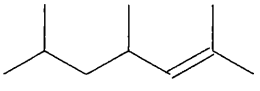 , with 3,3,5-trimethylcyclohexanone possible but less likely
2.47	Xylene	3.19	Unidentified. Probably a substituted aliphatic cyclic hydrocarbon.
2.52	Phenylethyne 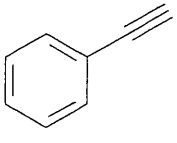 co-eluting with a little xylene	3.29	Unidentified. Probably a substituted aliphatic cyclic hydrocarbon.
2.63	Probably 4-methyl-3-hepten-2-one, 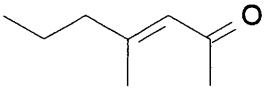	3.54	Possibly cyclohexyl ester 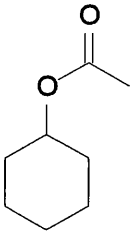 acetic acid
2.67	Probably 3,3,5-trimethylcyclohexene, 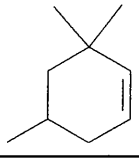	3.74	4-methyl-2-heptanone 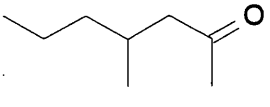

Table 3.13 (continued)

Retention Time	Product	Retention Time	Product
3.86	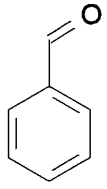 Benzaldehyde	6.10	Silicone contaminant
4.27	Unidentified. Probably a silicone contaminant	6.51	4-methylbenzaldehyde 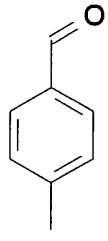
4.80	Phenol	9.75	Naphthalene
4.90	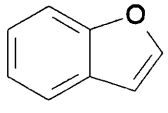 Benzofuran	10.60	Silicone contaminant
4.99	4,6-dimethyl-2-heptanone 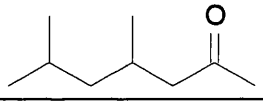	11.10	Silicone contaminant
5.06	Trimethyl- or methylethyl-benzene	15.45	Silicone contaminant
5.94	Silicone contaminant	16.61	Acenaphthylene 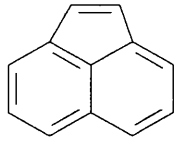 or biphenylene 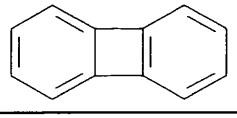

3.6 THERMAL DEGRADATION OF POLYESTER DNOP 43

Section 3.3 describes the limited information provided on this sample. The thermal stability was studied by thermogravimetry. The sample was also degraded for product analysis under dynamic nitrogen, dynamic air and flaming conditions.

3.6.1 Thermogravimetric Analysis

The TG traces obtained under nitrogen and air are presented in Figure 3.14. A heating rate of 10°C/min was used here and for all other temperature programmed degradations. The important temperatures are tabulated below:

Table 3.14: Key temperatures from thermogravimetry of Polyester DNOP 43

Conditions	T_{thresh}(°C)	T_{end}(°C)	%Residue
Dynamic Nitrogen	315	425	4
Dynamic Air	270	500	2

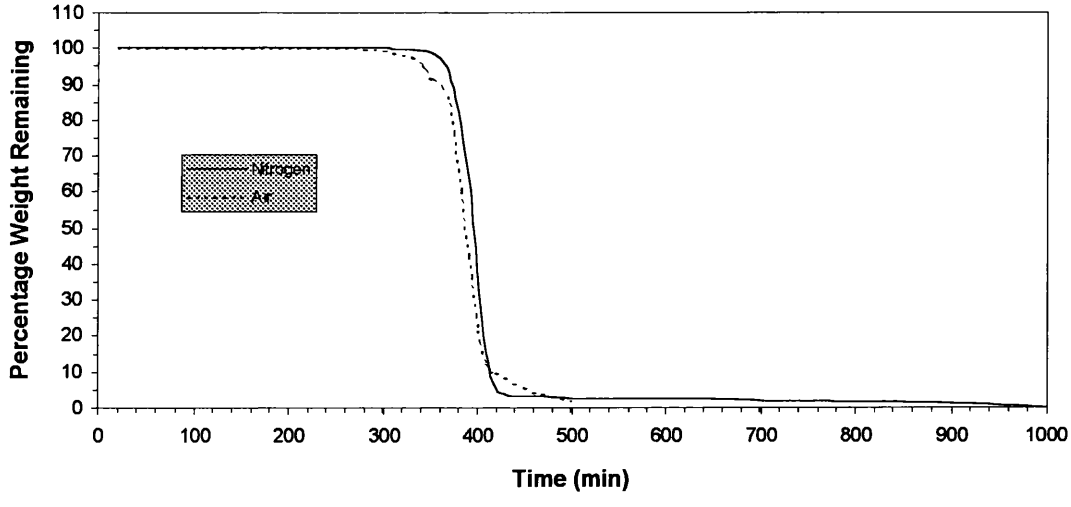

Figure 3.14: Thermogravimetrc Analysis traces from Polyester DNOP 43

It can be seen that the onset of weight loss was earlier under air. The profiles of the traces were nearly identical by around 400°C, suggesting that there was a stage in the degradation uninfluenced by the oxygen in the air. This implies that the air degradation

is a multi-stage process, although the trace has the appearance of having a single stage. It may also be seen that the end of the air study has a reduced rate of weight loss.

3.6.2 Product Analysis — Dynamic Nitrogen

This degradation was initially performed using programmed heating to 435°C, and subsequently repeated twice to a maximum temperature of 600°C. The higher temperature was used as an unexpectedly large residue was obtained at the lower temperature. This was probably due to either a time delay for the sample in the flow tube to reach the oven temperature, or because of the larger sample size in the flow tube. The differences in the percentage weight of residue obtained are shown in the following table:

Table 3.15: Residue percentages from nitrogen degradation of DNOP 43

	Weight Remaining	
Temperature	**Thermogravimetry**	**Flow tube**
435°C	4%	30.6%
600°C	4%	2.7%

No new products were observed at the higher temperature. A typical SATVA trace for the volatilisation of condensable degradation products obtained is shown in Figure 3.15. The products volatilised to form peaks 1 and 2 at 8 and 14 minutes were collected together for analysis by infrared spectroscopy. This spectrum only showed the absorptions for butadiene. The mass spectrometer showed a weak response for CO_2 during the first peak. This also showed the third and final peak to be dominated by water, although there was a weak response for benzene. No GC-MS data were obtained from the liquid fraction for this sample. These findings are summarised in the following table:

Table 3.16: SATVA peak assignments from Figure 3.15

Peak	Assignment
1	CO_2
2	Butadiene
3	Mainly water with some benzene

3.6.3 Product Analysis — Dynamic Air

The sample was degraded at a heating rate of 10°C/min up to a maximum of 510°C. The TG curve indicated that this temperature marked the end of the degradation. There was no residue present from the initial degradation, and a very small amount on a subsequent study.

A SATVA trace for the volatilisation of condensable degradation products is presented in Figure 3.16. Peak 1 at 10 minutes was due to the evolution of CO_2. This was observed by the previously quoted infrared absorptions, and mass spectrum peaks at m/e = 44, 28, 12 and 16. The products from peaks 2 and 3 were collected together for study by FT-IR spectroscopy. This revealed many absorptions, primarily associated with various C—H and carbonyl environments. The presence of formaldehyde was deduced from absorptions at 2650 to 3050 cm^{-1}, around 1745 cm^{-1} and at 1502 cm^{-1}.

Table 3.17: SATVA peak assignments from Figure 3.16

Peak	Assignment
1	CO_2
2 and 3	Formaldehyde with other products, possibly including propionaldehyde and butadiene.
4	Mainly water. See below for further analysis.

The products forming peak 4 were collected together in a cold finger. Diethylether was added to form an extract for GC-MS analysis. The TIC trace for the GC separation is shown in Figure 3.17. The peak assignments are provided in the following table:

Table 3.18: GC-MS peak assignments from Figure 3.17

Retention Time	Product	Retention Time	Product
2:46	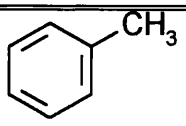	8:05	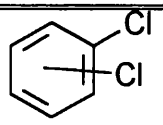 (contaminant)
3:07 3:34	Unidentified hydrocarbon	8:16	No matches. Probably a substituted aromatic.
4:06	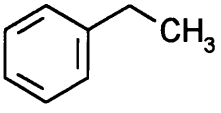 or 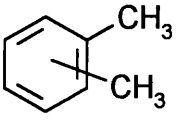	8:43	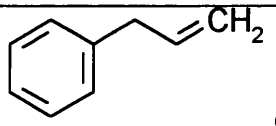 or isomers
4:54	Perhaps styrene	9:04	No matches
5:36 6:03 6:35	Unidentified hydrocarbon	9:15	Good match with 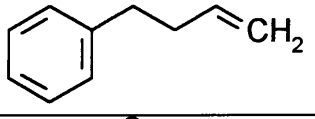
6:51	Probably 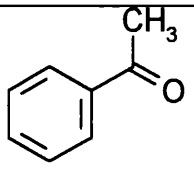	9:47	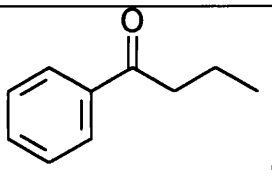 or 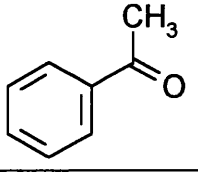
7:49	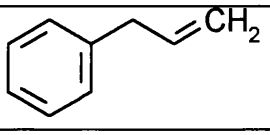	10:13	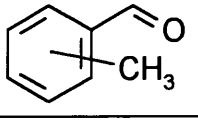

Table 3.18: (continued)

Retention Time	Product	Retention Time	Product
10:40	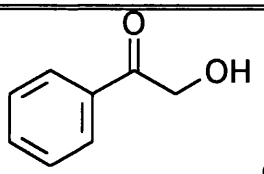 or 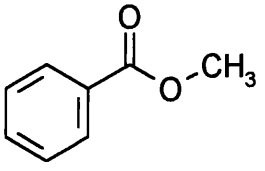	15:28	No definite matches. Perhaps structurally similar to 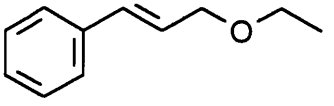
12:37	No matches	15:39	No matches
12:59	similar spectrum to 9:47 and 10:40, perhaps due to 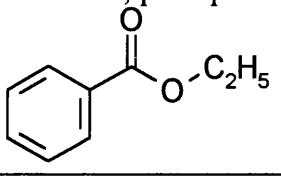	15:49	Spectrum similar to 9:47, 10:40 and 12:59. Perhaps the ethyl- group has been replaced with a butyl-
13:15	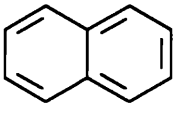	18:19	Very good match with 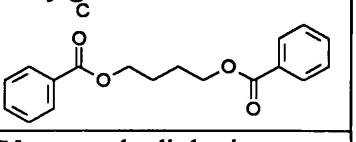
13:41	No matches	20:01	Very weak aliphatic hydrocarbon spectrum

3.6.4 Product Analysis - Flaming Conditions

The apparatus was arranged as was described in the previous chapter. The observations made during the degradation are summarised in the following tables:

Table 3.19: Observations from DNOP 43 under flaming conditions

First Run	
Sample Size:	326.1 mg
Time (min)	**Observations:**
1:15	Melting started. Opaque.
2:15	Formed single clear drop.
3:40	Ignition. Burnt for 5-8s.
4:40	Residue started to char.
5:00	Charring complete
6:30	Heater switched off.
Comments:	There was much smoke produced. Oxygen starvation may have occurred.

Table 3.19: (continued)

Second Run	
Sample Size:	93.7 mg
Residue:	3.7 mg (3.9%)
Time (min)	**Observations:**
5:15	Ignition. Burnt for 5 seconds.
6:30	Heater switched off.
Comments:	Discoloured before ignition.

A sample of the SATVA trace obtained for the volatilisation of the condensable degradation products is presented in Figure 3.18. Non-condensable trapping was also used during the degradation. FT-IR analysis of this fraction revealed four products. CO absorptions were observed at 2168 and 2127 cm^{-1}. Methane was indicated by absorptions at 1305 cm^{-1} and around 3017 cm^{-1}. There were weak absorptions at around 950 cm^{-1} suggesting ethene, and at 731, 3314 and 3268 cm^{-1} implying acetylene. The first peak on the SATVA trace at 6 minutes was due to the evolution of ethene and acetylene. This was observed through the same FT-IR absorptions as listed for the non-condensables study. It would appear that these components were only partly condensed in the trap on the degradation apparatus. The products forming the main gas peak and the peak at 30 minutes were collected together for study by FT-IR spectroscopy. This fraction contained mainly CO_2, as was seen by the usual absorptions. Formaldehyde was also observed through the characteristic absorptions at 2650 to 3000 cm^{-1} and at around 1745 cm^{-1}. It may be supposed that this latter product formed peak 3 at 30 minutes. These findings are summarised in the following table:

Table 3.20: SATVA peak assignments from Figure 3.18

Peak	Assignment
Non-condensables	CO, methane, ethene, acetylene
1	Acetylene and possibly some ethene
2 and 3	Mainly CO_2. Also a small amount of formaldehyde
4	Mainly water. See below for GC-MS of ether extract

The products from 32 minutes onwards were collected together in a cold finger. This fraction had the appearance of water with droplets of non-aqueous material also present. Diethylether was added to the liquid fraction to provide a non-aqueous extract for study by GC-MS analysis. The TIC trace from this study is shown in Figure 3.19. The peak assignments are given in the following table:

Table 3.21: GC-MS peak assignments from Figure 3.19

Retention Time	Product	Retention Time	Product
1.90	Benzene	6.40	Indene or 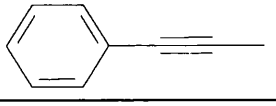
2.60	Toluene	6.55	Contaminant (decamethylcyclopentasiloxane)
3.52	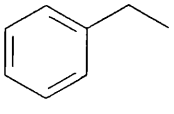 or (less 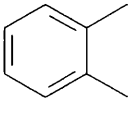 likely)	7.85	Phenol
4.00	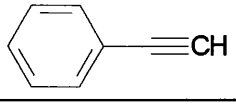	8.80	Naphthalene
4.10	Styrene or 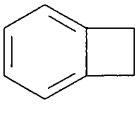	11.55	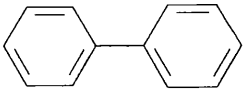 fits best, although it could be 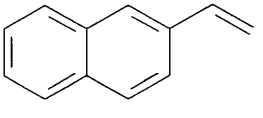
4.40	Contaminant (octamethyl-cyclotetrasiloxane)	12.80	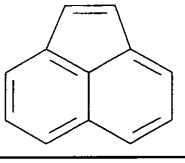
5.85	Probably 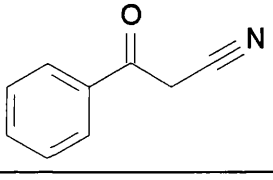		

3.7 MAJOR PRODUCT SUMMARIES AND MECHANISMS

The major products detected from the degradation of the polymer samples are presented in this section. Work has been performed in the past on the polymers studied, so only a brief summary is provided here.

3.7.1 Polypropylene FBF and Polypropylene Wax

These samples were structurally similar. The only difference cited was that the wax was of lower molecular weight. This was the reason that the two studies are presented together.

3.7.1.1 Dynamic Nitrogen

This degradation was performed under programmed heating at 10°C/min to 500°C. This temperature was well beyond the end of the degradation, as seen from the thermogravimetric analysis result. Little work was done on the wax. The SATVA traces between the two samples were very similar, although the first major gas peak was absent for the wax. It was, however, observed from the thermogravimetric analysis trace that the wax decomposed at a lower temperature. This suggested that either there was some stabiliser present in the Polypropylene FBF, or that the lower molecular weight promotes the degradation. It is also possible that the methods of polymerisation differed between the two samples. Differences in the initiator can influence the degradation.

Isobutene was the main gas detected for the FBF sample, although the corresponding peak was absent in the SATVA trace for the wax. There was also a small amount of propene, perhaps because there was only a small amount produced or because the trap on the degradation apparatus was too warm to condense it completely. The liquid

fraction appeared to be composed of other aliphatic hydrocarbons. A detailed analysis was not performed.

Different studies on polypropylene degradation have resulted in variations in the products evolved and their relative proportions[40-43]. Changes in the heating conditions, sample size and atmosphere (vacuum or inert gas), all appear to affect the degradation. A typical result was to have 2,4-dimethyl-1-heptene, 2-pentene, propene, 2-methyl-1-pentene and isobutene among the major products. The findings from the study here were clearly somewhat limited, but the products found were all predicted. A more detailed product analysis can be found in Chapter 8, where the colourant had been added to the polymer. The other predicted products were all present, with the exception of 2-pentene.

3.7.1.2 Dynamic Air

The wax and the FBF samples were heated to 350°C and 360°C respectively. The SATVA traces obtained for these samples were very similar with only small changes in intensity of some of the peaks. The gaseous products detected were also very similar. Liquid fraction analysis was not available for the wax sample.

Carbon dioxide, formaldehyde and acetone were all detected as gases. The wax also produced some acetaldehyde or propionaldehyde. The mass spectra from the GC-MS analysis of the liquid fraction non-aqueous extract from the FBF sample were not very clear. It was however apparent that the major products were 2,4-dimethylhept-1-ene and the corresponding ketone 4-methyl-2-heptanone. The alkene was predicted above, and could have been produced in the absence of oxygen. The ketone was a predicted product for thermal degradation under air.

The TG trace showed that there was oxidation before the onset of weight loss. It seems reasonable to suppose that this oxidation follows the same mechanism as that documented for polypropylene under processing[44]. This oxidation pathway is illustrated in Scheme 1.

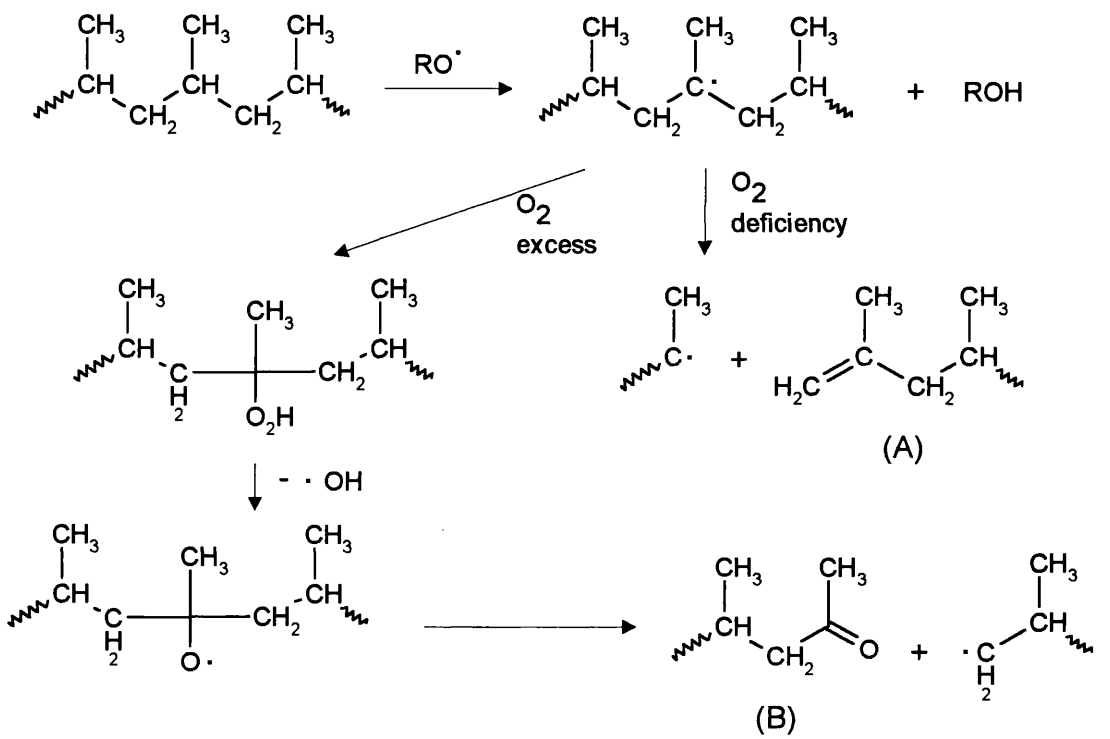

Scheme 1: Chain scission in PP during processing

The source of alkenes can be seen from (A) in the scheme, and the ketone source from (B). The favourable points on the chain for the formation of the radical are the tertiary hydrogens. This explains why the alkenes are 2-methyl alkenes, and the lack of aldehydes among the products.

3.7.1.3 Flaming Conditions

Some differences between the behaviour and the products from the wax and FBF samples were observed for the degradation under flaming conditions. The time to ignition was quite different. The wax ignited at an average of slightly over 2 minutes after the blocker was turned, whereas the FBF took only just over 1 minute from exposure to the heater. There were also some differences in the products.

CO_2 and water were by far the major products in both cases. Formaldehyde, acetone and ethylene were also detected from the wax, and ethylene with a little acetylene from the FBF. The polypropylene wax liquid fraction contained naphthalene along with the ketone and alkene described in section 3.7.1.2 in equal ratios. Benzaldehyde was also present. The polypropylene FBF produced toluene, the same alkene and either the same ketone or an isomer. The remaining products were mainly methylated alkenes and some ketones.

The hydrocarbon products were observed in the dynamic air and nitrogen studies. It may be concluded that the hydrocarbons were volatilised from the sample an ignited when the necessary mass flux was obtained. These samples would appear to follow the candle model for the combustion of polymers.

3.7.2 Polyester DNOP 43

It has been explained in section 3.1 that little information was available on the structure of this sample. It was known that it was probably a blend or copolymer of PET and PBT. It will be seen in the following sections that the degradation products were more in accord with those expected for PBT.

3.7.2.1 Dynamic Nitrogen

This degradation was performed under programmed heating at 10°C/min to 600°C. This temperature was chosen as preliminary studies to the end of degradation from the TG curve (435°C) left a residue much larger than predicted. Comparison of the TG curve obtained in this study with the literature[45] yielded some more information on the nature of this sample. The onset of weight loss was roughly consistent with either PET or PBT. However PET is expected to have around 20% weight remaining at 450°C, whereas PBT leaves only a very small amount of residue (<5%).

Butadiene was the major gas evolved on degradation under dynamic nitrogen. Some CO_2 was also produced. Much water was detected in the liquid fraction, along with benzene. The GC-MS of the liquid fraction was dominated with silicone contaminants.

Butadiene is not a predicted major product from PET degradation, but is expected from PBT[45]. Carbon dioxide is expected from either PET or PBT. The mechanism accompanying these predictions are shown in scheme 2.

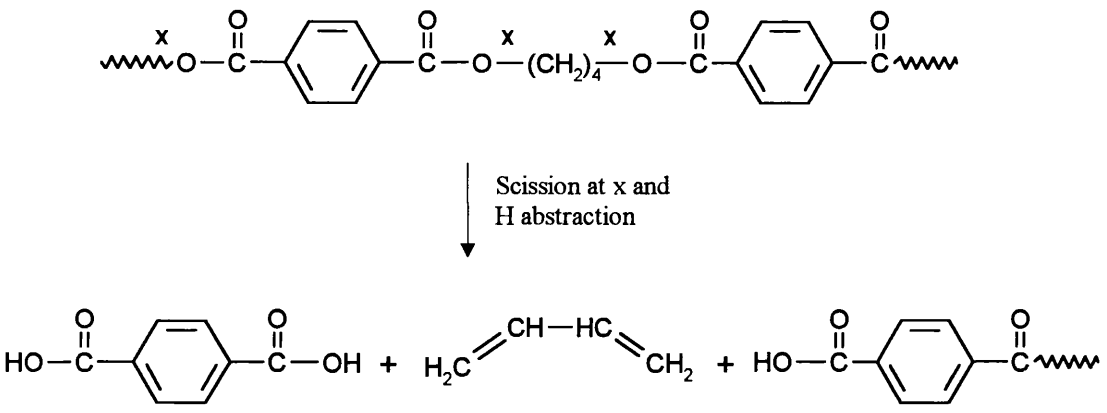

Scheme 2: Formation of butadiene

The mechanism of formation of CO_2 and benzene may involve the decomposition of the terephthalic acid. An alternative pathway is through the scissions of the polymer illustrated in scheme 3.

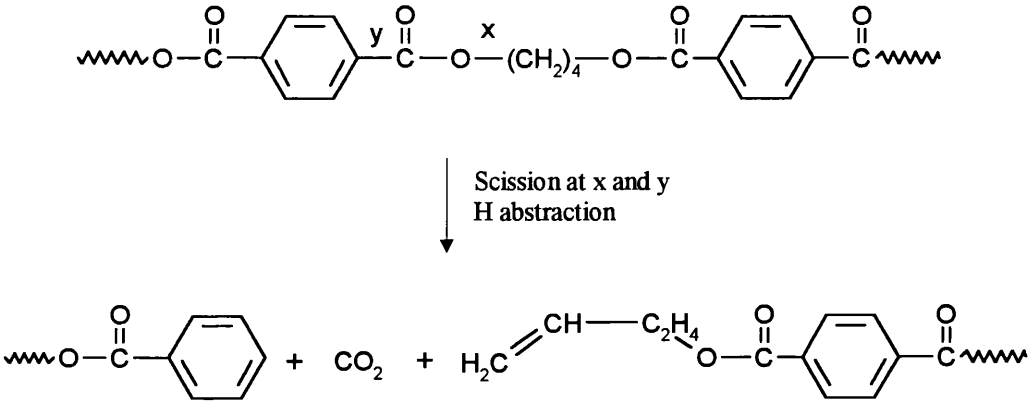

Scheme 3: Formation of carbon dioxide

These two processes account for all three of the major products.

3.7.2.3 Dynamic Air

This degradation was performed under programmed heating at 10°C/min to 500°C. Only a small amount of residue was remained. This was consistent with the results obtained from TG analysis. The TG curve obtained under dynamic air differed only slightly from that under dynamic nitrogen. A slightly earlier onset of weight loss was followed by the major weight loss closely following the dynamic nitrogen curve, at a lower temperature of only 10°C. It was apparent from the products that the mechanism of degradation must have been more complicated than that illustrated for dynamic nitrogen in schemes 2 and 3.

The major gas produced was CO_2. There was also much formaldehyde evolved. In addition there was also some propionaldehyde and butadiene detected. There was much water in the liquid fraction. The major non-aqueous component of the liquid fraction was an unidentified alkene. There was also much ethylbenzene or xylene, styrene and 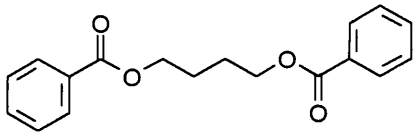 (ester A) detected, along with a lesser amount of toluene. There were also three products of the form 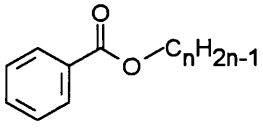 (ester B).

Styrene often arises in these studies as a contaminant. This could be due to a long residence time in the vacuum system, or from the injection port of the GC-MS analyser. The GC-MS instrument used in this study often failed to detect more volatile liquid products. This meant that benzene may have been present, but was not observed.

Products such as ester A and ester B show that the bond between the aromatic ring and the carbonyl group can be broken during the degradation. If this were to occur at both substitutions on the ring then benzene would be a predicted product. It can be seen in the following section that benzene was detected once more under flaming conditions.

The products of the type ester B show that the C_4 aliphatic sections of the polymer can undergo scission at any point along their length. The xylene and toluene detected initially implied that the carbon from the carbonyls could remain attached to the aromatic ring while the carbonyl oxygen was lost. Although this process may not be eliminated, it should also be noted that there were aromatics observed with aliphatic substitutions of length greater than C_1 but no longer than C_4. This implies some kind of transfer from the aliphatic section of the polymer backbone.

The formaldehyde may have been produced directly from scissions of the chain at each side of the carbonyl, followed by hydrogen abstraction. Once again this cannot be ruled out, but it does not explain the detection of propionaldehyde. This product adds additional support to the theory that scission is occurring within the aliphatic hydrocarbon section of the backbone. This may follow a mechanism similar to that described for polypropylene in scheme 1. This polymer does not have the methyl pendants to provide a favoured site for the initiating hydrogen abstraction. Following through the mechanism shows that this would produce aldehydes in this case rather than the ketones for polypropylene.

The butadiene detected here implies that the mechanisms suggested in scheme 2 and scheme 3 were still applicable for this degradation. It is clear that several competing degradation pathways were active in this particular study.

3.7.2.4 Flaming Conditions

This sample was slow to ignite. On first study the 326.1 mg sample ignited at 3 minutes 40 seconds then burned for 5 to 8 seconds. On the repeat study the smaller 93.7 mg sample took over 5 minutes to ignite, then burned for 5 seconds. In both cases the sample was masked from the heater for the first minute.

The major products from this degradation were CO_2 and water. Other gases detected were acetylene, formaldehyde, ethane, methane and carbon monoxide. The non-aqueous extract of the liquid fraction had benzene as the major component. There was also much phenol and naphthalene. Lesser amounts of styrene, toluene and perhaps biphenyl were also detected.

These were the only conditions under which the sample was degraded where non-condensables could be analysed. This means that the more volatile gases may have been evolved under the other conditions, but were not observed. The source of these materials may have been the decomposition of the aliphatic section of the polymer backbone. Alternatively, they may have been products of the incomplete combustion of the flammable products described in the preceding two sections.

Some naphthalene was detected as a minor product under dynamic air. There is clearly no obvious pathway for the formation of this product. The mechanism for the formation of the phenol is also unclear. The benzene ring from the polymer was the

probable source of the aromatic ring in the phenol. The source of the hydroxyl group is a mystery. Perhaps an RO· radical combined with a benzyl radical left by the cleavage of the carbonyl from the ring. This could be followed by a further scission and a hydrogen abstraction to form the phenol. Any biphenyl may have been formed by the combination of two benzyl radicals.

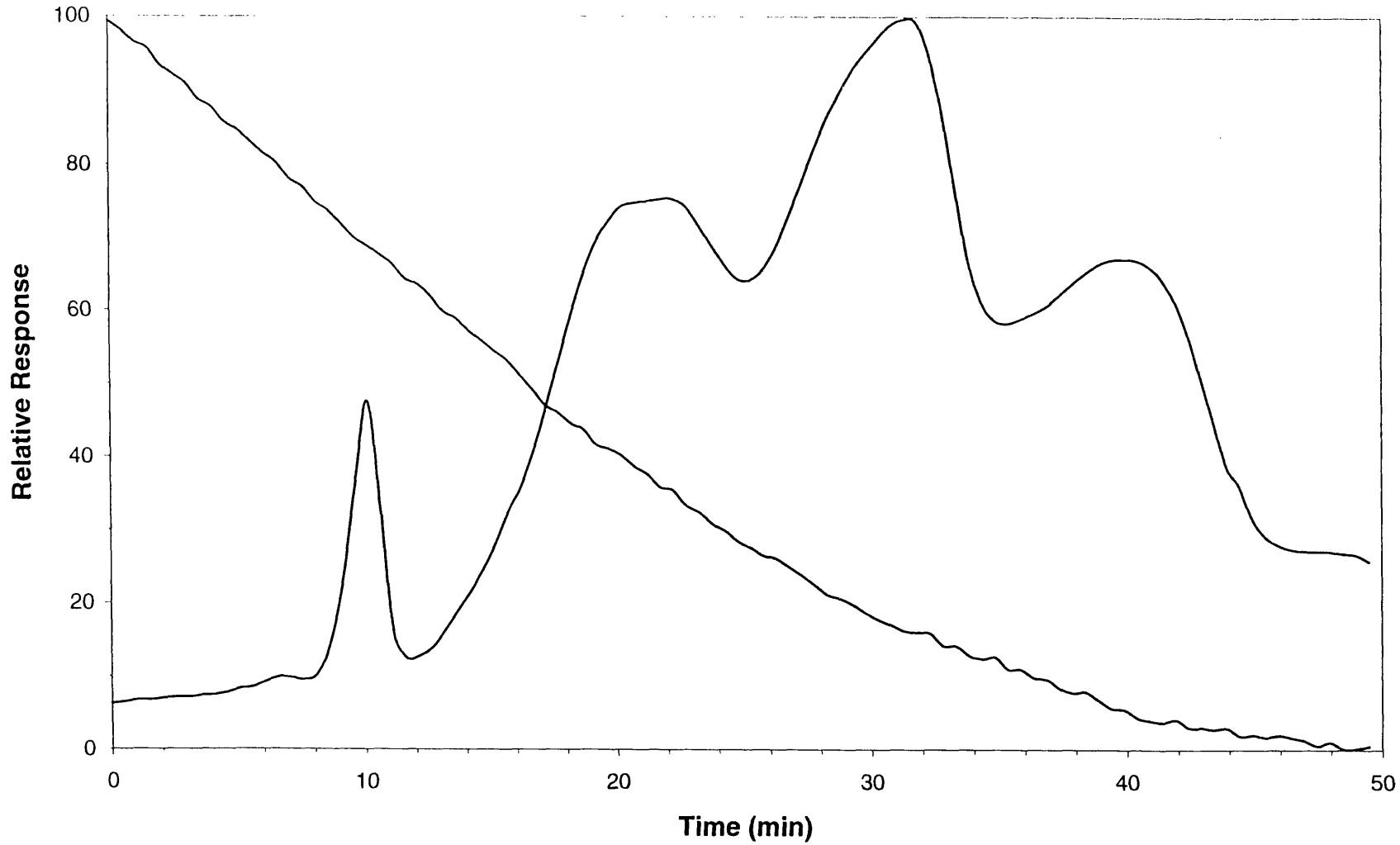

Figure 3.4: SATVA trace from the degradation of Polypropylene FBF under dynamic nitrogen

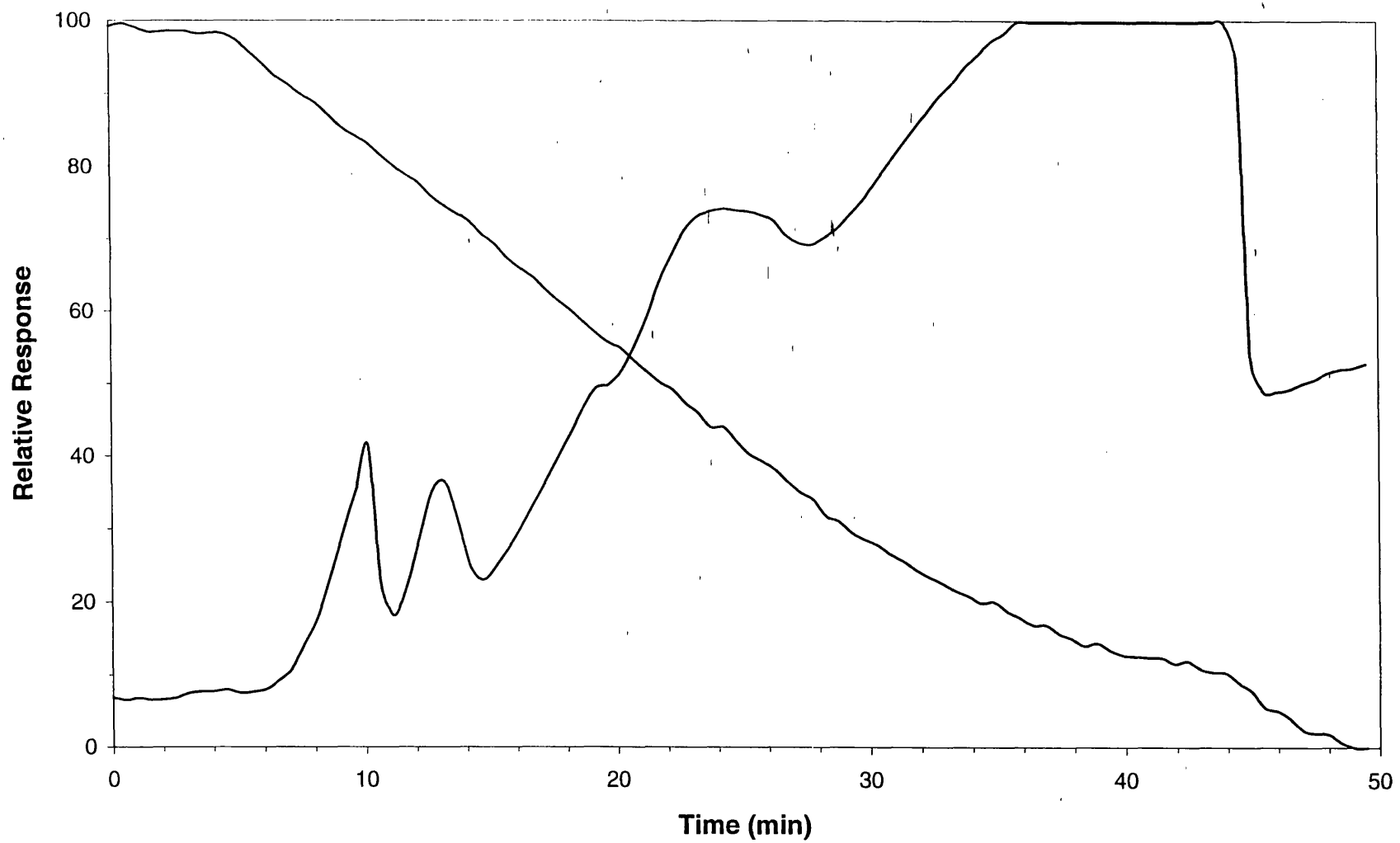

Figure 3.5: SATVA trace from the degradation of Polypropylene FBF under dynamic air

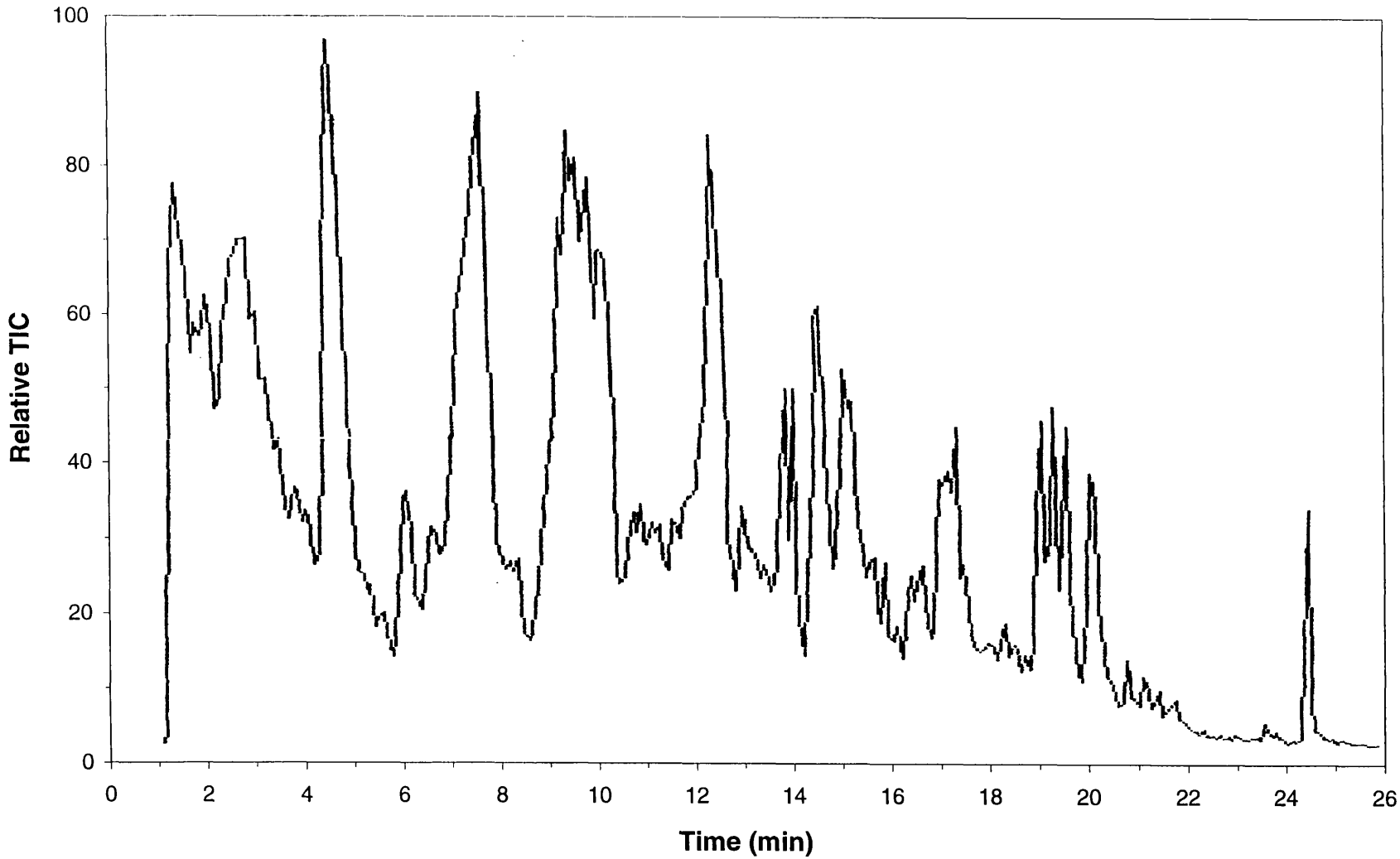

Figure 3.6: TIC trace for the liquid fraction from the SATVA curve in Figure 3.5

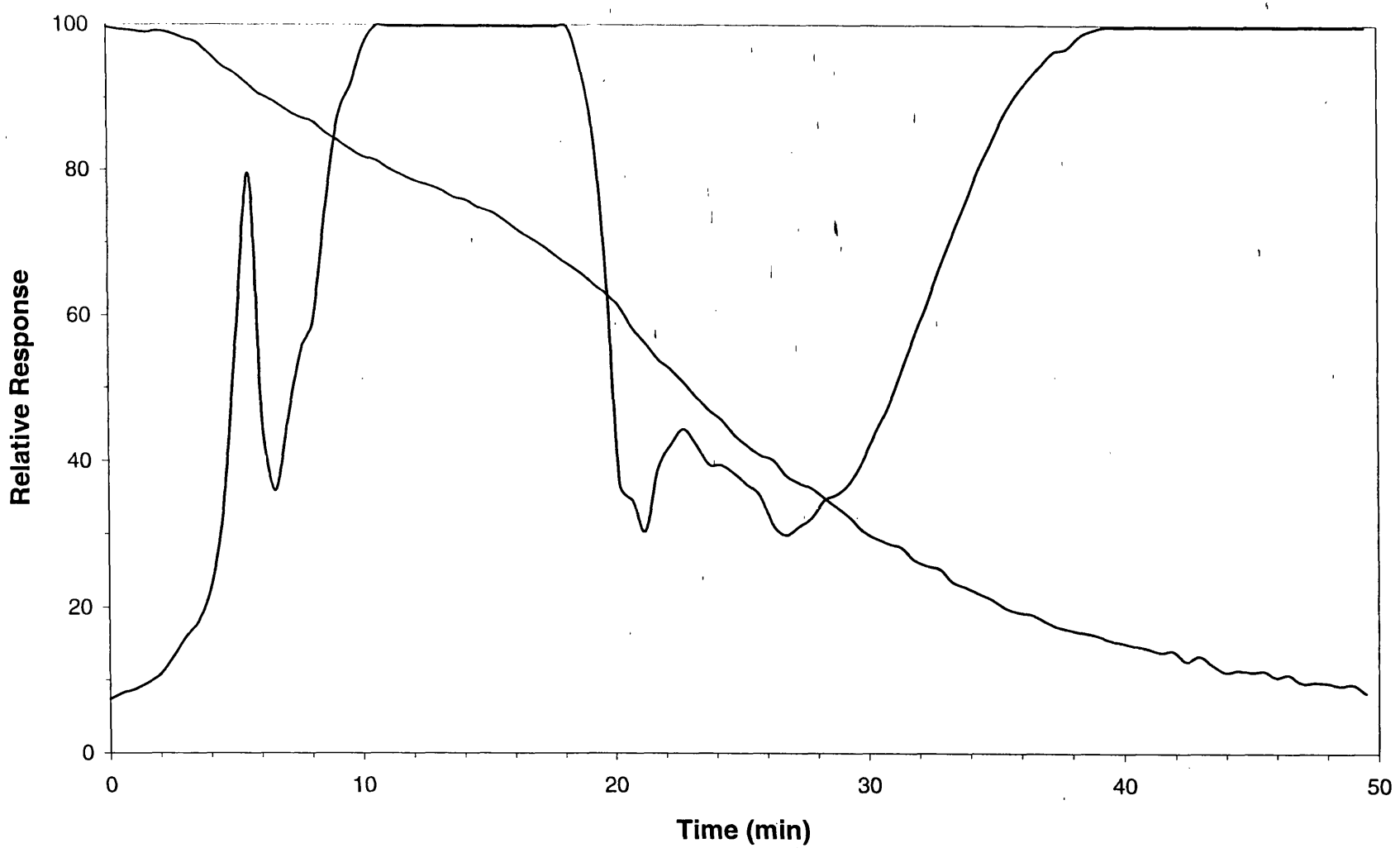

Figure 3.7: SATVA trace from the degradation of Polypropylene FBF under flaming conditions

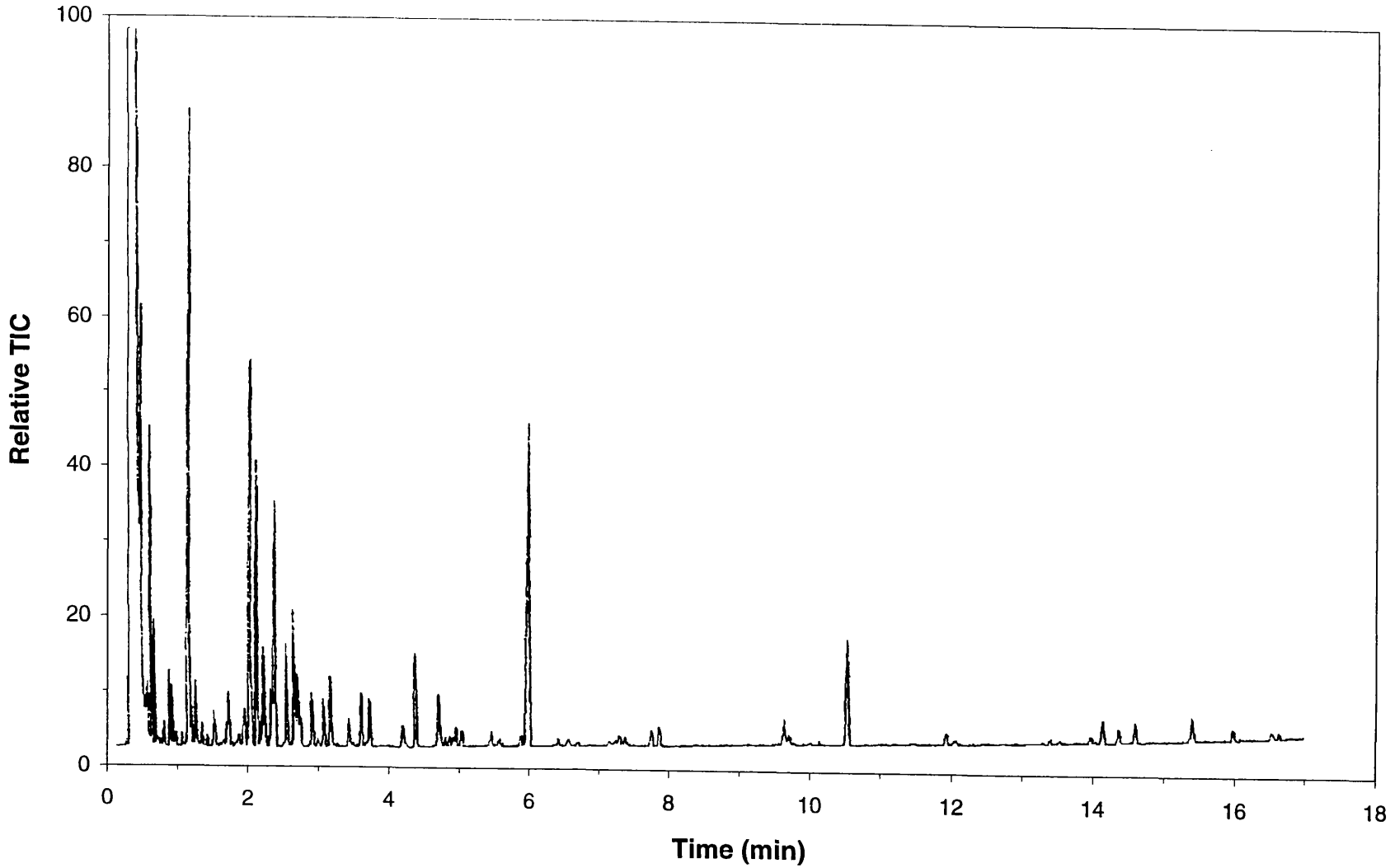

Figure 3.8: TIC trace for the liquid fraction from the SATVA curve in Figure 3.7

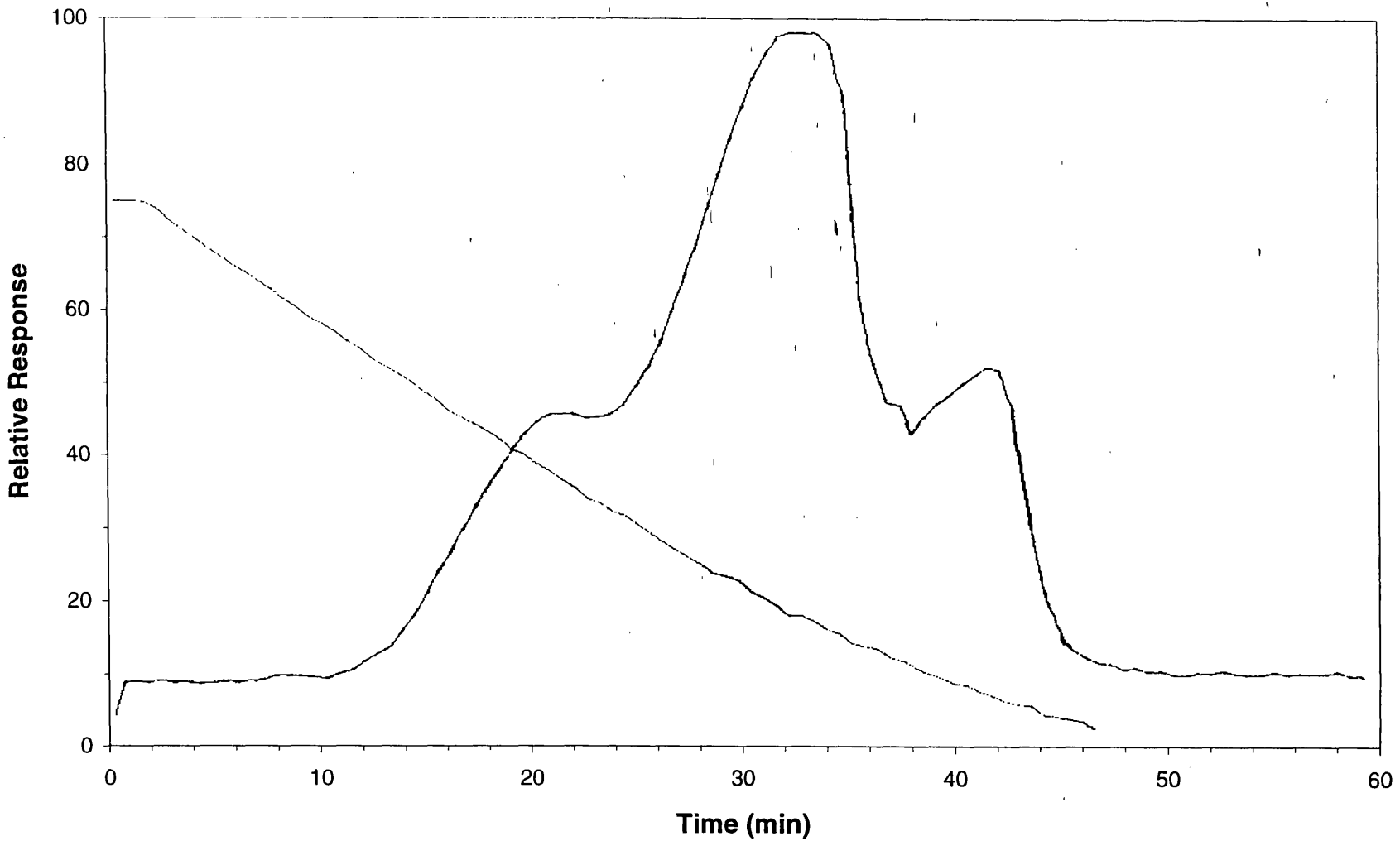

Figure 3.10: SATVA trace from the degradation of Polypropyene Wax under dynamic nitrogen

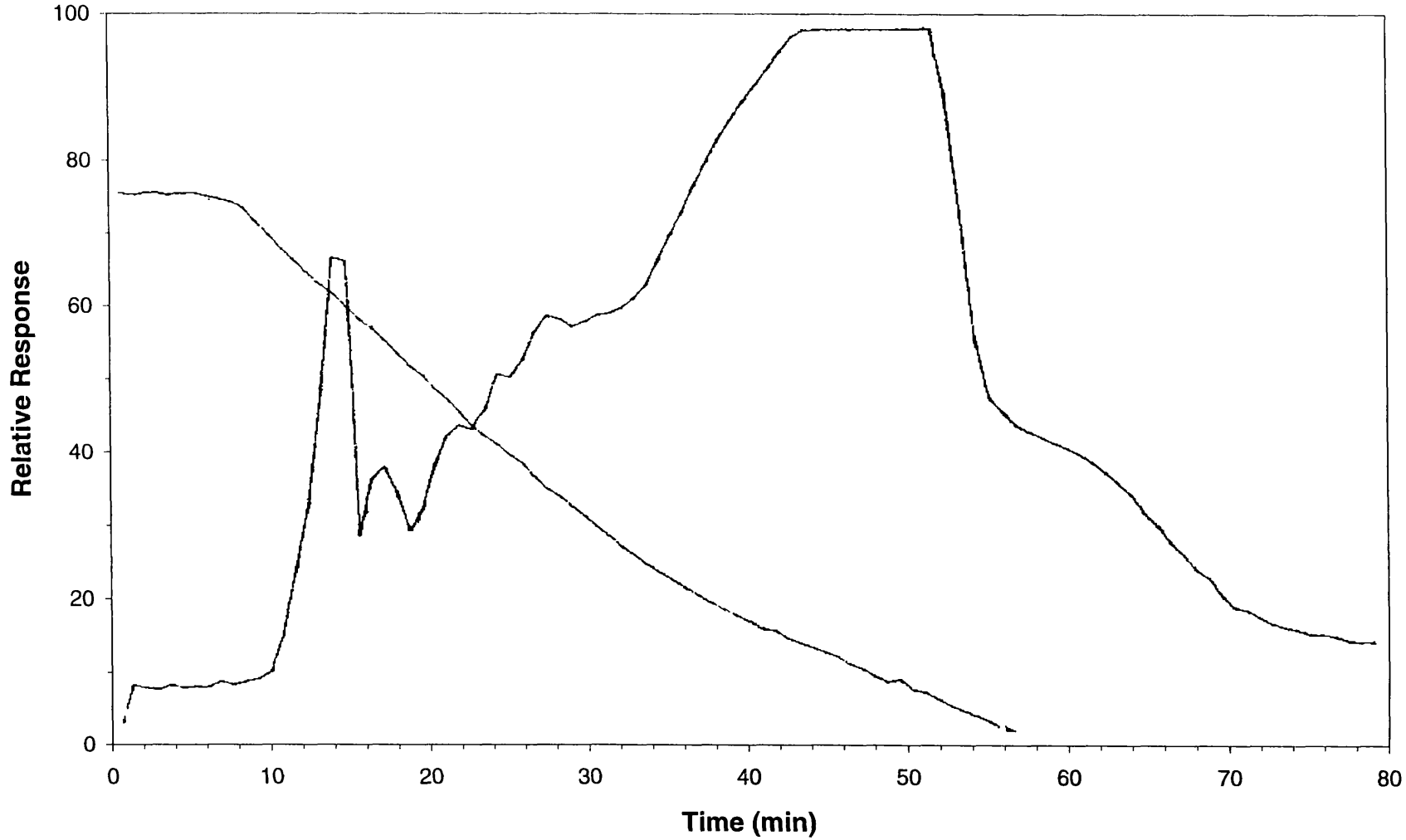

Figure 3.11: SATVA trace from the degradation of Polypropylene Wax under dynamic air

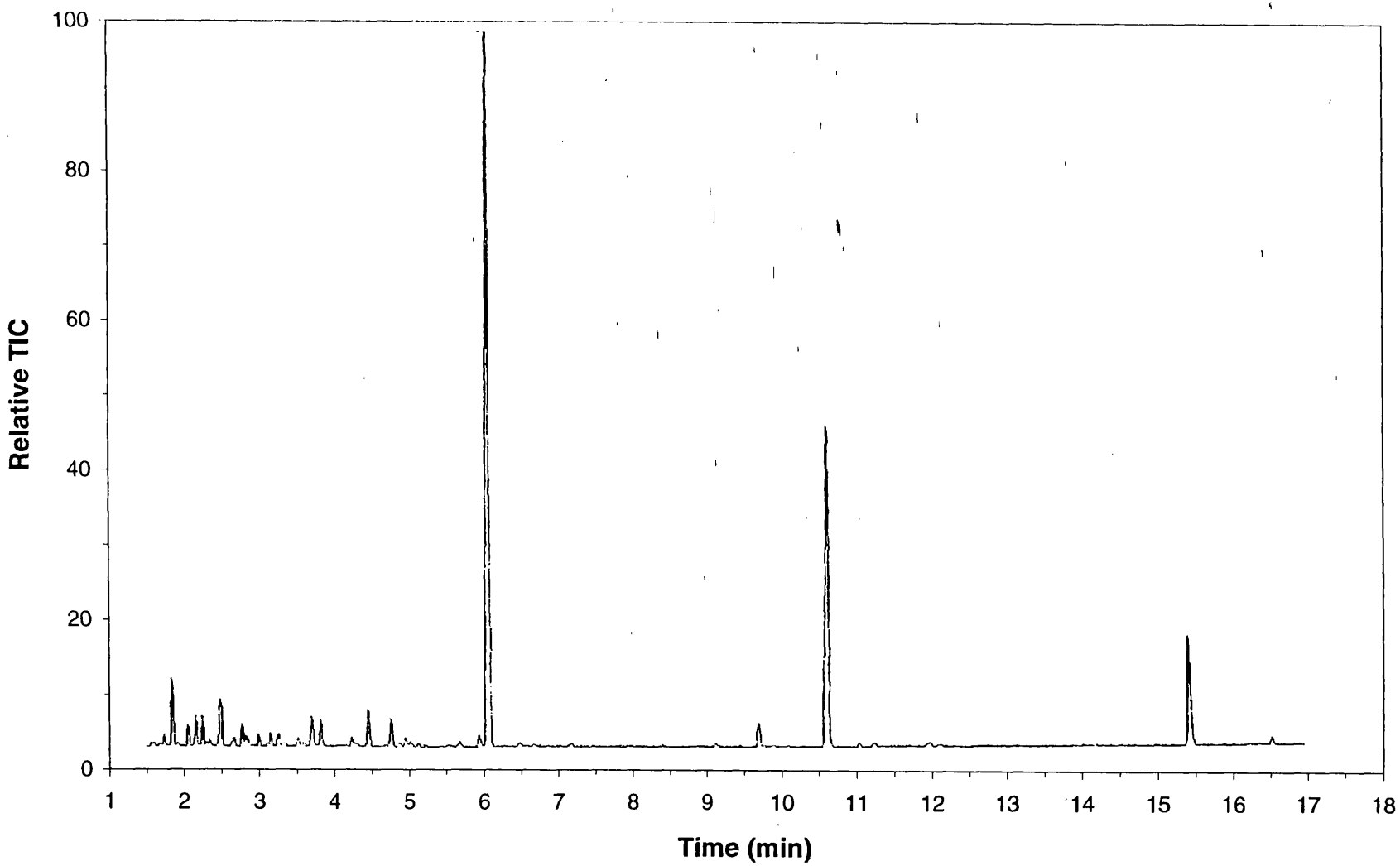

Figure 3.13: TIC trace for the liquid fraction from the SATVA curve in Figure 3.12

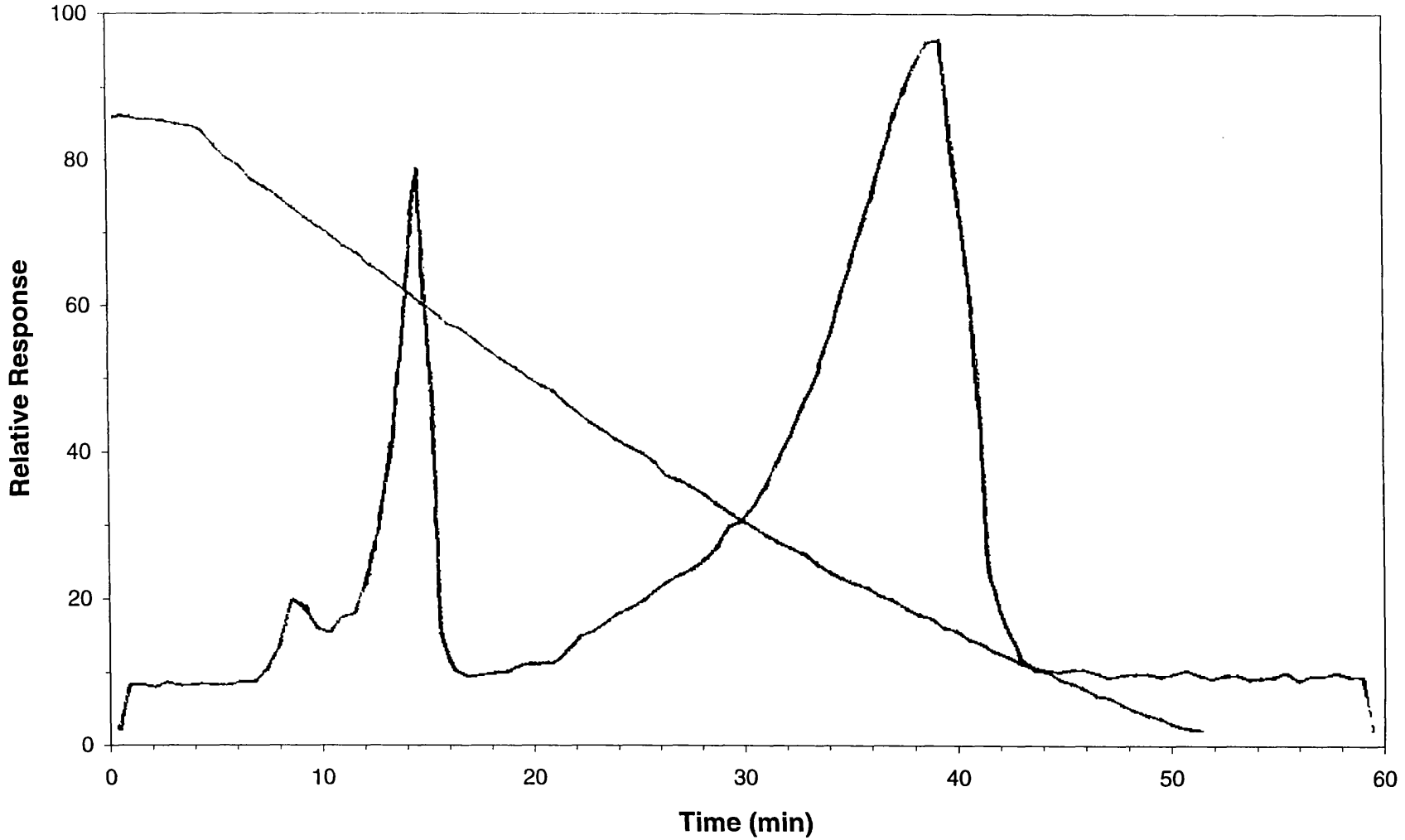

Figure 3.15: SATVA trace from the degradation of Polyester DNOP 43 under dynamic nitrogen

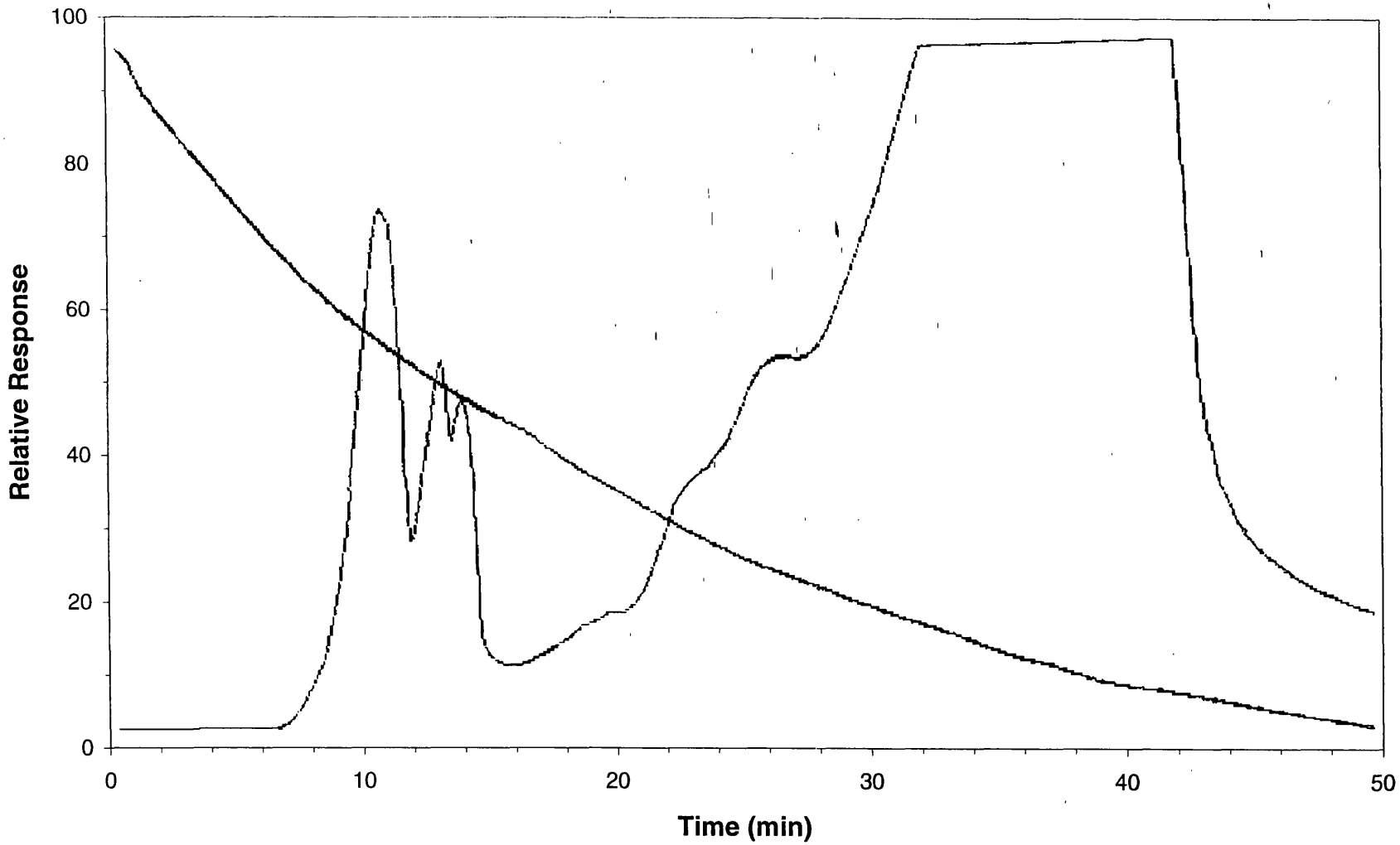

Figure 3.16: SATVA trace from the degradation of Polyester DNOP 43 under dynamic air

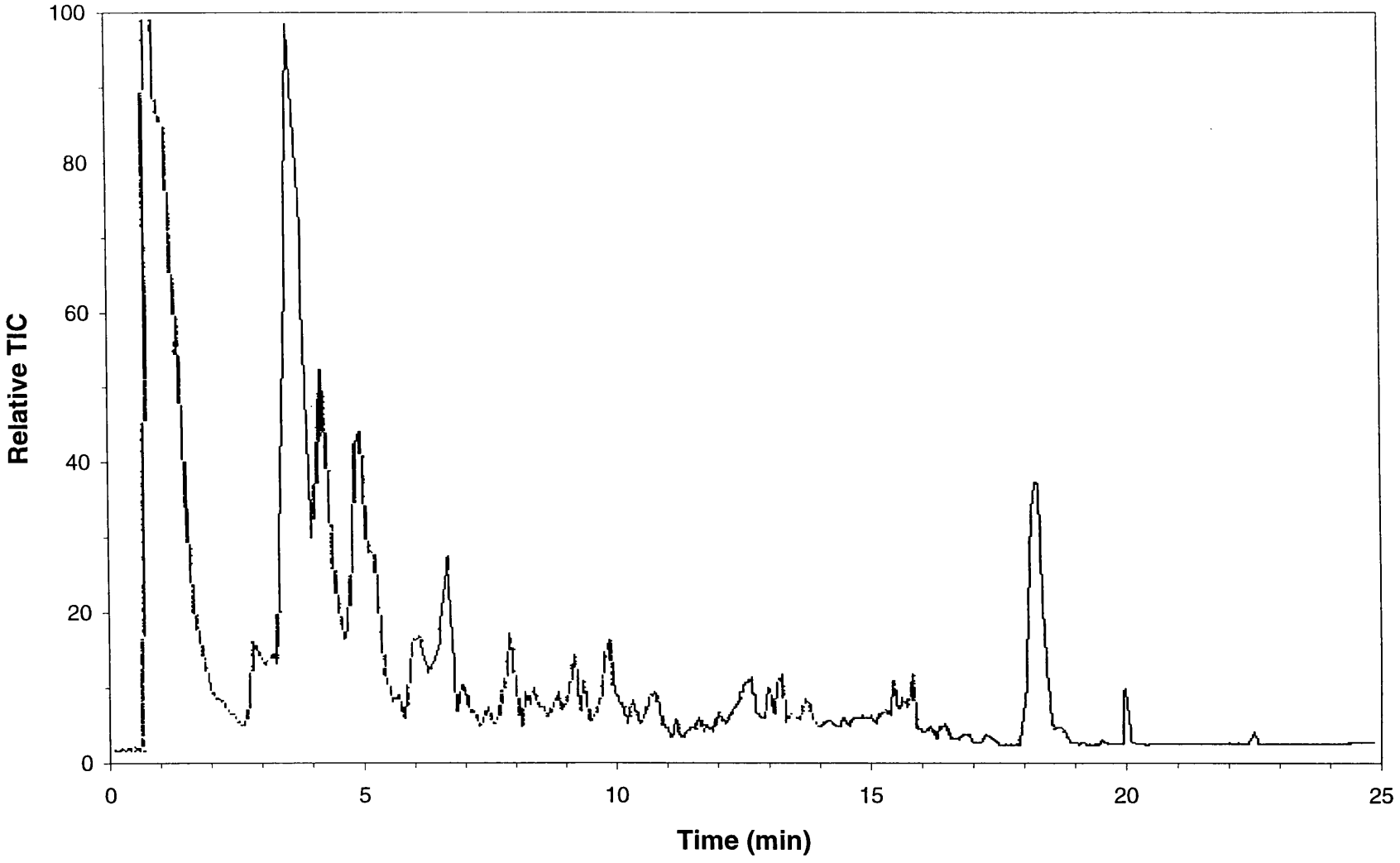

Figure 3.17: TIC trace for the liquid fraction from the SATVA curve in Figure 7.16

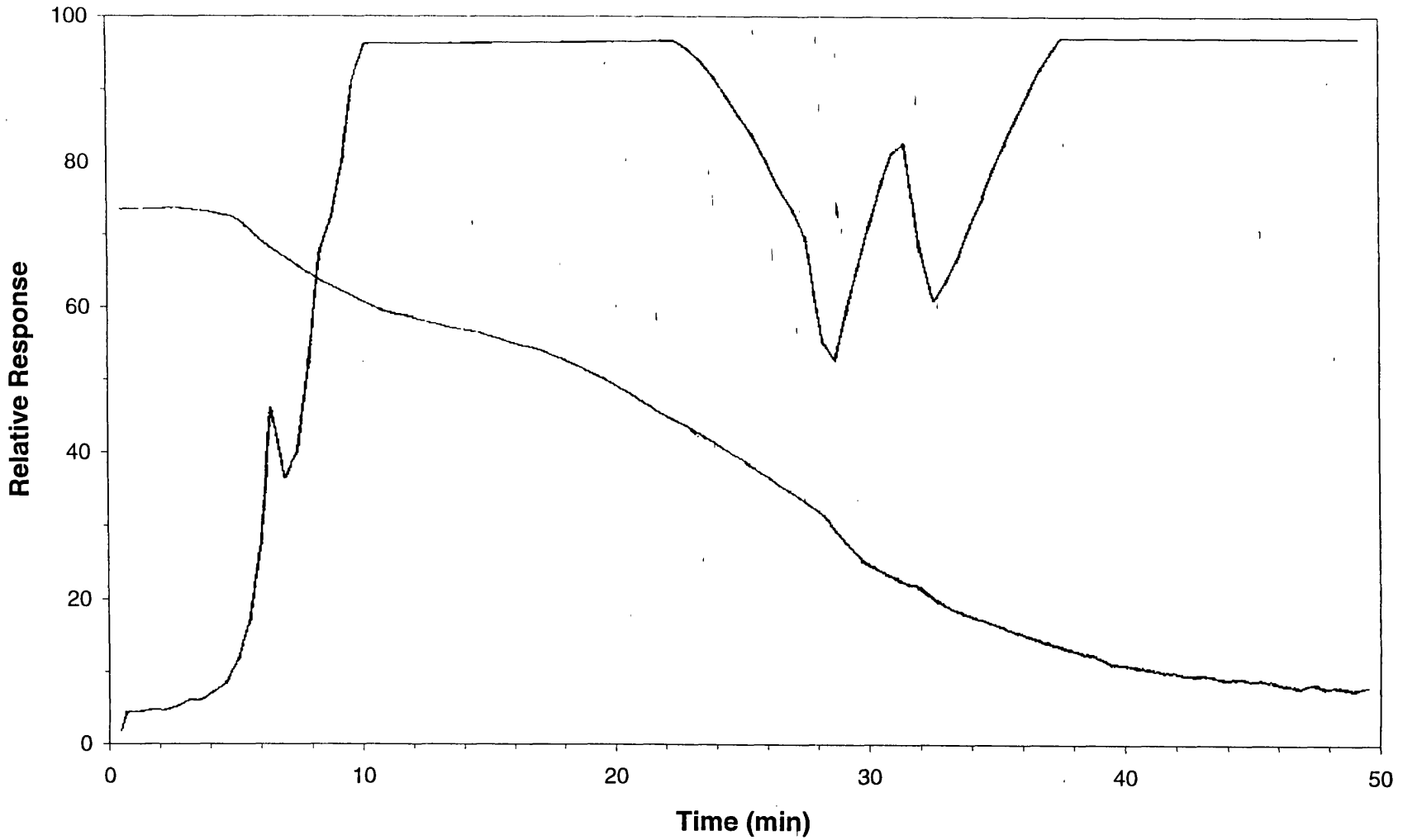

Figure 3.18: SATVA trace from the degradation of Polyester DNOP 43 under flaming conditions

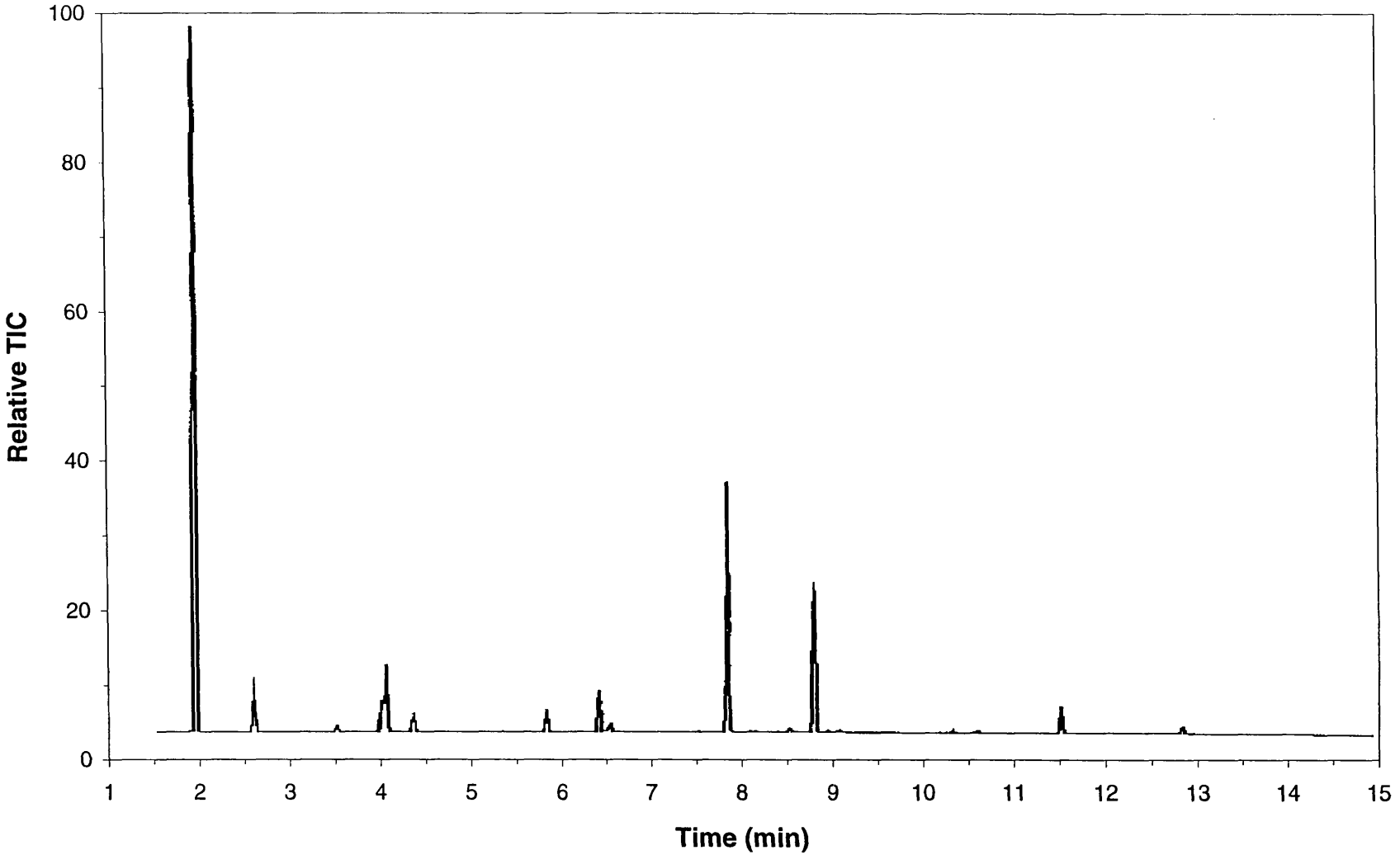

Figure 3.19: TIC trace for the liquid fraction from the SATVA curve in Figure 3.18

CHAPTER 4

ORGANIC AZO- AND DISAZO COLOURANTS

4.1 INTRODUCTION TO AZO DYES

Natural dyes dominated the world colourant market up until the start of the nineteenth century[14,17]. At this time the most significant synthetic dye was picric acid (discovered by Wolfe in 1771) which provided only a fraction of a percent of world dye production. The revolutionary change towards synthetic dyes was initiated in 1856 with the discovery of mauveine by W.H.Perkin, while working with Hofmann.

Azo dyes account for more than half of the total world dyestuffs production, making them the most important class. This has arisen due to good tinctorial strength, fastness, cheap and easy synthesis, and covering the whole shade range.

4.2 CHEMISTRY OF AZO DYES

Azo dyes normally contain one or more azo linkage[15,16]. All azo dyes contain at least one but normally two aromatic groups attached to the azo linkage. Normally the azo group is in the more stable trans position, as illustrated below:

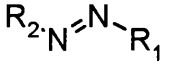

The primary classification of the azo series of dyes is related to the number of azo linkages present, *i.e.* azo, disazo, trisazo, *etc.* It is rare for a dye to contain more than four azo groups.

4.2.1 Azo-Hydrazone Tautomerism

In 1884 Zincke and Bindewald correctly suggested the rearrangement illustrated in Figure 4.1[17]. This is known as the Azo-Hydrazone Tautomerism.

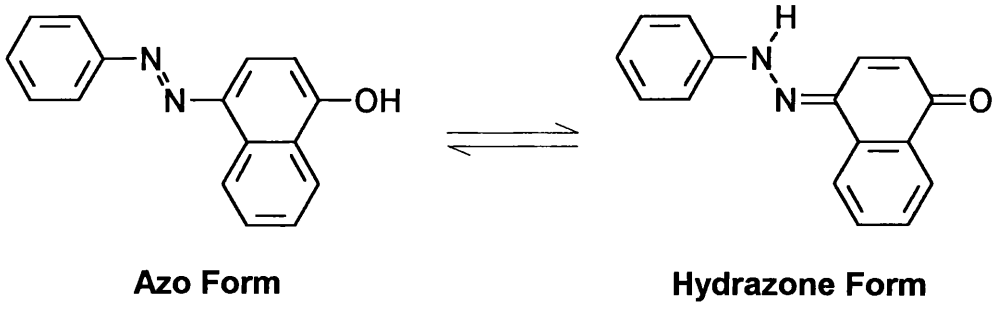

Figure 4.1: The Azo-Hydrazone Tautomerism

This phenomenon is clearly of significance when considering the mechanism for the degradation of these materials. The hydrazone form is not only bathochromic in comparison with the azo form, but also has a higher tinctorial strength. It therefore follows that dyes which exist predominately or exclusively in the hydrazone form are commercially desirable.

The hydroxy group must be conjugated to the azo group to allow this tautomerism to occur, *i.e. ortho-* or *para*-hydroxyarylazo compounds. The hydrazone is found to be more stable by bond energy calculations. However the resonance stabilisation energy of the ring system means that the azo form is still prefered for azophenol dyes, but not for fused benzene rings such as in the system illustrated.

Solvent effects may also influence the relative proportions of the tautomers, rendering UV-visible spectroscopic studies of the samples under study futile. Electron-accepting groups on the non-fused aromatic ring in the above system also generally increase the

proportion of the hydrazone form present, sometimes overriding solvent effects. This effect is most significant for para-substitution.

4.3 Organic Azo Dyes under Study

The samples provided consisted of one azo and two similar disazo dyes. One of the disazo samples, Sandorin Red BN, is very similar in structure to the published structure of Pigment Red 144[14], differing only by one chlorine on the bridging phenyl group. The supplied structures are illustrated in Figure 4.2.

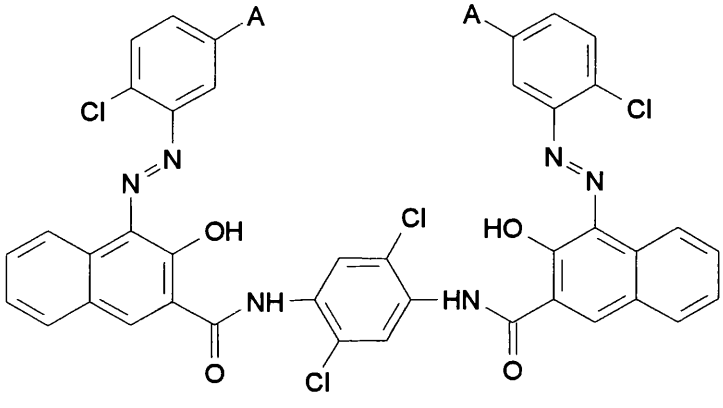

Sandorin Red BN: A=Cl

Sandorin Scarlet: A=CF_3

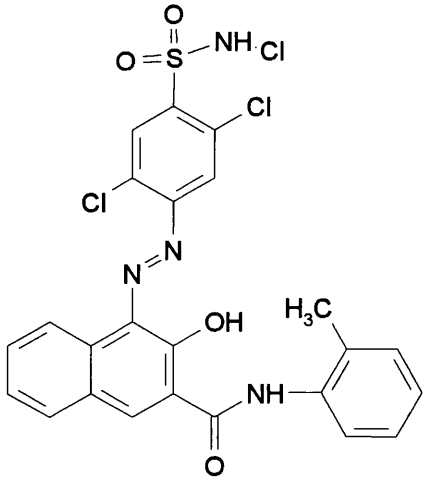

Graphtol Fast Red 2GLD

Figure 4.2: Organic Azo Dyes Under Study

The environment around the azo link may be redrawn as in Figure 4.3, where A and B are the substituents as illustrated in Figure 4.2. Further stabilisation of this structure may be supposed by considering the hydrogen bonding in the six-membered ring formations shown.

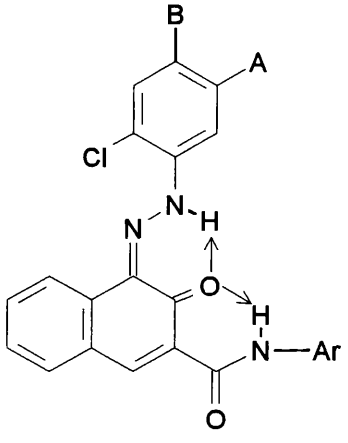

A = Cl or CF_3

B = H or SO_2NHCl

Figure 4.3: Proposed structure.

4.4 Thermal Degradation of Sandorin Red

This was studied first in this section as it was the most basic of the three organic azo compounds. The other two materials presented more complicated substituent groups.

4.4.1 Thermogravimetric Analysis

The TG plots are shown in Figure 4.4, and are sumarised in the following table:

Table 4.1: Key temperatures from thermogravimetry of Sandorin Red

Conditions	$T_{thresh1}$(°C)	$T_{thresh2}$(°C)	T_{end}(°C)	%Residue
Dynamic Nitrogen	350	440	>900	>30%
Dynamic Air	325	435	580	~2

The plot obtained under dynamic nitrogen shows one rapid loss starting at 350°C and ending at 440°C, with 64% of the initial weight remaining. From this temperature the

rate of weight loss was greatly reduced, implying that the residue was thermally quite stable from the first stage.

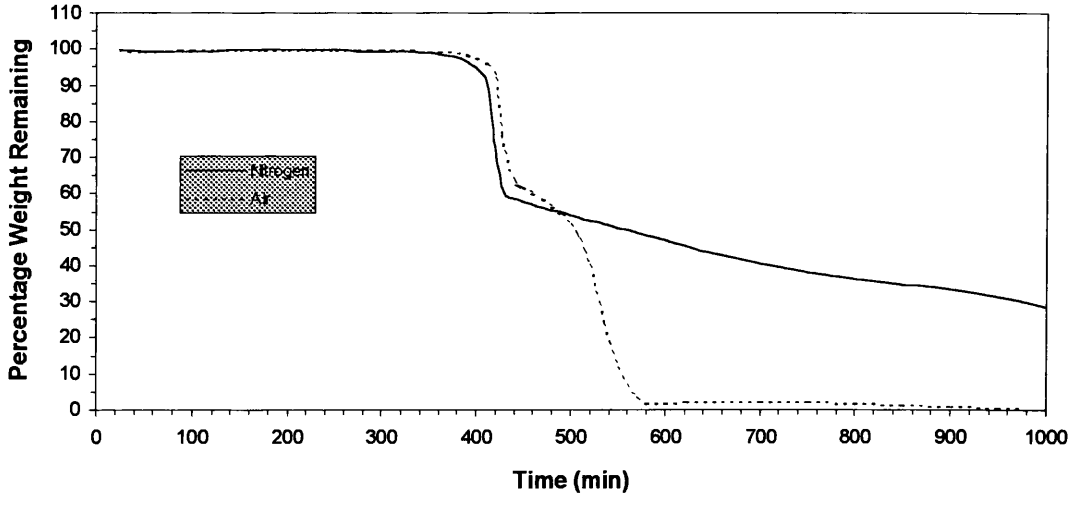

Figure 4.4: Thermogravimetric Analysis traces from Sandorin Red BN

When the experiment was repeated under dynamic air, two stages of rapid loss were observed. The first was similar to that for the inert atmosphere, with 65% of the residue remaining at 435°C. This observation implies that oxidation effects made only a minor contribution up to this temperature. The second stage left only 2% of the original weight by 580°C. This difference is to be expected, as the carbonaceous residue would have difficulty withstanding such elevated temperatures in air.

4.4.2 Product Analysis — Static Nitrogen

The sample was degraded at 10°C/min up to 425°C in these static nitrogen experiments. The sample sizes were from 100-150mg. It was the original intention to follow up these studies with analysis to higher temperatures, and then study the

difference in the products. This was not done, as the flow apparatus offered a superior method of study.

The typical SATVA trace obtained for the volatilisation of the condensable degradation products is illustrated in Figure 4.5. This shows three peaks before 25 minutes. The first two product fractions were collected together, and the IR spectrum is shown in Figure 4.6. The strong absorption at 2320 cm^{-1}, with the peaks at 665 cm^{-1} and overtone bands around 3600 cm^{-1}, indicate the presence of CO_2. The fine strucure around 2870 cm^{-1} and the peak at 714 cm^{-1} were caused by HCl. The rise in the trace at 20 minutes was attributed to HCN. This was seen through an IR absorption at 714 cm^{-1}, the spectrum being too weak to see the other absorptions clearly. By virtue of the HCl being the most volatile product, it can be taken as being responsible for the first peak. The following table summarises the assignments for the gas peaks:

Table 4.2: SATVA peak assignments from Figure 4.5

Peak	Assignment
1	HCl
2	CO_2
3	HCN with possible traces of HCNO

All the products after 25 minutes were collected together for study by GC-MS. The Total Ion Count (TIC) trace is presented in Figure 4.8. The peak assignments are shown in the table overleaf.

Table 4.3: GC-MS peak assignments from Figure 4.8

Retention Time	Product	Retention Time	Product
3:34	Solvent (ether)	15:02	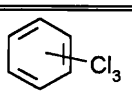
5:52	Styrene	16:00	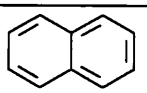
9:56	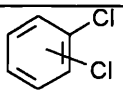	16:23	Unidentified aliphatic hydrocarbon
11:17	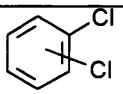	16:46	Unidentified aliphatic hydrocarbon
12:15	Styrene	17:15	Unidentified aliphatic hydrocarbon
13:30	Unidentified aliphatic hydrocarbon	22:20	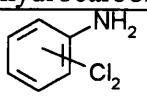
13:47	Unidentified aliphatic hydrocarbon		

The existence of two styrene peaks is not unusual for the GC-MS machine used here. Styrene can polymerise on the top of the column, and then degrade when the temperature increases. This results in a second styrene peak. This machine also has a reputation for giving a styrene peak when none has been present in the sample, presumably due to injection port contamination from previous analyses.

4.4.3 Product Analysis — Dynamic Nitrogen

The sample was degraded up to two selected temperatures at a rate of 10°C/min in order to see any possible difference in the products evolved in the different stages of the degradation, as seen in the thermogravimetric trace. The first runs were to 460°C, then the latter ones to 900°C.

The percentage residue obtained at the two temperatures under study are displayed in the table below. It can be seen that the residue for the flow tube experiments is larger than that predicted from the TG results. There are two possible reasons for this. The first is that the temperature in the tube may lag behind the oven by a few degrees. This effect should be offset by the 10 minute isothermal stage at the end of the degradation. The second, more plausible explanation is related to the larger sample size used for the flow tube studies. This would encourage side reactions, perhaps aiding the formation a more stable carbonaceous residue.

Table 4.4: Residue percentages from nitrogen degradation of Sandorin Red

	Weight Remaining	
Temperature	**Thermogravimetry**	**Flow tube**
460°C	60%	80%
900°C	35%	52%

The SATVA results for the 900°C degradations are presented here. No differences in the SATVA traces were observed between the two temperatures. The SATVA trace obtained is presented in Figure 4.9. The amount of product at peak 1 was insufficient for IR analysis, but was identified through MS. This spectrum gave a 100% molecular ion at m/e 44, with additional peaks at 28, 16 and 12. This is the unambiguous spectrum for CO_2. The IR spectrum of the products evolved at the start of peak 2 is displayed in Figure 4.10. The absorptions at 3345, 3300 and 714 cm^{-1} were produced by HCN. The remaining peaks at 2970, 1738, 1440, 1367 and 1215 cm^{-1} can be explained by the presence of acetone. These assignments were confirmed through MS analysis, which also showed methanol in some of the analyses. The following table summarises the study of the gas peaks:

Table 4.5: SATVA peak assignments from Figure 4.9

Peak	Assignment
1	CO_2
2 (start)	HCN, acetone, with possible traces of methanol.

The remaining less volatile liquid products were analysed through GC-MS analysis, giving the TIC trace presented in Figure 4.11. Although fewer peaks are shown here than under static nitrogen, this is more likely to be due to inconsistencies in GC-MS sensitivity than to the formation of fewer degradation products. It can be seen from the following peak allocation list that the same major products were detected.

Table 4.6: GC-MS peak assignments from Figure 4.11

Retention Time	Product	Retention Time	Product
8:10	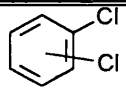	13:44	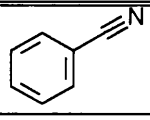
8:51	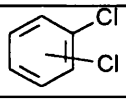		

4.4.4 Product Analysis — Dynamic Air

The sample was degraded at 10°C/min up to 560°C. The TG plots show that there was little point in proceding to a higher temperature for product analysis.

Table 4.7: Residue percentages from air degradation of Sandorin Red

	Weight Remaining	
Temperature	Thermogravimetry	Flow tube
580°C	3%	5-33%

A sample SATVA trace for the volatilisation of the condensable degradation products is given in Figure 4.12. The first peak was produced by CO_2, the IR evidence being the same as for under static nitrogen. This was supported with MS analysis. The second

peak gave only the IR absorptions attributed to HCN as presented in 4.4.3 for dynamic nitrogen. This was supported through MS with an m/e=27 peak at 100% and a weaker peak at m/e=26. It can be seen that there is much more CO_2 and HCN relative to the liquid fraction detected than under dynamic nitrogen conditions. The following table summarises the gases:

Table 4.8: SATVA peak assignments from Figure 4.12

Peak	Assignment
1	CO_2
2	HCN

The liquid fraction contained mainly water. Diethylether was used to extract the non-aqueous components for GC-MS analysis, which gave the TIC trace shown in Figure 4.13. The following table displays products against retention time:

Table 4.9: GC-MS peak assignments from Figure 4.13

Retention Time	Product	Retention Time	Product
1:51	Ether (Peak was split due to solvent dumping)	10:39	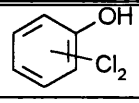
6:06	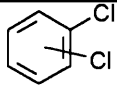	Note:	Other analyses showed 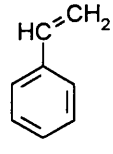 the presence of 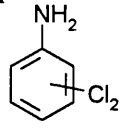 and
6:40	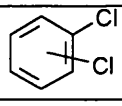		

4.4.5 Product Analysis - Flaming Conditions

The apparatus was set up as detailed in Chapter 2. The ensuing table shows the observations made during the degradations.

Table 4.10: Observations from Sandorin Red under flaming conditions

First Run	
Sample Size:	52.6 mg
Time (min)	**Observations:**
2:40	Blackening from the centre outwards started
5:30	Blackening almost complete. Some glow-burning
7:00	No more activity
10:00	Heater switched off
Comments:	No ignition.

Second Run	
Sample Size:	65.6 mg
Residue:	12.7 mg (a small amount was lost)
Time (min)	**Observations:**
1:30	Slight darkening in places
2:05	Blackening from the centre outwards started
3:00-3:40	Some ashing
4:50	Some glow-burning on the blackened region
6:00	Stopped. Some red remained at the edge of the planchet
Comments:	No ignition. Under room lighting the black parts appeared brown, with some red remaining below.

A sample SATVA trace is given in Figure 4.14. This trace is typical for the flaming studies of all the samples studied, where CO_2 and water are predominate. The IR spectrum from the non-condensable gases is shown in Figure 4.15. It can be seen that some of the CO_2 was not condensed in the spiral trap. The peaks at 2116 and 2168 cm^{-1} indicate that CO was produced. The products at peak 1 of the SATVA trace were split between two gas cells. Those at the start of the peak provided the IR spectrum in Figure 4.16, with the remainder of the gases producing the plot in

Figure 4.17. It is clear that CO_2 is the major product, as identified through the absorptions detailed in section 4.4.3. IR absorptions at 2238, 2213, 1299 and 1273 cm^{-1} showed that N_2O was present. The liquid fraction contained mainly water. These findings are summarised in the following table:

Table 4.11: SATVA peak assignments from Figure 4.14

Peak	Assignment
Non-condensables	CO
1	Mainly CO_2 with some N_2O
2	Mainly water.

Diethylether was used to provide the non-aqueous extract for GC-MS analysis. The resulting TIC trace is displayed in Figure 4.18. The peak allocation for this chromatograph is displayed in the following table:

Table 4.12: GC-MS peak assignments from Figure 4.18

Retention Time	Product	Retention Time	Product
3:05	Silicone contaminant		
4:18	Styrene	9:57	Silicone contaminant
5:44	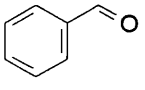	11:29	Possibly 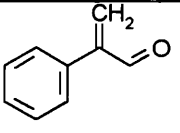
7:17	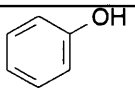	12:18	Mostly 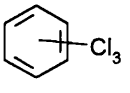 with some 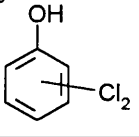
7:23	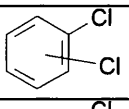	13:13	Silicone contaminant
8:00	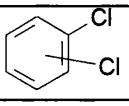	16:25	Probably an aliphatic substituted cyclohexane
8:24	Silicone contaminant	16:43	Probably a methylated alkane
8:55	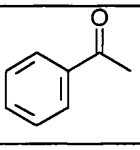 or 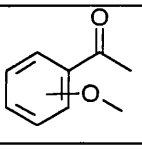	18:09 22:04 26:33	Silicone contaminant

The CRF was collected by washing the walls of the degradation vessel firstly with acetone and then with dichloromethane. These solutions were then studied through GC-MS analysis, resulting in the TIC traces in Figures 4.19 and 4.20. The following table gave the peak allocation for the acetone extract.

Table 4.13: GC-MS peak assignments from Figure 4.19

Retention Time	Product	Retention Time	Product
1.37	Hydrocarbon (unidentified)	4.69	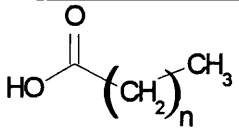 Like
1.52	Hydrocarbon (unidentified)	5.50	Unknown
1.93	Hydrocarbon (unidentified)	5.90	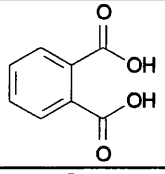
2.17	Possibly a 2-ol	6.11	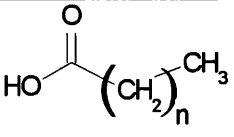 perhaps nonanoic acid
2.25 2.44 2.79	Hydrocarbon (unidentified)	6.85	Perhaps a furanone such 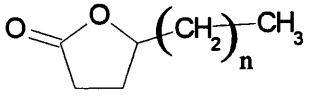 as
3.20	Possibly 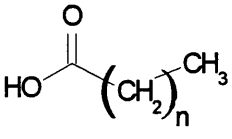	8.04	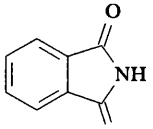 Possibly or 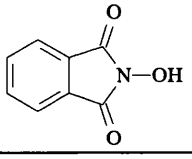
4.60	Perhaps 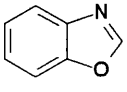 + 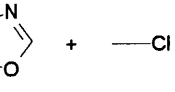 or 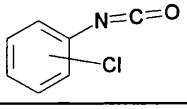	9.27	Dichloro aromatic 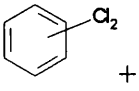 + substitutions of possibly 28 and 17 (mw189)

Table 4.13 (continued)

Retention Time	Product	Retention Time	Product
9.92	Probably a phthalate	17.50	Unidentified
10.46	Aromatic mw=231 with 2Cl, a 43 (C_3H_7) and a 27/70 loss	17.58	3Cl aromatic mw = 282
10.88	Redraw with second peak	17.68	1Cl mw = 272 possibly an aromatic ester or an anhydride
11.15	Unidentified hydrocarbon	17.91	Aromatic unknown, 1 or 2 Cl
11.41	Probably 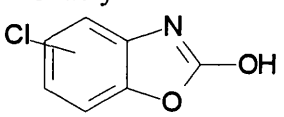	18.32	Possibly a cyclohexane substituted on a chloroaromatic
12.33	Possibly a 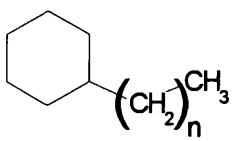	19.17	A dichloroaromatic mw=286
13.06	Probably a phthalate	19.35	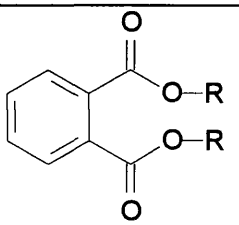
13.44	Unidentified hydrocarbon	20.17	Chloroaromatic. 277(100)+possible weak 351
14.02	A phthalate	20.49	Unidentified hydrocarbon
14.53	Perhaps a cyclohexane 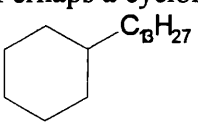		
15.09	2Cl aromatic mw = 248	21.57	Possibly a cyclohexane on a dichloroaromatic
15.63	Unidentified hydrocarbon	22.68	Probably an aromatic with large aliphatic hydrocarbon substitution
17.09	1Cl aromatic mw = 256		

The following table lists selected peaks form the dichloromethane washings:

Table 4.14: GC-MS peak assignments from Figure 4.20

Retention Time	Product	Retention Time	Product
15.60	Hydrocarbon	19.98	Hydrocarbon, possibly 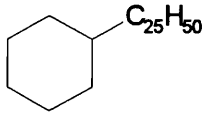
16.49	Hydrocarbon, possibly 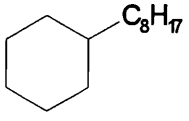	23.10	Unknown hydrocarbon, 55@100%, highest mass 393
18.31	Hydrocarbon, possibly 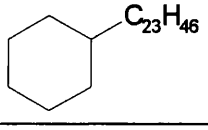		

It may be deduced rom the TIC trace that the other major peaks belong to the same series as those described above. The major products for this second extract, although not unambiguously identified, are certainly similar to those suggested. These materials are clearly not products of the degradation. The probable sources of contamination are

1. Vacuum grease
2. Pump oil (rotary or diffusion)
3. Impure solvents for extraction
4. Sample-bottle caps

The possibilty of contamination from containers has been minimised through the use of glass sample bottles, although it is still possible that the plastic caps (although usually foil lined) were a source. The solvents for fraction collection were analytical grade throughout. The oils in the vacuum pumps are more probable a source of these contaminants, yet inspection of the layout of the degradation apparatus shows the

presence of the cold trap which should prevent any materials from the pump from reaching the CRF region. The pump area itself was also protected with traps.

This leaves the vacuum grease as the most probable source. The suppliers of the grease (Apiezon L) were contacted, but provided no useful information. The grease is known to be composed chiefly of hydrocarbons of low volatility, so it is not improbable that some should be released under the elevated temperatures induced by the conical heater.

It was common for the CRFs for all of the samples inspected to require some concentration. This would have exaggerated the relative concentration of any contaminants present.

4.5 DEGRADATION OF SANDORIN SCARLET 4RF

Sandorin Scarlet 4RF differs from Sandorin Red BN by the substitution on two of the chlorine positions with trifluoromethyl- groups. This made it a logical choice to group this with the studies in section 4.4.

4.5.1 Thermogravimetric Analysis

The TG plots are shown in Figure 4.21, and are summarised in the following table:

Table 4.15: Key temperatures from thermogravimetry of Sandorin Scarlet 4RF

Conditions	$T_{thresh1}$(°C)	$T_{thresh2}$(°C)	T_{end}(°C)	%Residue
Dynamic Nitrogen	~230	~410	900	18
Dynamic Air	~270	~420	540	15

The first major weight loss is very similar for under air and nitrogen, leaving around 60% residue by around 400°C. This effect was also observed for Sandorin Red BN. Oxidation effects did not have a great influence until above this temperature.

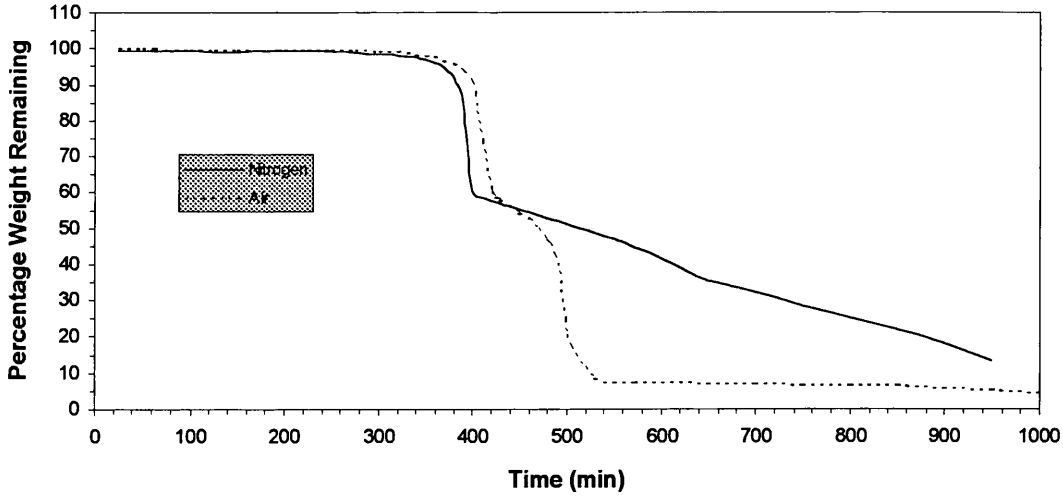

Figure 4.21: Thermogravimetric Analysis traces from Sandorin Scarlet 4RF

It is apparent from the study of the trace for the air atmosphere that there was some further weight loss after 540°C up to 900°C, albeit at a much slower rate, leaving a final residue of 6%. The second stage of degradation was probably split slightly, as can be seen from the gradient change at 500°C.

4.5.2 Product Analysis — Dynamic Nitrogen

These degradations were all carried out at 10°C/min up to 900°C as TG data were not available at the time of study. The following averages from the residue weights were calculated.

Table 4.16: Residue percentages from nitrogen degradation of Sandorin Scarlet 4RF

	Weight Remaining	
Temperature	**Thermogravimetry**	**Flow tube**
900°C	18%	33%

The flow tube apparatus gave a greater percentage residue than the TG studies predicted. This is the same effect as was observed in section 4.4.3.

The SATVA trace for the volatiles analysis are shown in Figure 4.22. Peak 1 was identified as due to CO_2 through MS, as described in section 4.3.3. The IR spectrum was too weak to provide any conclusions. Peak 2 was due to the evolution of HCN. This was confirmed through an MS peak at m/e = 27, and IR absorptions at around 3300 and 714 cm^{-1}. The volatile peak assignments are given below:

Table 4.17: SATVA peak assignments from Figure 4.22

Peak	Assignment
1	CO_2
2	HCN

The third and final peak on the SATVA trace was mainly from water, as was evidenced through the on-line MS. Diethylether was used to extract the non-aqueous

components, which were analysed through GC-MS. The TIC trace for this sample is given in Figure 4.23. The following table provides the peak allocations.

Table 4.18: GC-MS peak assignments from Figure 4.23

Retention Time	Product	Retention Time	Product
3:25	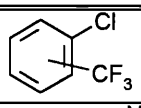	7:36	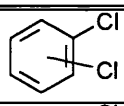
5:51	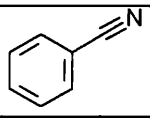	11:14	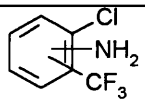

The cold ring fraction was extracted with acetone for GC-MS analysis. Difficulties arose in the interpretation of these results. The problem was the lack of reference data. This was for two main reasons. The first was the relative lack of known practical importance of these materials, rendering them unlikely additions to the already large database. The second was the presence of the CF_3 groups, further increasing the obscurity of many of these compounds. The MS database would have to be very large indeed to cover all chemical possibilities. The TIC trace obtained is shown in Figure 4.24. The main peak at 4.2 minutes was due to chloroaniline with a —CF_3 group on the ring. The product forming the second largest peak at 5.18 minutes was not properly identified. The spectrum showed it to be an aromatic with one chlorine and a molecular weight of 235. Only the first major peak was identified. The other components were clearly not common compounds as they were not present in the database.

4.5.3 Product Analysis — Dynamic Air

These studies were also carried out at 10°C/min up to 900°C, due to the lack of relevant TG information. These plots show that there was only around 2% weight loss between 540 and 900°C. The following comparisons for the weight of residue under TG and flow tube conditions were obtained:

Table 4.19: Residue percentages from air degradation of Sandorin Scarlet 4RF

	Weight Remaining	
Temperature	**Thermogravimetry**	**Flow tube**
900°C	15%	<1%

It can be seen from the other results that it is unusual for the larger samples in the flow apparatus to result in a lower residue weight than that for TG. This effect may have been due to errors from the TG instrument, or perhaps be related to the effect of side reactions within the bulk of the material. The latter appears less likely due to the structural similarities between Sandorin Scarlet 4RF and Sandorin Red BN.

The SATVA trace for the volatilisation of the condensable degradation products is given in Figure 4.25. The IR spectrum taken when the main gas peak was rising is presented in Figure 4.26. The absorptions at 2361 cm^{-1} and 668 cm^{-1} will be due to CO_2 from the small first peak seen on the SATVA trace. The second most volatile product was HCN, as can be seen from the pair of peaks at 3315 cm^{-1} and the spike at 713 cm^{-1}. The most dominant features of this IR spectrum were caused by acetone, these being the absorptions around 3460, 2970, 1739, 1366, 1217 and 900 cm^{-1}. These deductions were all supported through the use of the on-line MS analyser. The volatile products are summarised in the following table:

Table 4.20: SATVA peak assignments from Figure 4.25

Peak	Assignment
1	CO_2
2	Mainly water. Acetone was detected at the start of the peak.
Comments	A small amount of HCN was detected at around 15 minutes.

Further studies were not carried out on the liquid fraction. It was believed that the dynamic air studies were of the least significance, so further time was not spent in this area.

4.5.4 Product Analysis — Flaming Conditions

The apparatus was set up as detailed in Chapter 2. The following observations were made during the degradations:

Table 4.21: Observations from Sandorin Scarlet under flaming conditions

Sample Size:	92.2 mg
Residue:	10.1 mg (11.0%)
Time (min)	**Observations:**
2:30	Blackening started from centre.
4:20	Centre started to go grey.
5:00	Centre had hardened, lifting up from the remaining sample.
6:00	No red remaining. The hard area had blackened and crumbled.
10:00	Stopped. The residue was a brown/black colour.
Comments:	No ignition.

The SATVA trace for the volatilisation of the condensable degradation products is given in Figure 4.27. Non-condensables were also captured, and revealed CO through the normal IR absorptions. Figure 4.28 shows the IR spectrum obtained for the gas peak. Unsurprisingly, CO_2 was the major product for this peak. N_2O was also detected. This can be seen through the strong absorptions at around 2235 cm^{-1} and the

weak peaks around 3470, 2565 and 1290 cm^{-1}. The identification of the gases is summarised below:

Table 4.22: SATVA peak assignments from Figure 4.27

Peak	Assignment
Non-condensables	CO
1	Mainly CO_2 with some N_2O detected

The second SATVA peak was due almost exclusively to water. The usual ether extract was taken for GC-MS study. The resulting TIC trace is displayed in Figure 4.29. The identification of the peaks is shown in the following table:

Table 4.23: GC-MS peak assignments from Figure 4.29

Retention Time	Product	Retention Time	Product
5:28	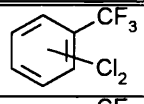	6:32	Silicone contaminant
5:40	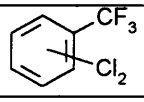	8:53	Silicone contaminant
6:21	Silicone contaminant	9:45	Possibly 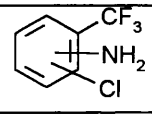

All the remaining peaks were caused by silicone contaminants. It should be noted that it is possible that the first two peaks were separated due to limitations of the machine rather than actually being separate isomers.

4.6 DEGRADATION OF GRAPHTOL FAST RED 2GLD

Graphtol Fast Red 2GLD was the last sample chosen for this section. This was due to it having the most individual structure of the three, since it presents the added complication of having an SO_2NHCl group.

4.6.1 Thermogravimetric Analysis

The TG plots are illustrated in Figure 4.30, and are summarised in the following table:

Table 4.24: Key temperatures from thermogravimetry of Graphtol Fast Red 2GLD

Conditions	T_{thresh}(°C)	T_{end}(°C)	%Residue
Dynamic Nitrogen	120	>900	/
Dynamic Air	130	~1000	0

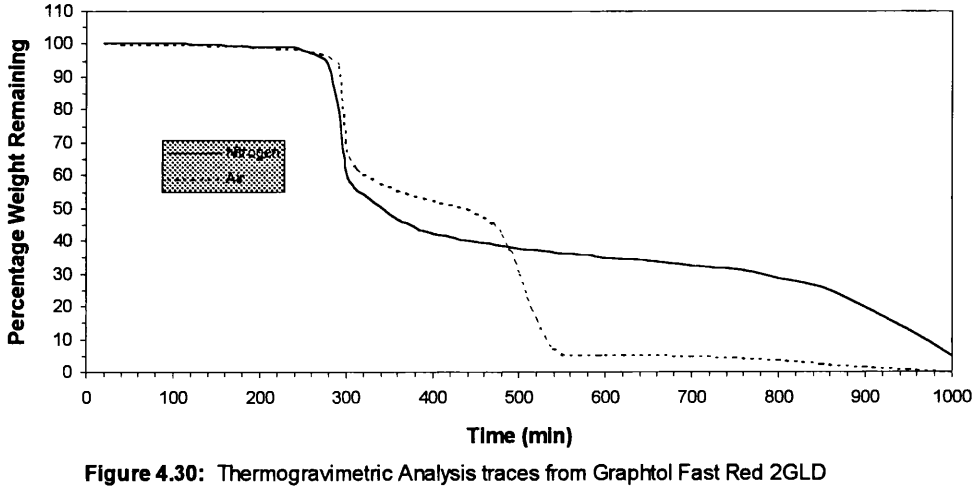

Figure 4.30: Thermogravimetric Analysis traces from Graphtol Fast Red 2GLD

The isotherms for dynamic nitrogen overlapped, making it difficult to assess the temperatures at which distinct stages of degradation occurred. The weight was still falling off at 1000°C. The faster stages of degradation appeared to be complete by 420°C. Similarly, there was some overlap for the dynamic air environment, with the second (~350°C) of four stages overlapping with its neighbours. There was only 5% weight remaining by 560°C.

4.6.2 Product Analysis — Dynamic Nitrogen

These studies were carried out using a temperature program of 10°C/min up to 900°C then isothermal for 10 minutes. The high temperature was used as TG data were not available at the time of these studies. The average residue weight is shown in the following table:

Table 4.25: Residue percentages from nitrogen degradation of Graphtol Fast Red

	Weight Remaining	
Temperature	**Thermogravimetry**	**Flow tube**
900°C	20%	40%

The residue from the flow tube experiments had the appearance of an open-celled foam. Typically, the flow tube residue was greater than that from the TG studies.

The SATVA trace for the separation of volatile products is presented in Figure 4.31. Only one gas peak can be seen, and this was found to be due to CO_2. The quantity of material forming this peak was too small for IR studies, but the MS evidence was conclusive through the normal m/e ratios as described in section 4.3.3. No other gases were detected. The liquid fraction contained much water. An ether extract of this fraction was studied by GC-MS. The TIC trace obtained is presented in Figure 4.32. The peak allocation can be viewed in the table on the following page:

Table 4.26: GC-MS peak assignments from Figure 4.32

Retention Time	Product	Retention Time	Product
1:16	Unidentified	8:29	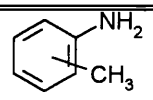
1:53	Unidentified	11:14	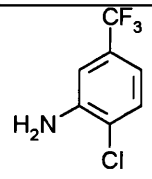 or isomers, 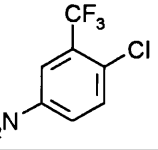 but not
5:56	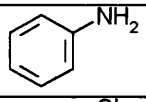	11:50	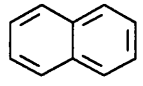
7:36	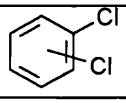		

Acetone was used to extract the cold ring fraction. The TIC for this is shown in Figure 4.33. There are many unidentified components, which is once again due to the lack of relevant reference data. It should be noted when reading the table below that quinolines and isoquinolines are indistinguishable through MS alone.

Table 4.27: GC-MS peak assignments from Figure 4.33

Retention Time	Product	Retention Time	Product
1.38 1.90	Unknown hydrocarbon	2.94	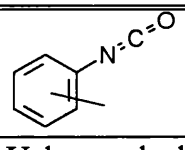
2.88	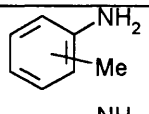 or 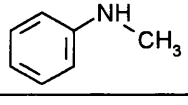	5.69	Unknown hydrocarbon

Table 4.27: (continued)

Retention Time	Product	Retention Time	Product
6.21	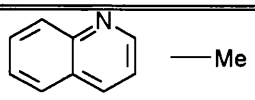	12.60	Possibly 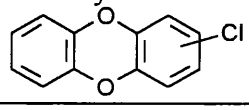
6.45	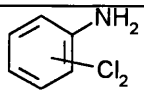	12.77 12.92	Unidentified. Possibly isomers
7.64	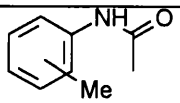 or 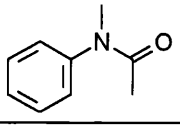	13.43	Unknown aromatic
7.95	Unidentified	13.74	Unknown 2Cl aromatic
8.23	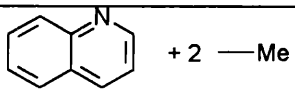	13.84	2 products. One has similar spectrum to 12.77. The other is possibly 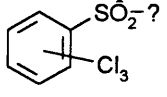 like
8.30	Unidentified	13.90	Lone 232 1Cl peak
8.83	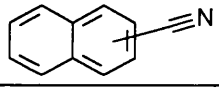	14.02	A phthalate
8.99	Unidentified	15.69	Similar spectrum to 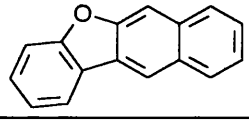
9.10	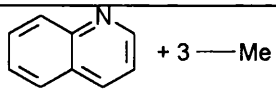	16.47 Major peak	Two components, possibly isomers. Unknown 2Cl aromatic mw = 254. Possibly a hydrazine
9.79	Probably 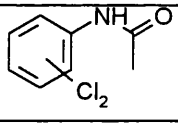	16.80	2 products, unidentified aromatic and unidentified chloro-aromatic
10.04	Unidentified, although a little like 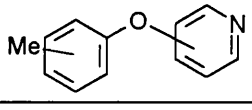	16.90	Undentified. Possibly a further substituted 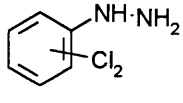
11.21, 11.58, 11.67, 11.78, 12.27, 12.38, 12.50	Unidentified	17.51	<u>Possibly</u> 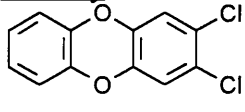

Table 4.27 (continued)

Retention Time	Product	Retention Time	Product
17.86	Unidentified	20.19	Unidentified aromatic possibly mw=277 Cl=1
18.13	Unidentified aromatic mw=296 possibly Cl=2	20.49	Unidentified aromatic mw=324 possibly Cl=2
18.37	Unidentified aromatic mw=324 possibly Cl=2	21.32	Unidentified aromatic mw=344 Cl=2
18.64	Unidentified aromatic mw=243	23.37	Unidentified aromatic possibly mw=309 Cl=1
19.50	Unidentified aromatic mw=311 Cl=1		

4.6.3 Product Analysis — Dynamic Air

These studies were carried out using a temperature program of 10°C/min up to 900°C then isothermal for 10 minutes. The high temperature was used as TG data was not available at the time of these studies. The average residue weight is shown in the following table:

Table 4.28: Residue percentages from air degradation of Graphtol Fast Red

	Weight Remaining	
Temperature	**Thermogravimetry**	**Flow tube**
900°C	~1.5%	2.5%

The SATVA trace for the separation of volatile products is shown in Figure 4.34. All the gaseous products were collected into the one gas cell for IR analysis. The simultaneous MS sampling gave a weak response at 10 minutes which was consistent with CO_2. This identification was confirmed through IR spectroscopy. At 18 minutes the MS plot matched that for HCN. IR absorptions at 718, 3297 and 3340 cm^{-1} confirm this deduction. The IR spectrum also indicated the presence of some

hydrocarbon, and perhaps carbonyl absorptions which could not be specifically assigned.

All the products after 25 minutes of the SATVA separation were collected together as a liquid fraction for GC-MS analysis. It was observed during SATVA through the on-line MS that this fraction contained mainly water. The ether extract provided the TIC trace shown in Figure 4.35, with the corresponding peak allocation being tabulated below:

Table 4.29: GC-MS peak assignments from Figure 4.35

Retention Time	Product	Retention Time	Product
5:12	Mainly 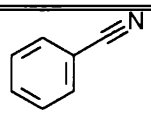 with some 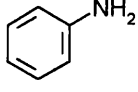	10:33	Unidentified aliphatic hydrocarbon
6:09	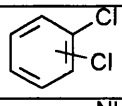	11:02	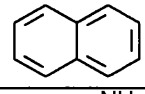
8:20	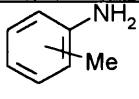 or 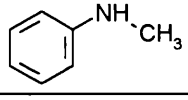	14:58	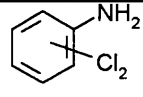
9:24	Probably 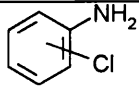		

4.6.4 Product Analysis — Flaming Conditions

The following tables display the observations made during the piloted pyrolysis studies. The ignition observed during the second run may have been related to the increase in the heater output with time.

Table 4.30: Observations from Graphtol Fast Red under flaming conditions

First Run	
Sample Size:	164.2 mg
Residue:	Not weighed.
Time (min)	**Observations:**
1:15	Small black drops (2-3 mm across) bubbled on the surface.
~3:00	Whole sample bubbled (was black).
~3:12	Started to flash, but did not remain lit.
3:40	Started to form a solid char.
5:00	Charring complete. No more activity.
6:00	Heater switched off.
Comments:	No Ignition.

Second Run	
Sample Size:	136.4 mg
Residue:	61.5 mg (45%)
Time (min)	**Observations:**
1:05	Discolouration commenced.
1:15	Some black droplets formed.
1:25	Ignition. Burned for 8 seconds.
2:00	Sample still a mixture of black and red.
2:50	Flashing, but no continuous burning.
3:00	Sample a black bubbling liquid.
4:00	Bubbling slowed down.
4:50	Residue was solid.
6:00	Heater switched off.
Comments:	Note that this second run resulted in ignition.

The SATVA traces obtained for the separation of the condensable volatile products for these degradations differed from the other piloted studies. A sample trace is presented in Figure 4.36. There were significant quantities of a gas produced other than CO_2. Simultaneous MS revealed the second gas peak to be due to a mixture of SO_2 and

HCN. The main gas peak was due to N_2O as well as CO_2. These findings are summarised in the following table:

Table 4.31: SATVA peak assignments from Figure 4.36

Peak	Assignment
Non-condensables	CO
1	Mainly CO_2 with some N_2O
2	SO_2 with HCN

The liquid fraction was composed mainly of water. GC of the ether extract provided the TIC trace in Figure 4.37, for which the peak allocations follow:

Table 4.32: GC-MS peak assignments from Figure 4.37

Retention Time	Product	Retention Time	Product
1.55	Unidentified aliphatic hydrocarbon	4.32	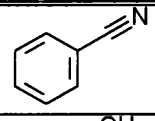
1.76	Unidentified aliphatic hydrocarbon	4.90	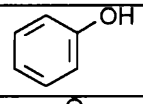
2.10	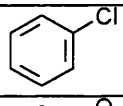	5.23	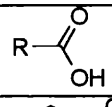
2.61	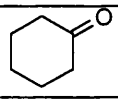	5.33	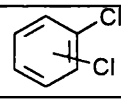
2.83	Probably 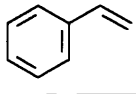	5.93	Unidentified Cl_1 aromatic mw = 196
3.00	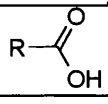	6.15	Silicone contaminant
3.92	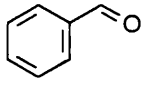	6.78	Probably 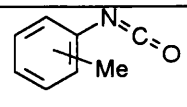 or 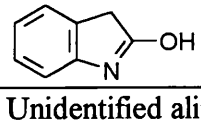
4.02	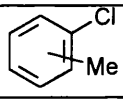	7.54	Unidentified aliphatic hydrocarbon

Table 4.32 (continued)

Retention Time	Product	Retention Time	Product
7.94	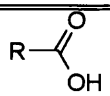	14.64	Reasonable match with 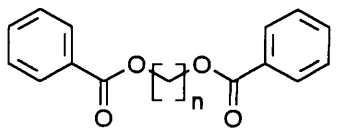
9.71	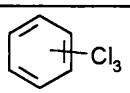	15.16	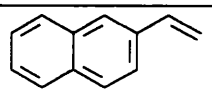 or 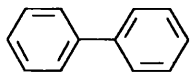
10.55	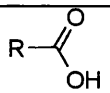	15.58	Silicone contaminant
10.74	Silicone contaminant	16.81	Aliphatic hydrocarbon
12.36	Possibly 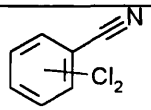	19.33	Aliphatic hydrocarbon
13.87	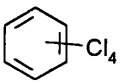	28.40	Probably a phthalate
14.40	Unidentified	29.32	Probably an aliphatic hydrocarbon

The acetone washings of the CRF were also analysed. The walls of the degradation vessel were washed with acetone. The GC trace for this fraction is displayed in Figure 4.38, and the peak allocation presented in the following table.

Problems were encountered during the interpretation of the MS. There were many spectra for which there were no comparable references. For this reason the major peaks have been also shown in the table. It should also be noted when reading these results that the MS for quinolines and their corresponding isoquinolines are indistinguishable.

Table 4.33: GC-MS peak assignments from Figure 4.38

Retention Time	Features	Products
1.47a	105(100), 120(38), 77(20), 79(18), 51(14), 103(11)	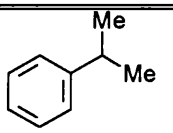
1.47b	43(100), 97(57), 112(41), 96(34), 41(14)	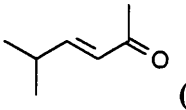 (needs 41(90))
2.24	146(87), 148(55), 111(26), 75(24), 50(15) [also 43(100), 58(15), 57(13)]	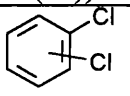
2.89	Aliphatic	
3.09	Aliphatic	
3.17	Probably Aliphatic	
3.71	88(100), 60(88), 131(68), 133(16), 43(57)57(54), 59(52), 71(17), 73(18)	Unidentified
4.36	162(100), 164(53), 43(67), 63(33), 59(24), 98(16), 99(10)	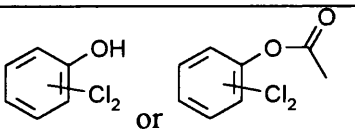 or 2,5- or 2,4-
4.58		Aliphatic
5.17	129(100), 128(21), 130(21), 102(18), 51(13), 50(9), 76(11)	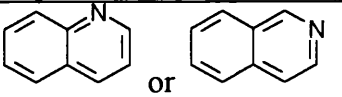 or
5.87 (shoulder of 5.90)	Weak 128(100), 43(57), 165(37), 167(30), 87(34), 101(32), 59(22)	
5.90	104(100), 76(93), 50(53), 148(31) Probably the anhydride due to the lack of peak tailing	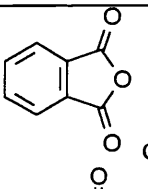 or 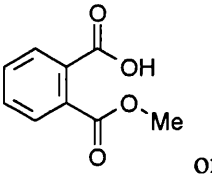 or 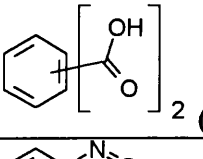 (best MS)
5.95 (shoulder of 6.02)	187(100), 188(55), 124(15), 76(14)	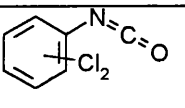

Table 4.33 (continued)

Retention Time	Features	Products
6.02	60(100), 73(86), 43(79), 41(32), 57(61), 55(39), 115(28), 98(6)	Probably 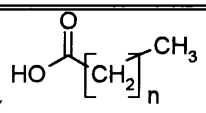
6.11	147(100), 146(83), 119(64), 121(48), 93(52), 90(18), 92(13), 66(29), 63(16), 51(13), 50(10)	
6.22	143(100), 142(14), 144(11), 128(15), 115(16), 101(5), 50(5), 51(6)	Probably 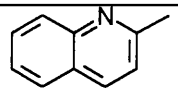 or possibly 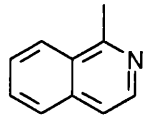
6.46	161(100), 163(75), 165(11) (and others - not ambiguous)	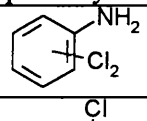
6.59	178(100), 180(67), 182(3), 114(30), 86(20), 88(9), 53(26), 51(20)	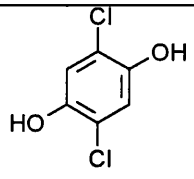 best isomer
6.88	143(100), 142(29), 144(8), 115(30), 89(7)	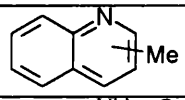
6.95	106(100), 135(62), 107(29), 77(28), 79(11)...	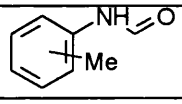
7.13	~As 6.88	As 6.88
8.03	157(100), 156(38), 158(12), 142(17), 141(4), 128(8), 115(6), 76(12), 77(9), 78(5), 104(10)	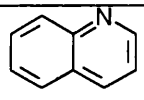 + $-Me_2$
8.22	As 8.03 without 104 peak	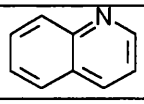 + $-Me_2$
8.57	177(100), 179(38), 115(14) [+154(26)]	Possibly 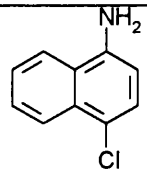
8.98	171(100), 170(23), 172(13), 156(14), 128(8), 127(4), 115(4), 77(5), 63(4), 51(3)	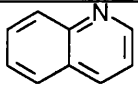 + $-Me_3$

Table 4.33 (continued)

Retention Time	Features	Products
	Note: If the following peak is a mixture as suggested here, then from single ion monitoring the co-elution is near perfect.	
9.18a	195(96), 197(100), 199(43), 160(9), 161(5), 133(17), 134(11), 124(15), 97(16), 62(15), 61(9), 63(9)	Possibly 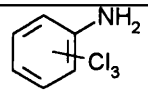
9.18b	170(56), 171(36), 143(7), 115(6)	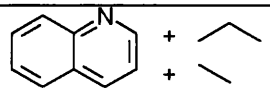 fits best.
9.26	189(27), 191(17), 193(2), 161(48), 163(29), 165(3), 154(100), 156(34), 126(13), 125(7), 99(16), 90(19), 73(10), 75(6), 63(21), 62(10), 52(6)	No NIST. Possibly 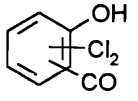
9.80	160(100), 159(16), 161(25), 132(29), 119(17), 92(10), 76(3), 63(6), 42(19), 43(17)	Possibly 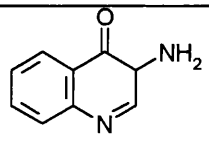 although this should have 104,5@~17%
9.98	Unidentified Aromatic	
10.31	Weak 191(100), 193(32), 190(5), 156(55), 231(9), 77(5), 63(6)	Unidentified
10.46	Probably one product. 43(100), 231(24), 233(16), 196(10), 188(23), 190(20), 187(7), 189(8), 161(27), 163(16), 160(13), 162(11), 169(10), 133(11), 135(6), 124(6), 126(2), 75(2), 63(6)	Unidentified
11.40	Peaks for 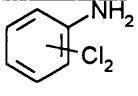 (mw 195), with added 188(97), 190(58), 223(40), 225(50), 227(5)	Need to add a mass of 28, yet retain the strong 195 peak. Perhaps 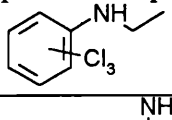
12.31	**Major Peak	Perhaps 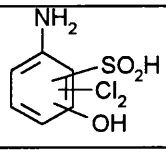

Table 4.33 (continued)

Retention Time	Features	Products
12.76	145(100), 147(70), 225(96), 227(52), 161(54), 162(32), 163(31), 164(28), 109(54), 74(32), 75(18), 64(31), 43(50)	Possibly 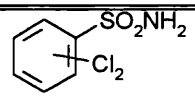
13.87	Cl_3 @273,245,211,212(w).....	Possibly 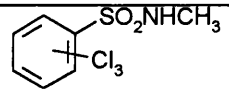 Many subst^{n}s possible
14.01		A phthalate, probably 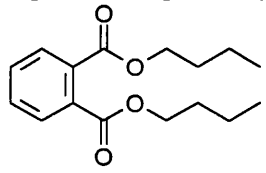
14.31	255(100), 257(68), 259(5), 225(39), 227(29), 191(15), 177(42), 179(25), 178(14), 161(33), 162(24), 163(21), 164(14), 133(26), 135(16), 97(30), 99(8), 73(15), 62(19), 63(16)	No NIST. Not too polar. Perhaps like 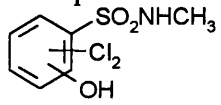
16.70	** Major Peak Cl_2@254(100)+224(49)+176(74)+160(44)+161(44)+133(21) 208(6), 210(4), 190(9), 192(6), 180(8), 124(31), 125(12), 126(12), 127(5), 97(16), 99(7)	No NIST. Possibly like 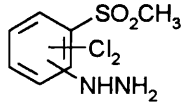
17.10		Unidentified 2Cl aromatic
17.25		Unidentified 3Cl aromatic mw=288
17.52	252(100), 254(29), 253(18), 255(10), 282(1), 223(1), 187(8), 188(5), 189(13), 190(2), 163(3), 126(7) (weak)	Possibly 1Cl aromatic mw=252
17.86	Cl_2@282(21)+176(18) Cl_1@247(100) 224(4), 226(3), 188(3), 190(3), 160(9), 161(7), 162(6), 163(4), 133(8), 135(6)	Unidentified
18.03	Cl_1@255(100), 247(5), 127(2)	Unidentified
18.16	Cl_2@296(30), 254(66), 224(25), 160(20), 161(27) Cl_1@261(100) 43(95)	Like 16.70 with a $-C_3H_7$ group

Table 4.33 (continued)

Retention Time	Features	Products
18.42	Similar to above, with relatively strong 43 peak +2Cl pattern@324(38)	Unidentified
19.36	Cl_1@286(88) 149(100), 167(31), 57(43), 254(5), 279(12)	Unidentified
20.17	Cl_1@277(100) 311(1), 248(1), 212(6), 213(3), 214(12), 215(2), 187(3), 138.5(6), 93.5(4)	Unidentified
20.48	324(44), 326(26), 267(100), 269(61), 271(22), 43(36)	Unidentified
21.11		Unidentified hydrocarbon

4.7 MAJOR PRODUCT SUMMARIES AND MECHANISMS

This section contains a summary of the major degradation product for the samples studied in chapter 4 under each of the degradation environments used. Some mechanisms for the formation of the products are suggested. It should be noted that these can only be suggestions, as the exact decomposition route cannot always be unambiguously determined through study of the products alone.

4.7.1 Sandorin Red BN

This sample was degraded under all four of the main sets of conditions; static nitrogen, dynamic nitrogen, dynamic air and flaming conditions. The first two of these studies are presented together here, as the similarity in the conditions resulted in the formation of similar degradation products.

4.7.1.1 Static and Dynamic Nitrogen

Hydrochloric acid was detected as a product from the degradation under static nitrogen. It is reasonable to assume that this was also formed in the dynamic nitrogen atmosphere, but was not detected as the trap temperature was to high to condense this product. Carbon dioxide and HCN were detected under both conditions, with much less of the latter found from the case of dynamic nitrogen atmosphere. Two isomers of dichlorobenzene were the major components of the liquid fractions, with one isomer in considerable excess. The static nitrogen study also produced some traces of trichlorobenzene and dichloroaniline. The dynamic nitrogen study revealed a small amount of benzonitrile.

The structure of Sandorin Red BN is illustrated in Figure 4.39. One side of the structure has been drawn considering the azo-hydrazone tautomerism represented in Figure 4.1. The weak links in the structure have been highlighted.

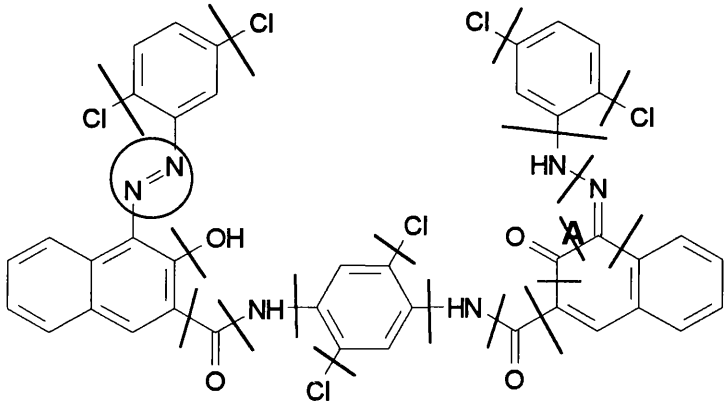

Figure 4.39: Sandorin Red BN weak linkages

The CO_2 was not detected in great amounts. The sensitivity of the SATVA system may have allowed the detection of the small quantity of CO_2 leaked in by the vacuum system from the atmosphere. The HCl probably arose from chlorine radicals breaking away from the aromatic structure, then abstracting a proton from elsewhere on the structure. The source of the third gas detected, HCN, is a little less clear. The hydrazone form may provide an answer.

If the —NH attached to the dichlorobenzene were to depart from the molecule, perhaps through a hydrogen abstraction or collecting a stray H^+, then the dichloraniline would be formed. This would leave an electron deficient CN^+ on the ring structure. The oxygen of the neighbouring carbonyl on the ring may support the breaking of bond A to provide electrons to the CN^+, forming a benzonitrile attached to the remainder of the colourant. This nitrile may be that forming the HCN, or the

benzonitrile may be released whole. It should be noted that benzonitrile was only detected when there was less HCN formed — the dynamic nitrogen case.

The remaining major products were the dichlorobenzene isomers. It may be of some relevance to interpreting the finding of more than one isomer to note that there was also a small amount of trichlorobenzene detected. One isomer, *p*- dichlorobenzene, could be expected as a degradation product, arising from any of the three chlorinated benzene rings in the structure. It is also known that HCl is a degradation product. The HCl or the chlorine radicals implicated in its formation may react with the benzene rings to produce a chlorine substitution at any point (or more likely the point of cleavage) on the ring. The only weakness in this theory is the absence of benzene or chlorobenzene in the product fraction. It should be noted that there was only a small amount of trichlorobenzene found, so there may have been insufficient of these other materials for detection. They also fall between the volatilities for gas and liquid detection giving a reduced sensitivity for SATVA.

4.7.1.2 Dynamic Air

There was now much more CO_2 evolved than in the degradation interpreted above. HCN was also still present. The dichlorobenzene isomers were still the major components of the liquid fraction, but there was also some dichlorophenol detected.

The increase in the CO_2 detected may be due to the oxidation of the residue. Alternatively, it may have been formed more directly. The explanation suggested for the formation of HCN given in section 4.7.1.1 leaves a carbonyl on the broken

naphthalene ring, which may be a source. There are also the carbonyls on the amide linkages.

The dichlorophenol may have formed through the azo linkages leaving as N_2 leaving a dichlorobenzene radical. This may be liable to form a peroxide which would degrade into the phenol.

4.7.1.3 Flaming Conditions

CO_2 and water were the major products. The liquid fraction contained much the same products as in section 4.7.1.2 with a few other oxidation products also present. This was the only condition in which CRF data was obtained. The strongest peaks were due to a phthalate and an unidentified aliphatic hydrocarbon. These were probably contaminants. Phthalate often arises as the platiciser in the sample bottle caps. After this discovery, sample bottles with foil lined resin caps were used. Other products included what appeared to be 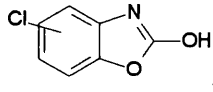

, 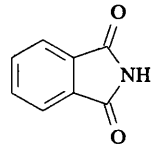

and 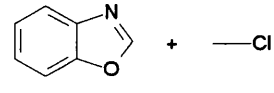

.

The first and third of these offer an explanation as to what became of the amide link on degradation. There would appear to be a cyclisation involving the central dichlorobenzene, involving oxidation in the first case, and chlorine loss in both examples.

4.7.2 Sandorin Scarlet 4RF

This sample was degraded under three environments, dynamic nitrogen, dynamic air and flaming conditions. The presence of a —CF_3 group meant that analysis of the degradation products was difficult. Reference spectra were hard to find for such relatively unusual materials.

4.7.2.1 Dynamic Nitrogen

A small amount of CO_2 was detected, along with a trace of HCN. The two major components of the liquid fraction were dichlorobenzene (one isomer) and 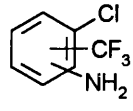

with less 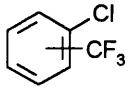

also detected. There was also a small amount of benzonitrile detected. CRF data was available, but the nature (fluorinated) of the products meant that identification was difficult. There were high molecular weight (>250) species, and example of multiple chlorination. This last observation suggests the presence of HCl, as described in section 2.7.1.1.

The structure of Sandorin Scarlet 4RF is shown in Figure 4.40, with the most likely points for degradation marked with hatched lines. The right side of the molecule has been drawn considering the azo-hydrazone tautomerism.

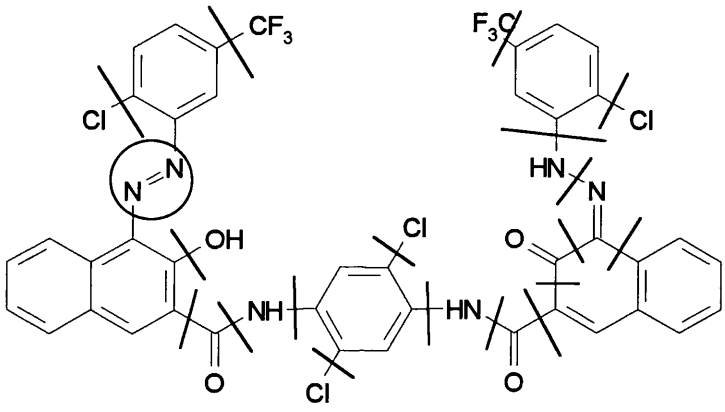

Figure 4.40: Sandorin Scarlet 4RF weak linkages

There was only one dichlorobenzene isomer detected, unlike the two found for the degradation of Sandorin Red BN. This suggests that the terminal dichlorobenzenes were the source of the other isomers, through either isomerisation of these dichlorobenzenes or more than one substitution present in the starting material. Clearly, for the Sandorin Scarlet 4RF there is only one obvious source for the dichloromethane.

The other major component of the liquid fraction, 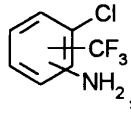

, was probably from the cleavage of the N—N bond of the hydrazone tautomer. The 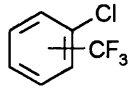

may have been formed from the pendant groups with loss of N_2 if the azo form was present. It may be suspected that only one tautomer is present at a time, in which case this product may be formed less directly, perhaps through decomposition of the previous aniline. Maybe the temperatures attained during the degradation process resulted in an equilibrium between the two tautomers, with the hydrazone in slight excess.

The CO_2 may by from the atmosphere, as suggested in section 4.7.1.1. Similarly, the HCN and the benzonitrile may have occurred through the mechanism suggested in section 4.7.1.1 for the degradation of Sandorin Red BN.

4.7.2.2 Dynamic Air

There were few products detected here, so no meaningful conclusions may be drawn.

4.7.2.3 Flaming Conditions

This sample did not ignite, probably due to the halogens present in the structure. CO_2 and water were the major products. N_2O was also detected, along with two isomers of 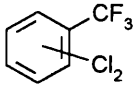

and one of 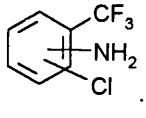

. The N_2O may be from the apparatus or the azo linkage, and the source of the 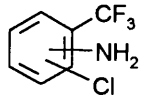

has been suggested in 4.7.2.1. The doubly chlorinated product is the only new one observed. Study of the structure in Figure 4.40 shows that this is not a simple fragment of the colourant. HCl is a probable undetected product, as was observed for the degradation of Sandorin Red BN. This may result in chlorination in the bulk of the sample, as the evolved gas will take a finite time to depart from the degrading sample. Consequently, chlorination may be observed at unexpected locations in the products. Alternatively the —CF_3 may have migrated onto the central dichlorobenzene segment. It is regrettable that so few materials are found in the evolved products, due to the small amount produced relative to the level of water.

4.7.3 Graphtol Fast Red 2GLD

This sample was most similar in structure to the Sandorin Red BN, differing by having a —SO_2NHCl group, and having only one azo section with the bridging dichlorobenzene replaced with a toluene substitution. The sample was degraded under dynamic nitrogen, dynamic air and flaming conditions.

4.7.3.1 Dynamic Nitrogen

The only gaseous product detected was a small amount of CO_2, perhaps from the air background. Methylaniline was by far the major component detected in the liquid fraction. The remainder were relatively trace, and included naphthalene, aniline and dichlorobenzene. There was also a small amount of a fluorinated product, which was probably a contaminant for the previous sample. This stands as a reminder of the possibility of contamination between analyses. All the other volatile materials are likely degradation products from the Graphtol Fast Red 2GLD.

The structure of Graphtol Fast Red 2GLD, with the weak linkages in the molecule highlighted, is shown in Figure 4.41. The hydrazone form has been illustrated. The products detected in the dynamic nitrogen degradation are consistent with the azo structure, although it will be shown that the dynamic air and flaming studies imply that the hydrazone is present.

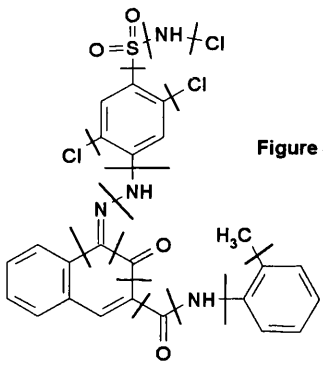

Figure 4.41: Graphtol Fast Red 2GLD weak linkages

The right hand aromatic ring clearly sourced the major product of methylaniline. Dichlorobenzene and naphthalene were detected, but no dichloroaniline or benzonitrile. These absent materials would be expected from the hydrazone form, as described for the degradation of Sandorin Red BN and Sandorin Scarlet 4RF. Loss of nitrogen from the azo link would be an initial step for the formation of naphthalene and dichlorobenzene. The lack of sulphated products was a curiosity. The degradation under flaming conditions shows some possible sulphated materials in the CRF. Aniline was detected in the dynamic nitrogen study. This may be from the loss of —CH_3 from the methyl aniline, or could be the only evidence for the hydrazone form. The loss of chlorine with cleavage of the upper ring at the N—N bond would lead to this product. Also, the loss of a methyl group over the cleavage of an Ar—N bond is thermodynamically favourable, rendering aniline a possible alternative product to the methylaniline.

4.7.3.2 Dynamic Air

HCN was detected, along with a small amount of CO_2. The latter of these may be from the background, as such a small amount was detected. Once again, methylaniline was very much the major component in the cold finger. Dichlorobenzene and naphthalene

were still present, although there was appreciable amounts of dichloroaniline. Benzonitrile, aniline and chloroaniline were also present.

The products which differ from the dynamic nitrogen degradation were relatively minor, but do give strong evidence for the hydrazone tautomer. The explanation suggested for the Sandorin Red BN degradation applies to these new products. The hydrazone form shows a reasonably direct route for the formation of benzonitrile, HCN and dichloroaniline as described in section 4.7.1.1. The difference in the materials obtained under nitrogen and air atmospheres suggests that the oxygen had some effect on the decomposition mechanism, although no direct oxidation products were detected.

4.7.3.3 Flaming Conditions

This sample ignited on the second analysis, when the power output of the heater had increased with time, as described in Chapter 2. CO_2 was now the major gas, with much SO_2 also present. There were smaller amounts of HCN and N_2O detected as well. Water was the major component of the liquid fraction. Disregarding aliphatic hydrocarbons and silicone contaminants, the other products were trichlorobenzene, chlorotoluene, tetrachlorobenzene, biphenyl or vinylnaphthalene, and benzonitrile. There were also some oxygen containing products including phenol and benzaldehyde. There was also a component with a mass spectrum comparable with that of 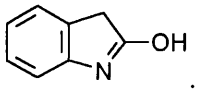

. Due to the presence of sulphur, the interpretation of the CRF GC-MS data was difficult. It would appear that some of the components of this fraction contained —SO_2— linkages, with the major product probably being like

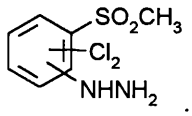

. Some rearrangement of the substitutions could be made to make this match an expected degradation product, such as moving the —NH— link to between the SO_2 and the methyl group. Clearly there is scope for speculation here, rendering definite statements on the products and mechanisms impractical. It may be said, with reasonable confidence, that some -SO_2- linkages remain in the products, and do not depart as SO_2 gas. This observation stands as an explanation of the lack of sulphated compounds present under the dynamic nitrogen and air atmospheres.

Mechanistically, we have slightly more information than normally obtained from degradation under flaming conditions. We have already cast light on the destination of the sulphur. The multiply chlorinated species indicate the migration of chlorine, and perhaps the presence of HCl which will not have been condensed in the dry ice/ acetone trap.

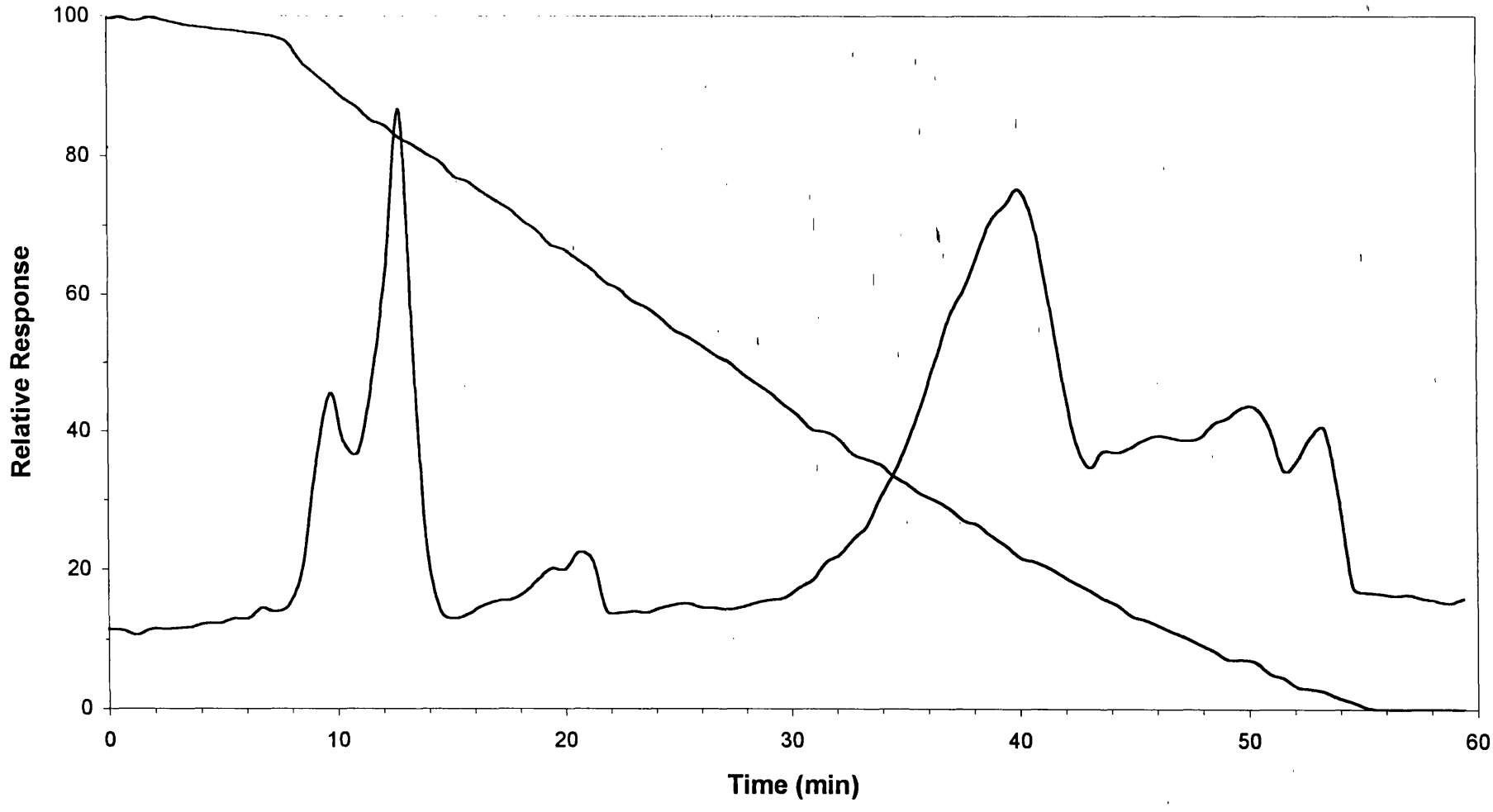

Figure 4.5: SATVA trace from the degradation of Sandorin Red BN under static nitrogen

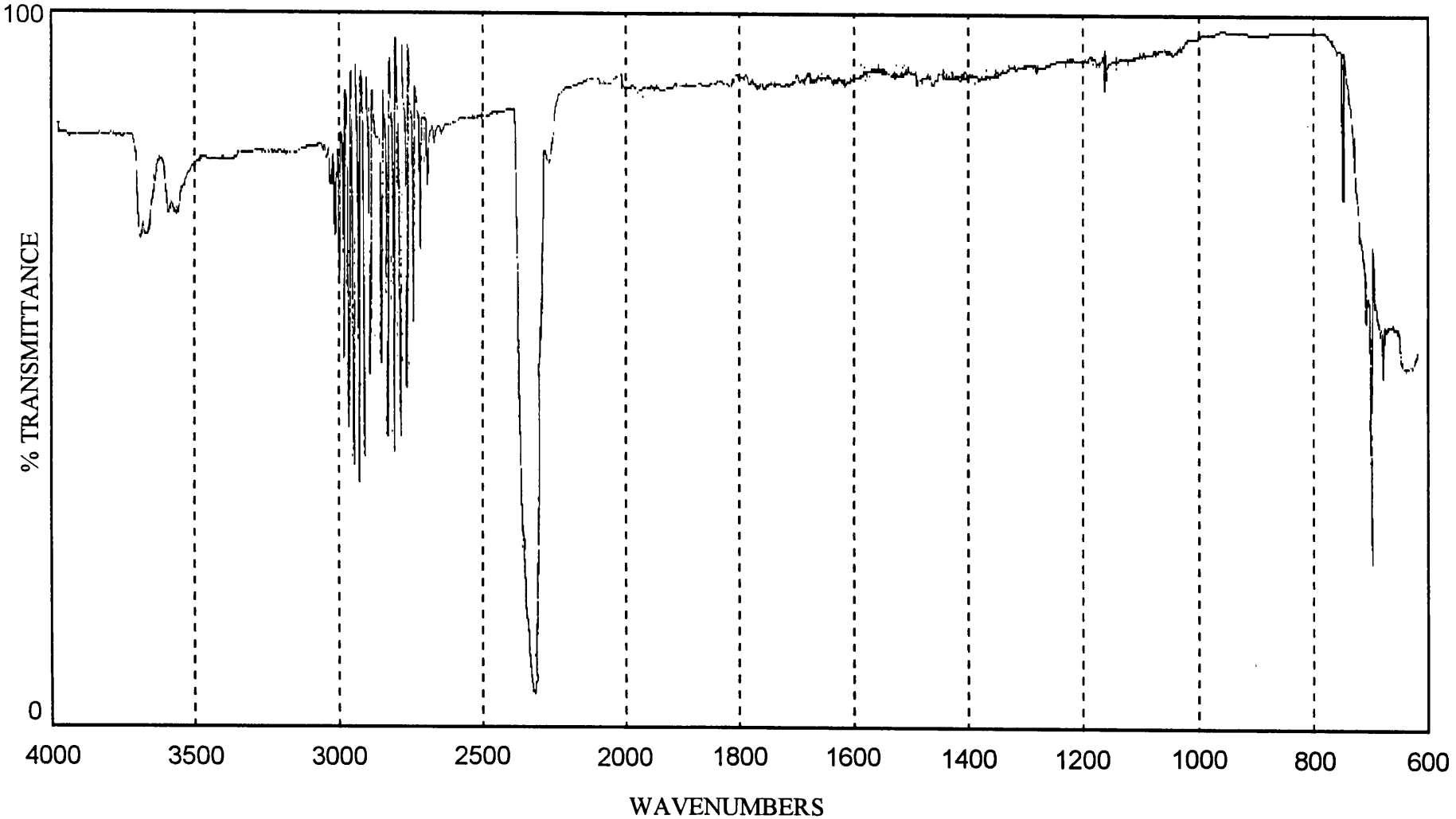

Figure 4.6: IR spectrum for peaks 1 and 2 from SATVA Figure 4.5

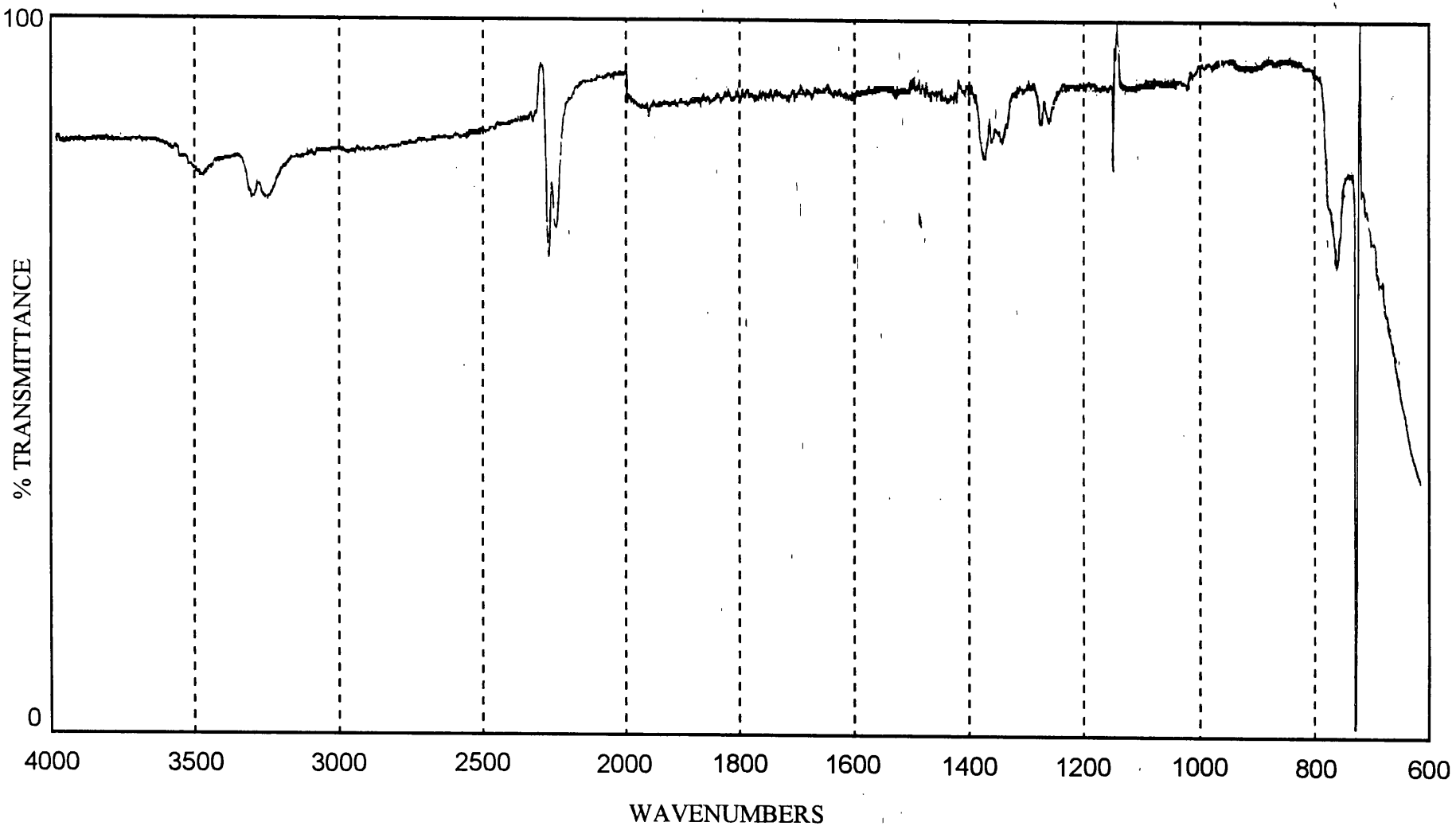

Figure 4.7: IR spectrum for peak 3 from SATVA Figure 4.5

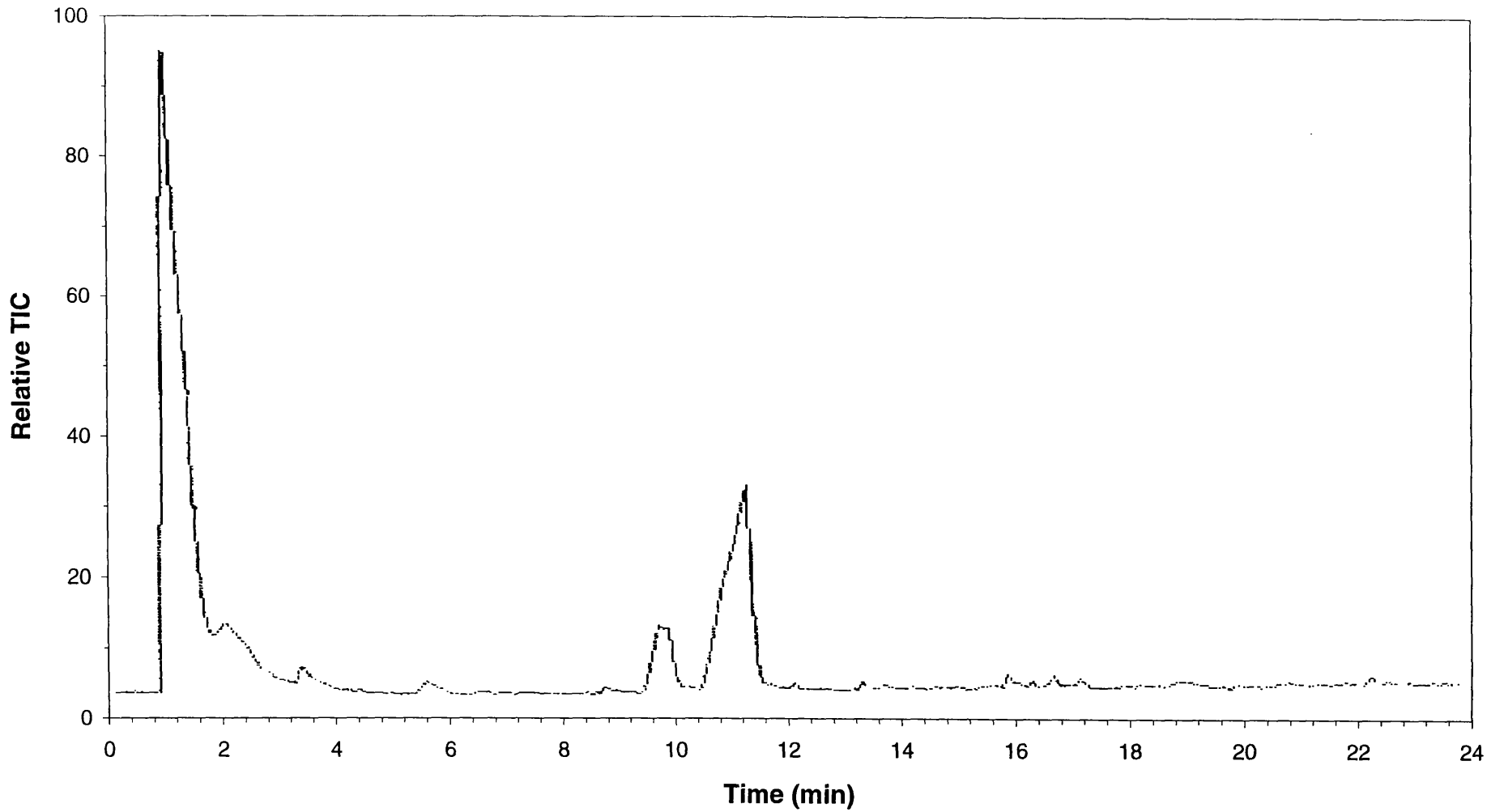

Figure 4.8: TIC trace for the liquid fraction from the SATVA curve in Figure 4.5

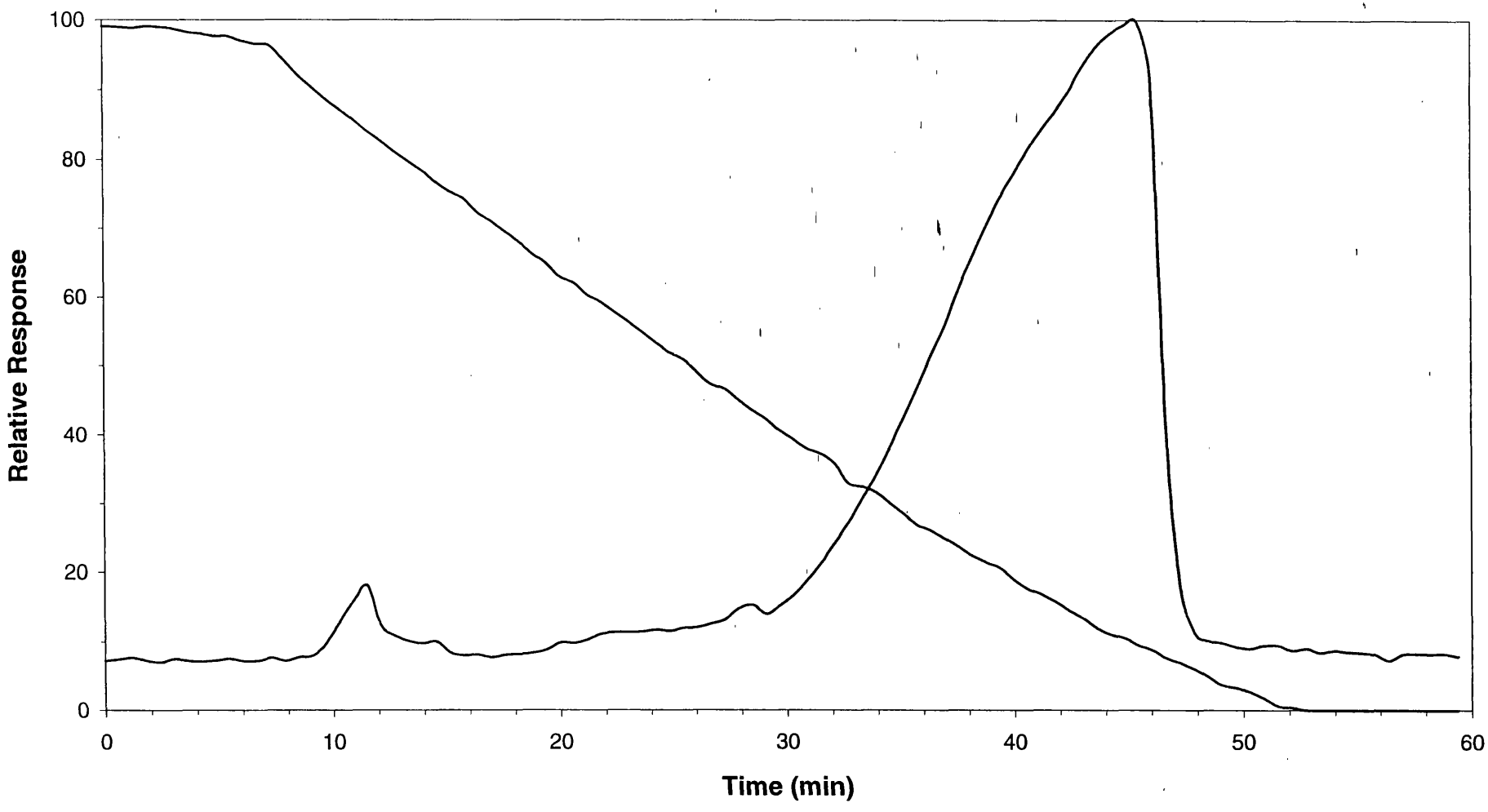

Figure 4.9: SATVA trace from the degradation of Sandorin Red BN under dynamic nitrogen

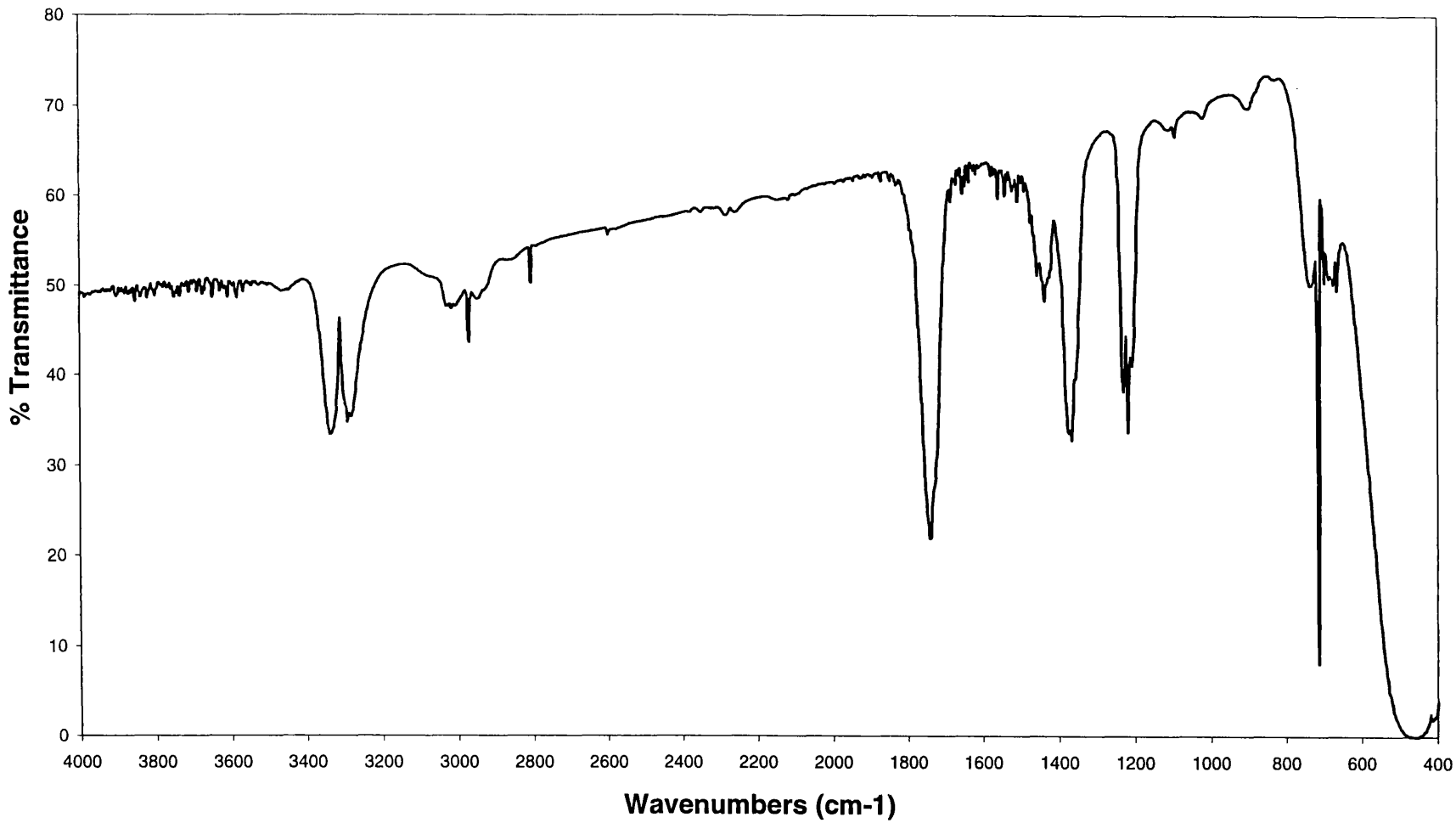

Figure 4.10: IR spectrum from start of peak 2 from SATVA curve in Figure 4.9

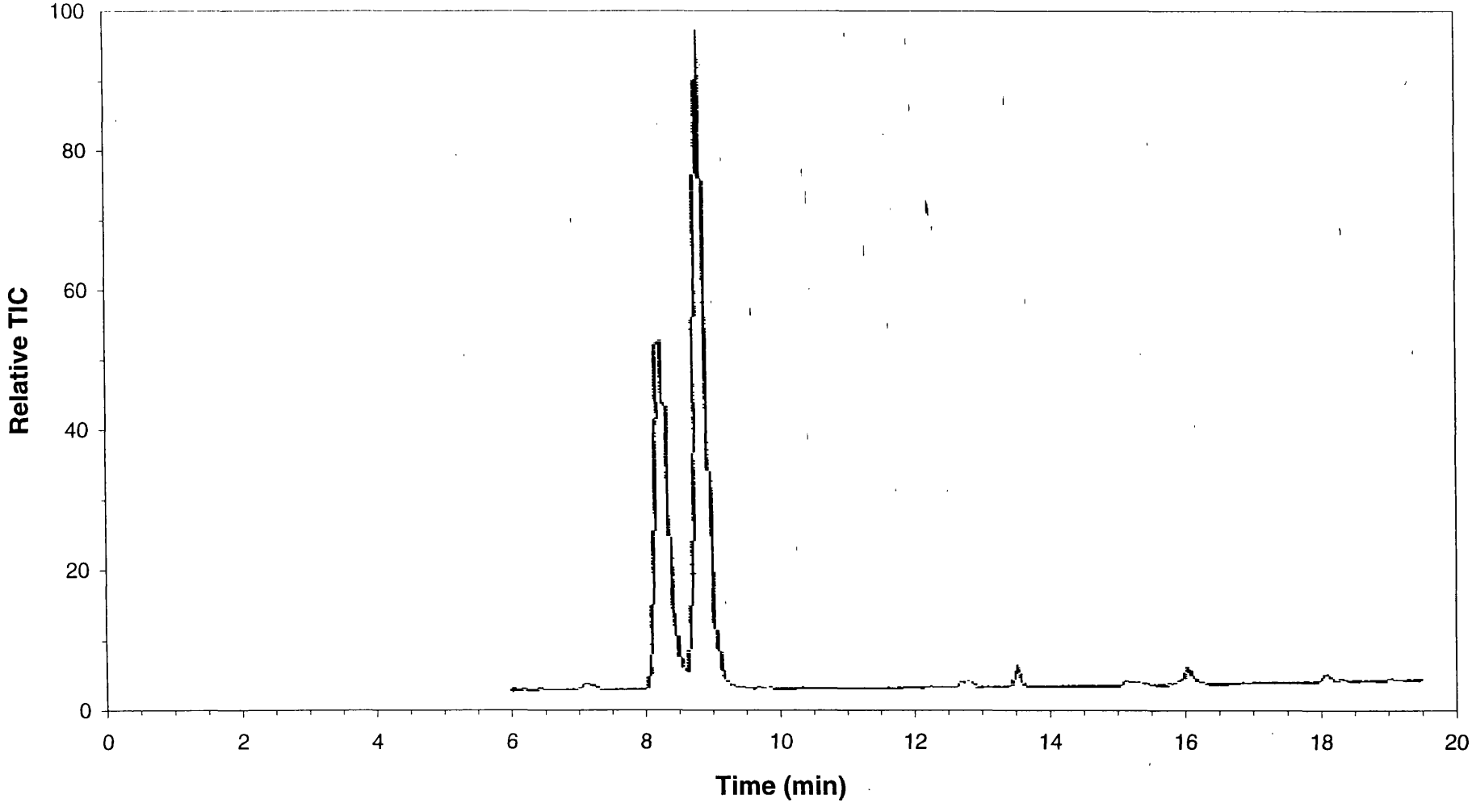

Figure 4.11: TIC trace for the liquid fraction from the SATVA curve in Figure 4.9

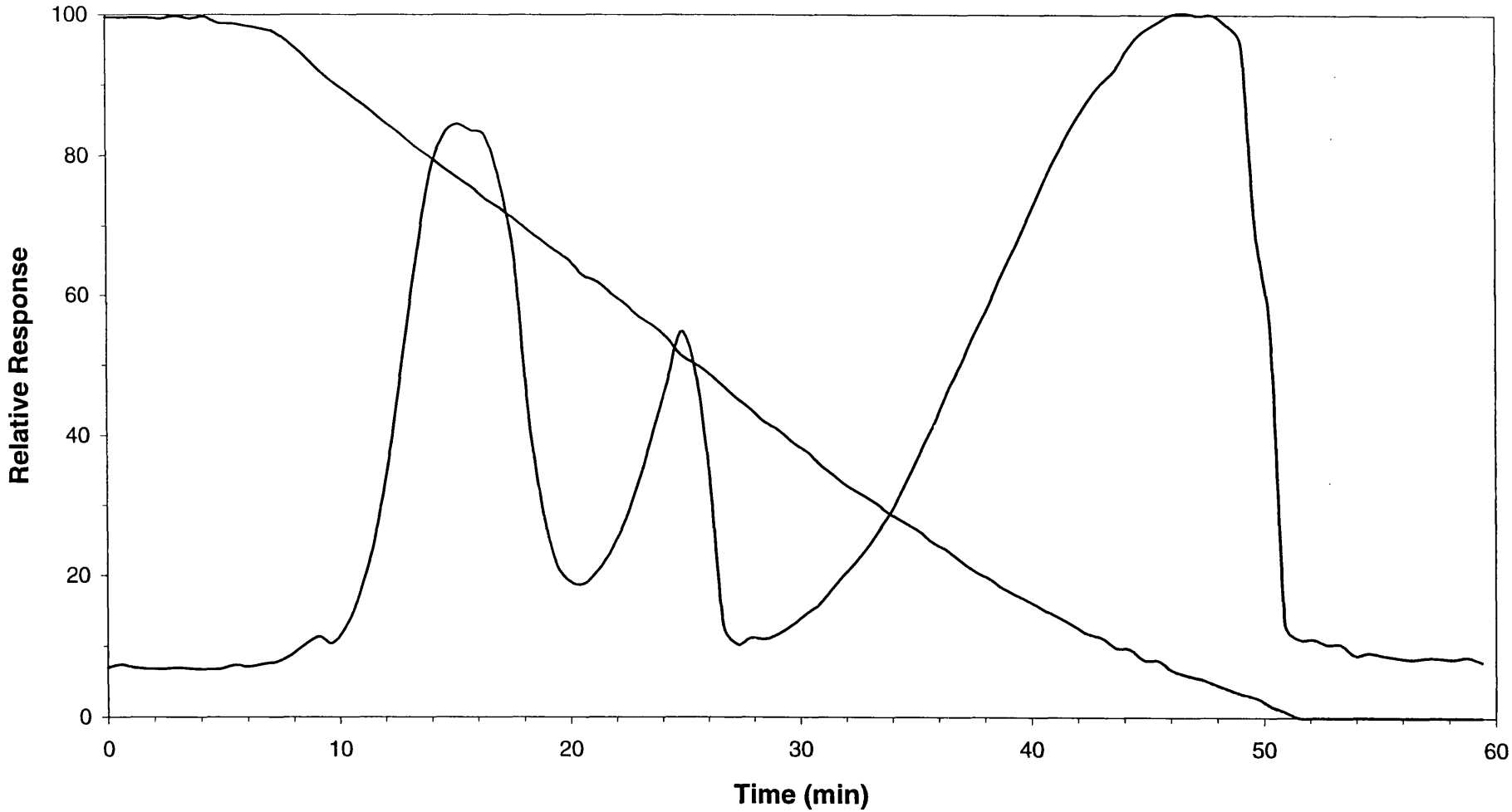

Figure 4.12: SATVA trace from the degradation of Sandorin Red BN under dynamic air

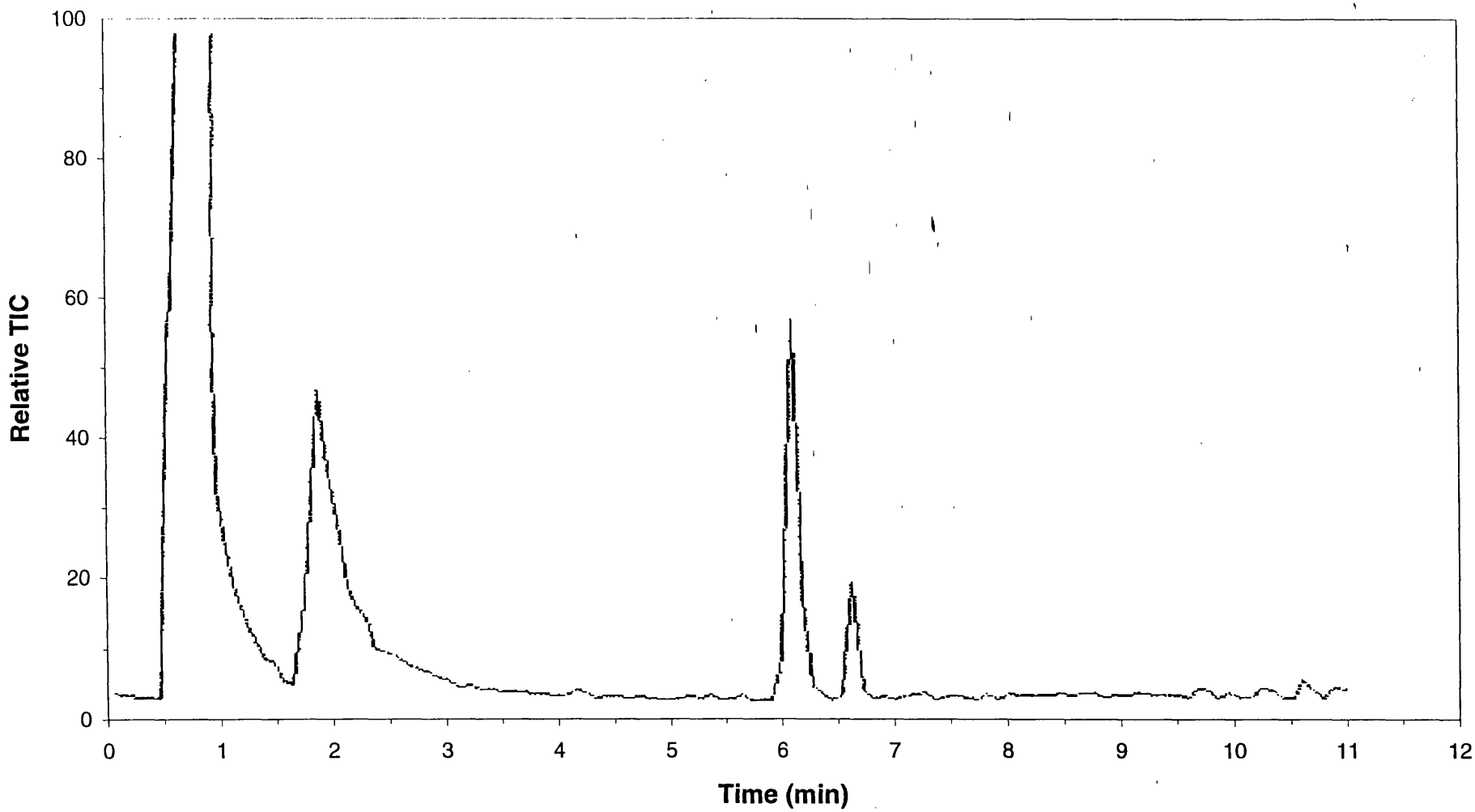

Figure 4.13: TIC trace for the liquid fraction from the SATVA curve in Figure 4.12

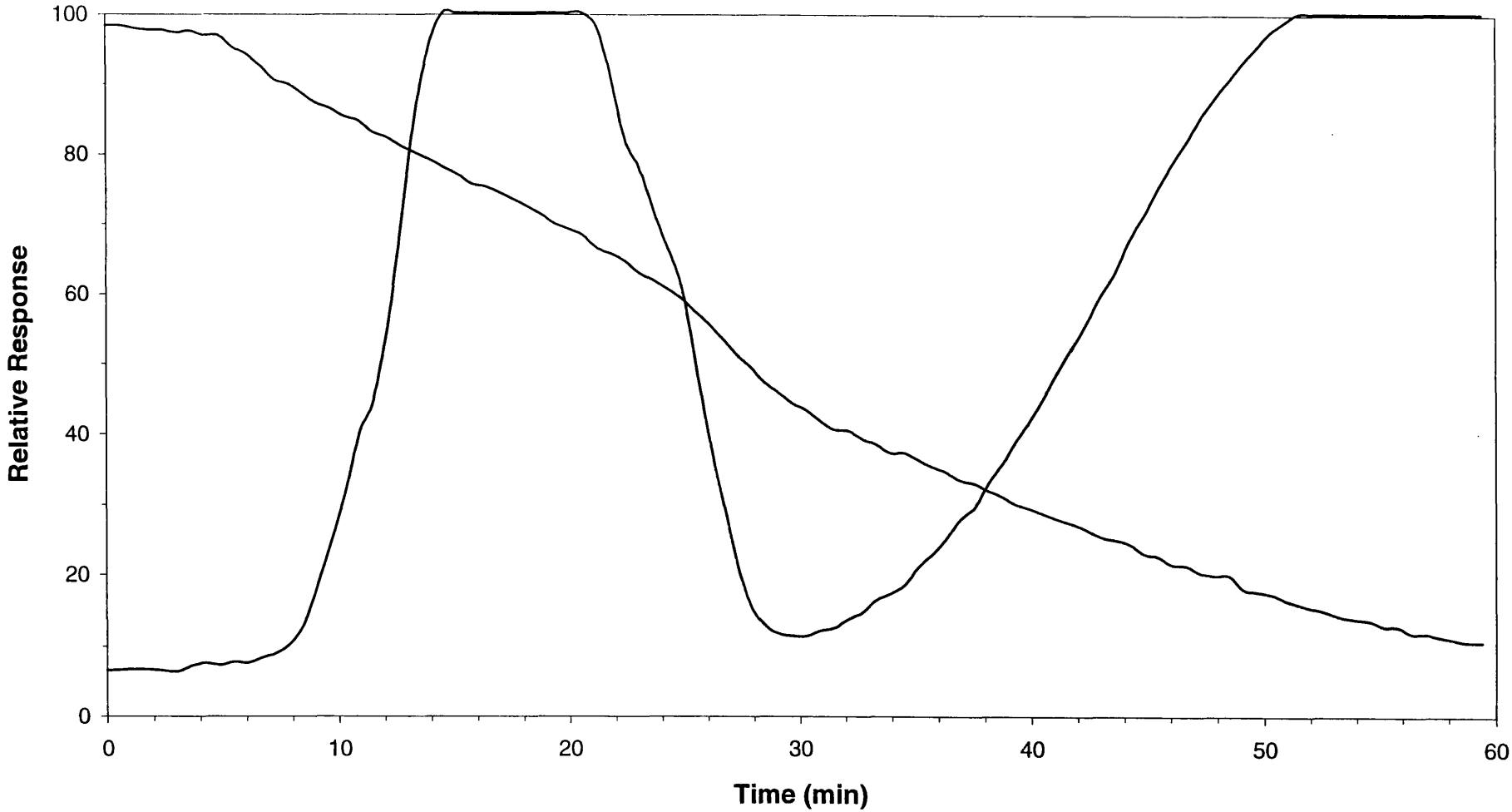

Figure 4.14: SATVA trace from the degradation of Sandorin Red BN under flaming conditions

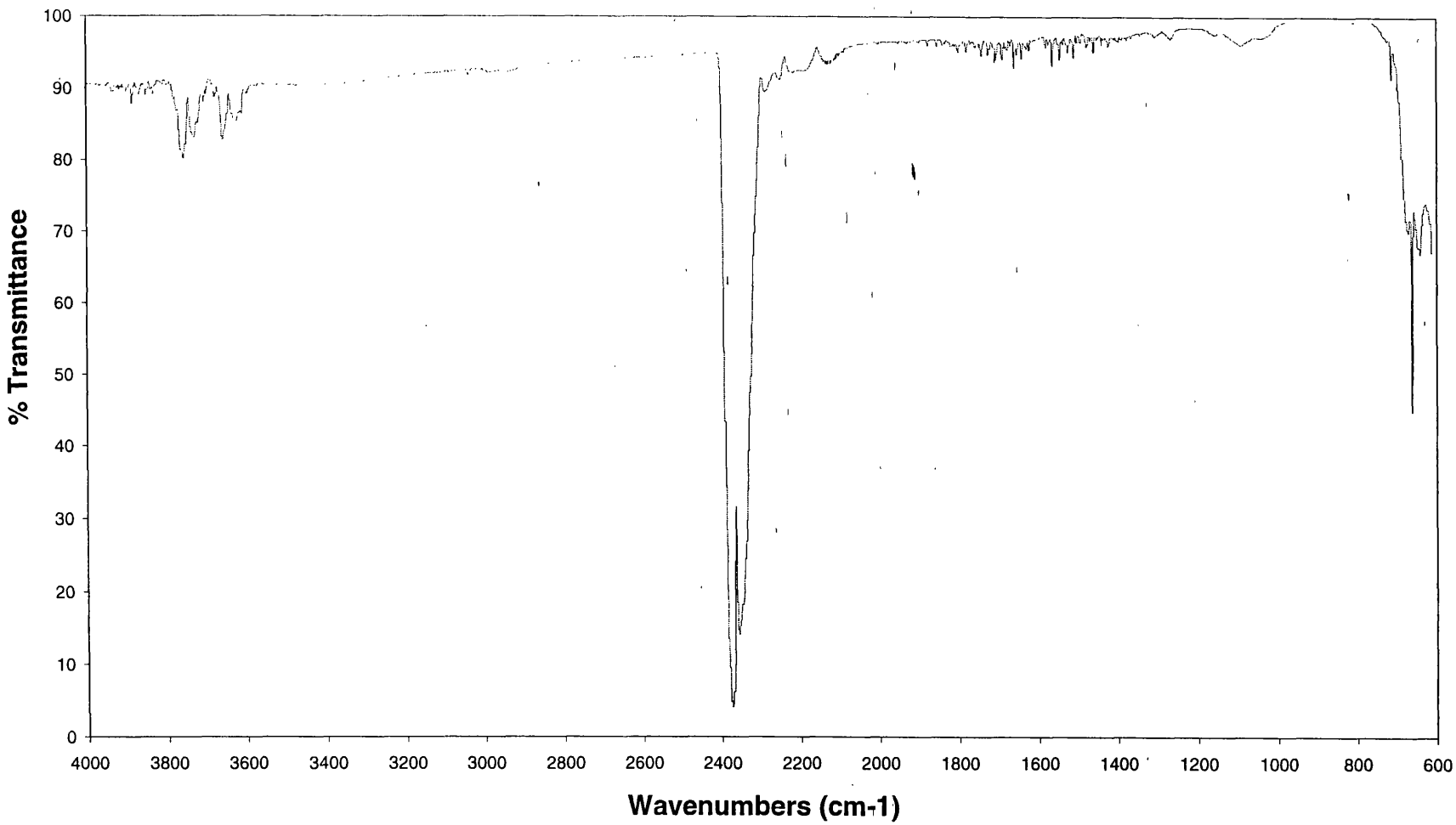

Figure 4.15: IR spectrum for non-condensable gases from SATVA separation in Figure 4.14

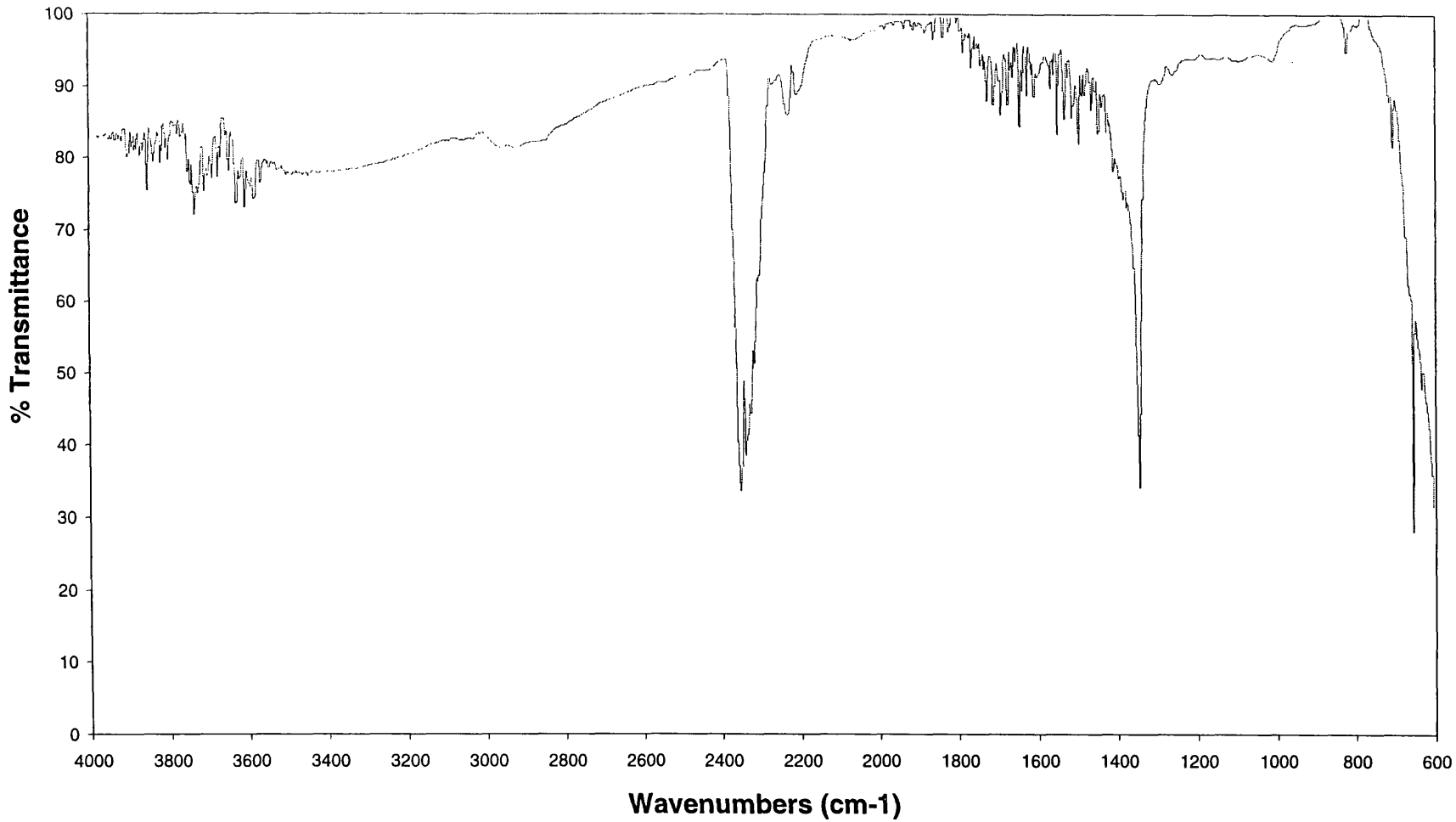

Figure 4.16: IR Spectrum from start of peak 1 from SATVA curve in Figure 4.14

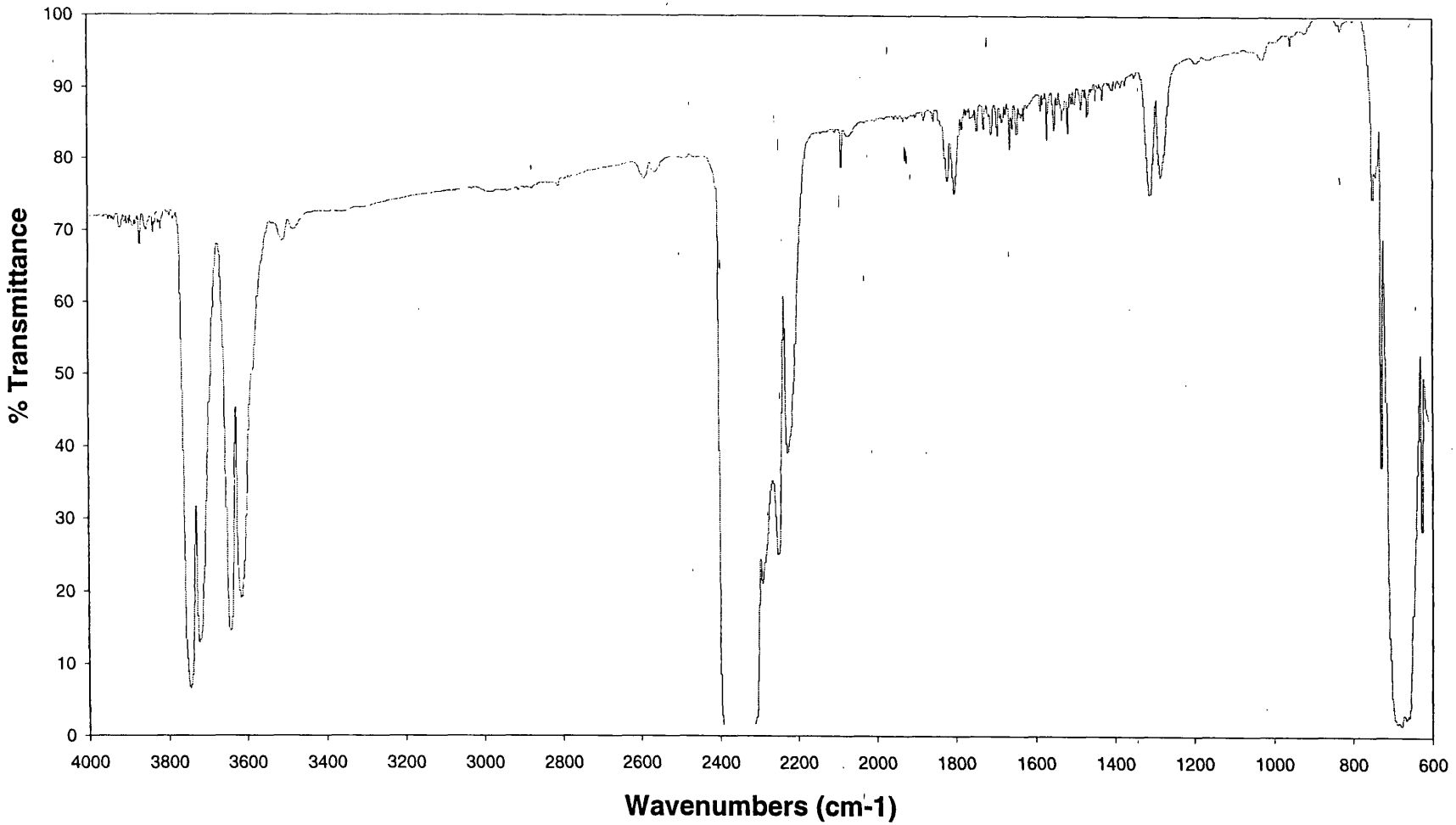

Figure 4.17: IR spectrum for remaining gases from peak 1 from SATVA curve in Figure 4.14

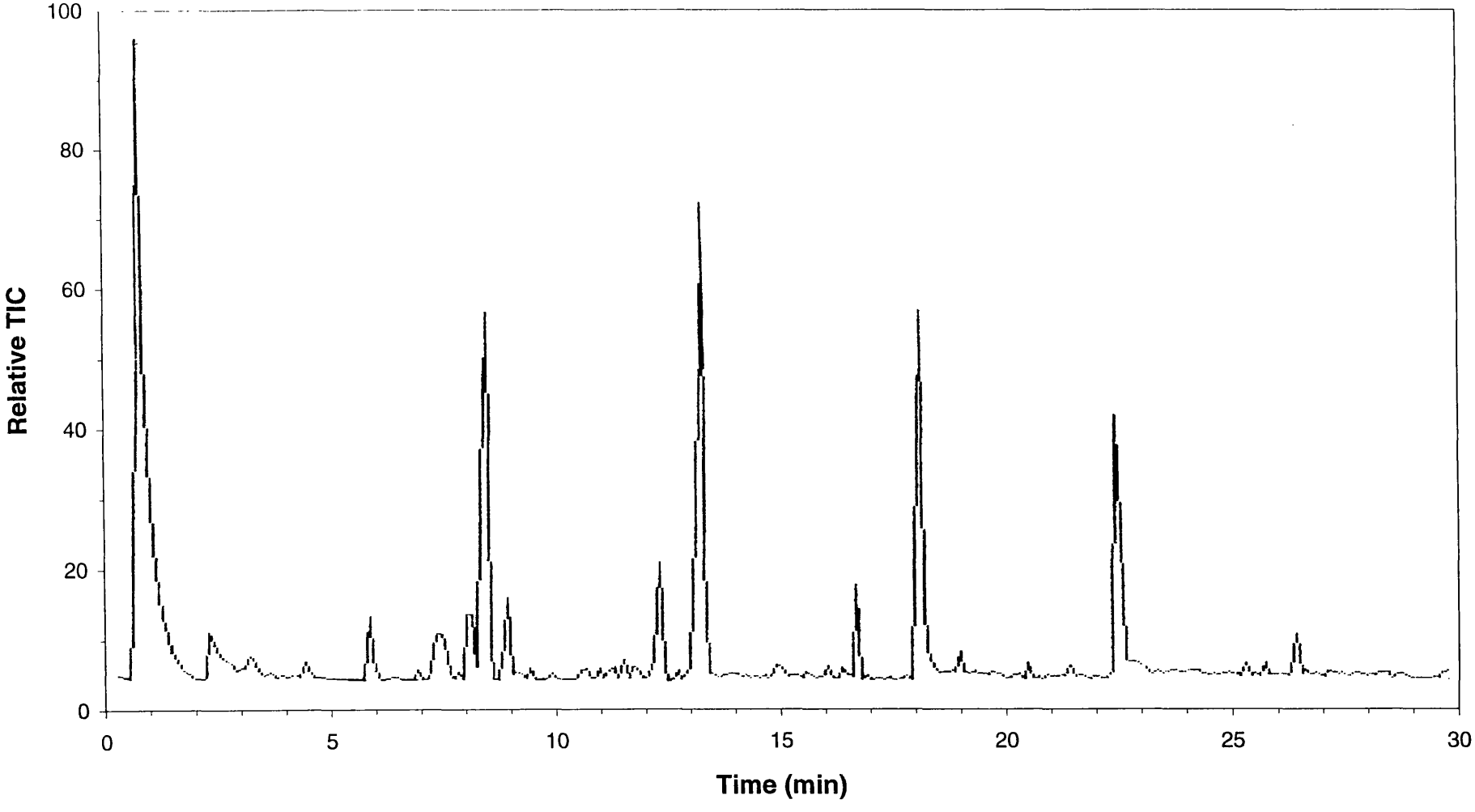

Figure 4.18: TIC trace for the liquid fraction from the SATVA curve in Figure 4.14

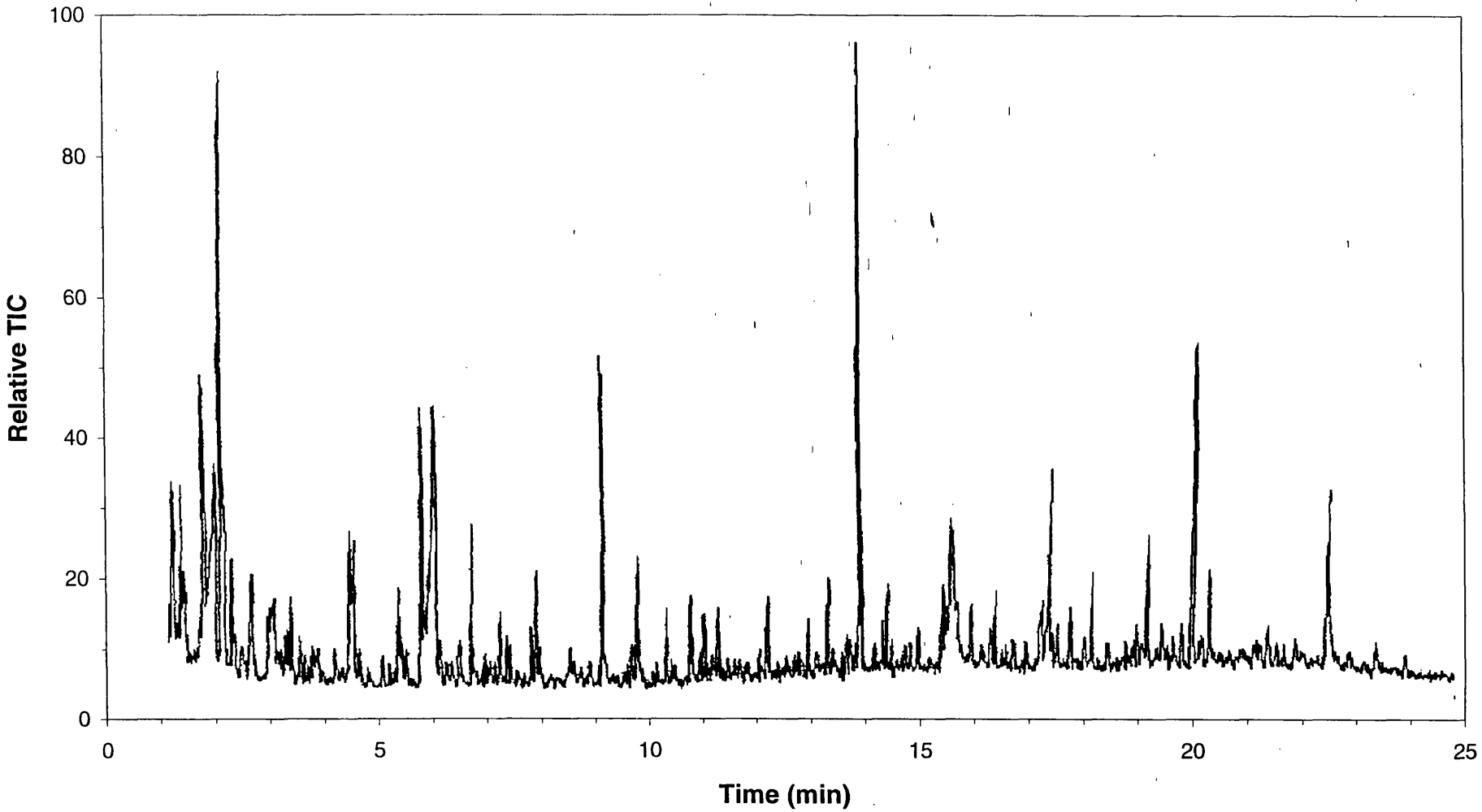

Figure 4.19: TIC trace for the cold ring fraction from the SATVA curve in Figure 4.14

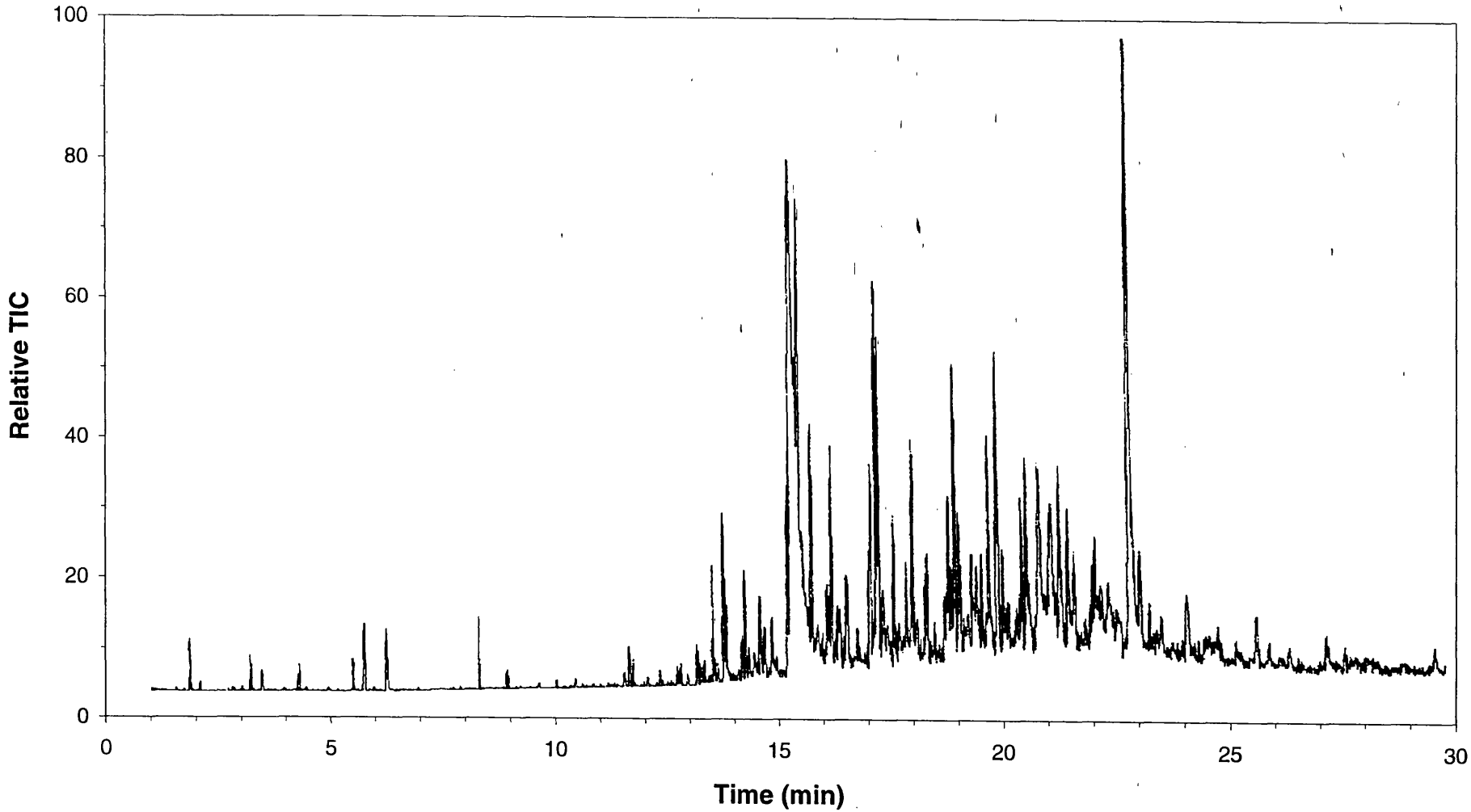

Figure 4.20: TIC trace for the cold ring fraction from the SATVA curve in Figure 4.14

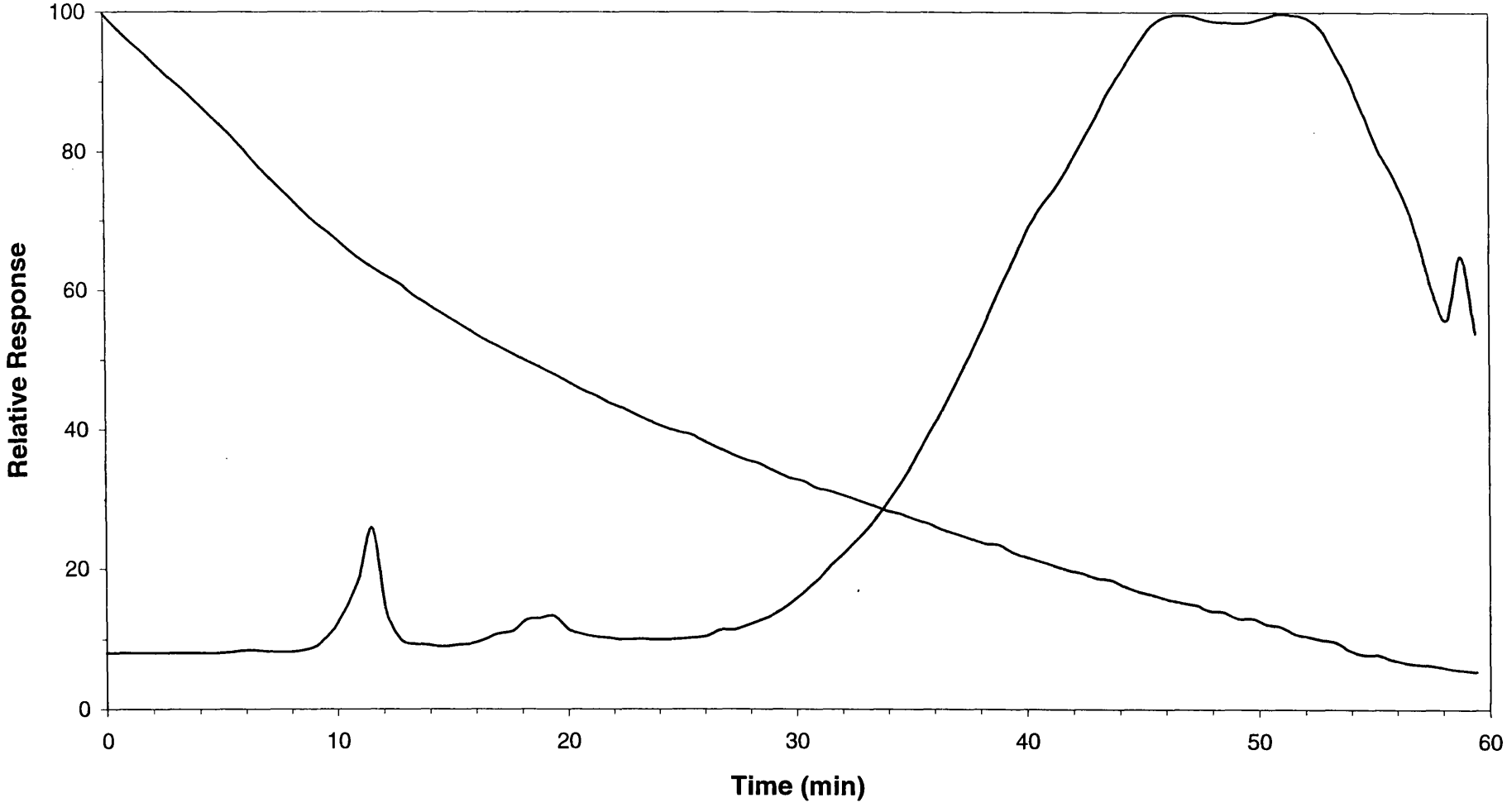

Figure 4.22: SATVA trace from the degradation of Sandorin Scarlet 4RF under dynamic nitrogen

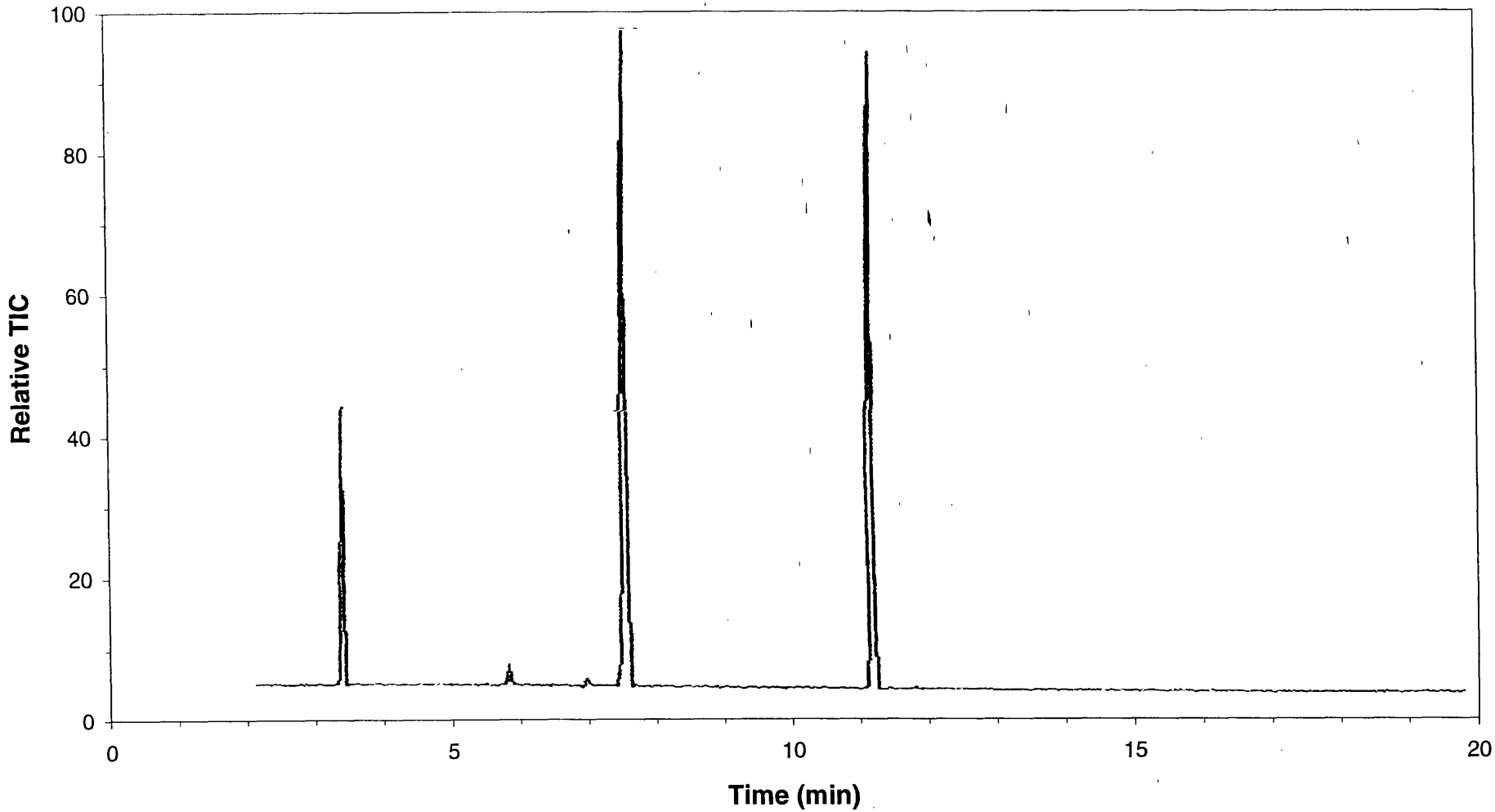

Figure 4.23: TIC trace for the liquid fraction from the SATVA curve in Figure 4.22

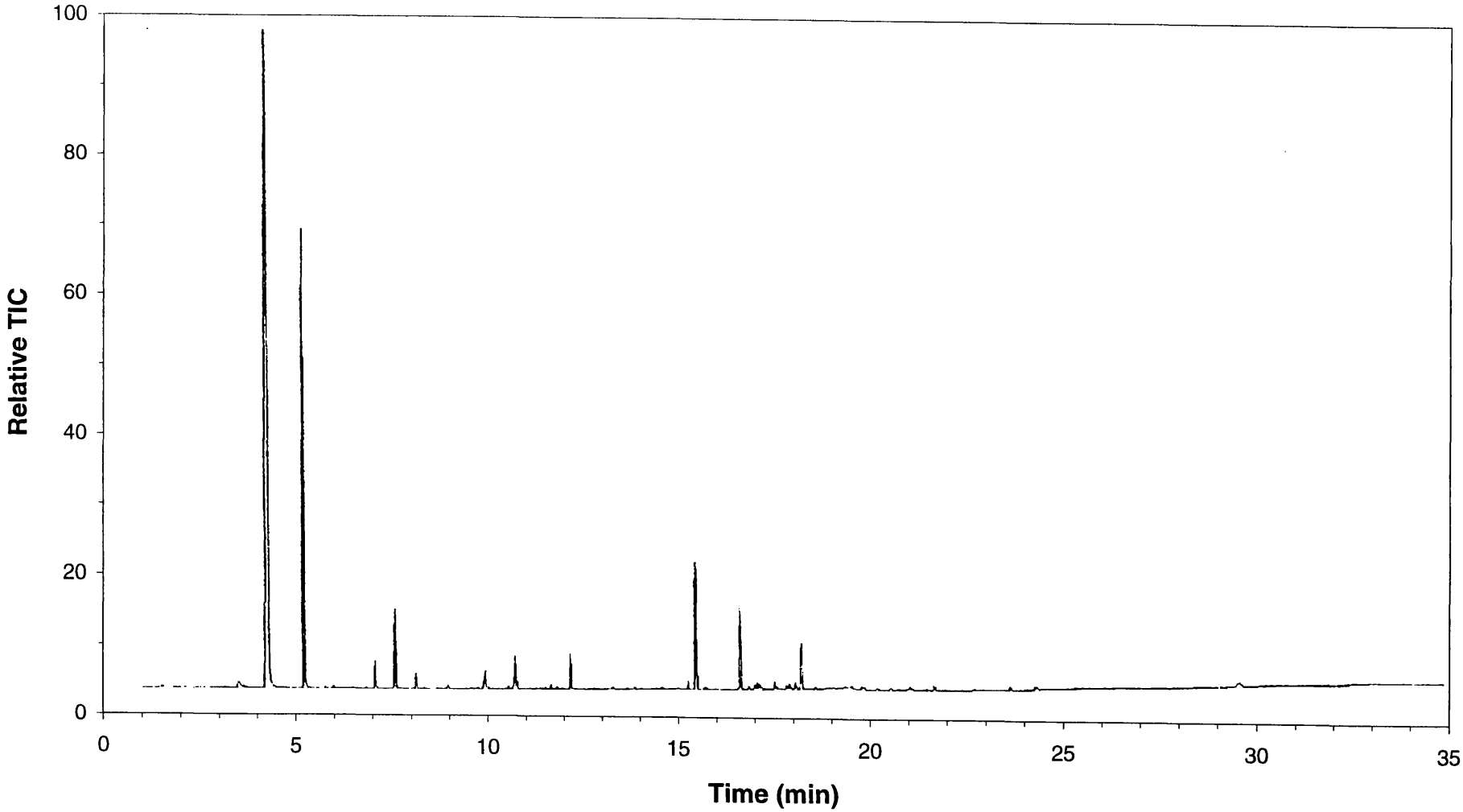

Figure 4.24: TIC trace for the cold ring fraction from the SATVA curve in Figure 4.22

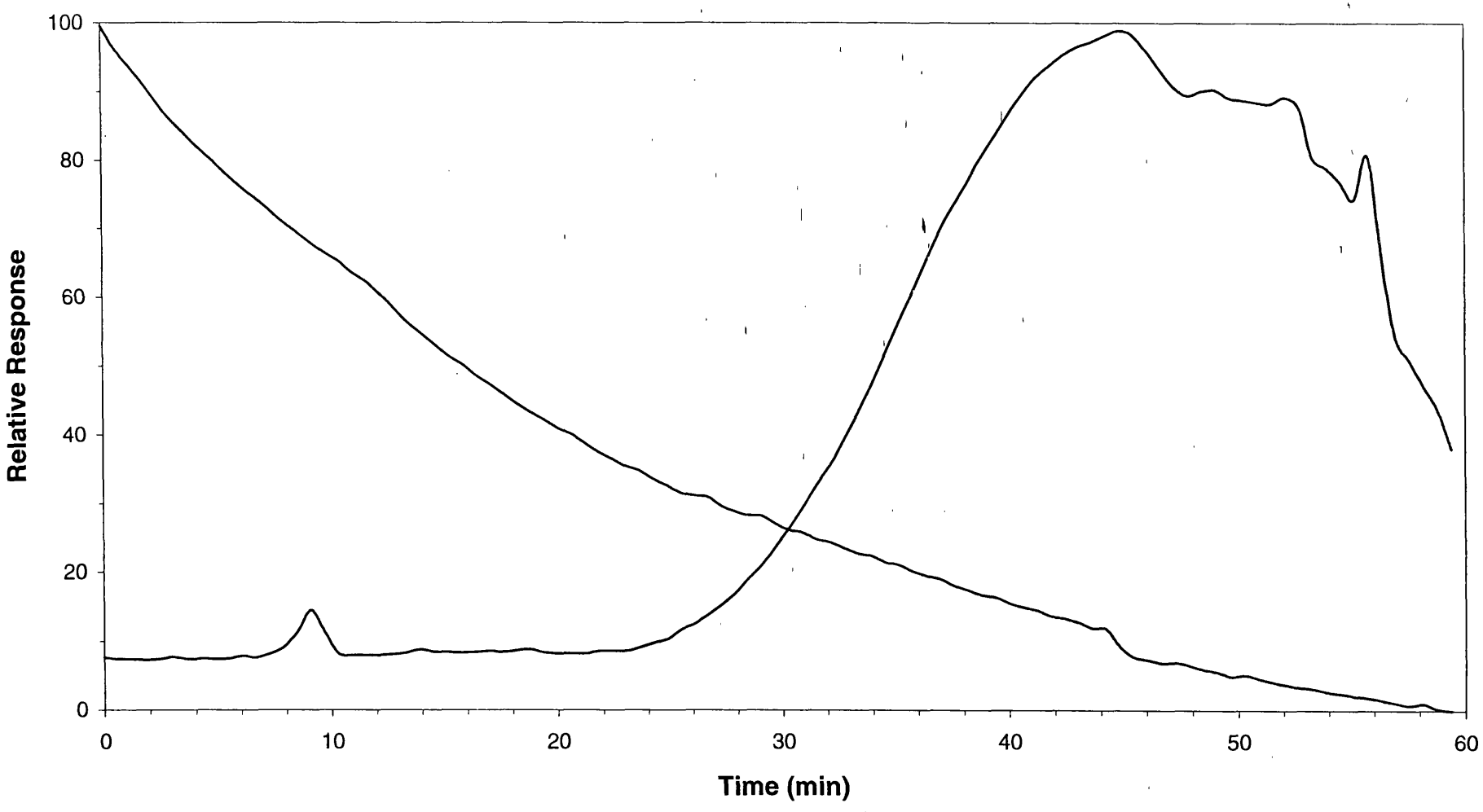

Figure 4.25: SATVA trace from the degradation of Sandorin Scarlet 4RF under dynamic air

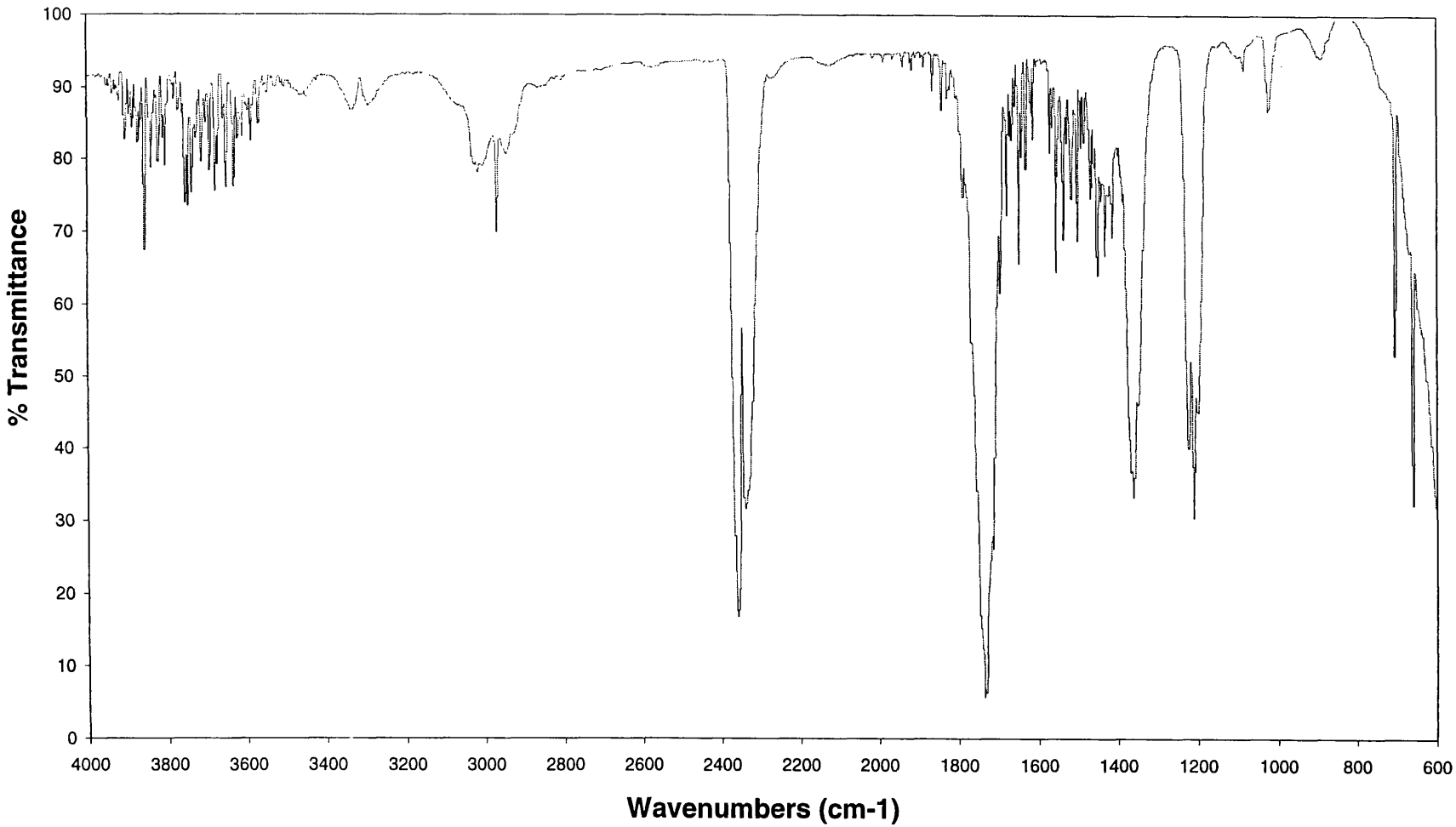

Figure 4.26: IR Spectrum from gas peak from SATVA Figure 4.25

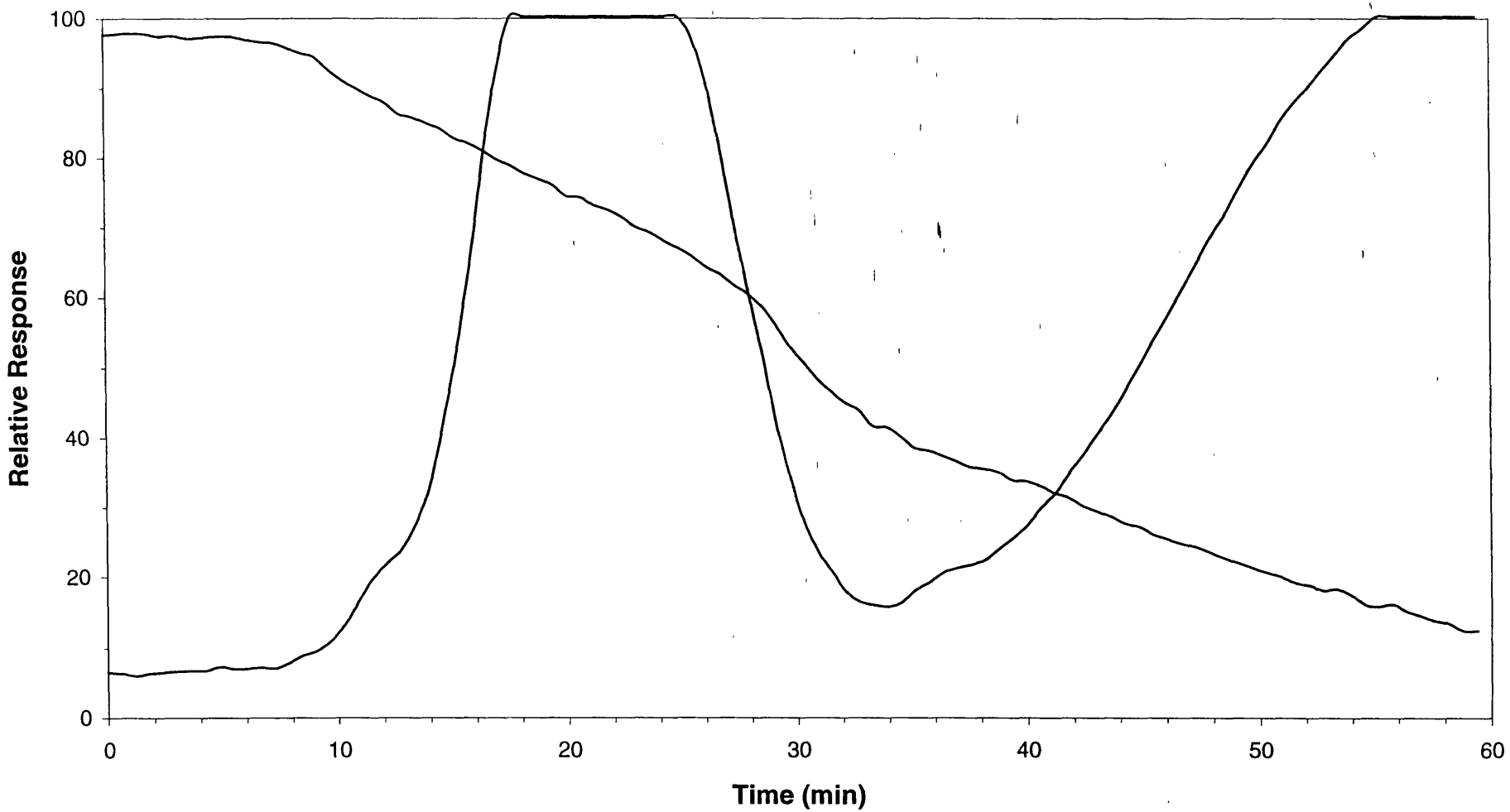

Figure 4.27: SATVA trace from the degradation of Sandorin Scarlet 4RF under flaming conditions

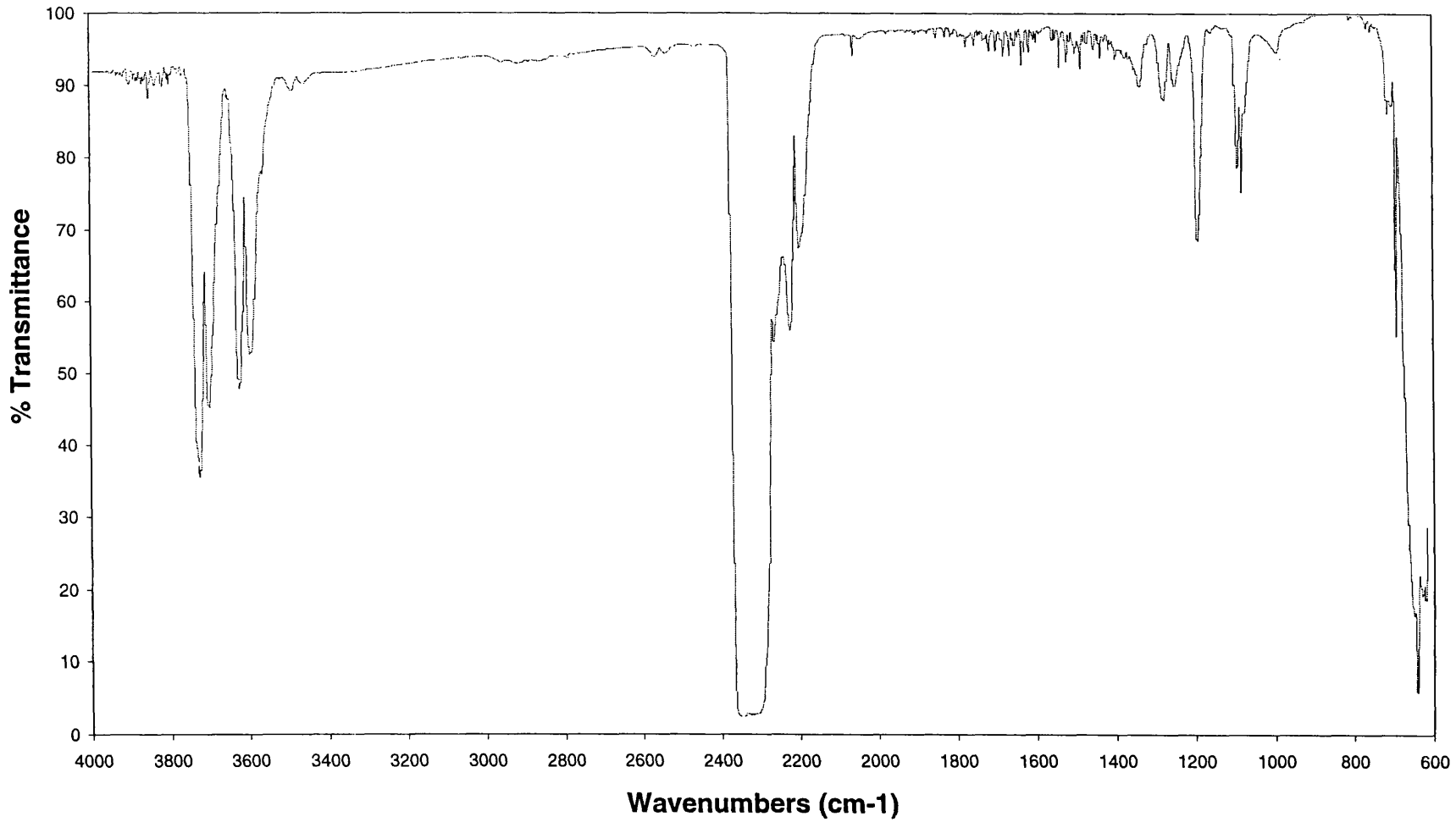

Figure 4.28: IR spectrum from gas peak from SATVA curve in Figure 4.27

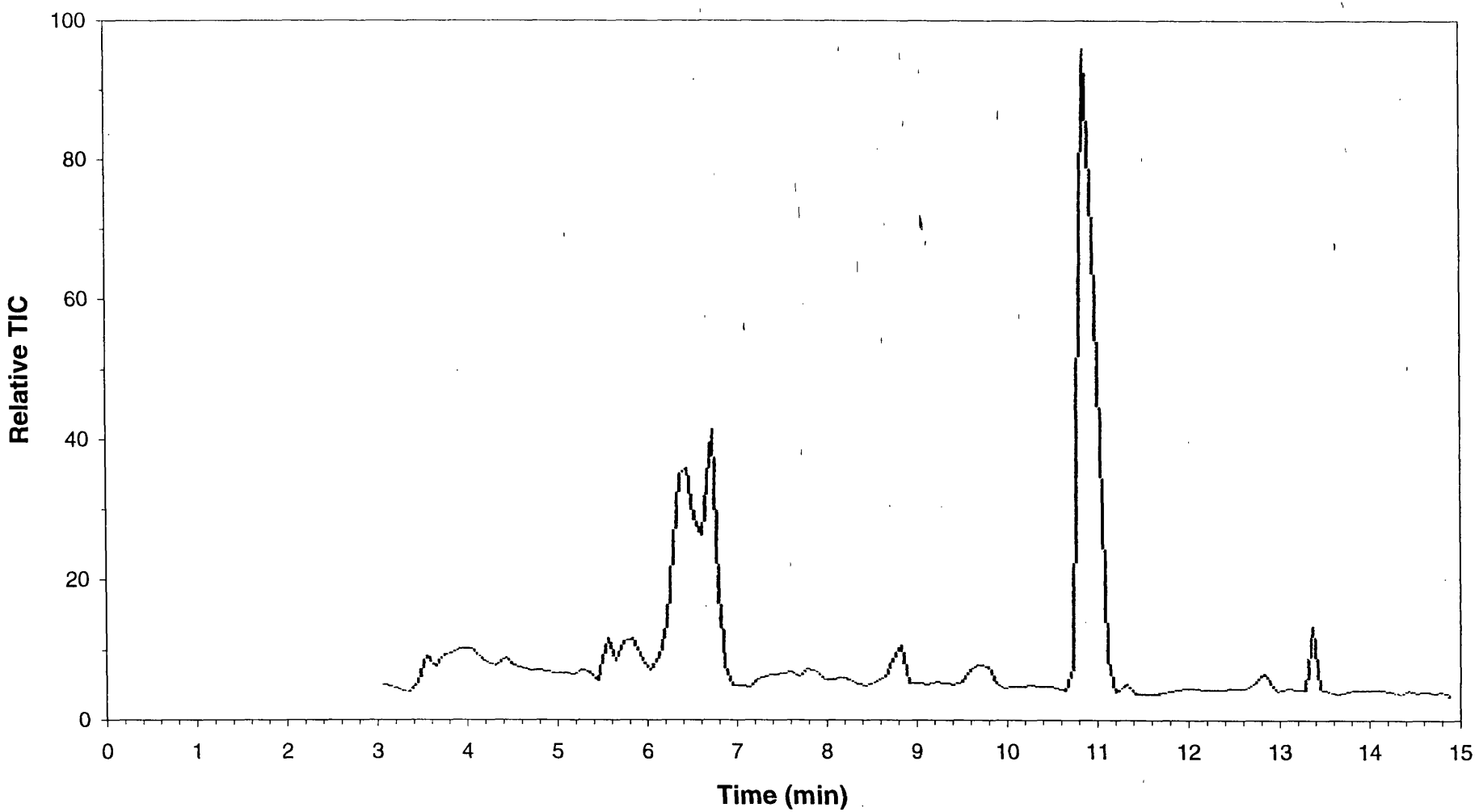

Figure 4.29: TIC trace for the liquid fraction from the SATVA curve in Figure 4.27

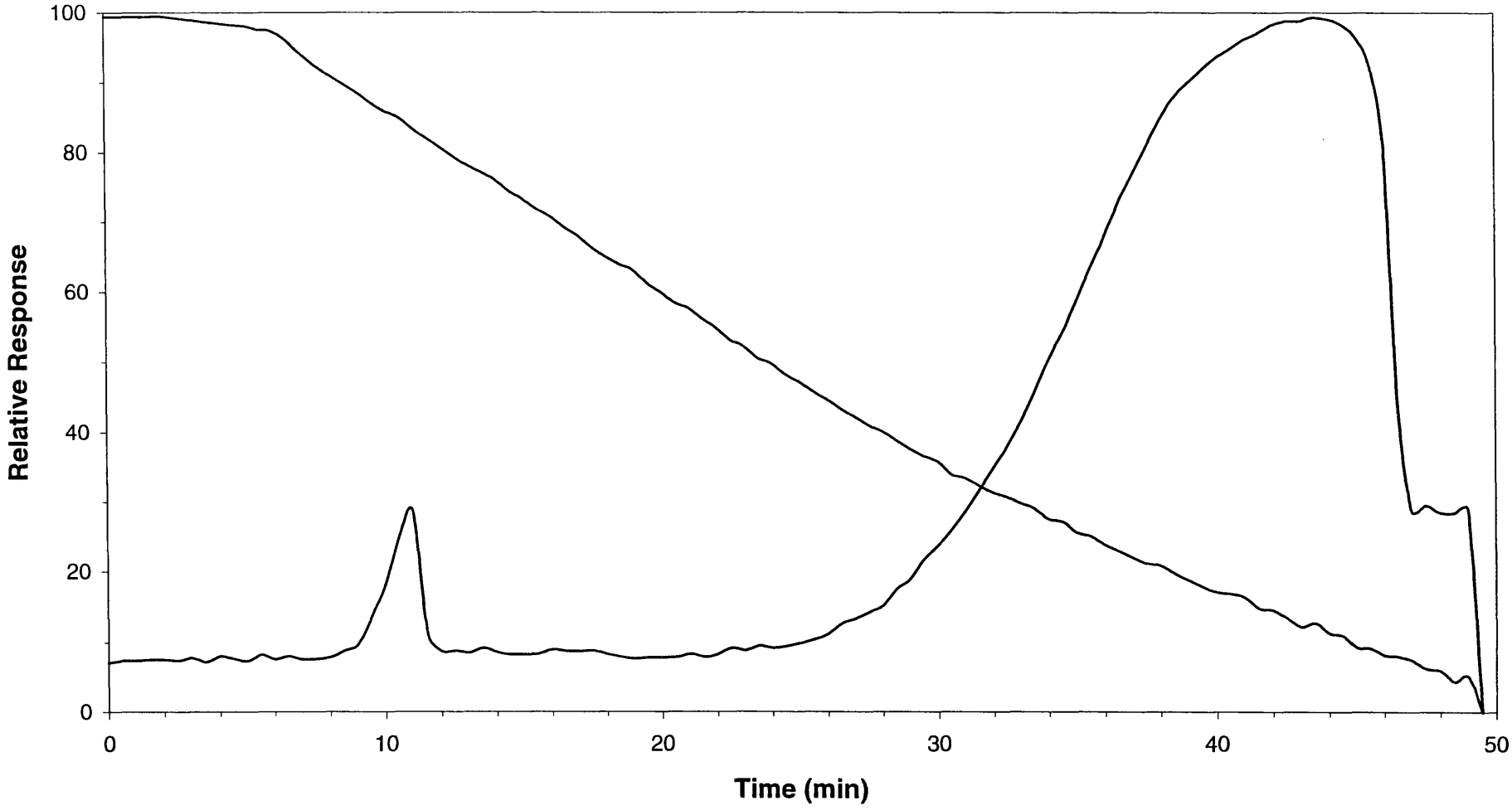

Figure 4.31: SATVA trace from the degradation of Graphtol Fast Red 2GLD under dynamic nitrogen

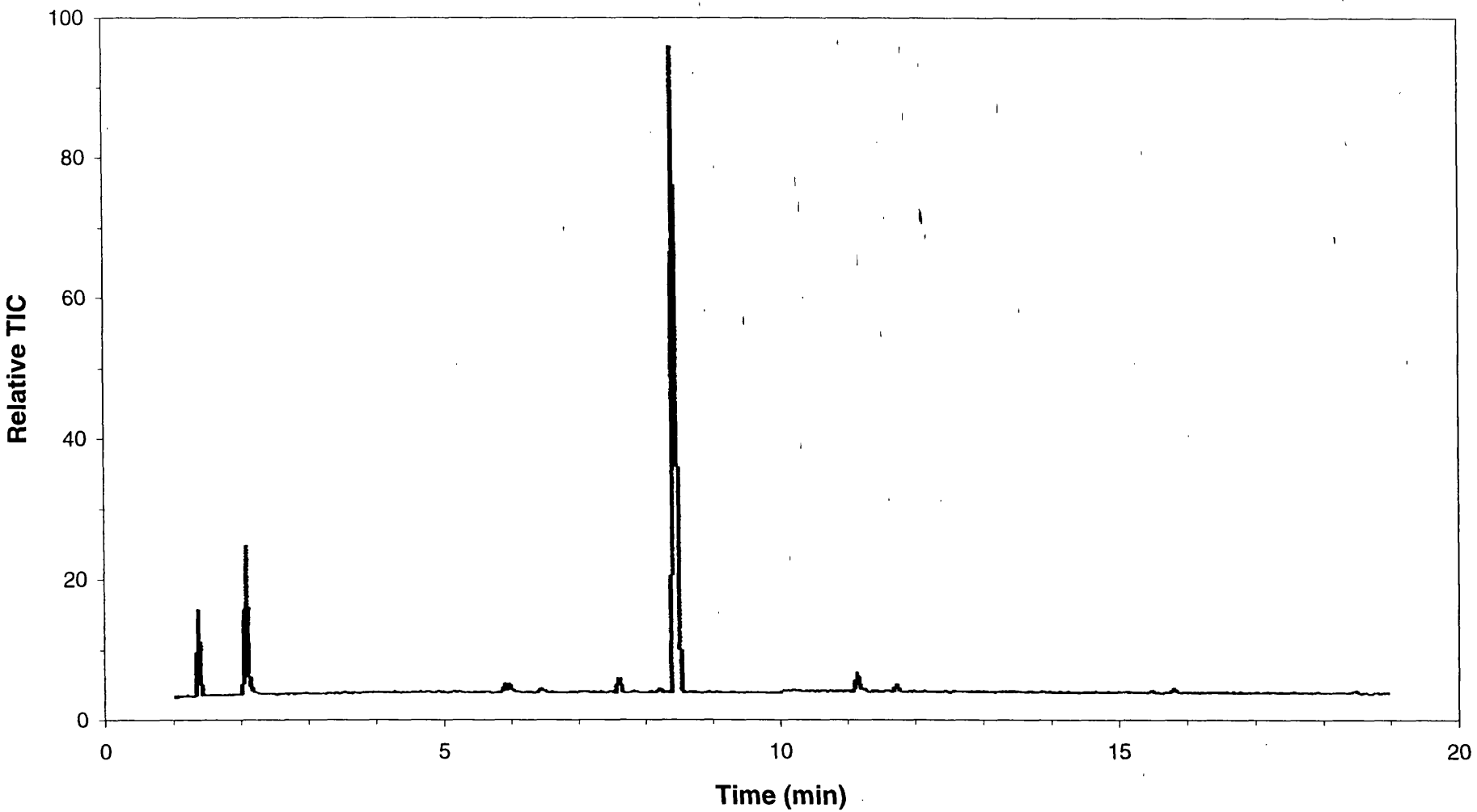

Figure 4.32: TIC trace for the liquid fraction from the SATVA curve in Figure 4.31

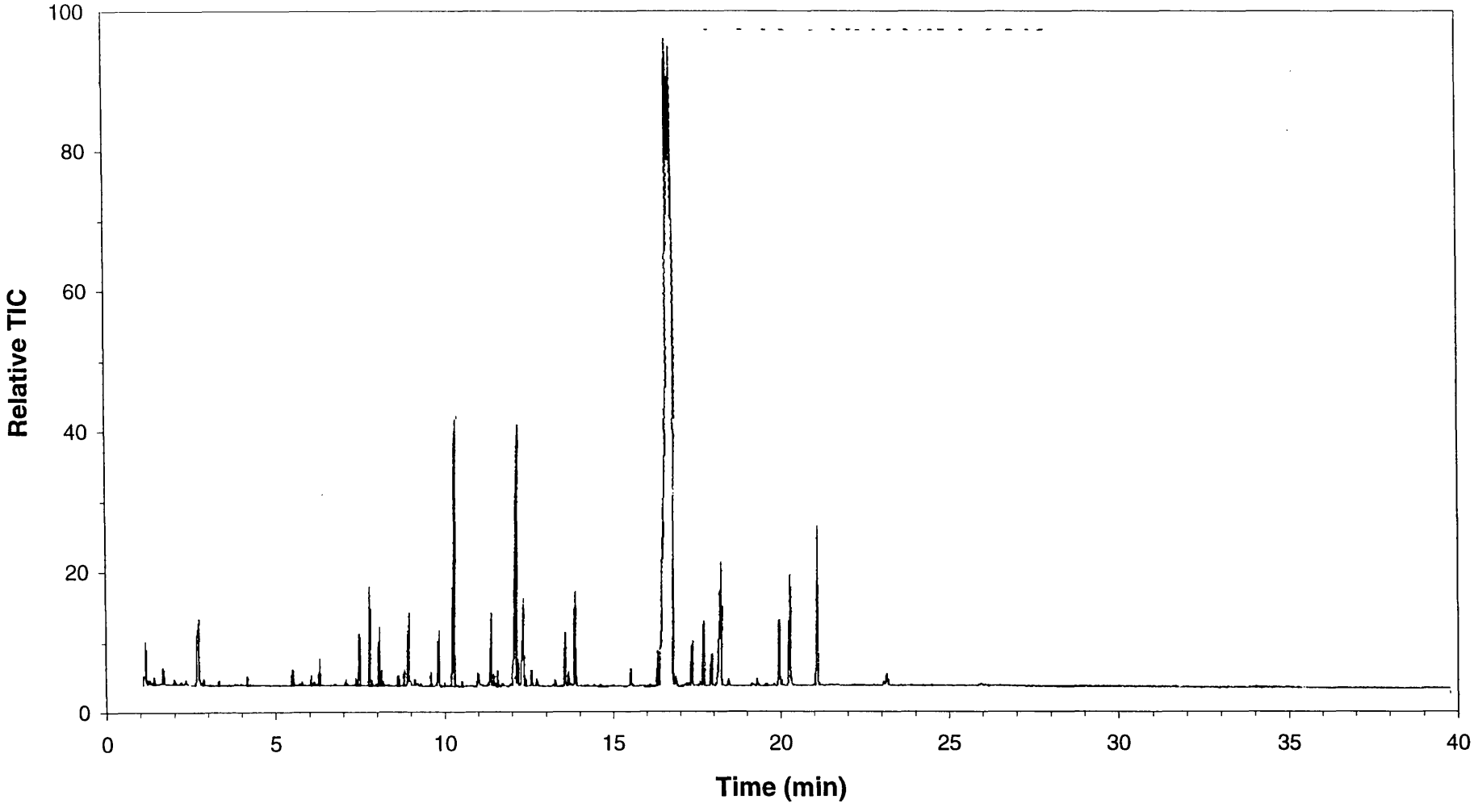

Figure 4.33: TIC trace for the cold ring fraction from the SATVA curve in Figure 4.31

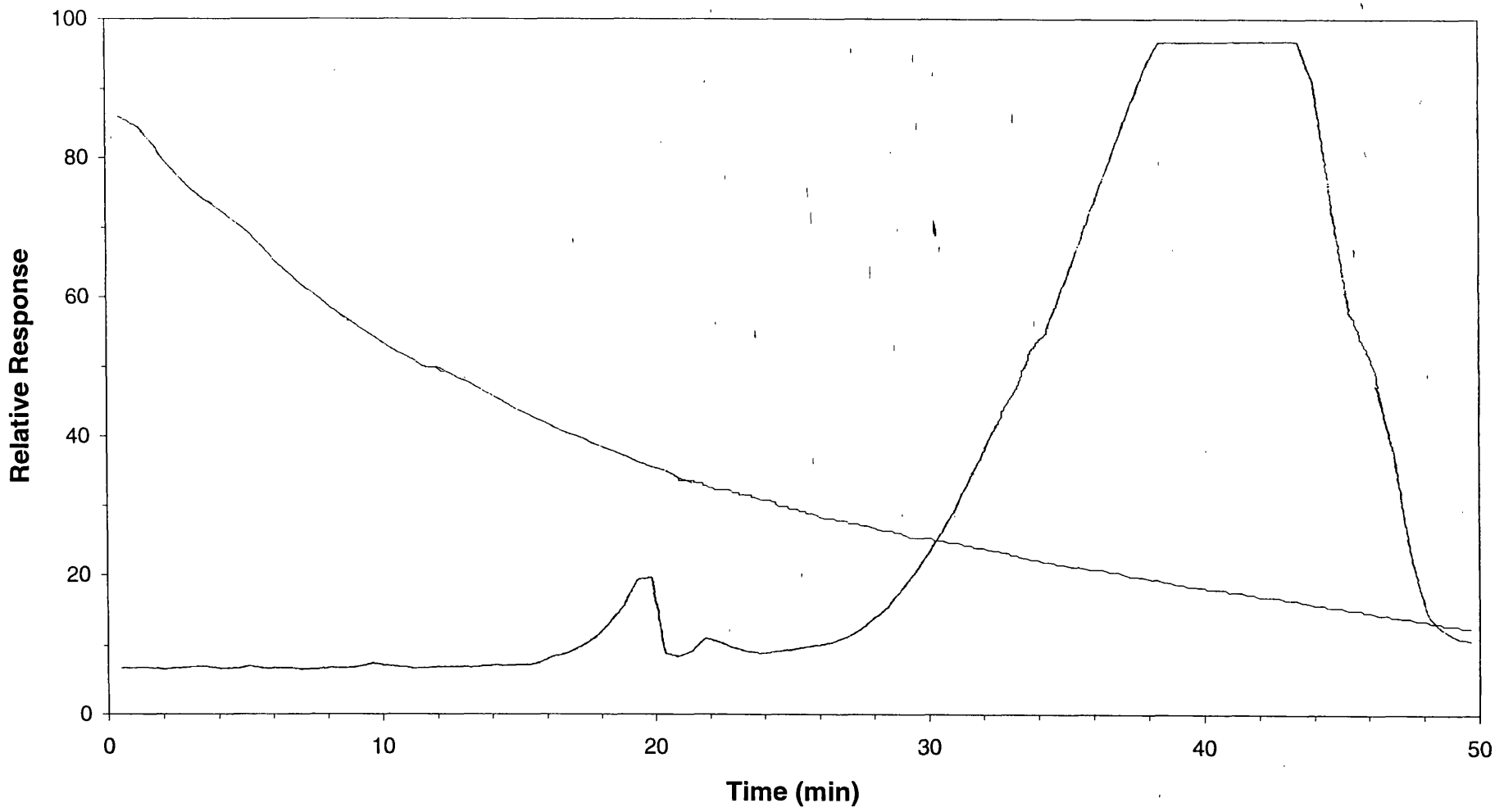

Figure 4.34: SATVA trace from the degradation of Graphtol Fast Red 2GLD under dynamic air

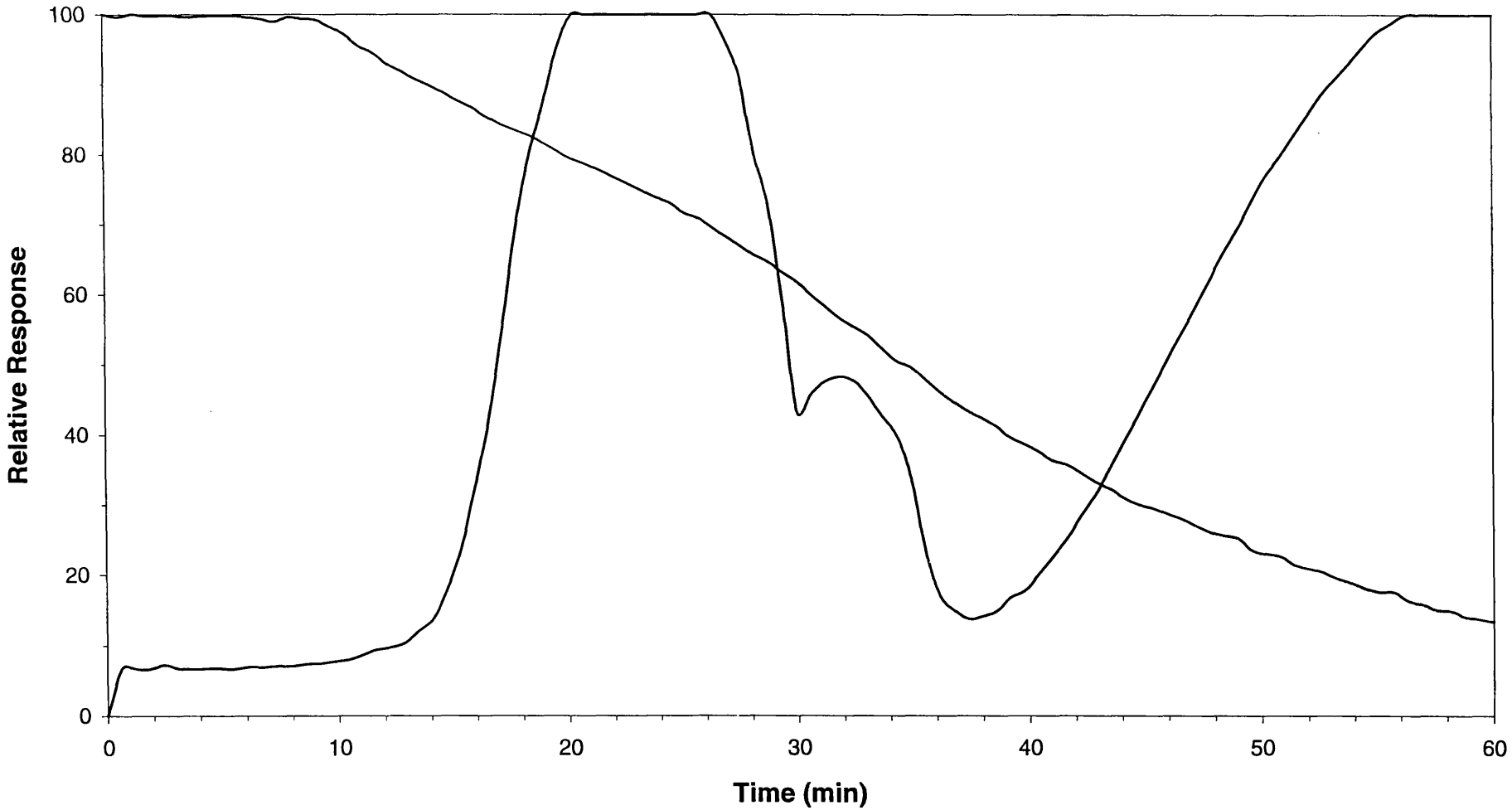

Figure 4.36: SATVA trace from the degradation of Graphtol Fast Red 2GLD under flaming conditions

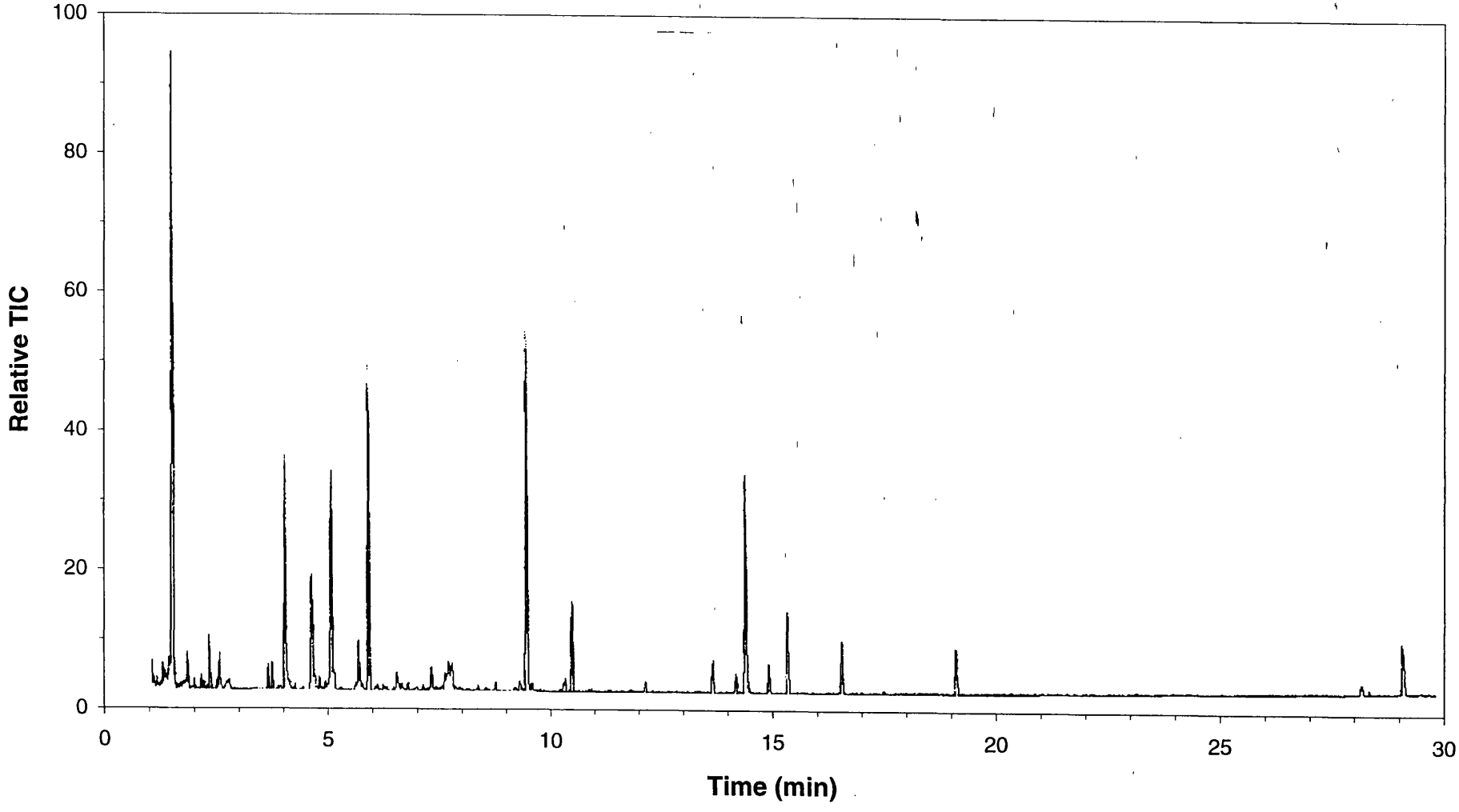

Figure 4.37: TIC trace for the liquid fraction from the SATVA curve in Figure 4.36

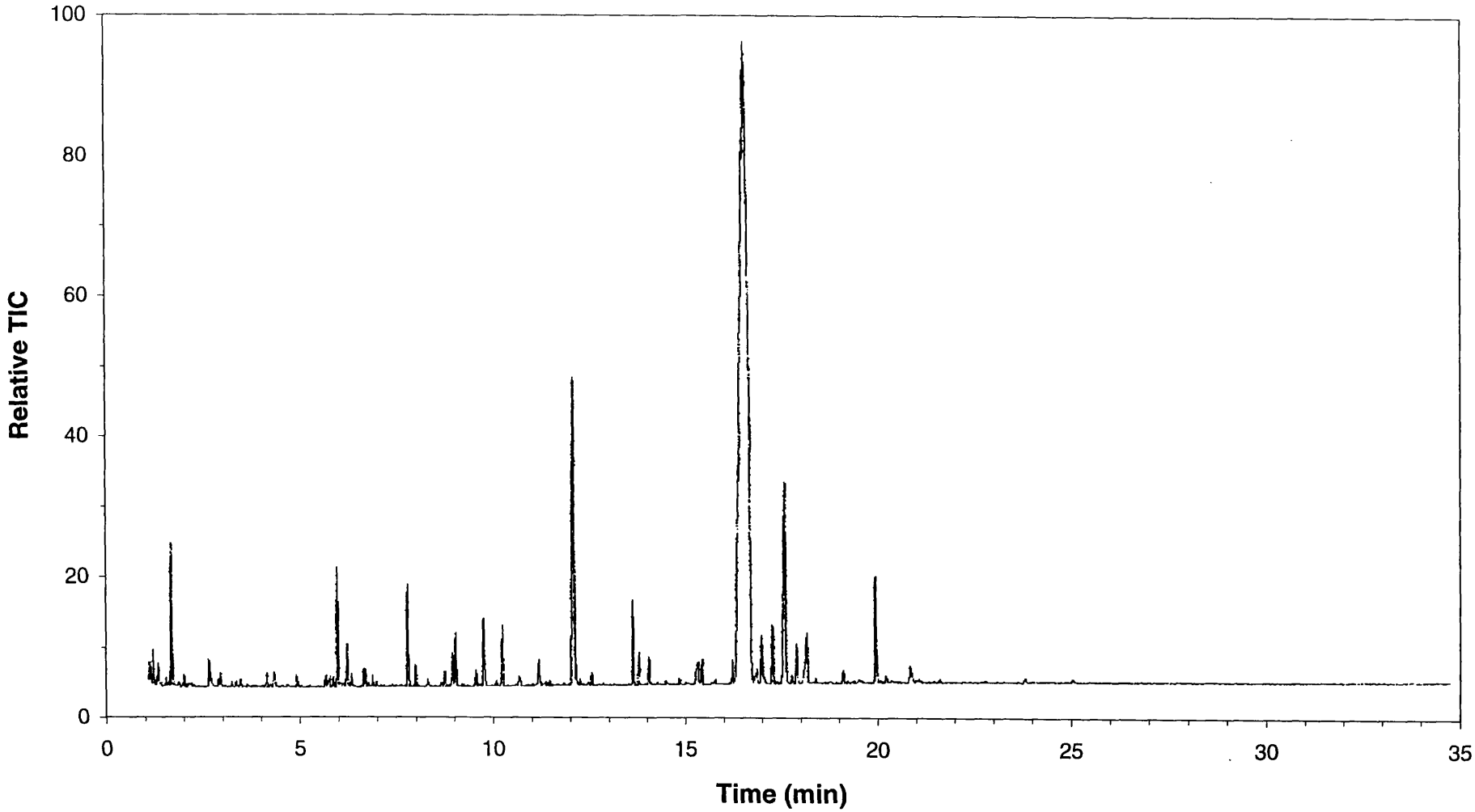

Figure 4.38: TIC trace for the cold ring fraction from the SATVA curve in Figure 4.36

CHAPTER 5

REMAINING ORGANIC COLOURANTS

5.1 INTRODUCTION

The two materials studied here do not fall into the same dye class. They were grouped together as they were the remaining all organic colourants.

5.2 CHEMISTRY

The first sample studied for this chapter was Estofil Blue S-RLS, which falls into the anthraquinone class of colourants[15,16]. This class is second only to the azo dyes in commercial importance.

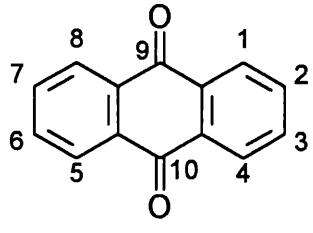

Figure 5.1: Anthraquinone structure

The basic anthraquinone structure is provided in Figure 5.1. The most common dyes have one or more electron-donating substituents on the 1, 4, 5 or 8 positions. The colourant studied here was substituted on the 1 and 4 positions.

The second colourant in this chapter was Sandorin Violet BL. Some difficulty was found classifying this material. The closest match was under the heading "Miscellaneous Dye Classes", where it was described as a triphendioxazine. The typical structure for this class is shown in Figure 5.2.

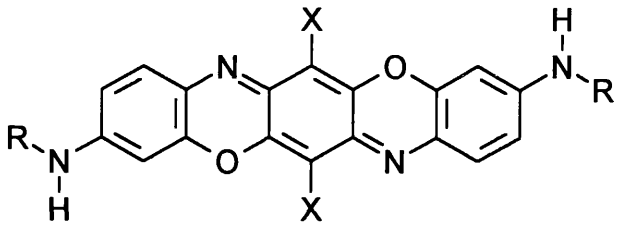

Figure 5.2: Triphendioxazine structure

The —X substituent is normally an electron donor. Chlorine, as was the case for this sample, is a typical example.

5.3 STRUCTURES

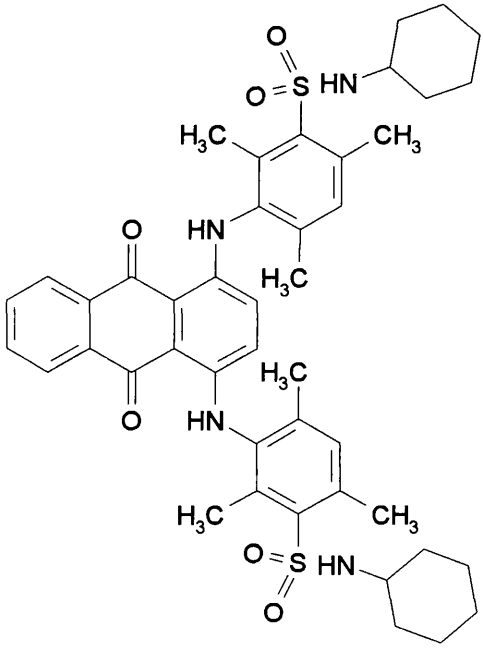

Estofil Blue S-RLS

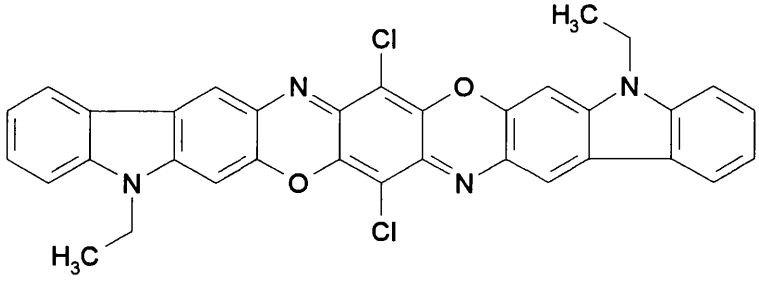

Sandorin Violet BL

Figure 5.3: Dyes studied in this chapter

The anthraquinone colourant, Estofil Blue S-RLS, is the first to be presented in this chapter. A glance at the structure in Figure 5.3 shows possible areas at which

degradation might first occur. The structure may be considered as a series of stable ring structures with relatively weak linkages.

The second material under study was Sandorin Violet BL, which is also displayed in Figure 5.3. This colourant is essentially a large conjugated molecule, with a less obvious thermal decomposition pathway.

5.4 THERMAL DEGRADATION OF ESTOFIL BLUE S-RLS

This material is presented first in this chapter as it should have had a more predictable degradation pathway than the other material.

5.4.1 Thermogravimetric Analysis

The TG plots are shown in Figure 5.4, and the main features are summarised in the following table:

Table 5.1: Key temperatures from thermogravimetry of Estofil Blue S-RLS

Conditions	$T_{thresh1}$(°C)	$T_{thresh2}$(°C)	T_{end}(°C)	%Residue
Dynamic Nitrogen	255	420	1000	0
Dynamic Air	250	420	620	2

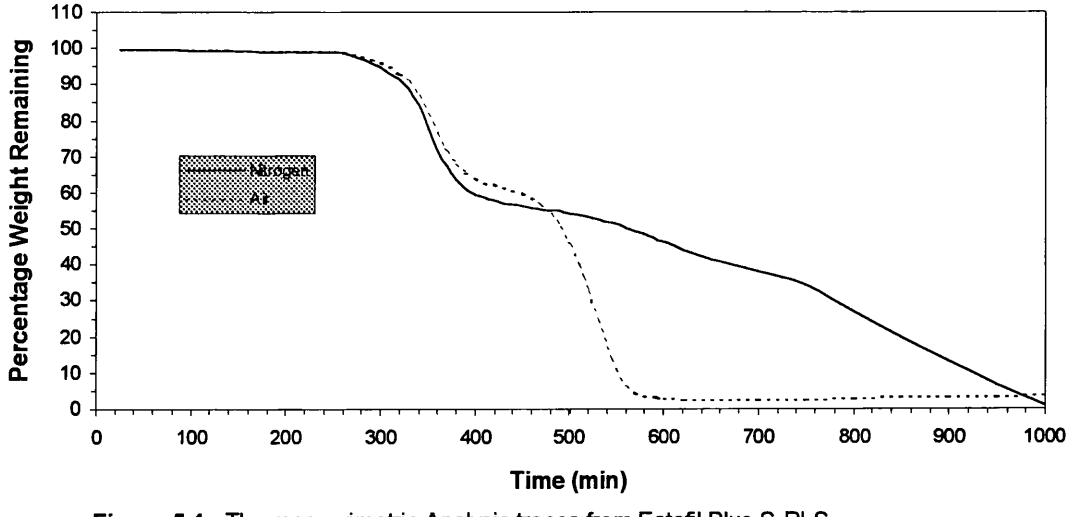

Figure 5.4: Thermogravimetric Analysis traces from Estofil Blue S-RLS

The profile for the dynamic nitrogen case displays some undulations between 420°C and the end, marked with a slight increase in rate at 735°C. The dynamic air degradation would appear to occur in two distinct stages. The first stage, up to around 460°C, closely follows the trace obtained for dynamic nitrogen. This would suggest that oxidation plays little or no part in the degradation up to this temperature. There is then a weight loss from this residue at a greater rate than that for the inert atmosphere case. Clearly oxidation effects are present in this second stage of the degradation. There is then a slight weight gain, implying that the residue is forming an involatile oxide.

5.4.2 Product Analysis — Dynamic Nitrogen

The sample was degraded at a rate of 10°C/min up to 400°C on the first run. This temperature was too low for the completion on the first stage of the degradation, so the higher temperature of 435°C was subsequently used. The resulting SATVA traces were identical. These studies resulted in the following residue weights:

Table 5.2: Residue percentages from nitrogen degradation of Estofil Blue S-RLS

	Weight Remaining	
Maximum Temperature	**Thermogravimetry**	**Flow tube**
400°C	62%	57.7%
435°C	57%	52.8%

The residue percentages fairly closely match between the TG and flow tube studies. This was one of the unusual samples which gave a lower residue weight through the flow-tube studies. It may be that there was a degradation product which promoted side reactions through the bulk of the larger sample.

A SATVA trace for the separation of the condensable volatile products is shown in Figure 5.5. The IR spectrum for the products forming peak 1 at 13 minutes was too

weak for any identifications. However, the on-line MS showed a pattern at m/e = 34, 33 and 32 which unambiguously proves H_2S was the major component forming this peak. There was also a weak response consistent with CO_2. The IR spectrum for the products collected at 16 to 25 minutes revealed the distinctive NH_3 absorptions. This was confirmed through the MS. The MS also continued to show H_2S until the water response started to rise. It is possible that this gas was trapped or dissolved into the water in the SATVA trap. These findings are summarised in the following table:

Table 5.3: SATVA peak assignments from Figure 5.5

Peak	Assignment
1	Mainly H_2S with trace CO_2
2	Ammonia
3	Much water. See below for GC-MS of ether extract.

The TIC trace for the GC-MS separation of the liquid fraction is presented in Figure 5.6. The peak allocation from this trace is presented in the ensuing table:

Table 5.4: GC-MS peak assignments from Figure 5.6

Retention Time	Product	Retention Time	Product
0:44	Solvent	13:20	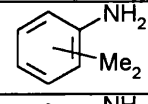
5:04	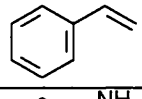	16:22	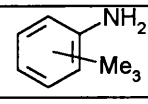
7:52	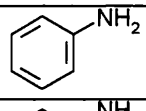	17:34	Aliphatic hydrocarbon
10:34	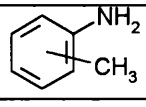	18:40	Too weak
12:30	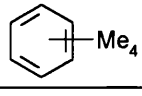		

The condenser on which the CRF gathered was washed firstly in acetone, and then with dichloromethane. These washings were then analysed by GC-MS. The mass

spectra for all the peaks were obtained for the acetone washings, with only the major TIC trace peaks considered for the dichloromethane.

The TIC trace from the separation of the acetone extract is shown in Figure 5.7. The identification for the peaks shown is presented in the following table:

Table 5.5: GC-MS peak assignments from Figure 5.7

Retention Time	Product	Retention Time	Product
3.02	Unidentified	12.02	Unidentified aromatic, highest mass detected = 212
2.95	Possibly 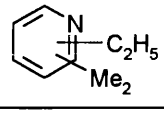	12.07	Unidentified
3.50	Unidentified	12.31	As 11.17
4.23	Possibly 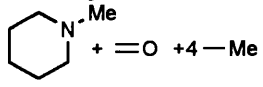	13.78	Unidentified
5.19	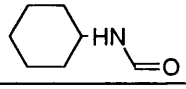	14.00	A phthalate
5.87	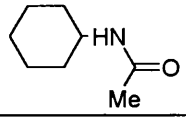	14.68	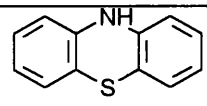
6.44	Perhaps a cyclohexane	16.55	Unidentified
7.07	Unidentified	16.66	Unidentified
8.45	Unidentified	16.79	Unidentified
8.69	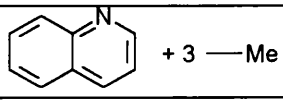	18.17	Unidentified
9.64	Probably 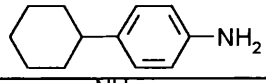	19.59	Unidentified
10.22	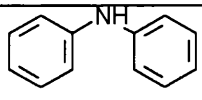 fits best, or perhaps 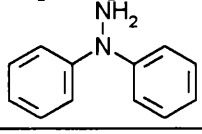	19.68	Unidentified
10.58	Unidentified	21.08	Probably an n-alkane
11.17	Highest mass detected = 209 with a 1Cl pattern.	23.73	Aromatic. Highest mass 341 at 100% abundance

The TIC trace from the dichloromethane extract is presented in Figure 5.8. Selected peaks have been identified and are presented below:

Table 5.6: GC-MS peak assignments from Figure 5.8

Retention Time	Product	Retention Time	Product
5.19	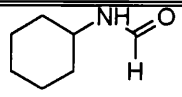	14.00	A phthalate (such as dibutylphthalate)
5.86	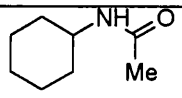	14.36	Spectrum very similar to molecular sulphur S8
9.63	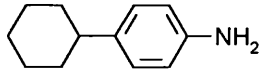 or isomers	14.66	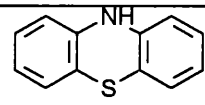

5.4.3 Product Analysis — Dynamic Air

The samples were heated at 10°C/min up to 430°C, then held isothermally for 10 minutes. The resulting residue was a solid foam.

Table 5.7: Residue percentages from air degradation of Estofil Blue S-RLS

	Weight Remaining	
Maximum Temperature	**Thermogravimetry**	**Flow tube**
430°C	55%	60%

It can be seen that the flow-tube studies resulted in a residue weight that was similar to that predicted by the TG studies. It would have been desirable to repeat these studies to a higher temperature, but the relative lack of significance of the dynamic air studies makes the omission less important.

A sample SATVA trace for the condensable volatile products from these degradations is displayed in Figure 5.9. The MS bleed during the volatilisation at peak 1 indicated CO_2 alone. The IR spectrum for the products from this peak also gave a weak absorption at around 2060 cm^{-1}, which would correspond to COS. The IR spectrum

for the products forming peak 2 displayed the distinctive absorptions for ammonia. There was also some COS present in this distillate. The MS at 20 minutes was dominated by peaks at m/e = 34, 33 and 32 which unambiguously signifies H_2S. There were also mass spectrometer peaks corresponding to the evolution of benzene. The MS taken during the volatilisation at the final peak was dominated by water peaks.

Table 5.8: SATVA peak assignments from Figure 5.9

Peak	Assignment
1	Mainly CO_2 with some COS
2	H_2S, NH_3 and some benzene
3	Contains water. See below for GC-MS from ether.

The TIC provided by the GC-MS separation of the liquid fraction is shown in Figure 5.10. The peak assignments are tabulated below:

Table 5.9: GC-MS peak assignments from Figure 5.10

Retention Time	Product	Retention Time	Product
1:22	Ether	16:58	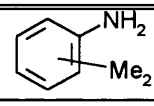
11:19	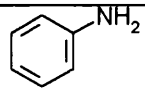	20:04	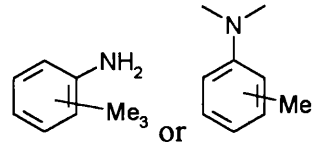
13:57	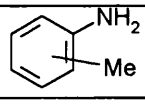	21:37	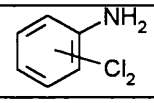

5.4.4 Product Analysis — Flaming Conditions

The apparatus was set up as described in Chapter 2. The following observations were made during the studies.

Table 5.10: Observations from Estofil Blue under flaming conditions

First Run	
Sample Size:	113.3 mg
Residue:	64.3 mg (57%)
Time (min)	**Observations:**
1:30-2:00	Formed droplets
4:28	Ignition. Then foamed.
Comments:	Sample puffed up to form a protective layer.

Second Run	
Sample Size:	199.3 mg
Residue:	99.3 mg (50%)
Time (min)	**Observations:**
1:20	Melted into droplets.
1:35	Droplets bubbled gently.
2:00	Drops started running together.
2:15	Drops fully joined and bubbling.
2:34	Sample started to flash.
2:50	Ignition.
3:10	Extinguished. Bubbled for <2s then formed slightly puffed residue.
5:00	Stopped.
Comments:	The topped puffed layer concealed 31.2 mg of shiny black lower layer.

The second run revealed an accelerated degradation with a much earlier ignition. This was probably due to an increase in the heater output with time. There were similarities in the residue weight and appearance.

The SATVA trace for the volatilisation of the condensable volatile degradation products is presented in Figure 5.11. It can be seen that two product fractions were volatilised. The IR spectrum for the products at the first peak is displayed in Figure 5.12. The major component was CO_2, as can be deduced from the absorptions at 2360 and around 3660 and 669 cm^{-1}. There was also evidence for N_2O, through the absorptions at around 2247, 3480 and 1285 cm^{-1}. The absorptions near 1360 cm^{-1} indicate the presence of SO_2. The non-condensables were also gathered during the

degradation. IR analysis of this fraction signalled the presence of CO as an additional product. These findings are summarised in the following table:

Table 5.11: SATVA peak assignments from Figure 5.11

Peak	Assignment
Non-Condensables	CO
1	Mainly CO_2,with N_2O and some SO_2 detected.
2	Mainly water. See below for GC-MS of ether extract.

The TIC for GC from the ether extract is presented in Figure 5.13. The peak assignments are listed below:

Table 5.12: GC-MS peak assignments from Figure 5.13

Retention Time	Product	Retention Time	Product
1:32	Possibly NO_2 perhaps indicating poor sample stability under GC conditions	3:11	Weak. Looks like silicone contaminant or 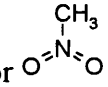
1:36	COS or 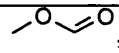 , also suggesting poor thermal stability	4:25	Silicon based contaminant
1:51	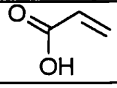	6:52	Silicon based contaminant
2:29	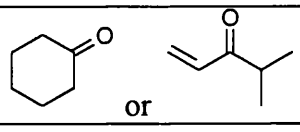	Note:	Some naphthalene was also detected on a subsequent analysis

The GC-MS of the cold-ring fraction extract was dominated by aliphatic products, probably contaminants from the SATVA line pump system. This meant that meaningful identification was not practicable.

5.5 THERMAL DEGRADATION OF SANDORIN VIOLET BL

This was the last of the metal free colourants to be studied. The structure is a fused nine-ring system. This makes the degradation pathway less predictable than for the others, which were predominately stable ring structures connected by relatively weak linkages.

5.5.1 Thermogravimetric Analysis

The TG plots are shown in Figure 5.14, and the main features are summarised in the following table:

Table 5.13: Key temperatures from thermogravimetry of Sandorin Violet BL

Conditions	$T_{thresh1}$(°C)	$T_{thresh2}$(°C)	T_{end}(°C)	%Residue
Dynamic Nitrogen	300	~450	>1000	<44
Dynamic Air	300	570	1000	0

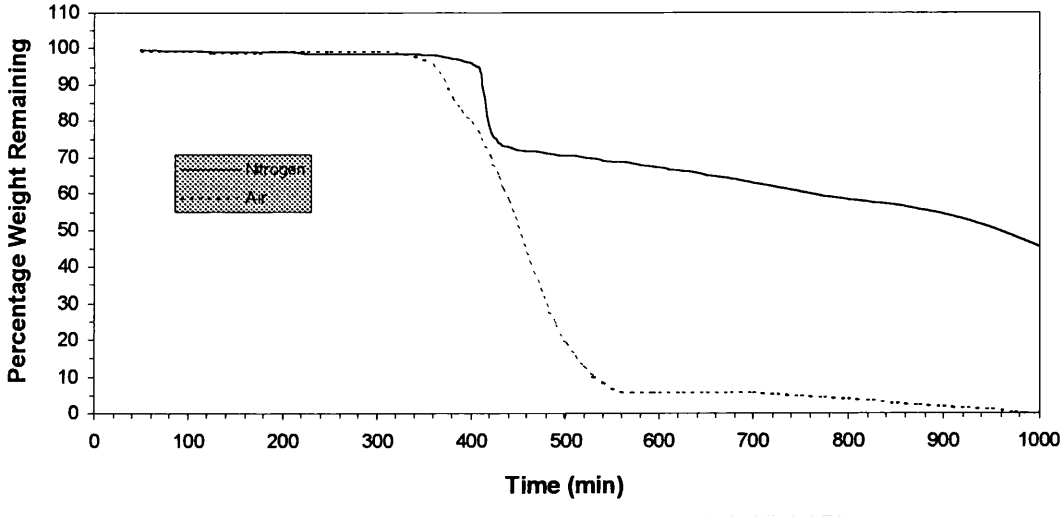

Figure 5.14: Thermogravimetric Analysis traces from Sandorin Violet BL

The trace for dynamic nitrogen displayed a slight weight loss from room temperature, reaching around 1% by the quoted $T_{thresh1}$. This small drop may be due to water in the sample. The gradual loss from $T_{thresh2}$ until the maximum of 1000°C for the thermobalance would appear to be incomplete. This profile for the end of the trace was

a common occurrence amongst the pigments, in particular for studies under inert atmosphere.

The TG analysis under dynamic air also displayed a small gradual weight loss up to the temperature of the first main weight loss. Close inspection of this section of the trace reveals a slight gain (~0.5%) starting at 140°C, indicating a small amount of oxidation of the sample. An estimation of the extent of this oxidation is 0.75% considering the differences in the nitrogen and air traces at 300°C. It is accepted that this is a very approximate calculation, as it is common for the air trace to show an earlier onset for the first major weight loss. The main loss on the trace from 300°C to 570°C left ~6% residue. This main loss was not very rapid, with a slight drop in the rate at ~375°C. This residue in turn gained under 0.5% weight by 650°C. This is indicative of some oxidation of the remaining residue.

It was also clear that the first stage of the degradation for air and nitrogen studies was not the same, as was seen for some of the earlier samples. Although the onset temperature was the same, the weight loss at this stage was far more rapid under dynamic air. The implication is that oxidation of the material occurred which promoted the degradation.

5.5.2 Product Analysis — Dynamic Nitrogen

These degradation studies were performed with a heating rate of 10°C/min up to 900°C under dynamic nitrogen, with the usual 10 minute hold at the maximum temperature. This high temperature was chosen as TG data was not available at the time of study. It can be seen that there was still weight loss to be found at the end of

the TG analysis (5.5.1). The percentage residue obtained for this degradation is compared with the TG result in the following table:

Table 5.14: Residue percentages from nitrogen degradation of Sandorin Violet BL

	Weight Remaining	
Temperature	**Thermogravimetry**	**Flow tube**
900°C	54%	55%

These residue percentages are in good agreement.

A SATVA trace for the volatile degradation products is given in Figure 5.15. The products forming the small peak at 10 minutes did not provide sufficient material for IR analysis. However, simultaneous MS did reveal CO_2. The second product fraction was studied through both MS and IR analysis. The IR spectrum is presented in Figure 5.16. This is indisputably the spectrum for HCN, through the absorptions at 714, 3345, 3330, 1437, 1389 and 2331 cm^{-1}. This result was confirmed through MS peaks at m/e = 27 and 26. The IR spectrum also shows weak absorptions with some fine structure at around 950 cm^{-1}. This indicates the presence of ammonia, which may have been the major constituent at the third peak. These identifications are summarised in the following table:

Table 5.15: SATVA peak assignments from Figure 5.15

Peak	Assignment
1	CO_2
2	HCN
3	Probably NH_3
4	Much water. See below for GC-MS of ether extract.

The MS from the start of peak 4 showed only water. The fraction was collected, and ether added for GC-MS analysis. The resulting TIC trace is presented in Figure 5.17, and the peak assignments are tabulated overleaf:

Table 5.16: GC-MS peak assignments from Figure 5.17

Retention Time	Product	Retention Time	Product
5:05	Probably 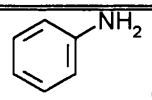 or perhaps 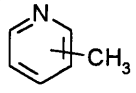	9:19	Unidentified aliphatic hydrocarbon
5:50	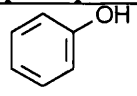	10:44	Possibly 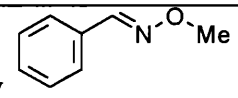
6:46	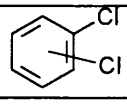		

5.5.3 Product Analysis — Dynamic Air

These degradations were performed with a heating rate of 10°C/min up to 900°C. The TG curve shows that this was higher than required, with only 6% of the residue remaining at 570°C.

A SATVA trace for the separation of the condensable volatile degradation products is given in Figure 5.18. This trace shows two gas peaks, with a third peak for the liquid fraction. Peak 1 was identified as being due to the volatilisation of CO_2. This was due to absorptions in the IR spectrum at 2361, 2338 and 667 cm^{-1}. Peak 2 was due predominately to HCN, established by both the IR and MS data. The IR spectrum is presented in Figure 5.19. There were IR absorptions at 3336, 3291, and around 1410 and 714 cm^{-1}, with an MS peak at m/e = 27 confirming the presence of HCN. There were also additional absorptions at 2282, 2257 and 1746 cm^{-1} indicating at least one other unidentified component. The former two of these absorptions suggested HCNO, but there were no other absorptions to support this. The latter suggested a carbonyl. It was decided to leave this product unidentified after much consideration of correlation

charts and reference spectra. The findings from the gas analysis are summarised in the following table:

Table 5.17: SATVA peak assignments from Figure 5.18

Peak	Assignment
1	CO_2
2	HCN
3	Mainly Water. See below for GC-MS of ether extract.

The on-line MS taken at the start of the third peak showed mainly water. This fraction was collected, and ether added to make an extract for GC-MS study. The TIC trace obtained is shown in Figure 5.20. The assignments for the peaks present are tabulated below:

Table 5.18: GC-MS peak assignments from Figure 5.20

Retention Time	Product	Retention Time	Product
3:11	Ether	14:05	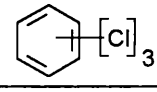
3:59	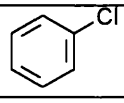	14:15	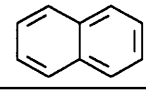
5:25	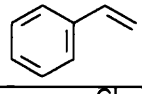	14:47	Silicon based contaminant
10:46	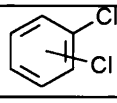	18:22	MS too weak to identify
12:07	Mainly as above, with what appears to be some 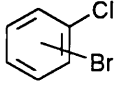	19:32	Weak, but 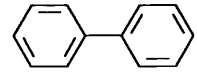 or 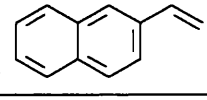
12:28	Mainly as 10:46, but with some 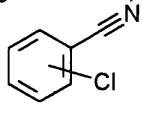		

5.5.4 Product Analysis — Flaming Conditions

The standard conditions for degradation under flaming conditions were used. The following observations were made:

Table 5.19: Observations from Sandorin Violet under flaming conditions

First Run	
Sample Size:	109.6 mg
Time (min)	**Observations:**
2:15	Ashing commenced.
8:00	Stop.
Comments:	No Ignition

Second Run	
Sample Size:	195.8 mg
Time (min)	**Observations:**
1:45	Ashing commenced.
4:00	Stop.
Comments:	No Ignition.

The material under study was dark before the start of degradation. This meant that it was difficult to observe the time at which discolouration commenced. The only change observed was the appearance of an ash effect, although the structure for the pure sample did not contain any inorganic elements. The lack of ignition is perhaps a little surprising when there was such a low extent of chlorination. It is possible that this fused ring conjugated structure formed a stable carbonised residue without the evolution of flammable volatile products. The would not provide the critical mass flux of fuel materials to allow ignition. The residue could not be weighed, as it was too fine to be transferred from the degradation apparatus to the balance.

The SATVA trace for the separation of the volatile degradation products is given in Figure 5.21. This is similar to the typical two-peak trace obtained for degradations under these conditions. However, it may be seen from the undulations on the fall of the first peak that there were some other gaseous products present.

The products from peak 1 were collected in a gas cell for IR analysis. The major product was identified as CO_2, through the normal absorptions. There was also a considerable quantity of N_2O produced, as was indicated by absorptions at 2239, 2214, 1273, 1299, 2577 and 2550 cm^{-1}. There were also weak peaks present for HCN, in both the IR spectrum (718 cm^{-1}) and the mass spectrum from the on-line mass spectrometer (m/e = 27). There were also very weak peaks in the IR spectrum consistent with the presence of formaldehyde (around 1790 and 1130 cm^{-1}), but these were not clear enough to be conclusive.

Non-condensable capture was also used during the degradation, as described in Chapter 2. The IR spectrum of this fraction revealed the presence of CO, through absorptions at 2168 and 2117 cm^{-1}. The findings for the studies of the gaseous products are summarised below:

Table 5.20: SATVA peak assignments from Figure 5.21

Peak	Assignment
Non-condensables	CO
1	Mainly CO_2 with much N_2O. Also traces of HCN and perhaps formaldehyde.
2	Mainly Water. See below for GC-MS of ether extract.

The on-line MS displayed only the spectrum for water during the volatilisation of the final peak. The products were collected into a cold-finger and diethylether was added. This extract was then studied through GC-MS, with the TIC trace being presented in Figure 5.22. The peak assignments revealed only silicon-based compounds, except the peak at 10:20 (the shoulder to the main peak after solvent) which was due to

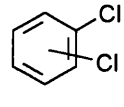

The cold ring fraction was extracted into two separate solvents, acetone and dichloromethane. These were both examined with heated probe mass spectrometry, and the latter through GC-MS analysis. The probe results showed predominately aliphatic hydrocarbons through strong peaks at 41, 43, 55, 57 *etc.* with decreasing intensity. This was confirmed through the GC-MS study of the dichloromethane extract. Consideration of the starting material suggests that these materials detected were contaminants.

5.6 MAJOR PRODUCT SUMMARIES AND MECHANISMS

The major products obtained for the degradation of each of the samples in this chapter are presented in this section, along with possible mechanisms.

5.6.1 Estofil Blue S-RLS

This sample was degraded under three different conditions, dynamic nitrogen, dynamic air and flaming conditions. The first of these provides the best guide to the unstable areas of the molecule, as there is less scope for secondary degradation of the products.

5.6.1.1 Dynamic Nitrogen

The major gases were NH_3 and H_2S with a small amount of CO_2. This latter product often arises in small amounts in these studies. When it is only a minor product, it may be assumed that it has entered the SATVA apparatus through inevitable minor leaks or by being physically trapped within the sample. Aniline was by far the major product in the liquid fraction. There were also significant quantities of trimethylaniline, along with smaller amounts of mono- and dimethylaniline. The cold ring fraction was dominated by 4-cyclohexylbenzamine.

Consideration of the structure makes the formation of H_2S and the NH_3 hard to explain, although the origin of the anilines is a little clearer. The structure may be considered as a series of thermally stable aromatic units, connected by relatively weak linkages. This is illustrated in Figure 5.23.

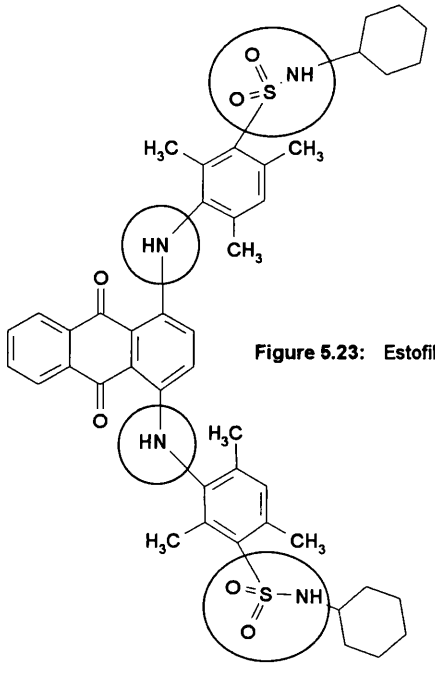

Figure 5.23: Estofil Blue S-RLS Weak Linkages

No products clearly related to the anthraquinone unit were detected. It is supposed that this was a major contributor to the carbonaceous residue. This in turn would be a source of hydrogen for the volatile product fraction, as could the methyl and cyclohexane fragments. Alternatively, the cleaved fragments may have extracted protons from the anthraquinone, a process aided by resonance stabilisation through its structure.

The major aromatic product was aniline, with smaller amounts of methylated aniline. This suggest that the NH linkage remains with the trimethylbenzene unit, extracting a proton from somewhere — perhaps freed with the formation of the residue. Some of the methyl groups are probably cleaved as methyl radicals. Regrettably, the degradation method employed did not allow the detection of methane, the logical product after coupling with hydrogen atoms. Small amounts of tetramethylbenzene was also detected, implying the migration of methyl groups, supporting homolysis of the methyl groups.

Cyclohexane was not detected, although 4-cyclohexylbenzamine was. This may be due to the formation of a cyclohexyl radical, combining with a radical site from a departing methyl group on the aniline. Another possible source of the aniline may be hydrogen loss of a cyclohexanamine fragment. There was no cyclohexanamine detected, implying that if this pathway was followed then the aromatic ring was formed first.

It is unclear what became of the SO_2NH linkage. Sulphur dioxide was not present as a degradation product, although H_2S was. This linkage may also be the major source of NH_3 as the other NH link would appear to remain with the neighbouring benzene ring. Molecular sulphur (S_8) was detected in the CRF, although it does have a boiling point of 445°C. This means that only a small amount of this product would leave the hot zone of the degradation apparatus to be detected. It may be supposed that the sulphur formed molecular sulphur and then reacted with protons from the degrading residue. This would result in the formation of the H_2S.

5.6.1.2 Dynamic Air

The products here were essentially the same as above, as was the percentage residue obtained. The main difference was the increase in the amount of CO_2 and the water. These may be easily explained as the oxidation of the residue for CO_2 or the cyclohexane for both of these new products. The presence of oxygen around hydrogen radicals would also produce water.

5.6.1.3 Flaming Conditions

This sample did ignite. CO_2 and water were the major products. There were few others detected, including N_2O, SO_2, CO. The products listed in 5.6.1.1 and 5.6.1.2 probably fuelled the flame observed. Full oxidation of these products would yield CO_2 and water as the major products, with partial oxidation allowing the formation of CO. This also explains SO_2, which may have also formed on oxidation of the residue. The ferocity of the heater may provide a more severe environment for oxidation than that experienced using dynamic air. A common product in all the flaming experiments was N_2O. This may be a genuine product, a theory supported by the large amount detected for the degradation of azo colourants. Alternatively, the hot metal element and spark pilot may have produced some from the air.

5.6.2 Sandorin Violet BL

This sample was degraded under the same three conditions as Estofil Blue S-RLS. The major degradation products identified under each set of conditions are summarised in the following sections. Some mechanistic suggestions are also supplied.

5.6.2.1 Dynamic Nitrogen

CO_2 was the major gaseous product, although there was only a small amount evolved. Some HCN and perhaps NH_3 was also detected. The former of these was not necessarily a genuine product (see 5.6.1.1). Dichlorobenzene was by far the major product detected. There were also small amounts of aniline and phenol present in the liquid fraction.

HCl could not be detected. There was a 45% weight loss for this degradation. Dichlorobenzene would account for 25% of the weight if it was produced with 100% efficiency. CRF data were not available.

Inspection of the structure of Sandorin Violet BL suggests some likely weak areas, which would be less thermally stable. The more breakable bonds are highlighted in Figure 5.24.

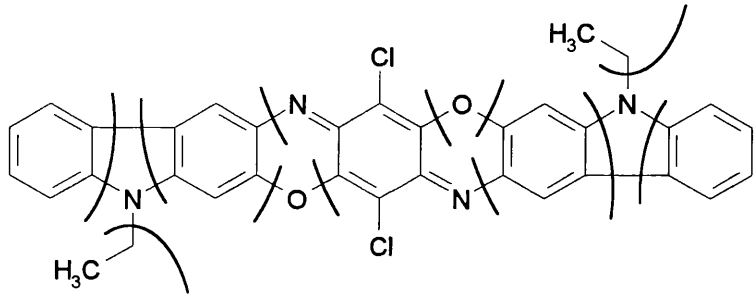

Figure 5.24: Sandorin Violet BL Weak Linkages

The source of the dichlorobenzene was probably the central chlorinated ring. This raises the question of what happens to the CN double bond. This may not be a true double bond due to possible delocalisation of electrons along the molecule. If this CN was to gain hydrogen, then this nitrogen may be that found in the aniline. The most probable sources of the hydrogen would be the C_2H_5 or hydrogens lost on the formation of the carbonaceous residue. Alternatively, HCN may be formed as an alternative to dichlorobenzene. It is also quite feasible that the other nitrogen is that observed in the aniline, after the cleavage of the ethyl group. With a boiling point of -88.6°C, ethane as a product would not have been trapped in the dry-ice/acetone trap.

The third ring from the end is the most likely source of phenol. This may be deduced by considering the location of the oxygen, which clearly does not remain connected to the centre ring when so much dichlorobenzene is produced.

It is surprising that benzene was not detected. It was not uncommon for benzene to be lost in the ether peak on the GC-MS machine used. It could, however, be detected by the on-line MS during the SATVA separation. There was no evidence found here either. It may be supposed that the end aromatic ring provided the aniline, and the next benzene the phenol. However, phenol and aniline formation was considerably less favourable than the evolution of dichlorobenzene. This observation, along with the 55% residue, implies that all but the centre of the molecule favoured residue formation.

5.6.2.2 Dynamic Air

The same major products were observed as for dynamic nitrogen. There were some changes in the relative quantities. There was more CO_2, and the dichlorobenzene was even more major a product. Aniline and phenol were not detected. There was only a small residue.

The oxidation of the carbonaceous residue by the high temperature would have produced CO_2. The increase in the relative amount of dichlorobenzene does not mean that more was produced, but that there was more relative to the other liquid products. This means that the presence of the oxygen either encouraged the formation of dichlorobenzene, or inhibited the development of the other products detected in 5.6.2.1.

The oxygen may help support a radical decomposition pathway, analogous to that found for polypropylene (see chapter 3). Trichlorobenzene was also detected. This requires the migration of chlorine. This may be explained by considering the presence chlorine radicals.

5.6.2.3 Flaming Conditions

The sample failed to ignite. With dichlorobenzene as the major volatile product, it seems reasonable that there was no ignition. Water and CO_2 were the major products, with all others being very minor. Dichlorobenzene was the only product identified in the liquid fraction.

The CO_2 and water are both predictable products for these conditions. The N_2O may have been a product of the apparatus itself, as suggested in 5.6.1.3.

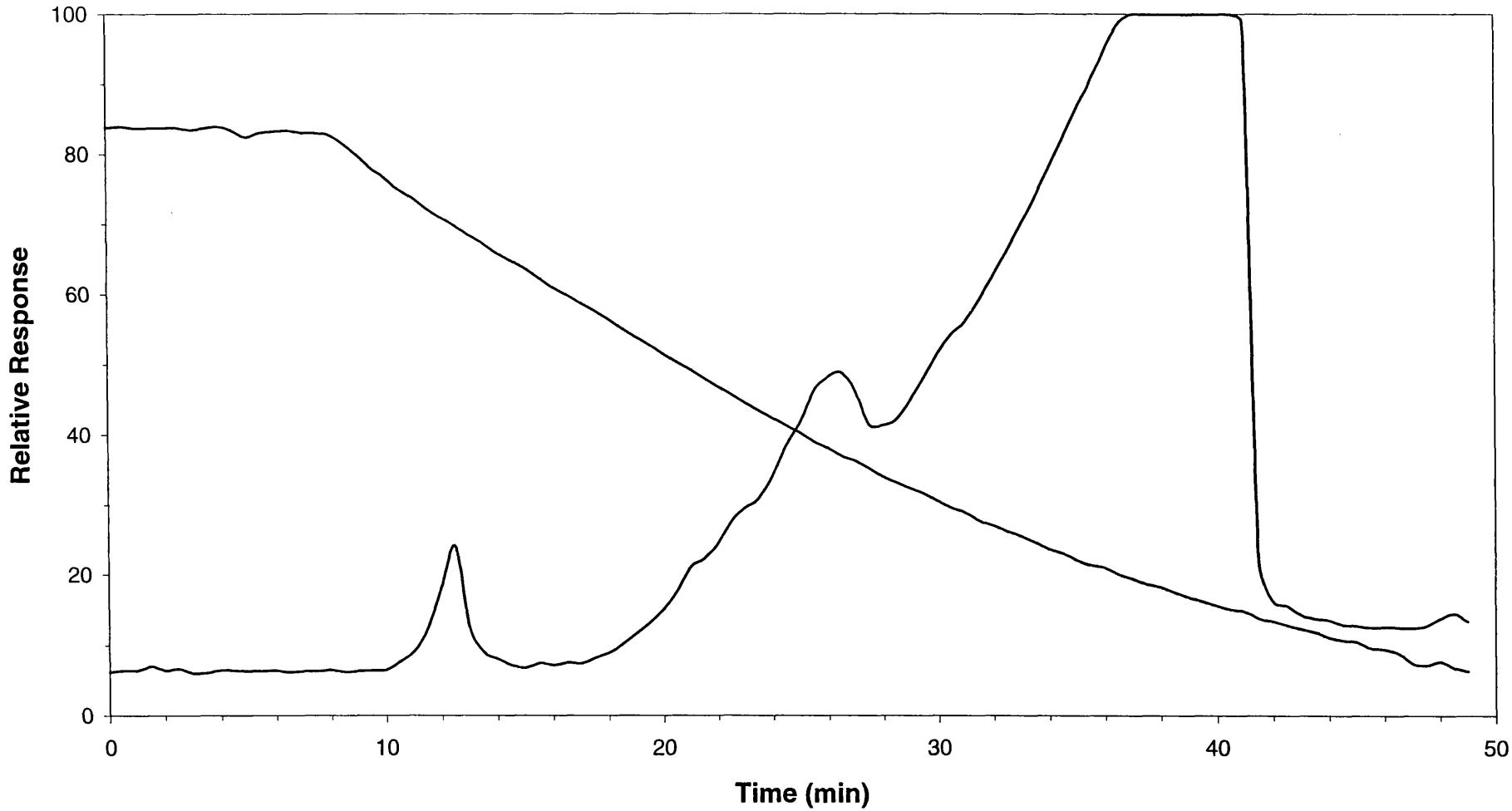

Figure 5.5: SATVA trace from the degradation of Estofil Blue S-RLS under dynamic nitrogen

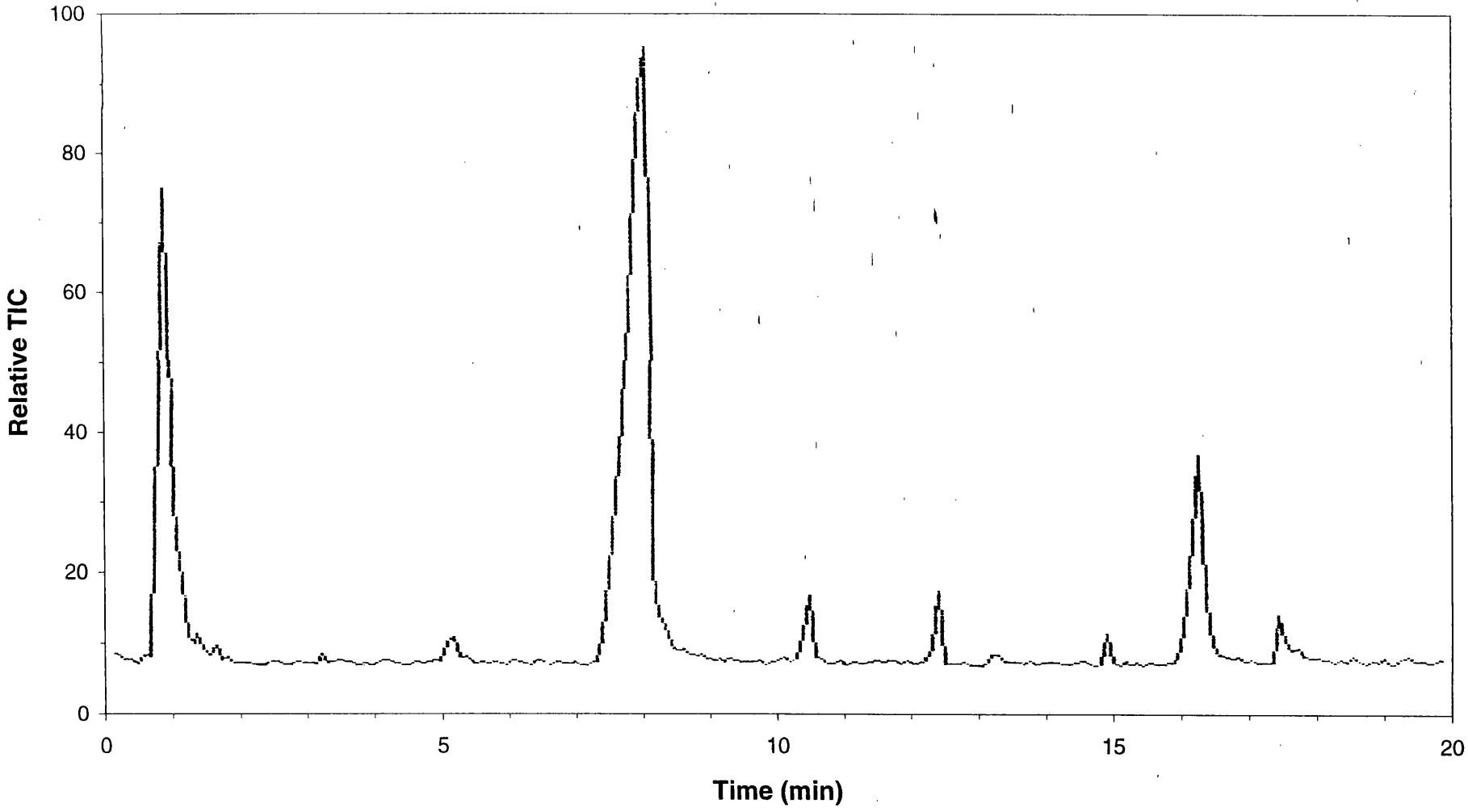

Figure 5.6: TIC trace for the liquid fraction from the SATVA curve in Figure 5.5

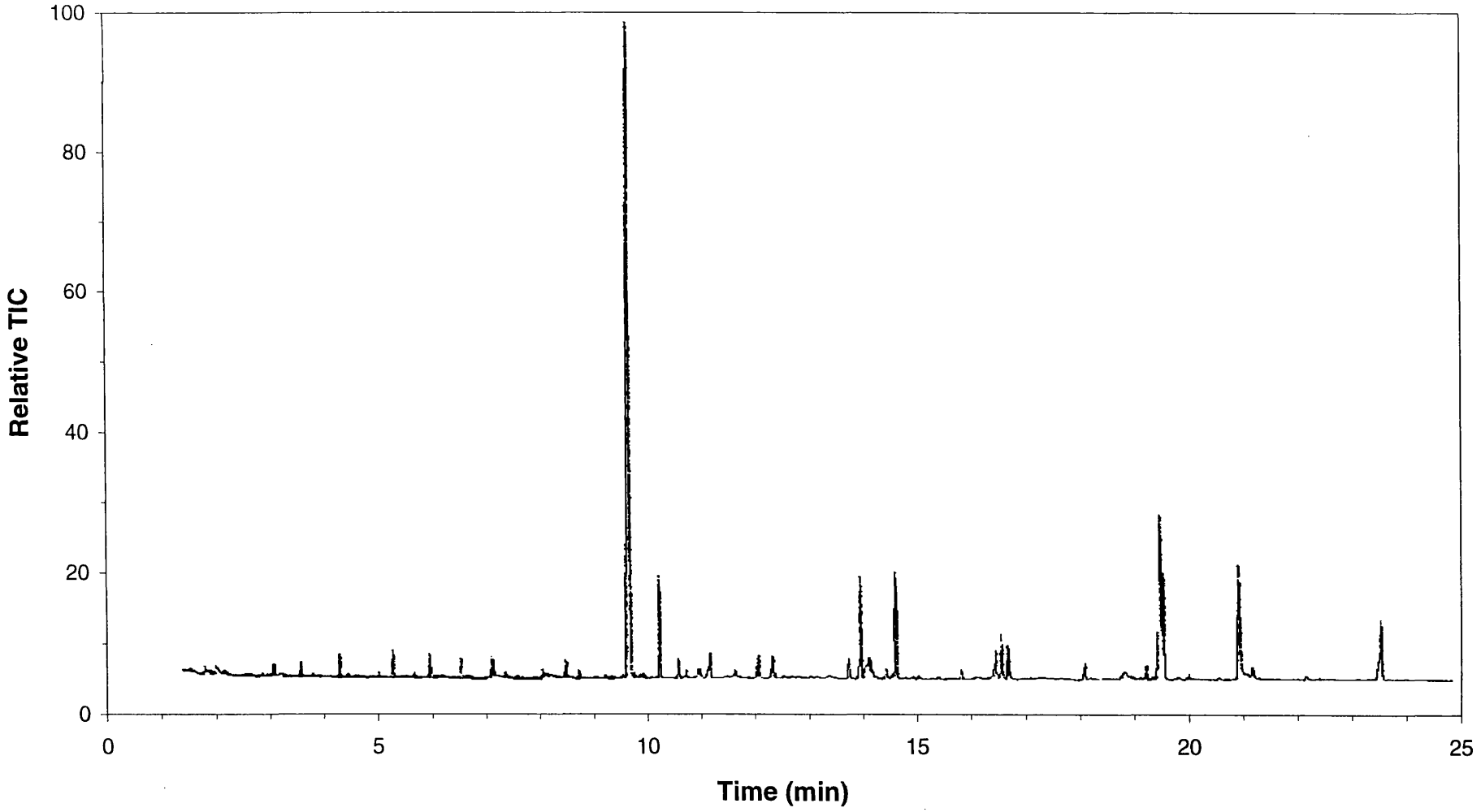

Figure 5.7: TIC trace for the acetone washings from the CRF from the SATVA curve in Figure 5.5

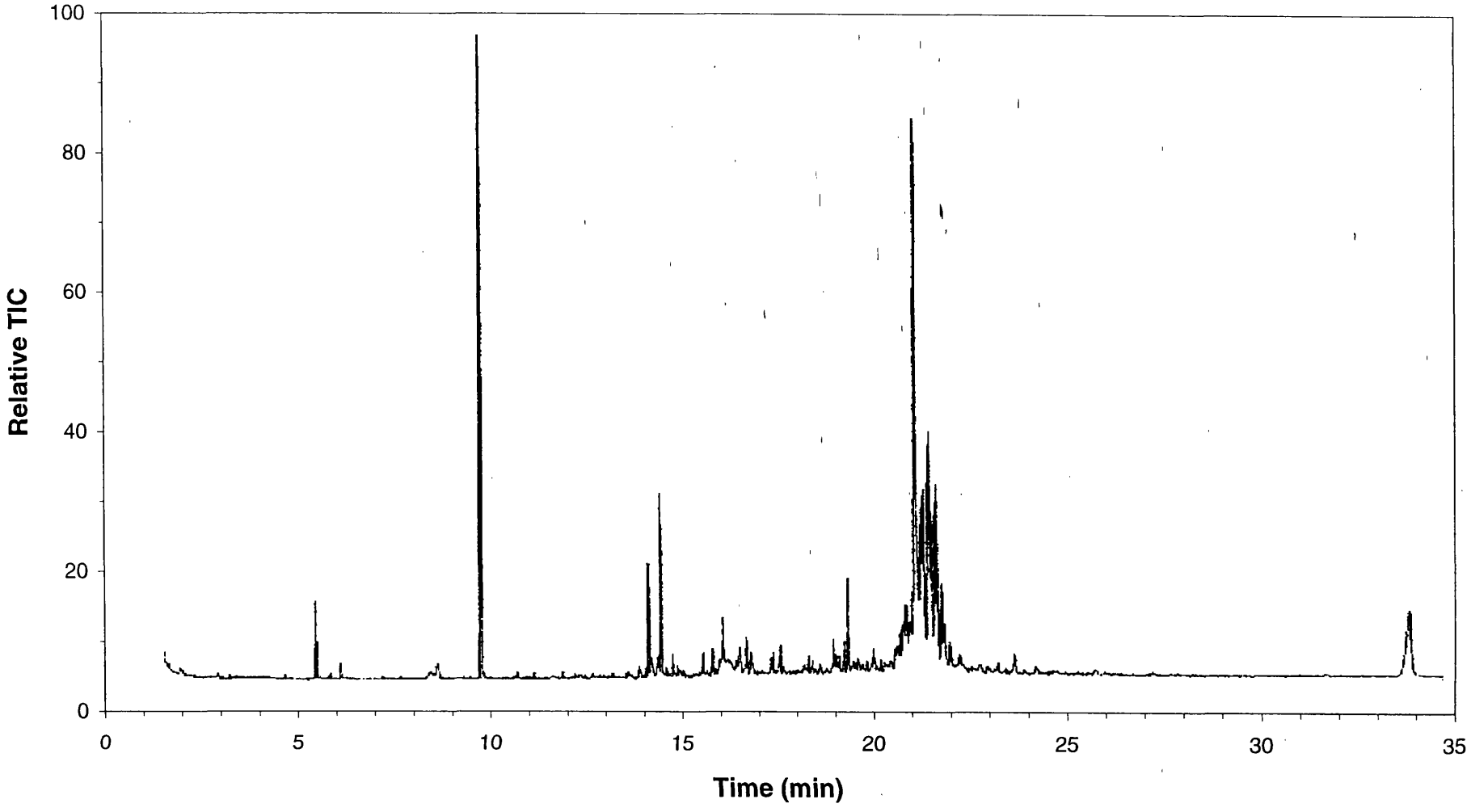

Figure 5.8: TIC trace for the dichloromethane washings from the CRF from the SATVA curve in Figure 5.5

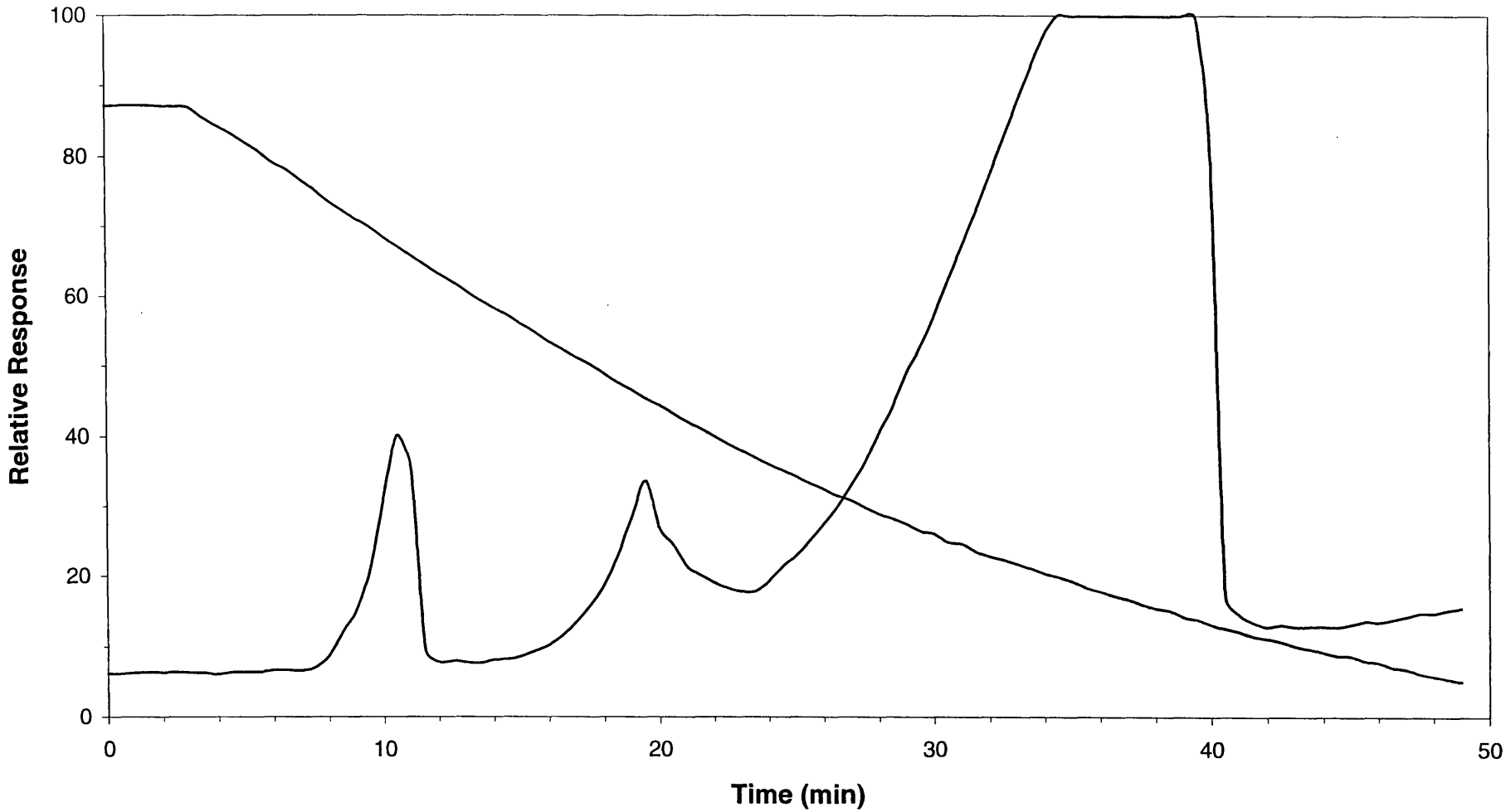

Figure 5.9: SATVA trace from the degradation of Estofil Blue S-RLS under dynamic air

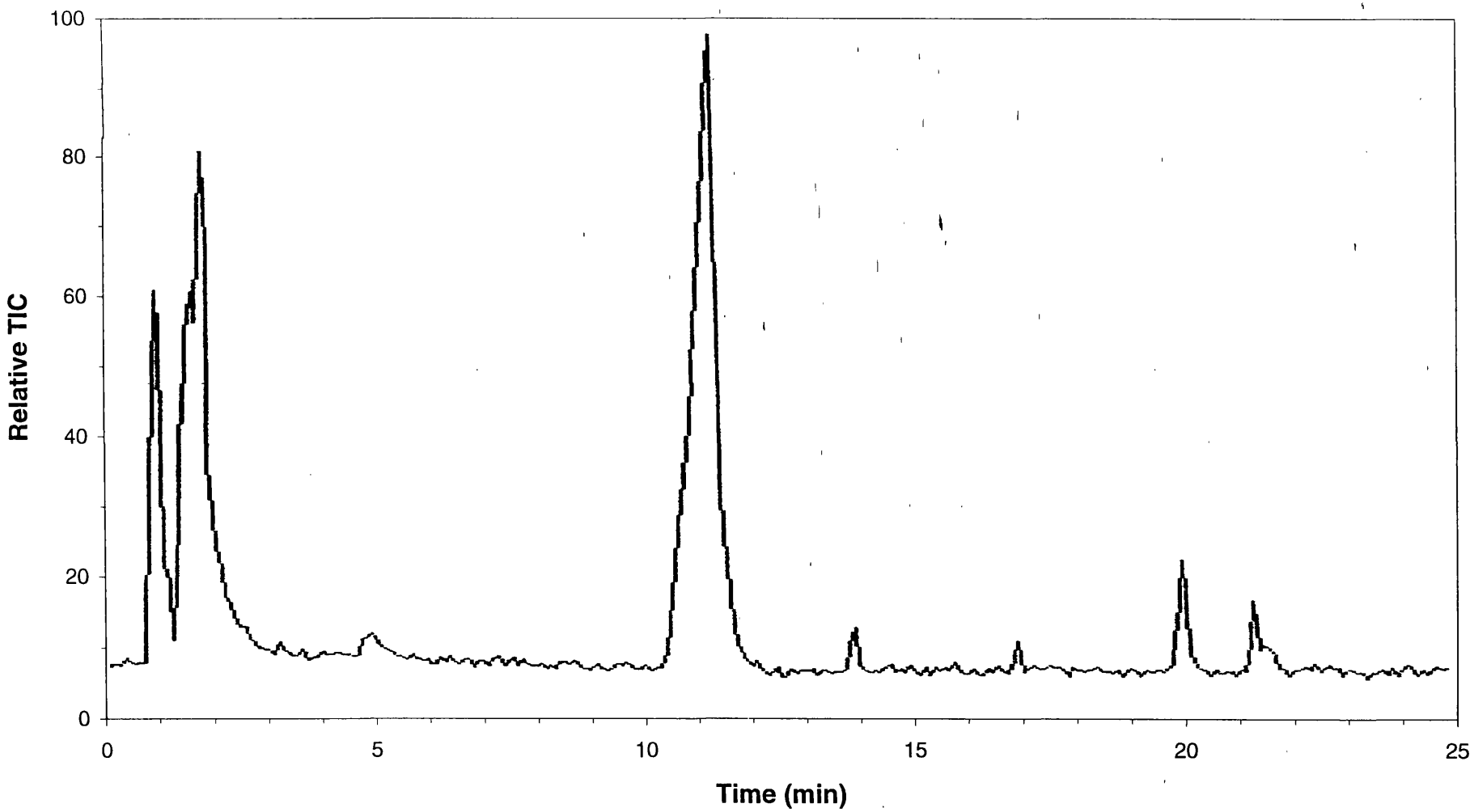

Figure 5.10: TIC trace for the liquid fraction from the SATVA curve in Figure 5.9

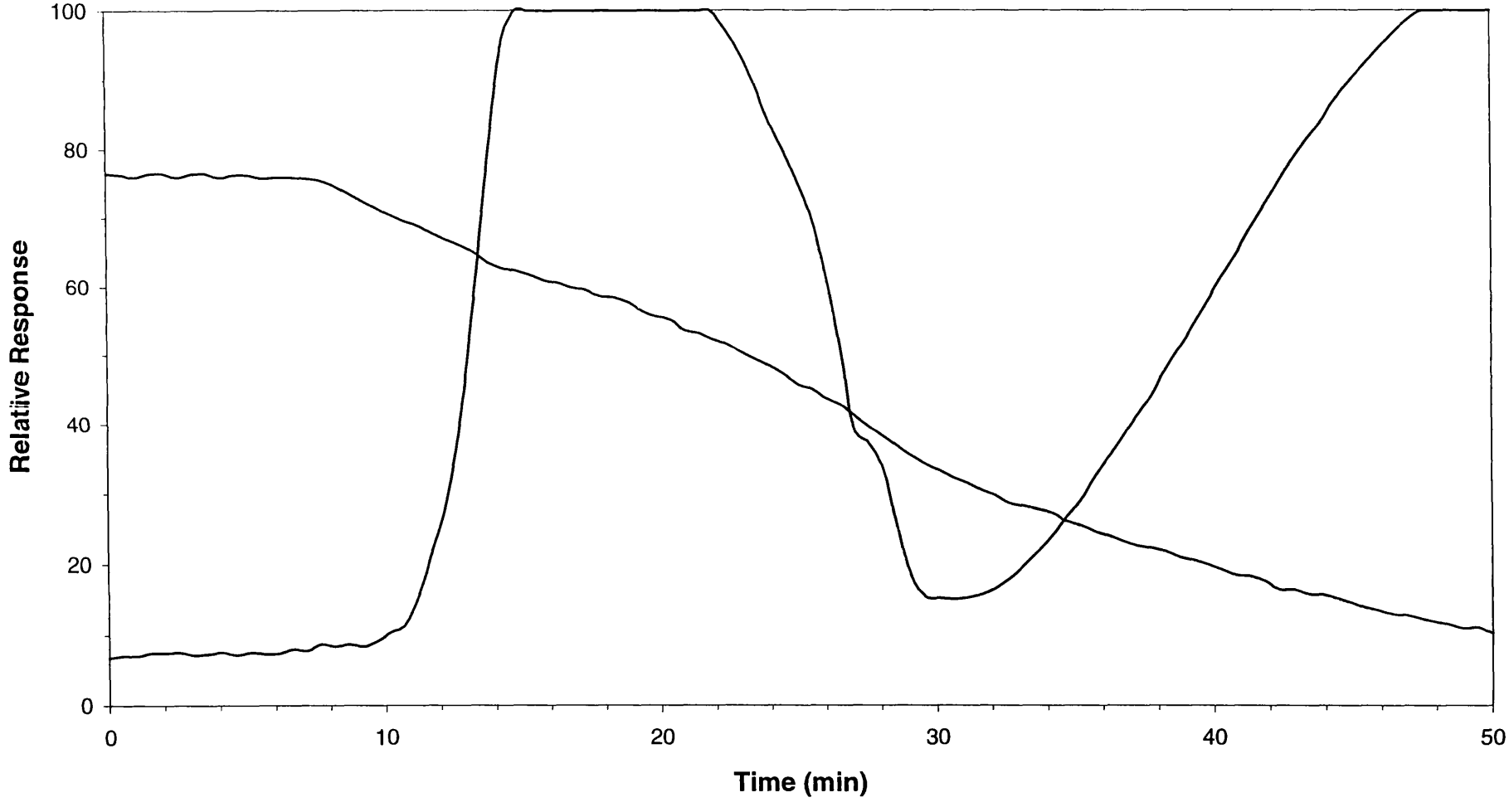

Figure 5.11: SATVA trace from the degradation of Estofil Blue S-RLS under flaming conditions

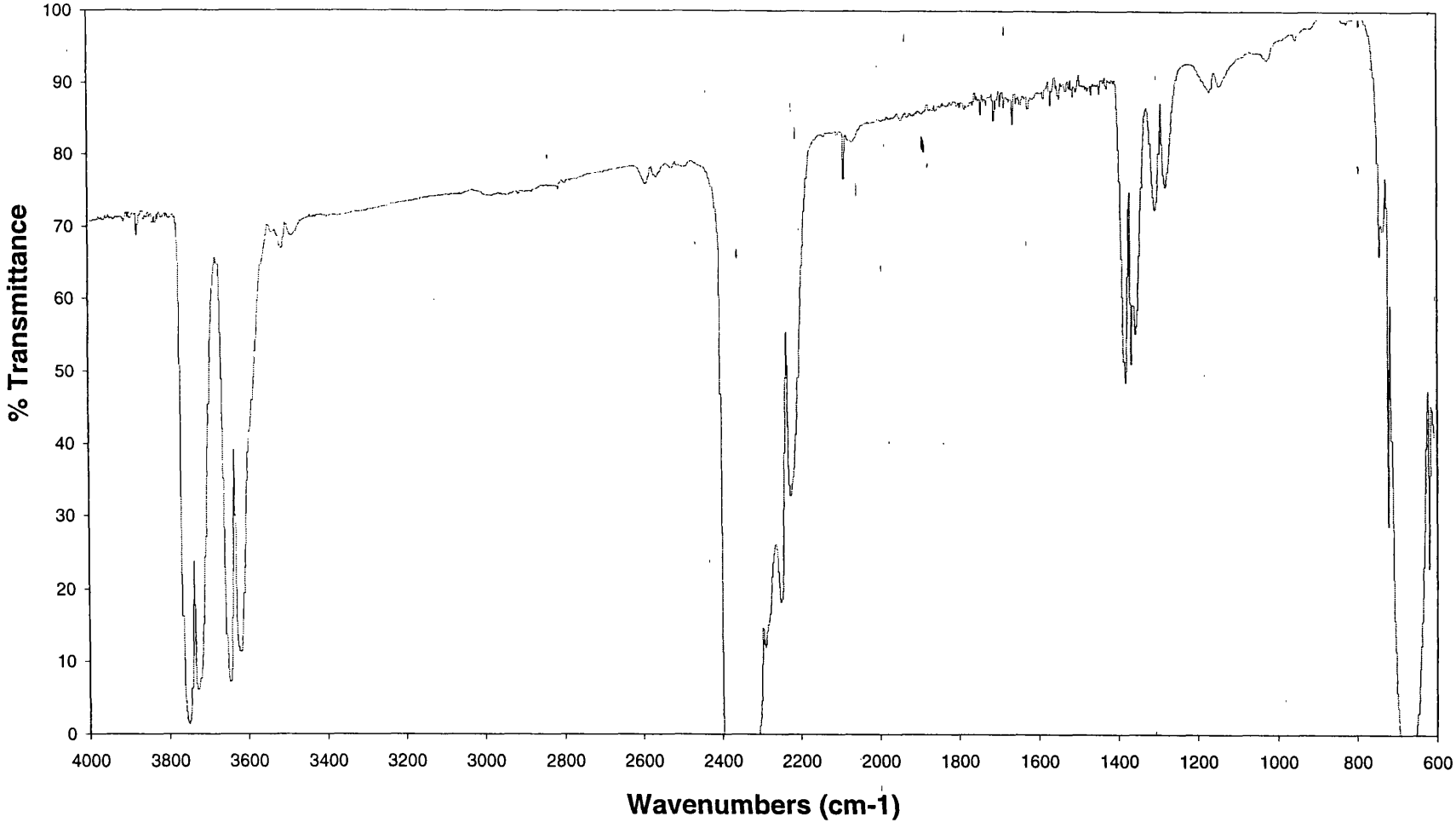

Figure 5.12: IR spectrum from peak 1 products in the SATVA curve in Figure 5.11

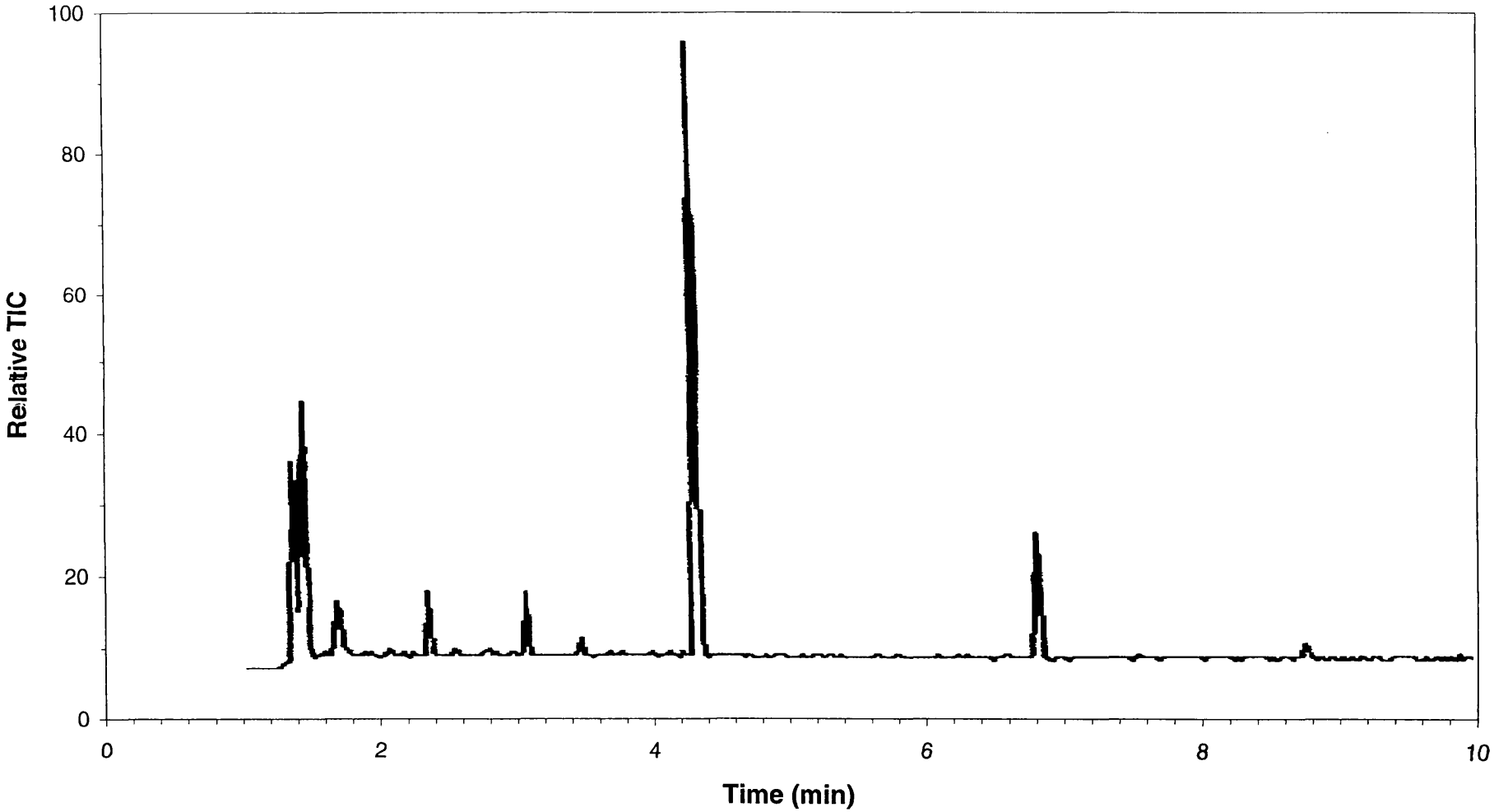

Figure 5.13: TIC trace for the liquid fraction from the SATVA curve in Figure 5.11

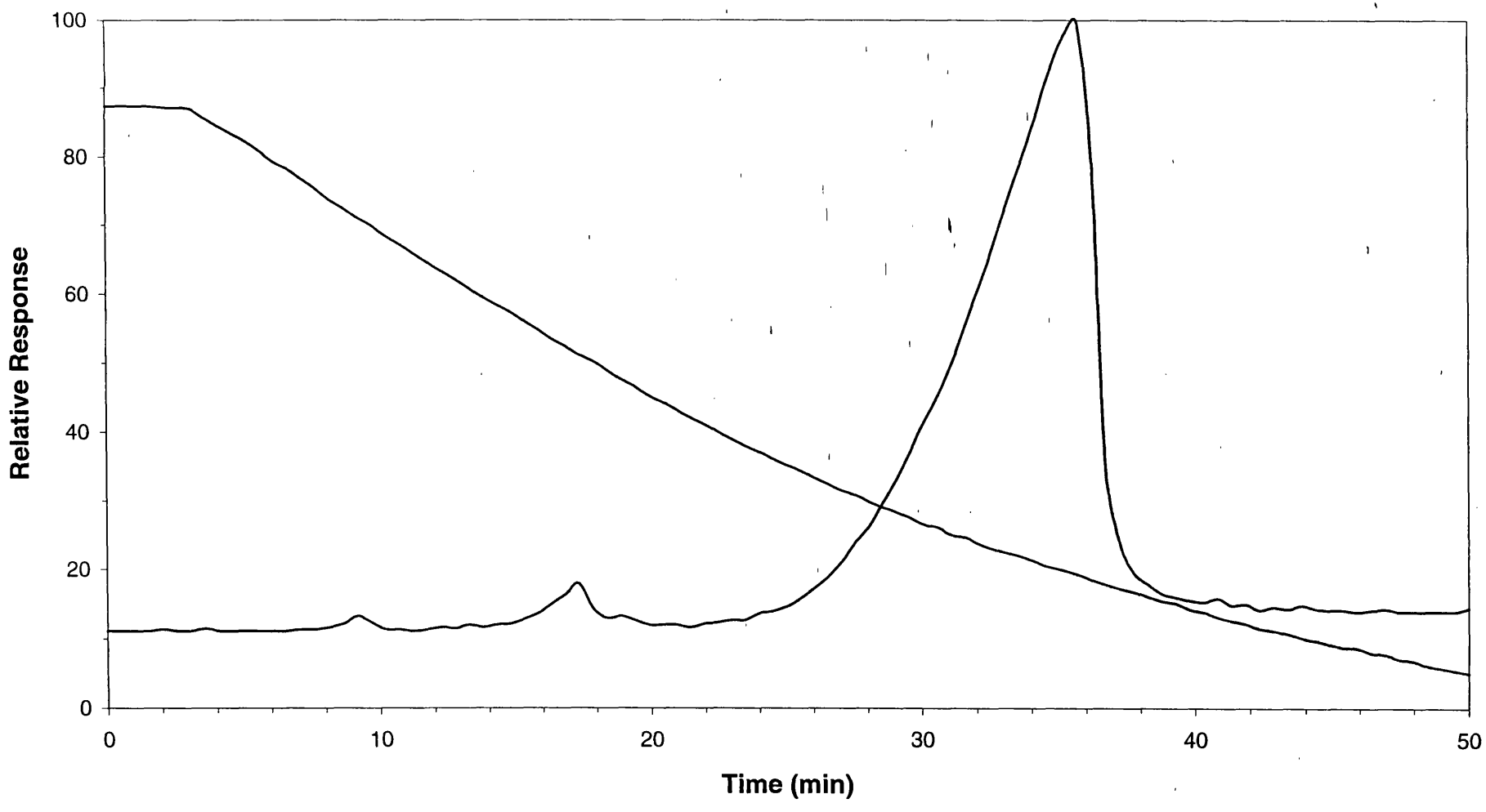

Figure 5.15: SATVA trace from the degradation of Sandorin Violet BL under dynamic nitrogen

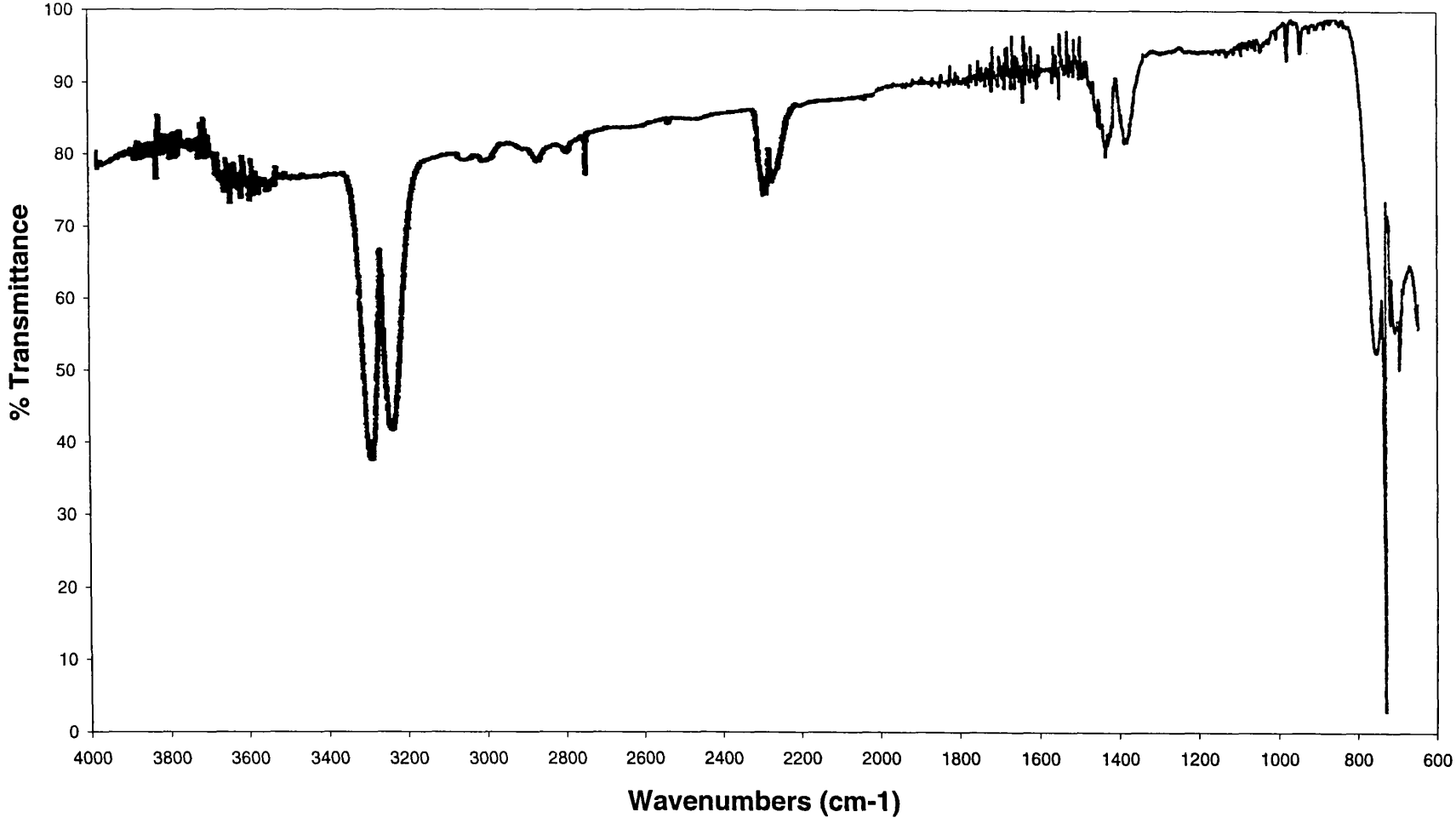

Figure 5.16: IR spectrum from peak 2 products for the SATVA curve in Figure 5.15

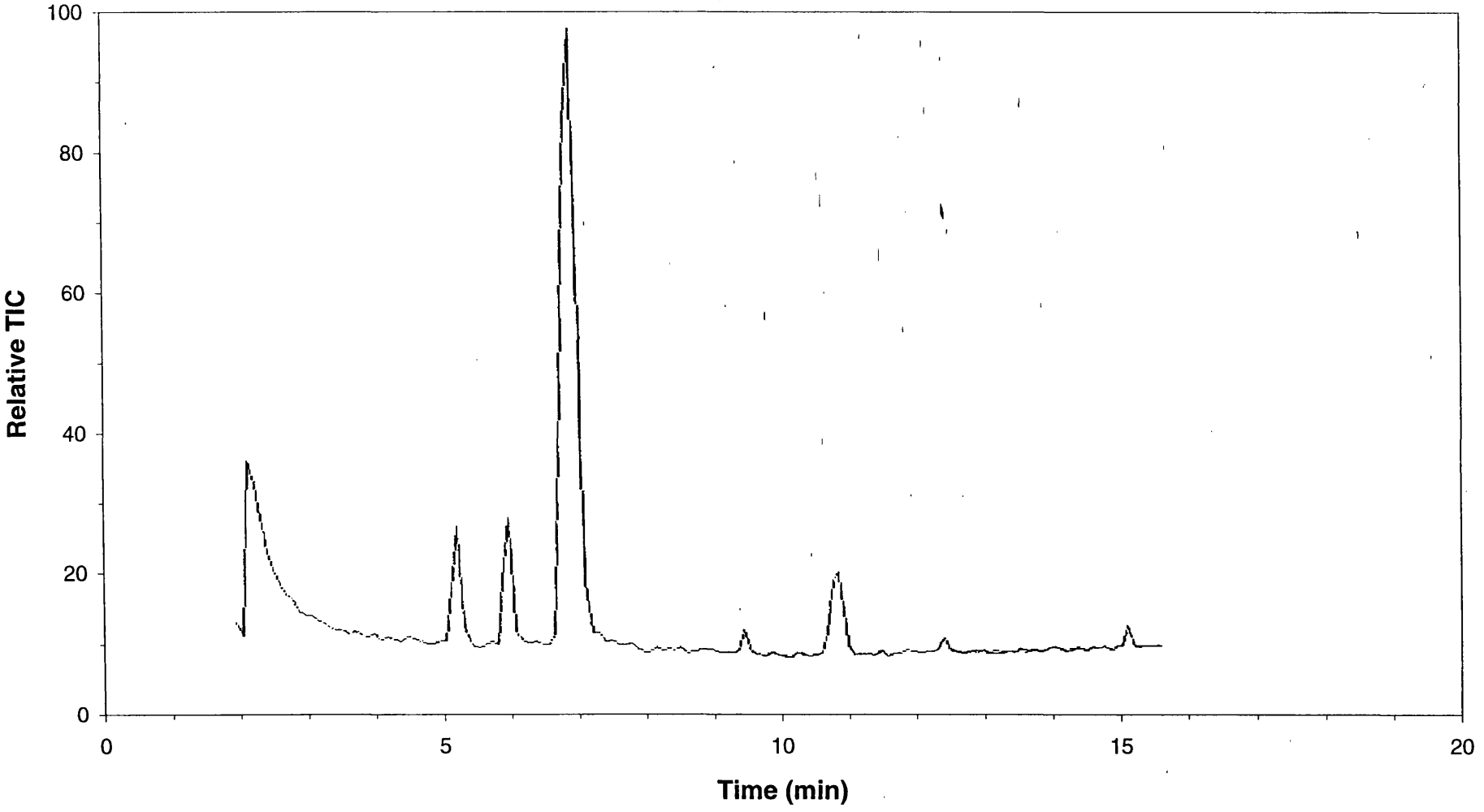

Figure 5.17: TIC trace for the liquid fraction from the SATVA curve in Figure 5.15

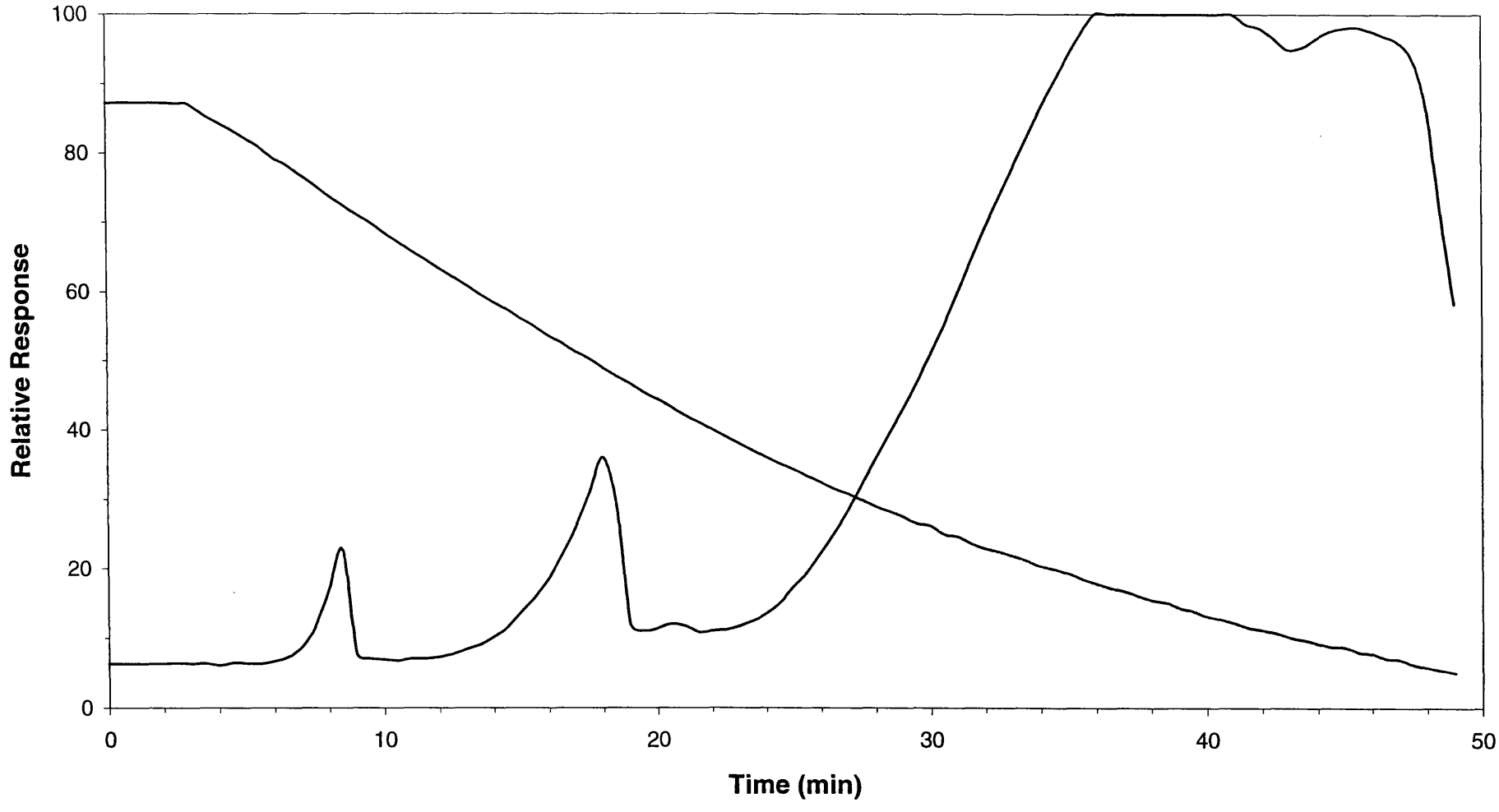

Figure 5.18: SATVA trace from the degradation of Sandorin Violet BL under dynamic air

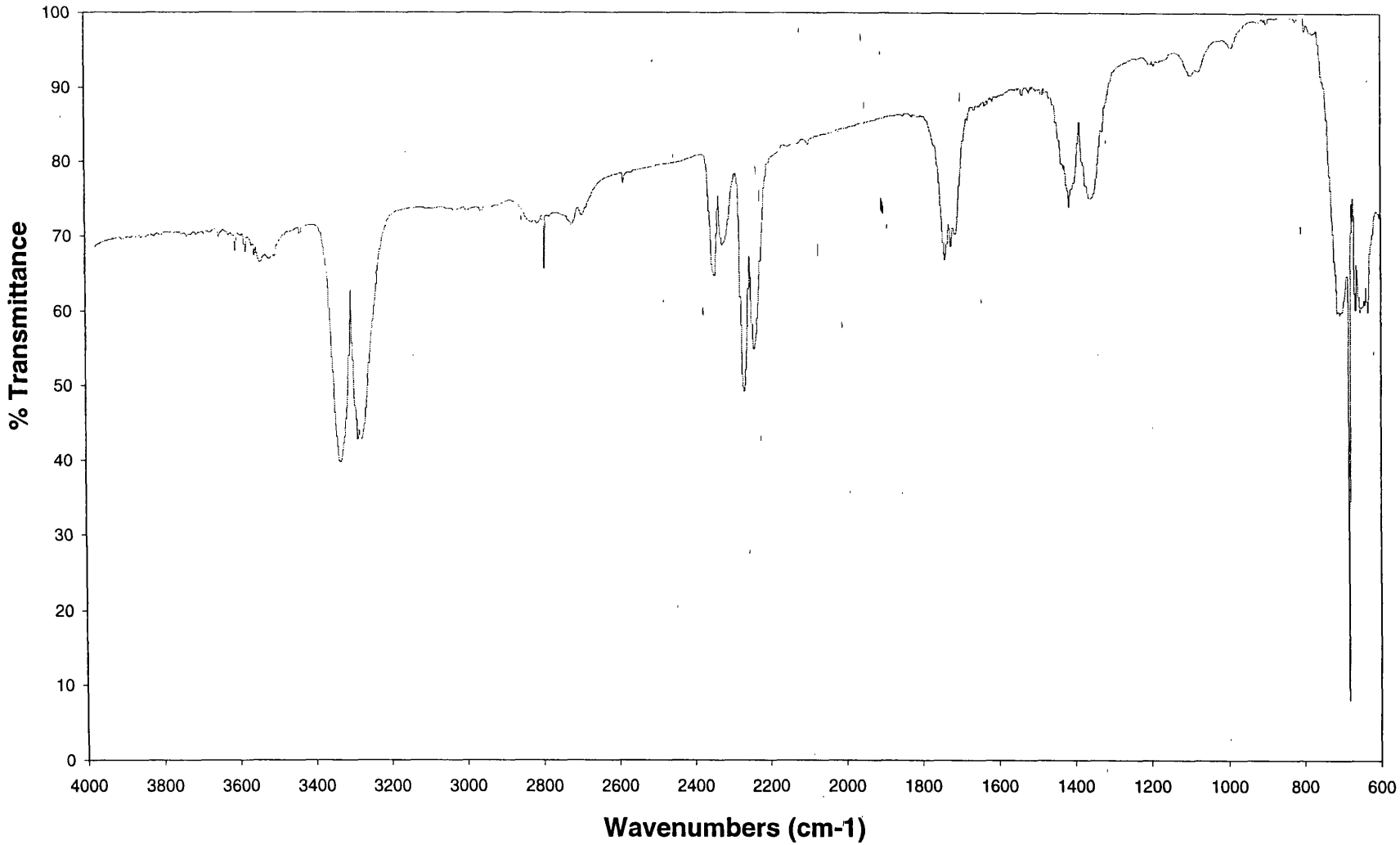

Figure 5.19: IR spectrum from peaks 1 and 2 products for the SATVA curve in Figure 5.18

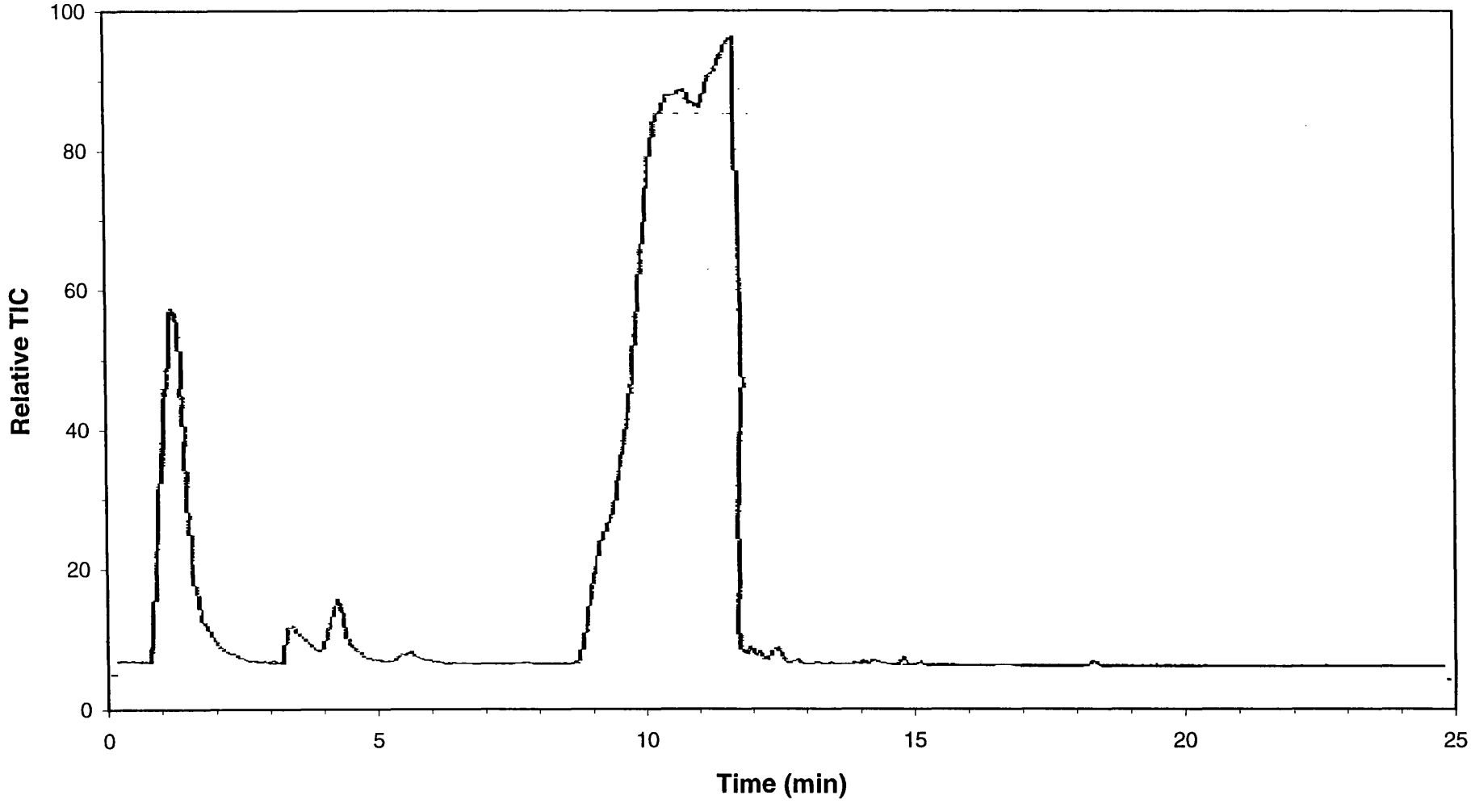

Figure 5.20: TIC trace for the liquid fraction from the SATVA curve in Figure 5.18

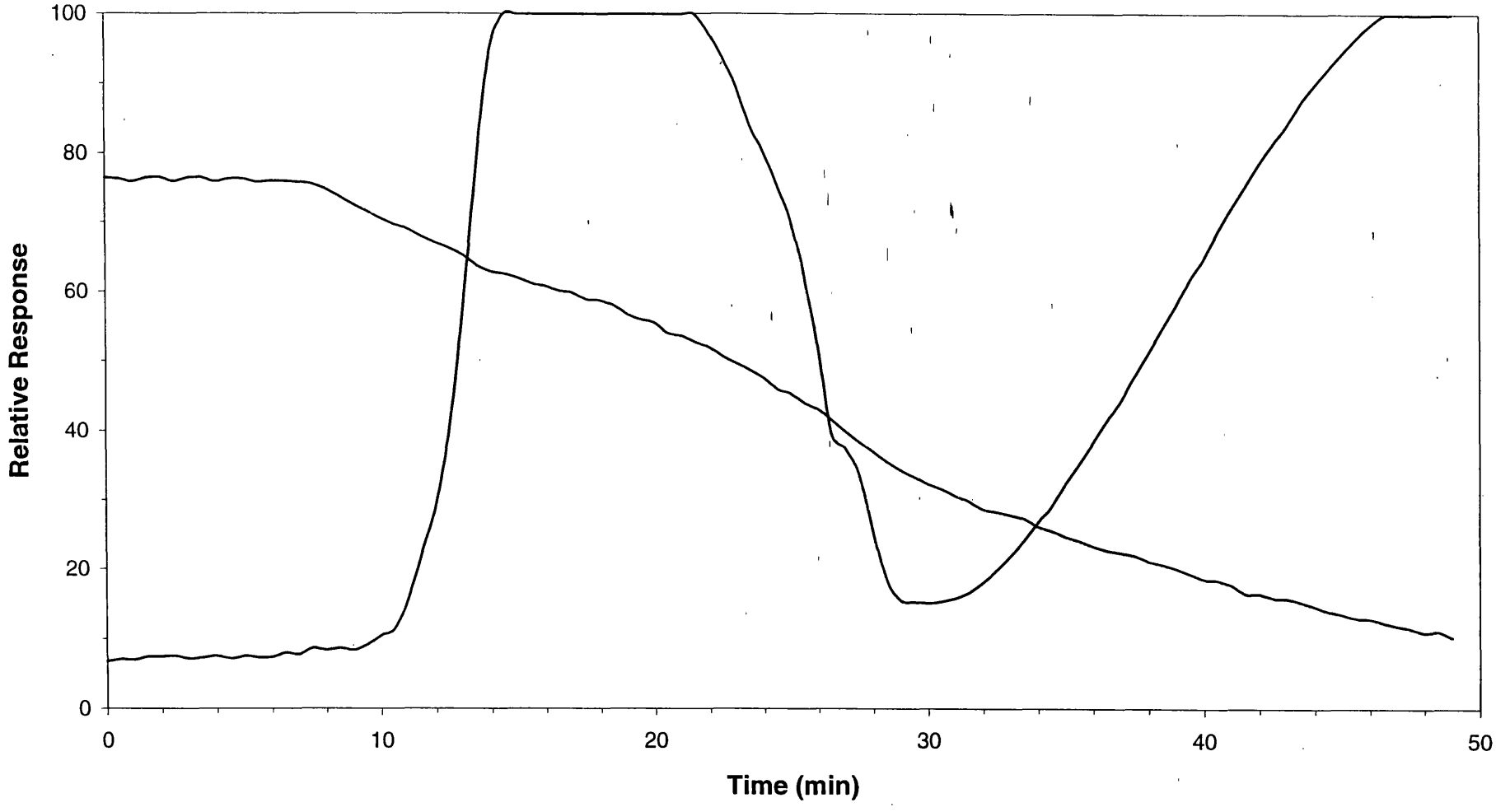

Figure 5.21: SATVA trace from the degradation of Sandorin Violet BL under flaming conditions

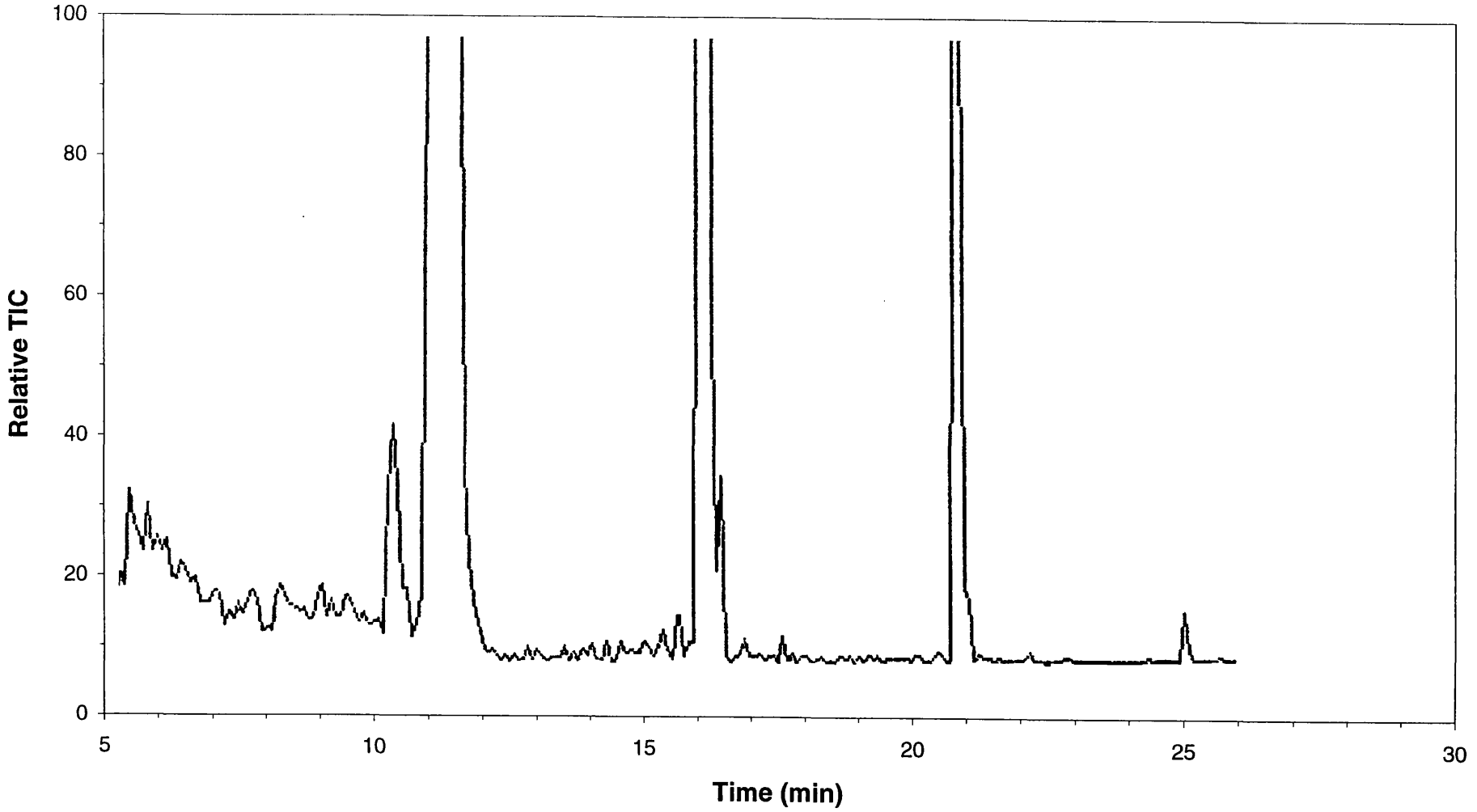

Figure 5.22: TIC trace for the liquid fraction from the SATVA curve in Figure 5.21

CHAPTER 6

METAL COMPLEX AZO DYES

6.1 INTRODUCTION

The colourants studied in this and the following chapter had the added complication of having a transition metal in the structure. The samples in this chapter were metal complex azo dyes. Historically, metal complex formation was a feature of dyestuffs chemistry from a very early time. Mordant dyeing depended on the formation of metal complexes[15]. Metallisation was an important process during the development of azo dyes. It was not until 1991 that Ciba and IG introduced the first premetallised dyes[14]. There are two main types of metallised azo dyes, those where the azo group is a coordinating ligand to the metal and those where it does not coordinate. The former case is of the most commercial importance, and would appear to be the type under study in this chapter.

6.2 CHEMISTRY

Chromium III, cobalt III and copper II are most commonly used metal ions for metal complex azo dyes. Copper II forms square planar complexes. This metal was not present in the samples studied, and will not be discussed further. The other two ions are of relevance. Chromium III has a d^3 configuration, and cobalt III d^6. This means that the crystal field stabilisation energy is at maximum for octahedral complexes, rendering this the preferred structure. Complexes formed from *o,o'*-hydroxyazo dyes

have a meridial (*mer*) structure, and those from o-carboxy-o'-hydroxyazo dyes a facial (*fac*) arrangement. This is illustrated in Figures 6.1 and 6.2 respectively.

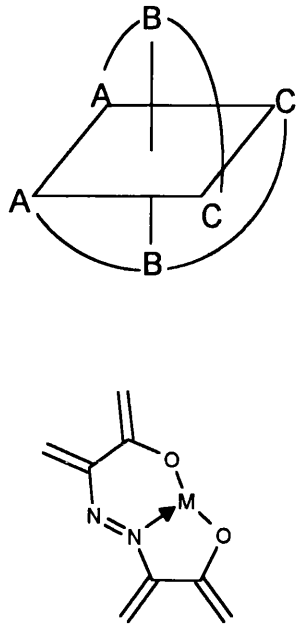

Figure 6.1: *Mer* type

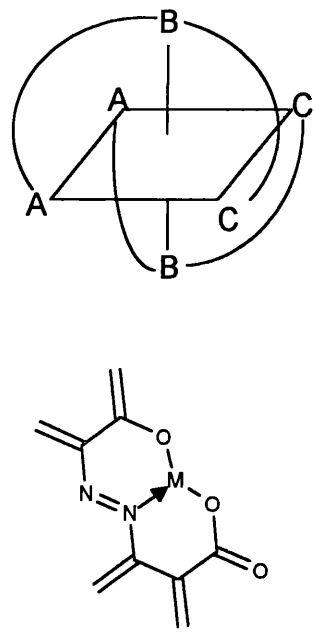

Figure 6.2: *Fac* type

The samples studied in this chapter would appear to be of the type illustrated in Figure 6.1.

6.3 STRUCTURES

The first two colourants presented in this chapter were structuraly similar. The first was a cobalt complex, and the second was a chromium complex. The other difference was with one of the aromatic substituents. The structures are illustrated in Figure 6.3. For ease of interpretation of the diagrams the structures are drawn in two dimensions. Consideration of Figure 6.1 suggests that the two ligands were spacially well separated, so intramolecular interactions during degradation seem improbable.

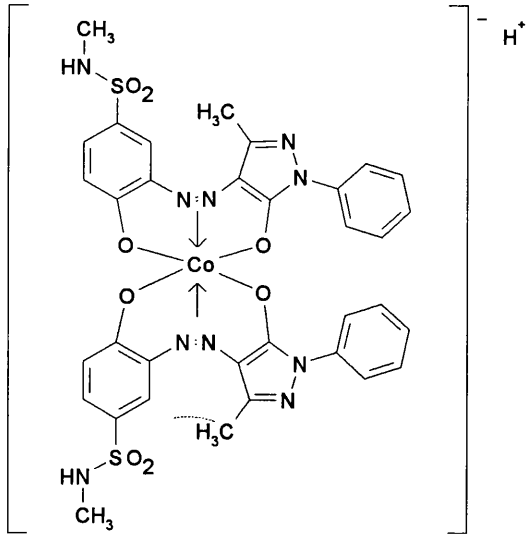

Savinyl Yellow 2RLS

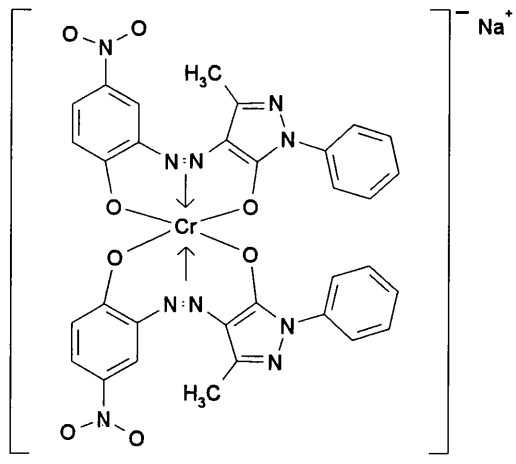

Savinyl Orange RLSE

Figure 6.3: The first two metal complex azo dyes in this chapter

The third colourant in this chapter was another chromium complex. The structure provided differed from those for the other two dyes by having different ligands and two counter ions. The ratio of the counter ions was not provided. The structure for this dye, Savinyl Black RLS, is shown in Figure 6.4.

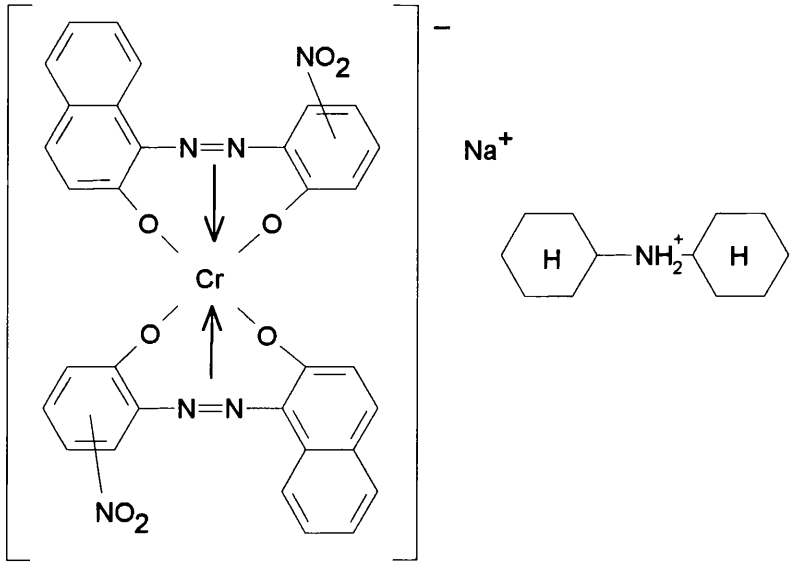

Figure 6.4: The structure of Savinyl Black RLS

The unconventional style of illustrating used for the complex ammonium ion was taken to indicate that the ion was $(cyclohex)_2NH_2^+$.

6.4 THERMAL DEGRADATION OF SAVINYL YELLOW 2RLS

This colourant has many similarities with the second studied in the chapter. These two materials share the same aromatic organic groups, but differ through the bonded metal, counter ion, and one substituent on the organic portion.

6.4.1 Thermogravimetric Analysis

Figure 6.5 shows the TG traces obtained. The table outlining the important temperatures has been omitted for this study. This was because the trace obtained under nitrogen did not show well defined changes of rate.

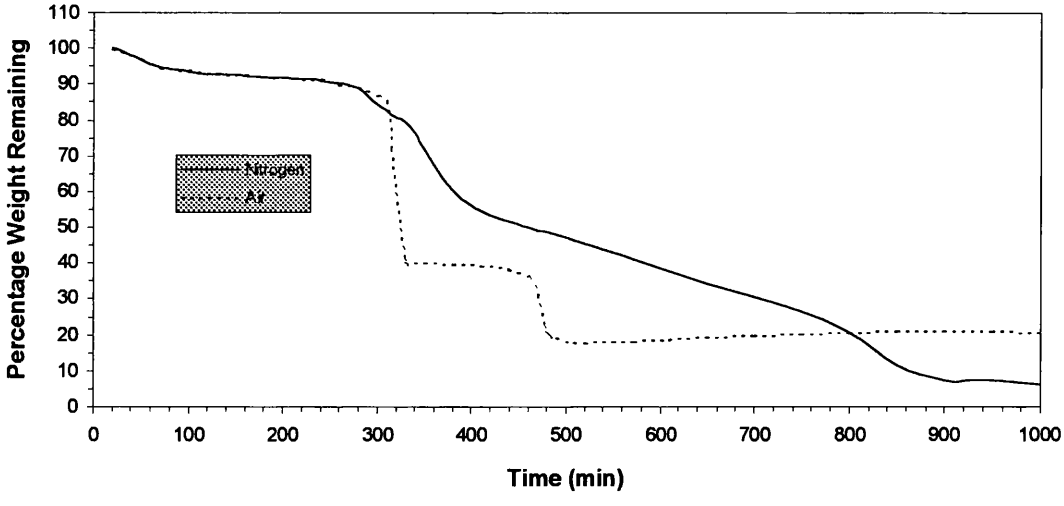

Figure 6.5: Thermogravimetric Analysis traces from Savinyl Yellow 2RLS

It is apparent that there is an early weight loss probably due to water, as was suggested for previous samples. The trace under nitrogen displays a decrease in rate of weight loss at around 420°C. The slower rate following this was probably due to the

degradation of a relatively stable residue. It was for this reason that the degradations for product analysis were only performed to this temperature. The trace under dynamic air displayed a very sharp weight loss at around 320°C. This clearly indicates that oxidation plays a significant part in the degradation of this sample. The degradations for product analysis were carried out to 350°C, as this major weight loss stage should have been complete by this temperature. In retrospect this may not have been the case. It is not unknown for a sample which degrades rapidly, or forms a foam, to fall off the thermobalance pan. Ideally the product analysis should have been repeated to a higher temperature, but time constraints did not permit this.

6.4.2 Product Analysis — Static Nitrogen

These studies were carried out with a heating rate of 10°C/min up to 420°C. This meant that the first stage of degradation (as seen from the TG) was completed.

A typical SATVA trace for the volatilisation of the condensable degradation porducts is shown in Figure 6.6. The major product forming peaks 1 and 2 was CO_2, as identified through IR absorptions at 2319, 669, 3727, 3706, 3627, and 3602 cm^{-1}. A small quantity of COS was also indicated, through IR absorptions at 2072 and 2035 cm^{-1}. Peak 3 was predominately due to the evolution of SO_2. This was seen through IR absorptions at 1373, 1360, 1350, 1165 and 1136 cm^{-1}. There were also traces of HCN, signalled by weak absorptions at 714, 3338 and 3291 cm^{-1}. Ammonia was also detected in small amounts, through the distinctive IR bands at around 920 and 950 cm^{-1}. These findings are summarised in the table on the following page.

Table 6.1: SATVA peak assignments from Figure 6.6

Peak	Assignment
1	CO_2
2	COS
3	SO_2 with a little HCN. Some NH_3 was also detected
4	See below for GC-MS from ether

Diethylether was added to the liquid fraction, which was then analysed by GC-MS. The TIC trace obtained is displayed in Figure 6.7. Only three products were identified. These are listed below:

Table 6.2: GC-MS peak assignments from Figure 6.7

Retention Time	Product	Retention Time	Product
11:35	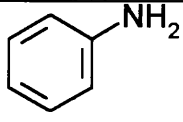	20:08	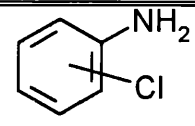
15:12	Good match with 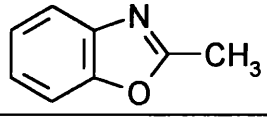		

6.4.3 Product Analysis — Dynamic Nitrogen

These studies were carried out with a heating rate of 10°C/min up to 420°C. The percentage residue by weight compared with the TG results is tabulated below:

Table 6.3: Residue percentages from nitrogen degradation of Savinyl Yellow 2RLS

	Weight Remaining	
Maximum Temperature	**Thermogravimetry**	**Flow tube**
420°C	57%	65%

A typical SATVA trace for the volatilisation of the condensable degradation products is shown in Figure 6.8. The same temperature programme was used as for the static nitrogen studies. It was found that the products obtained were quite different. This implies that some side reactions may have been occurring in the bulk of the sample.

The mass spectrum obtained at 11 minutes into the SATVA run was typical and unambiguous for CO_2. This provided less clear evidence for the nature of the product at the second peak, as there were other products from the liquid fraction also appearing on the spectrum. The IR spectrum obtained for this fraction did suggest the presence of methanol as the major product. Although this trace was weak, there was some absorption at 2800-3000 cm^{-1} for —CH_3 symmetric and asymmetric stretching, and at around 1065 cm^{-1} which is typical for methanol and perhaps due to C—O stretch.

Subsequent analyses also provided mass spectrometric evidence for SO_2 and acetonitrile, the latter of which gave quite a strong spectrum. Unfortunately the IR spectra were too weak to provide additional evidence. Another degradation of this material also provided the unambiguous IR spectrum for ammonia. The deductions made from the SATVA evidence are summarised in the following table:

Table 6.4: SATVA peak assignments from Figure 6.8

Peak	Assignment
1	CO_2 with a little SO_2
2	Methanol and some acetonitrile and ammonia
3	See below for GC-MS of ether extract

The products in the cold finger had ether added, and the fraction was analysed through GC-MS. The TIC trace obtained is presented in Figure 6.9. The peak assignments are tabulated below. The dichloromethane may have been added in error by the analysis service used.

Table 6.5: GC-MS peak assignments from Figure 6.9

Retention Time	Scan Number	Product
0:58	53	SO_2, either due to solubility in the products/solvent mix, or poor sample stability under GC conditions.
1:19	72	Solvent (diethyl ether)
1:29	81	Dichloromethane
5:14	286	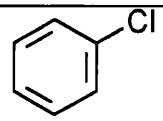
5:58	326	Styrene
7:10	392	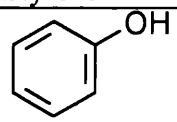
7:18	399	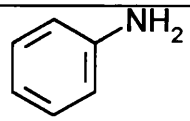
7:34	413	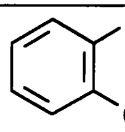 (other isomers do not match spectrum so well)
9:27	516	Possibly 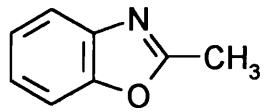
10:37	580	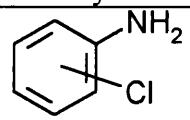
14:47	807	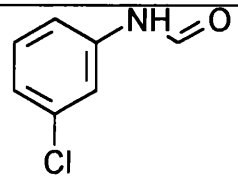

The cold-ring fraction was extracted with dichloromethane, and was also analysed through GC-MS. The TIC trace for this is presented in Figure 6.10. The identification of these peaks is tabulated below. Some of the spectra could not be assigned through the MS reference data available. These have been labelled "NO NIST", representing absence from the NIST MS database used.

Table 6.6: GC-MS peak assignments from Figure 6.10

Retention Time	Product	Retention Time	Product
1.70	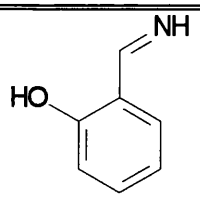 Unclear. very possible, or perhaps 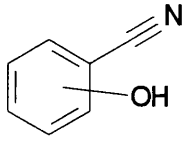	12.49	3-chloroformanilide, 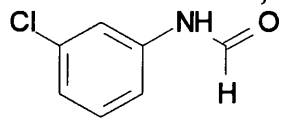 1- and 4- less likely
1.84	Phenol	12.80	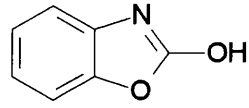
2.90	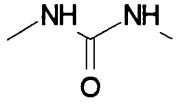 most likely, or perhaps 1,4-dioxin	14.05	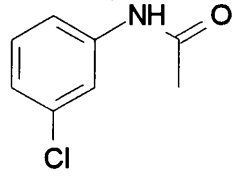 Most likely substitution shown
3.90	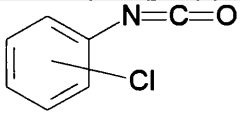 , 1,4- or 1,2- more likely than 1,3-	15.01	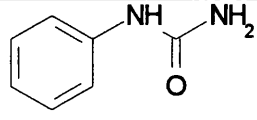
4.32	Similar to peak 1, but 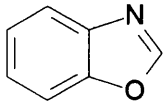 more like 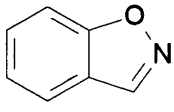 or	12.80	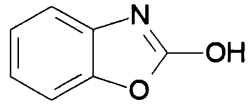
5.18	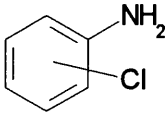	14.05	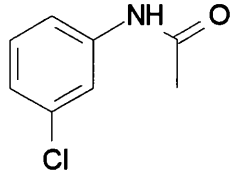 Most likely substitution shown
6.42	Not Identified (weak)	15.01	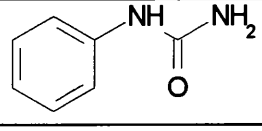

Table 6.6 (continued)

Retention Time	Product	Retention Time	Product
15.60	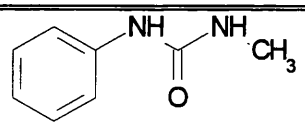	22.50	No NIST
20.16	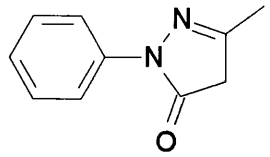 + —Cl at unknown location (no NIST)	27.20	No NIST. From non-chlorinated spectra, possibly 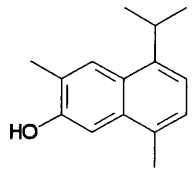 + —Cl
20.71	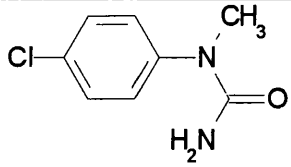	36.32	Aliphatic hydrocarbon
21.86	No NIST		

6.4.4 Product Analysis — Dynamic Air

These studies were carried out with a heating rate of 10°C/min up to 350°C. This temperature should have allowed the initial stage to reach completion. The percentage residue by weight compared with the TG results is tabulated below:

Table 6.7: Residue percentages from air degradation of Savinyl Yellow 2RLS

	Weight Remaining	
Maximum Temperature	**Thermogravimetry**	**Flow tube**
350°C	33%	73%

The percentage residue from the flow-tube studies was significantly higher than that from TG. In hindsight, this may be related to the sample falling off of the thermobalance pan, this possibility having been explained earlier in this chapter.

A typical SATVA trace for the volatilisation of the condensable degradation products is shown in Figure 6.11. Peak 1 was found to be due to the evolution of CO_2, through

the usual MS and IR methods. COS was also observed, but in a much smaller quantity. The IR spectrum of the products from peak 2 showed predominantly the absorptions for SO_2, as described in section 6.6. A small amount of HCN was also observed. The MS evidence confirms these findings. The timing of the MS data shows that the HCN was the product responsible for forming the shoulder following the second peak. The products forming peak 3 gave only a weak IR spectrum, but strong enough to suggest the presence of acetonitrile with absorptions at around 1450, 1030 and 750 cm^{-1}. This identification was confirmed by the MS data. This displayed peaks with m/e = 41, 40, 39, 38 of decreasing intensity, with an additional peak at m/e = 14, as expected. There was also some more SO_2 still being evolved by this time. These findings are summarised in the following table:

Table 6.8: SATVA peak assignments from Figure 6.11

Peak	Assignment
1	Mainly CO_2 with a little COS
2	Mainly SO_2 with some HCN
3	Acetonitrile and SO_2 detected.
4	Much water. See below for GC-MS of extract.

The liquid fraction contained much water, so diethylether was added to extract the other degradation products for GC-MS analysis. The TIC trace for this fraction is displayed in Figure 6.12. The peak assignments for this trace are presented in the following table:

Table 6.9: GC-MS peak assignments from Figure 6.12

Retention Time	Scan Number	Product
0:21	19	Solvent (ether and dichloromethane)
1:20	73	Contaminant (hexamethyltricyclosiloxane)
1:26	78	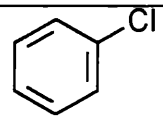
1:44	95	Styrene
2:20	128	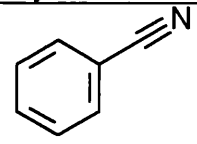
2:26	133	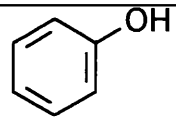
2:33	139	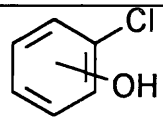
2:42	148	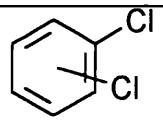
2:49	154	Contaminant (octamethyltetracyclosiloxane)
3:41	201	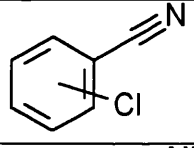
4:26	242	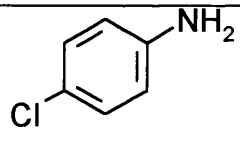 *ortho-* is also possible but *meta-* unlikely
6:07	334	Contaminant (decamethylpentacyclociloxane)
6:15	342	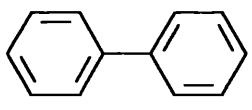 or 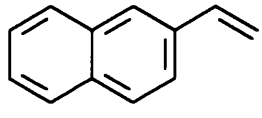
7:17	398	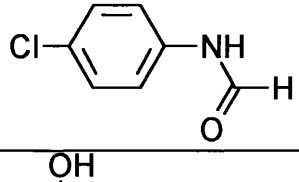
7:25	405	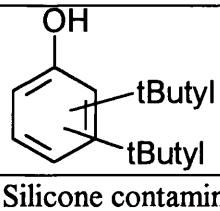
7:40	419	Silicone contaminant

6.4.5 Product Analysis — Flaming Conditions

The apparatus was set up as described in chapter 2. The following observations were made during the degradation:

Table 6.10: Observations from Savinyl Yellow under flaming conditions

First Run	
Sample Size:	236.1 mg
Residue:	77.8 mg (33.0%). A small amount was lost on removal.
Time (min)	**Observations:**
1:20	Started foaming. The sample slowly grew into a column of char.
2:35	Ignition. Burned for under 10 seconds.
7:00	Heater switched off.
Comments:	The residue was a solid foam column around 2 cm tall. This was mainly a brown crumbly foam, with a thin brittle black char around the lower edges.

Second Run	
Sample Size:	262.3 mg
Time (min)	**Observations:**
1:10	Sample started to foam in the centre, releasing occasional smoky puffs.
2:30	Ignition. Extinguished in 5 seconds.
~4:00	The column of residue stopped growing (at ~2 cm tall).
5:00	Heater switched off

The two degradations were carried out within a short time of each other. The previously mentioned heater power output increase with time will not have had an effect on these studies. This explains the similarity between the two results.

The SATVA trace is presented in Figure 6.13. This differed slightly from the typical flaming conditions two peak trace with a small rise after the first peak. Peak 1 was mainly due to the presence of CO_2. This was ascertained through the normal IR absorptions. There was also an appreciable quantity of N_2O observed, also through IR spectroscopy. The SATVA products evolved during the small second peak at around 38 minutes were collected into a separate gas cell. IR spectroscopy showed that some

CO_2 was still being released, although there were also strong absorptions at 1373, 1360 and 1349 cm^{-1} and weak absorptions at 1165 and 1136 cm^{-1}. These absorptions indicated that this rise in Pirani response was due to SO_2.

The on-line mass spectrometer only detected water at the third peak. A cold finger was used to collect this fraction. A small amount of ether was then added to study the sample through GC and GC-MS analysis. Only silicone contaminants were detected. The SATVA findings are summarised in the following table:

Table 6.11: SATVA peak assignments from Figure 6.13

Peak	Assignment
1	Mainly CO_2. A reasonable quantity of N_2O was also detected.
2	SO_2
3	Mainly water. Only silicon contaminants detected in solvent extract.

6.5 THERMAL DEGRADATION OF SAVINYL ORANGE RLSE

This sample had three structural differences from Savinyl Yellow 2RLS. The bonded metal was chromium rather than copper, and the counter ion was Na^+ as opposed to H^+. The SO_2NHCH_3 groups were also replaced by NO_2.

6.5.1 Thermogravimetric Analysis

The plots for TG of Savinyl Orange RLSE under dynamic nitrogen and air are shown in Figure 6.14. These results are summarised in the following table:

Table 6.12: Key temperatures from thermogravimetry of Savinyl Orange RLSE

Conditions	$T_{thresh1}$(°C)	T_{end}(°C)	%Residue
Dynamic Nitrogen	335	>1000	21
Dynamic Air	335	475	13

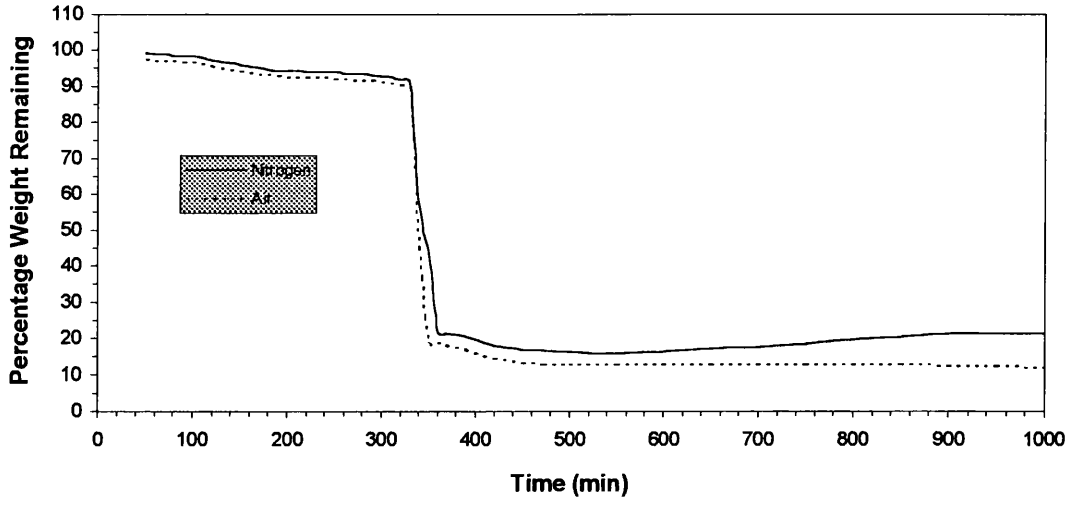

Figure 6.14: Thermogravimetric Analysis traces from Savinyl Orange RLSE

A steady fall in the weight remaining from room temperature up to over 300°C is probably indicative of water loss. The fact that this loss continues up to such a high temperature suggests that this sample has a strong affinity for the water. The alternative would be a contaminant in the sample, such as one of the precursors in the synthesis.

This point was clarified by a TVA study. The sample (1.63 g) was placed under vacuum and heated to 70°C. The temperature was held isothermally for 3 hours, the products collected, and a SATVA separation performed. This gave a very large peak which IR analysis showed to be due to water. There was also an earlier peak, in the region where CO_2 is normally evolved. This may have been due to a small leak in the vacuum system, or perhaps degassing from the sample.

Both traces display a very sharp weight loss. It was suggested in section 6.4.1 that this effect may be due to all or part of the sample falling off of the balance pan.

6.5.2 Product Analysis — Static Nitrogen

These studies were carried out at two maximum temperatures, 330°C to correspond with the start of the first major onset of weight loss and 500°C, as this was the maximum available with this apparatus.

6.5.2.1 Products of Degradation to 330°C

A SATVA trace is given in Figure 6.15. The product evolved at peak 1 was identified as CO_2 through IR analysis, by the absorptions previously reported. The second gas fraction only provided a weak IR spectrum. This had peaks at 750, 1019, 1202, 1275, 1790, 1813 and around 1610 cm^{-1}. All but the absorptions at around 1800 cm^{-1} match those expected for N_2O_4. This product also requires a strong absorption at 1735 cm^{-1}. The product may well be an oxide of nitrogen, but no positive identification has been made. There was no supporting MS evidence. These findings are summarised in the following table:

Table 6.13: SATVA peak assignments from Figure 6.15

Peak	Assignment
1	CO_2
2	Unidentified. Possibly a nitrogen oxide, but not NO_2
3	Mainly water. GC-MS only showed some aliphatic hydrocarbons, particularly a C_8 compound.

Study of the TG trace shows that little was expected to be released at this temperature. Consequently any contamination from the pumping system or a sample impurity will be emphasised in the analysis.

6.5.2.2 Products of Degradation to 500°C

A SATVA trace is presented in Figure 6.16. The temperature used here is into the main degradation stage, as seen in the TG trace. This resulted in more peaks in the

SATVA separation. Peak 1 was due to the evolution of CO_2, indicated by the normal IR absorptions. The second peak, at 30 minutes, provided the distinctive IR spectrum for NH_3 and HCN. These absorptions have been listed previously. All of the less volatile products were collected together for study by GC and GC-MS. On one re-run of this degradation the products forming the peak at 44 minutes were collected for IR analysis, but the spectrum only showed NH_3. These conclusions are presented in the following table:

Table 6.14: SATVA peak assignments from Figure 6.16

Peak	Assignment
1	CO_2
2	NH_3 and HCN
3	Includes lingering NH_3
4	See below for GC-MS

Notes: Ammonia tends to linger in the system, resulting in its detection at more than one peak.

The sample was dried, so little water was detected.

The liquid fraction had diethylether added, and was studied by GC-MS. The TIC trace is presented in Figure 6.17, and the peak assignments are listed in the following table. All products other than aniline were very minor.

Table 6.15: GC-MS peak assignments from Figure 6.17

Retention Time	Product	Retention Time	Product
9:58	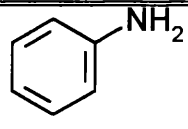 - by far the major product.	17:14	Weak spectrum
14:54	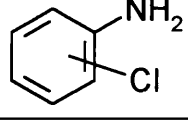	18:50	Possibly 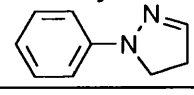 + $—CH_3$

6.5.3 Product Analysis — Dynamic Nitrogen

The sample was degraded at 10°C/min up to 500°C. There was an additional study to 850°C, which gave an identical SATVA trace to the lower temperature analysis. The percentage residue obtained for the latter run is shown below:

Table 6.16: Residue percentages from nitrogen degradation of Savinyl Orange RLSE

	Weight Remaining	
Temperature	**Thermogravimetry**	**Flow tube**
850°C	18%	36%

A SATVA trace for the separation of the volatile degradation products is shown in Figure 6.18. IR Spectroscopy was the only technique used for analysing the gaseous products from this SATVA separation. The absorptions for the materials present have been documented elsewhere. The peak assignments are tabulated below:

Table 6.17: SATVA peak assignments from Figure 6.18

Peak	Assignment
1	CO_2
2	NH_3 and HCN (more of the latter than for static N_2)
3 and 4	See below for GC-MS of ether extract.

The TIC from the GC-MS of the liquid fraction is displayed in Figure 6.19. The peak assignments are listed in the following table:

Table 6.18: GC-MS peak assignments from Figure 6.19

Retention Time	Product	Retention Time	Product
7:34	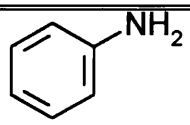 with a small amount of 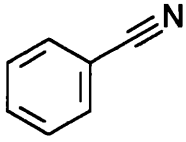	14:46	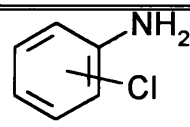
10:20	Unidentified hydrocarbon, possibly mw = 112	18:53	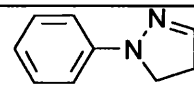
12:05	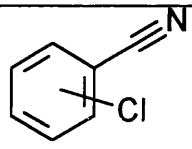		

Note : in one subsequent study the aniline peak was stronger than the hydrocarbon.

6.5.4 Product Analysis — Dynamic Air

These experiments were executed with a heating rate of 10°C/min up to 365°C, as this is past the main stage of weight loss from the TG trace. It was observed that the residue from the flow-tube degradations was a black foam. The foaming can cause the sample to fall off of the thermobalance pan, which may have attributed to the sharp fall in weight detected in the TG. The sharp end to the main weight loss may also be indicative of this effect, so some doubt may be cast on the accuracy of the thermogram obtained. Furthermore, the residue from the flow-tube broke up too easily to permit weighing.

A sample SATVA trace for the volatilisation of the condensable degradation products is given in Figure 6.20. The IR spectra for the gas peaks showed the presence of CO_2. There were also weak absorptions at 721, 3330 and 2990 cm^{-1} which are the strongest absorptions for HCN. These findings were confirmed through the on-line MS data.

There were also weak MS peaks at m/e = 41, 40 and 39 present at around 30 minutes into the SATVA separation. These peaks may indicate the presence of acetonitrile or isocyanomethane. There was also much water present at this point in the SATVA separation. These findings are summarised in the following table:

Table 6.19: SATVA peak assignments from Figure 6.20

Peak	Assignment
1	CO_2
2	NH_3 and HCN (similar as found for static N_2). Perhaps a little isocyanomethane or acetonitrile.
3 and 4	Mainly Water. See below for GC-MS of ether extract.

The TIC trace obtained during the GC-MS analysis of the liquid fraction is displayed in Figure 6.21. The peak assignments for the major product peaks are listed in the following table. The peak at 1:30 is due to solvent.

Table 6.20: GC-MS peak assignments from Figure 6.21

Retention Time	Product	Retention Time	Product
8:41	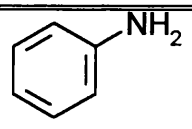 and 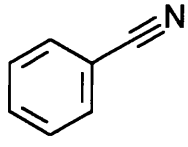 of equal intensity in mass spectrum	13:21	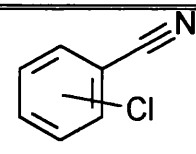
10:56	Aliphatic hydrocarbon, possibly mw = 112		

6.5.5 Product Analysis — Flaming Conditions

The following observations were made during the degradation of this sample under flaming conditions:

Table 6.21: Observations from Savinyl Orange under flaming conditions

First Run	
Sample Size:	152.9 mg
Time (min)	**Observations:**
1:38	Ignition. Burned violently for <2 s
Comments:	Formed into a thermally stable conical shape composed of vertical strata during the burning. This residue had a greenish hue.

Second Run	
Sample Size:	159.6 mg
Residue:	57.1 mg (36%)
Time (min)	**Observations:**
1:24	Started to discolour.
1:30	Ignition. Burned violently for <2 s
Comments:	Residue of same appearance as for the first run.

This sample burned in a violent manner, leaving a large volume of low density material as a residue. The fact that the residue was coloured indicated that it consisted of significant amounts of metal oxide. The only green chromium oxide is α-Cr_2O_3 and is probably the source of the colour. The aggressive way in which the sample was transformed from a layer of powder to this inflated cone would imply that this material may disperse Cr_2O_3 into the smoke under a fire situation.

The SATVA trace obtained from these degradations is displayed in Figure 6.22. The curve is not smooth at around 27 minutes. This may have been caused by an air leak in the vacuum system, as product evolution tends to appear as a smooth peak. This shape is more typical of a partial loss in vacuum. The second run of the degradation did not provide a presentable trace, due to flaws in the new software in use.

The IR spectrum for all the gases evolved under the SATVA separation is presented in Figure 6.23. The strongest absorptions indicate the presence of CO_2. These absorptions have been listed previously. The absorptions at 2273, 2238, 2212, 1299

and 1272 cm^{-1} are indicative of N_2O. Acetylene is indicated by the absorptions at 731, 3337 and 3290 cm^{-1}. These findings are summarised in the following table:

Table 6.22: SATVA peak assignments from Figure 6.22

Peak	Assignment
Non-Condensables	CO
1	Mainly CO_2 with a large quantity of N_2O and a little acetylene.
2	Mainly water. See below for GC-MS of ether extract.

The liquid fraction had diethylether added to provide an extract for GC-MS analysis. The resulting TIC trace is presented in Figure 6.24. The peak assignments are listed in the following table:

Table 6.23: GC-MS peak assignments from Figure 6.24

Retention Time	Product	Retention Time	Product
2:26	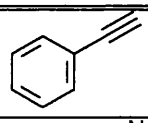	6:43	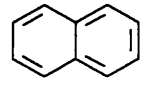
3:34	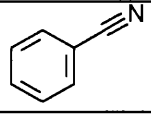	6:52 and 9:24	Silicone contaminant
4:26	Silicone contaminant	13:20	Spectrum matches 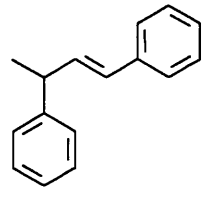 well

The walls of the degradation vessel were washed with dichloromethane, and the resulting extract studied through GC-MS. The TIC trace is presented in Figure 6.25, and the peak assignments listed in the ensuing table:

Table 6.24: GC-MS peak assignments from Figure 6.25

Retention Time	Product	Retention Time	Product
1.69	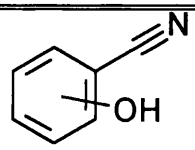	5.10	Chloroaniline
1.81	Aniline	26.73	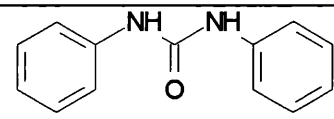
3.91	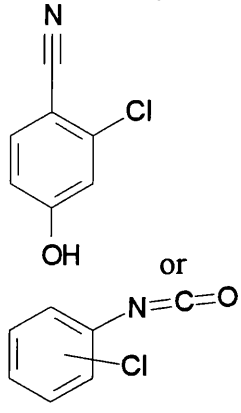		

6.6 THERMAL DEGRADATION OF SAVINYL BLACK RLS

This sample was the final co-ordinated disazo inorganic colourant studied. The organic substitutions differ quite significantly from the other two in this chapter. It also has two counter ions — a sodium ion and a bicyclohexyl ammonium ion.

6.6.1 Thermogravimetric Analysis

Figure 6.26 shows the TG traces obtained. The major threshold temperatures are not tabulated for this sample as there are no clear transitions in the rate of weight loss. Both traces follow a similar profile up to around 200°C. This slight weight loss may be due to the loss of water. The trace obtained under nitrogen shows no well defined

stage of weight loss, but rather a gradual decomposition, which was still incomplete by 1000°C.

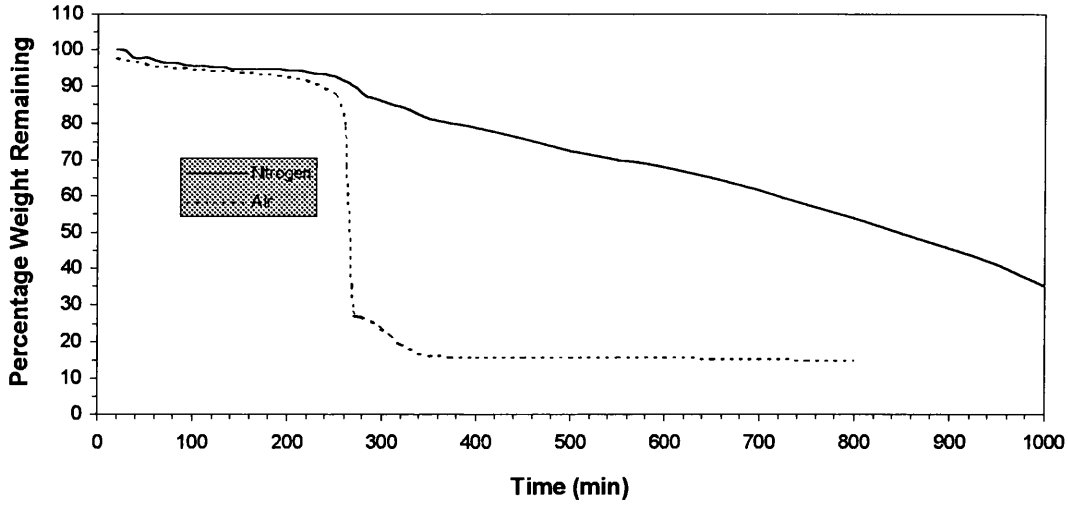

Figure 6.26: Thermogravimetric Analysis traces from Savinyl Black RLS

The trace obtained under air did show a sharp drop in weight at around 265°C. Although sharp, it can be seen that there was a steady increase in the rate of weight loss from around 210°C. This suggests that this was a genuine weight loss, and not a consequence of the sample falling off the balance pan.

6.6.2 Product Analysis — Dynamic Nitrogen

These studies were carried out with a heating rate of 10°C/min up to 900°C. This was chosen as TG information was not available at the time the degradations were carried out. It may be seen from the TG trace in Figure 6.26 that there was no clear temperature from which to determine a suitable maximum temperature for the degradation.

A typical SATVA trace for the separation of the volatile condensable degradation products is presented in Figure 6.27. The products were all studied through mass

spectrometry and IR spectroscopy. Peak 1 was identified as being due to the volatilisation of CO_2, and peak 2 to NH_3. The peak at 19 minutes provided MS peaks at m/e = 41, 40, 39, 28, 27 and 26. This is consistent with the presence of acetonitrile. These peaks were very weak, so it is not surprising the IR confirmation was not observed. The peak at 23 minutes (peak 4) supplied unambiguous MS and IR spectrometry data for HCN. The on-line MS information for the final peak showed only water. These conclusions are summarised in the following table:

Table 6.25: SATVA peak assignments from Figure 6.27

Peak	Assignment
1	CO_2
2	Ammonia
3	Acetonitrile
4	HCN
5	Mainly water. See below for GC-MS of ether extract.

Diethylether was added to the cold-finger to provide an extract for GC-MS analysis. The TIC trace for this study is shown in Figure 6.28. The peak assignments are listed in the following table:

Table 6.26: GC-MS peak assignments from Figure 6.28

Retention Time	Scan Number	Product
1:15	68	Possibly 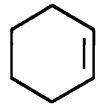
3:52	211	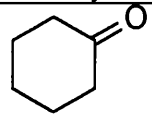
4:59	272	Good match with 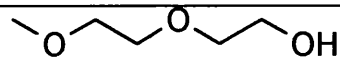
5:55	323	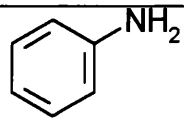
6:23	349	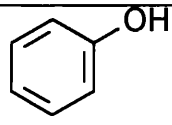

Table 6.26 (continued)

Retention Time	Scan Number	Product
7:49	427	Unidentified aliphatic.
8:13	449	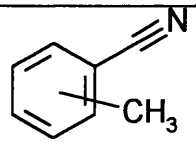
9:16	506	Unidentified
11:32	630	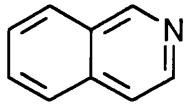 (note that quinolines and isoquinolines are indistinguishable by MS alone)
11:49	646	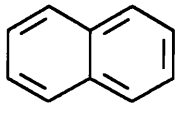
20:23	1114	Spectrum similar to 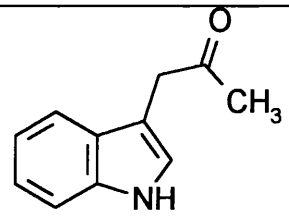
24:13	1323	Unidentified

6.6.3 Product Analysis — Dynamic Air

These studies were also carried out with a heating rate of 10°C/min up to 900°C. The reason was that TG information was not available at the time the degradations were performed, to provide a more significant choice of maximum temperature.

A typical SATVA trace for the volatilisation of the condensable degradation products is shown in Figure 6.29. Mass spectrometry and FT-IR spectroscopy were used to analyse the gaseous products. Peak 1 at 10 minutes was confirmed as being due to the evolution of CO_2. All the products from 12 to 22 minutes were collected into the one gas cell for IR analysis. This only revealed the presence of NH_3 and some lingering CO_2. The on-line mass spectrometer only detected ammonia. There was no distinct product identified for the small rise in Pirani response at 21 minutes. The mass

spectrometer displayed only water peaks for the third major peak, starting at 24 minutes. These findings for the three major peaks summarised in the following table:

Table 6.27: SATVA peak assignments from Figure 6.29

Peak	Assignment
1	CO_2
2	NH_3
3	Mainly water. See below for GC-MS of ether extract.

The cold finger had diethylether added, to provide an extract for GC-MS analysis. The TIC trace from this study is presented in Figure 6.30. The peak assignments are tabulated below:

Table 6.28: GC-MS peak assignments from Figure 6.30

Retention Time	Scan Number	Product
1:40	91	
1:51	101	
4:09	227	O
5:29	300	N
6:13	340	Cl Cl
6:48	372	H Me
6:59	382	N Me
8:48	481	N
9:02	494	
12:28	681	Unidentified aliphatic hydrocarbon

6.6.4 Product Analysis — Flaming Conditions

The apparatus was arranged as described in Chapter 2. The following observations were made during the degradation.

Table 6.29: Observations from Savinyl Black under flaming conditions

First Run	
Sample Size:	158.4 mg
Time (min)	**Observations:**
1:15	Ignition.
4:00	Heater switched off.

Second Run	
Sample Size:	332.4 mg
Residue:	117.3 mg (53%)
Time (min)	**Observations:**
1:09	Ignition. Burned rapidly.
3:00	Heater switched off.
Comments:	The sample auto-ignited almost immediately after the blocker had been removed. The pilot had not been started. The residue puffed up and had formed three distinct layers: 1) Ash on the top. 2) Middle layer of a "clumpy" brown powder. 3) Lower layer of black powder.

The layering of the residue suggests that the sample may have been protected by the residue layers.

The SATVA trace obtained did not differ from the usual for degradation under flaming conditions. There were two large peaks, one for CO_2 and one for water. For this reason it has not been reproduced here. There were small amounts of other materials also detected. The IR spectrum of the gaseous products also showed the absorptions previously attributed to N_2O. Weak absorptions at 3311, 730 and 3267 cm^{-1} may have been be due to a small amount of acetylene. Other weak absorptions at around 1755, 1630 and 1602 cm^{-1} suggested N_2O_4 was present. Ethane was also detected through

the on-line MS. The non-condensable collection showed weak IR absorptions for CO.

These conclusions are summarised in the following table:

Table 6.30: SATVA peak assignments from Savinyl Black under flaming conditions

Peak	Assignment
Non-Condensables	CO
1	Mainly CO_2, with N_2O, N_2O_4, acetylene and ethane.
2	Mainly water. See below for GC-MS of ether extract.

The TIC trace for the diethylether extract from the cold finger is presented in Figure 6.31. The peak assignments are given in the following table:

Table 6.31: GC-MS peak assignments from Figure 6.31

Retention Time	Scan Number	Product
3:12	175	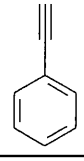
3:34	195	Contaminant (octamethylcyclotetrasiloxane)
5:01	274	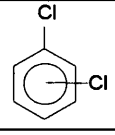
5:46	315	Mostly contaminant (decamethylcyclopentasiloxane) co-eluting with some benzonitrile
6:53	376	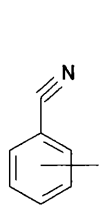 or 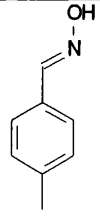
7:05	387	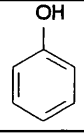
8:01	438	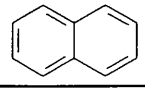
8:12	448	Contaminant (dodecamethylcyclohexasiloxane)
8:50	482	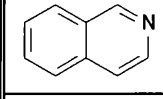 or possibly 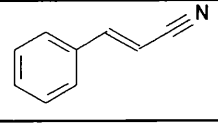
10:27	571	Siloxane contaminant

6.7 MAJOR PRODUCT SUMMARIES AND MECHANISMS

The major products for each of the degradations in this chapter are summarised in this section. Proposed mechanistic routes for the decomposition of the materials are also suggested.

6.7.1 Savinyl Yellow 2RLS

These degradations were performed under four environments, static nitrogen, dynamic nitrogen, dynamic air and flaming conditions. The first two are discussed together, as this demonstrates the difference between these similar conditions.

6.7.1.1 Static and Dynamic Nitrogen

The main difference between these two studies was in the gases produced. The same temperature program was used for both analyses. The static nitrogen degradation gave CO_2 and SO_2 as the major products, along with smaller amounts of COS, HCN and NH_3. The dynamic nitrogen degradation provided CO_2 and MeOH as the major gases, along with smaller amounts of SO_2, NH_3 and a little acetonitrile. It has been suggested in Chapter 2 that the static nitrogen environment would permit more side reactions than the dynamic studies. The acetonitrile may have been the source of the HCN, with methane being formed as a by-product. This latter product was not detectable by the analysis procedures employed. Similarly, the methanol may have been further degraded if retained in the hot decomposing sample.

The liquid fraction contained mainly aniline and chloroaniline under both environments, with phenol also detected in the dynamic nitrogen studies. CRF analysis was only performed for the dynamic nitrogen case. Here the major product was apparently

chlorinated 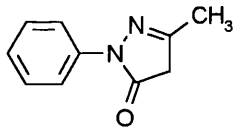 which, although not in the MS database was identified through the comparison of the spectra from structurally similar materials.

The most surprising aspect to these findings were the chlorinated products. The structure provided for this colourant shows no chlorine. It may be that some chlorinated intermediates were used in the synthesis, these residues remaining in the sample although the purity of the samples was claimed to be high.

The most obvious weak links in the structure of Savinyl Yellow 2RLS are marked in Figure 6.32.

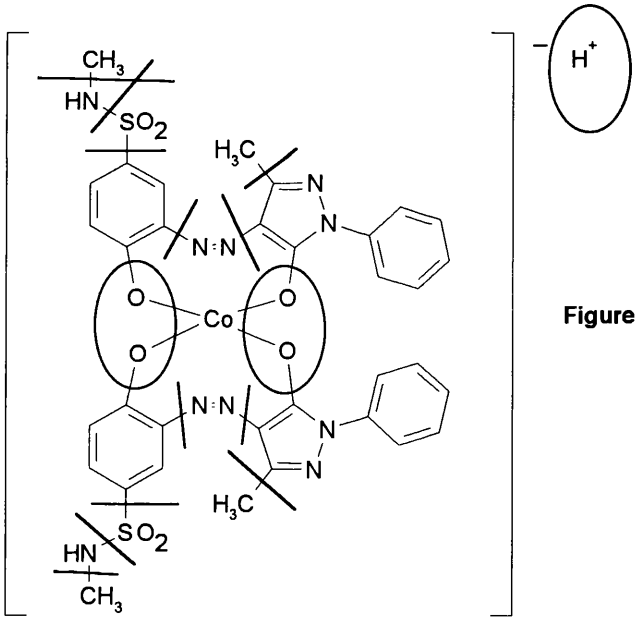

Figure 6.32: Savinyl Yellow 2RLS weak linkages

The source of the major CRF component can be seen from the structure of the colourant, if the chlorine could be accounted for. This suggests that the central oxygen atoms may remain with the aromatic rather than the cobalt. This means that the benzene rings to the left are a likely source of the phenol. These rings are also the probable source of the aniline via the azo linkage, or perhaps the five-membered ring

degrades to make the right-hand benzene rings the aniline source. If the SO_2 leaves directly, then the remainder of that substitution would be the source of acetonitrile and ultimately HCN. This may also be the source of NH_3. Alternatively, it has been supposed here that the azo linkage or the five membered ring may decompose, allowing ammonia to come from this pathway. The source of the COS, CO_2 and methanol is less clear. Loss of the methanol groups as radicals may result in the formation of methanol from water — the substance is hydrophilic. The CO_2 may be formed from the decomposition of the residue, which probably contained a cobalt oxide and carbonaceous material.

6.7.1.2 Dynamic Air

The gases detected were CO_2, SO_2, CH_3CN and HCN. There was relatively more phenol with chloroaniline and chlorobenzene but no aniline.

The lack of aniline is an interesting observation, yet chloroaniline was present. If the oxygen promoted the formation of the chloroaniline/aniline, then this fragment may be liberated without the chlorine being separated from the aromatic ring. If one were to suppose that the right-hand aromatic was chlorinated in contradiction to the structure supplied, then it may be supposed that the decomposition of the five membered ring initiated the formation of the anilines. Simple cleavage of the benzene ring would also provide the chlorobenzene.

6.7.1.3 Flaming Conditions

There were very few products detected here, with there being no liquids found other than water and background silicone contaminants. Major components were CO_2 and water, with some N_2O and SO_2 also detected. This offers no new information, with the

N_2O being a suspect genuine product, as explained previously. It cannot be ruled out that the azo linkage was the source. The ferocity of the flaming may have promoted the near total decomposition resulting in few products being detected.

6.7.2 SAVINYL ORANGE RLSE

This sample was also degraded under the four major environments, with the static nitrogen studies being performed to a maximum temperature of 300°C and 500°C. The lower temperature degradation produced only CO_2 and water at detectable levels. The 500°C products closely matched those for the degradation under dynamic nitrogen, as have been described together.

6.7.2.1 Static and Dynamic Nitrogen

The gases produced were CO_2, NH_3 and HCN. The static nitrogen environment produced considerably more CO_2. There was also a higher ratio of HCN to NH_3 under dynamic nitrogen. The dynamic nitrogen degradation produced a hydrocarbon with a molecular weight of 112 as the major product. This was not present in the study under static nitrogen. This material appeared in some of the other analyses, and may be a contaminant. Disregarding this, aniline was a major liquid in both cases, with much chloroaniline also being present. There was also some 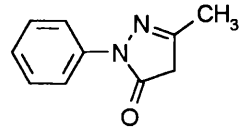

detected. Benzonitrile was also present in the degradation under dynamic nitrogen.

The structure of Savinyl Orange RLSE is illustrated in Figure 6.33, with the most obvious weak linkages indicated.

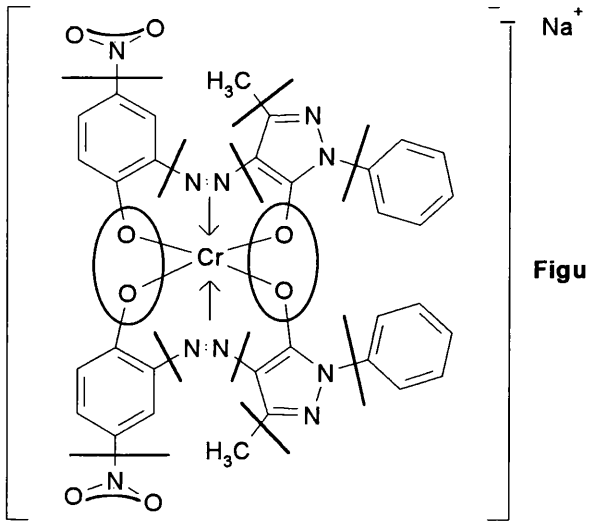

Figure 6.33: Savinyl Orange RLSE weak linkages

One source of the HCN for the Savinyl Yellow 2RLS was the CH_3NH substituent, which is not present here. This points towards the five membered ring as being the source. Partial hydrogenation of this ring could result in the production of both the HCN and the aniline. This whole fragment also left complete, in order to provide the

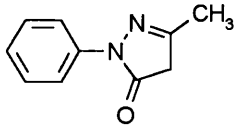

. Chloroaniline was also produced, once again implying that there was chlorination of the benzene rings drawn to the right in Figure 6.33.

There is no direct source of the CO_2. One possible pathway for this formation is the residue. This may be a combination of a carbonaceous residue with a chromium oxide dispersed through it. There may be reduction of the Cr_xO_y by the carbon to produce the CO_2.

The source of the ammonia is harder to suggest. Nitrogen dioxide was not detected, and NO would not be trapped as it has a boiling point of -151.8°C. Similarly, N_2 from the azo linkages would not be condensed in the trapping system. It is apparent from the structure that hydrogenation was required for the formation of the ammonia, but

there is no obvious source of the nitrogen for this product. The Savinyl Yellow 2RLS may have provided a more apparent source, the structural similarities with this colourant suggest that there was another source common to this material.

6.7.2.2 Dynamic Air

The same gases were produced as under the nitrogen conditions, but with addition of a little acetonitrile. The NH_3/HCN ratio was much the same as for under the static nitrogen conditions. Water was the major liquid detected, with the ether extract containing aniline, benzonitrile and the mw = 112 product in equal amounts. There was also a smaller yet significant amount of chlorobenzonitrile.

The main difference between the products obtained under dynamic air and nitrogen conditions was the acetonitrile and the benzonitrile. The acetonitrile may have been formed through the decomposition of the five-membered ring, which would provide a methyl group connected to a CN. The fact that this product was not detected under a nitrogen atmosphere implies that this particular degradation of the ring was promoted by the presence of oxygen.

The source of the benzonitrile is a little harder to determine. The structure has no carbons directly bonded to a benzene ring. Isocyanobenzene is less stable than benzonitrile, so it was initially thought that this was formed and then rearranged into the benzonitrile. However, study of the structure of the starting material indicates that this would require the breaking of a double bond, while a single bond remains unbroken (and ultimately the source of a triple bond). It seems more likely that the benzene ring picks up a nitrile group, perhaps from the acetonitrile.

6.7.2.3 Flaming Conditions

Water and CO_2 were the major products, as is typical for study under flaming conditions. Some N_2O and acetonitrile were also detected as gaseous products. Benzonitrile was the major product in the liquid fraction, with some naphthalene and acetobenzene also detected. The cold ring fraction had what was either a hydroxybenzonitrile or isocyanatobenzene as the major component, with a lesser amount of the chlorinated form also present. There was also some 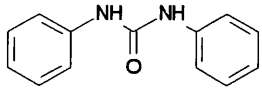 detected.

The N_2O may have come from the azo linkages or the piloting system. The other new products have no obvious pathway to their formation. The chlorinated products found in this and the environments above would be consistent with the benzene ring drawn to the right in Figure 6.33 being singly chlorinated. Under the aggressive conditions used here, the benzonitrile path described in section 6. may have been followed, with additional oxidation occurring to form either the hydroxyl group or the isocyanato-substituent. The 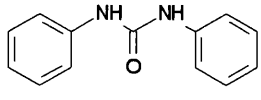 also has no direct route for formation. As there are no pairs of nitrogen separated by a single carbon in the starting structure. There are many possible indirect pathways, including perhaps the combination of other detected products. By way of example, there may be some combination between an isocyanatobenzene and an aniline. This can only be speculation, with the information available unable to offer any firm conclusions.

6.7.3 SAVINYL BLACK RLS

Structurally, this sample did not have the similarities shared by the other two in this chapter. It has been included in this section as it was the only other transition element complex studied. The degradations were performed under three environments, dynamic nitrogen, dynamic air and flaming conditions.

6.7.3.1 Dynamic Nitrogen

Ammonia was the major gas, with CO_2 also present in reasonable amounts. There was also a small amount of acetonitrile and even less HCN detected. Much water was also evolved. The non-aqueous liquids had aniline as a slightly major product, with much phenol, naphthalene and what appeared to be 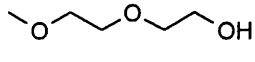

also produced.

The structure provided for Savinyl Black RLS is shown in Figure 6.34 with the weak linkages highlighted.

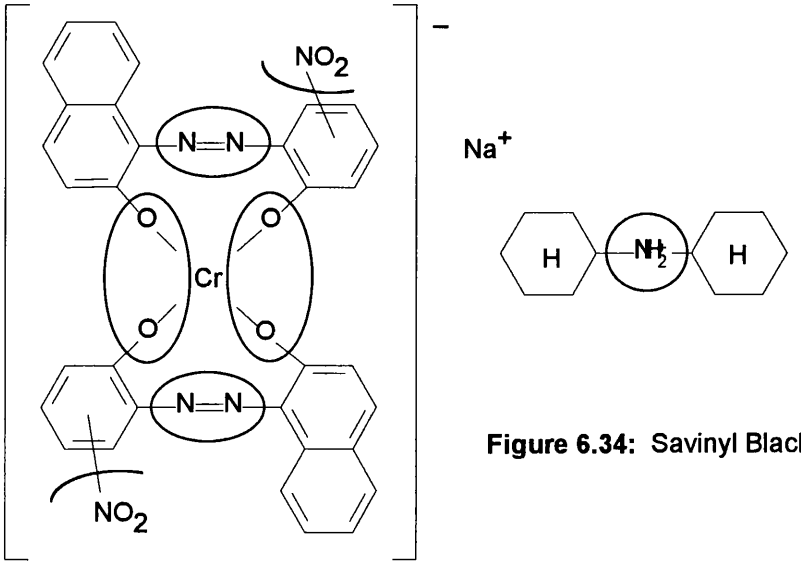

Figure 6.34: Savinyl Black RLS weak linkages

Nitrobenzene was not detected from either this sample or the Savinyl Orange RLSE. This suggests that the bond to the azo or the oxygen is more thermally stable than the

bond to the NO_2 or the NO_2 itself. Aniline and phenol were both detected. These may be from the benzene ring with hydrogenation of the azo linkage or the oxygen. An alternative but less likely source of the aniline could be the counter ion, with the cyclohexane losing hydrogens to form an aromatic. There is no apparent source for the diether alcohol. It seems likely that this was incorrectly identified, the mass spectra for many aliphatic materials being more ambiguous than for the aromatic products. The CO_2 may have been formed through the reduction of a chromium oxide by the carbonaceous residue.

The most likely source of the ammonia is the NH_2 in the counter ion. There is no clear source of the acetonitrile and HCN. Decomposition of the counter ion is again the most likely origin, as the azo link or the NO_2 group offer no C—N bond where the carbon is not part of a stable aromatic ring structure.

6.7.3.2 Dynamic Air

Similar amounts of CO_2 and NH_3 were detected as under dynamic nitrogen. Acetonitrile and HCN were not present. The CO_2 and NH_3 were probably formed the same way as under dynamic nitrogen, as the quantity found here was very similar. Naphthalene was now the major component (after water) in the liquid fraction. Much quinoline or isoquinoline, benzonitrile and dichlorobenzene were also detected. The last of these was probably a contaminant, as it was not found under the dynamic nitrogen environment. It could result if the structure for the colourant provided were incorrect, or if an impurity from the original synthesis were present.

The oxygen may have influenced the degradation of the counter ion. The aniline, acetonitrile and hydrogen cyanide were attributed to the decomposition of the counter

ion in the dynamic nitrogen study, but were not detected under dynamic air. The quinoline/isoquinoline and the benzonitrile are hard to explain. The pathway for the formation of these products must be quite indirect, perhaps occurring in the residue.

6.7.3.3 Flaming Conditions

Predictably, CO_2 and water were the major products. The only other products detected were CO, N_2O, N_2O_4, acetylene and ethane. Suspicion has already been cast on the authenticity of nitrogen oxides as genuine degradation products, although the azo linkage or the NO_2 group may have been the source. Interestingly, the decomposition of the quinoline detected under dynamic air conditions may result in the formation of benzonitrile (detected under dynamic air) and acetylene. It is a little surprising that acetylene and ethane could withstand the vigour of this degradation environment. One possible explanation is that the rapid burning observed allowed these products to leave the hot zone unoxidised. Perhaps rapid decomposition of the aromatic structures produced these small hydrocarbon fragments. Note that, as is normally observed under these conditions, CO (a partial oxidation product) was also detected.

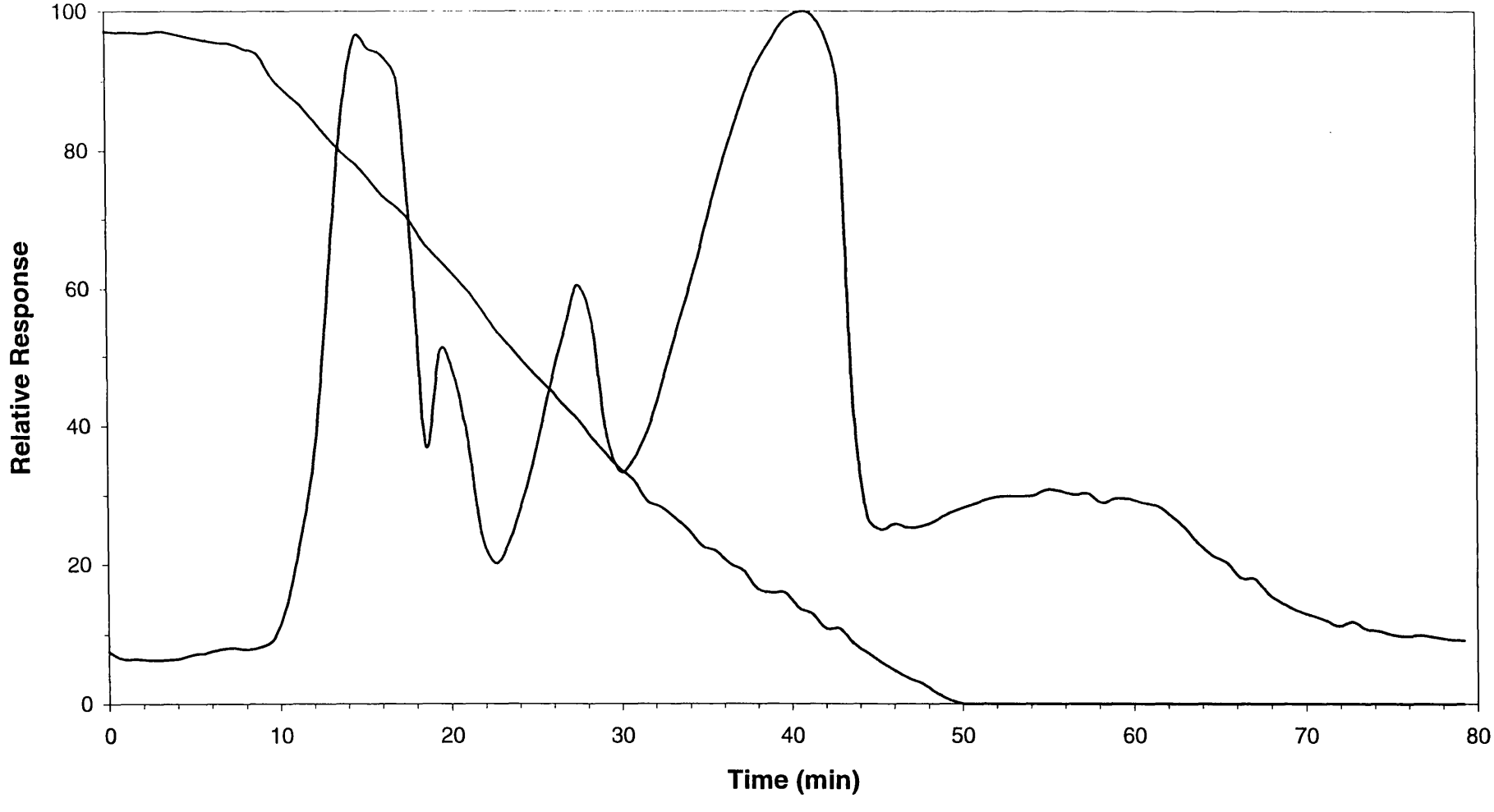

Figure 6.6: SATVA trace from the degradation of Savinyl Yellow 2RLS under static nitrogen

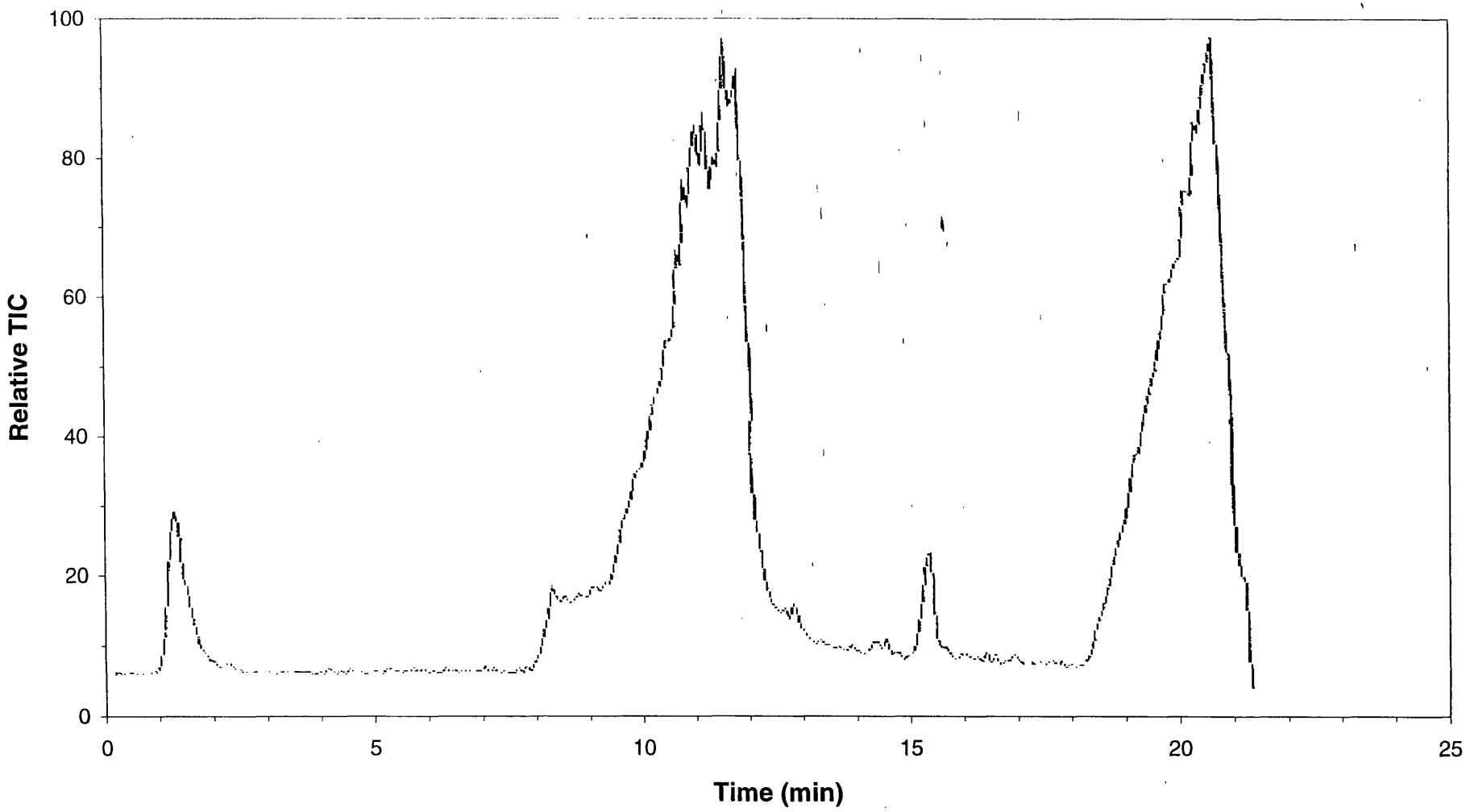

Figure 6.7: TIC trace for the liquid fraction from the SATVA curve in Figure 6.6

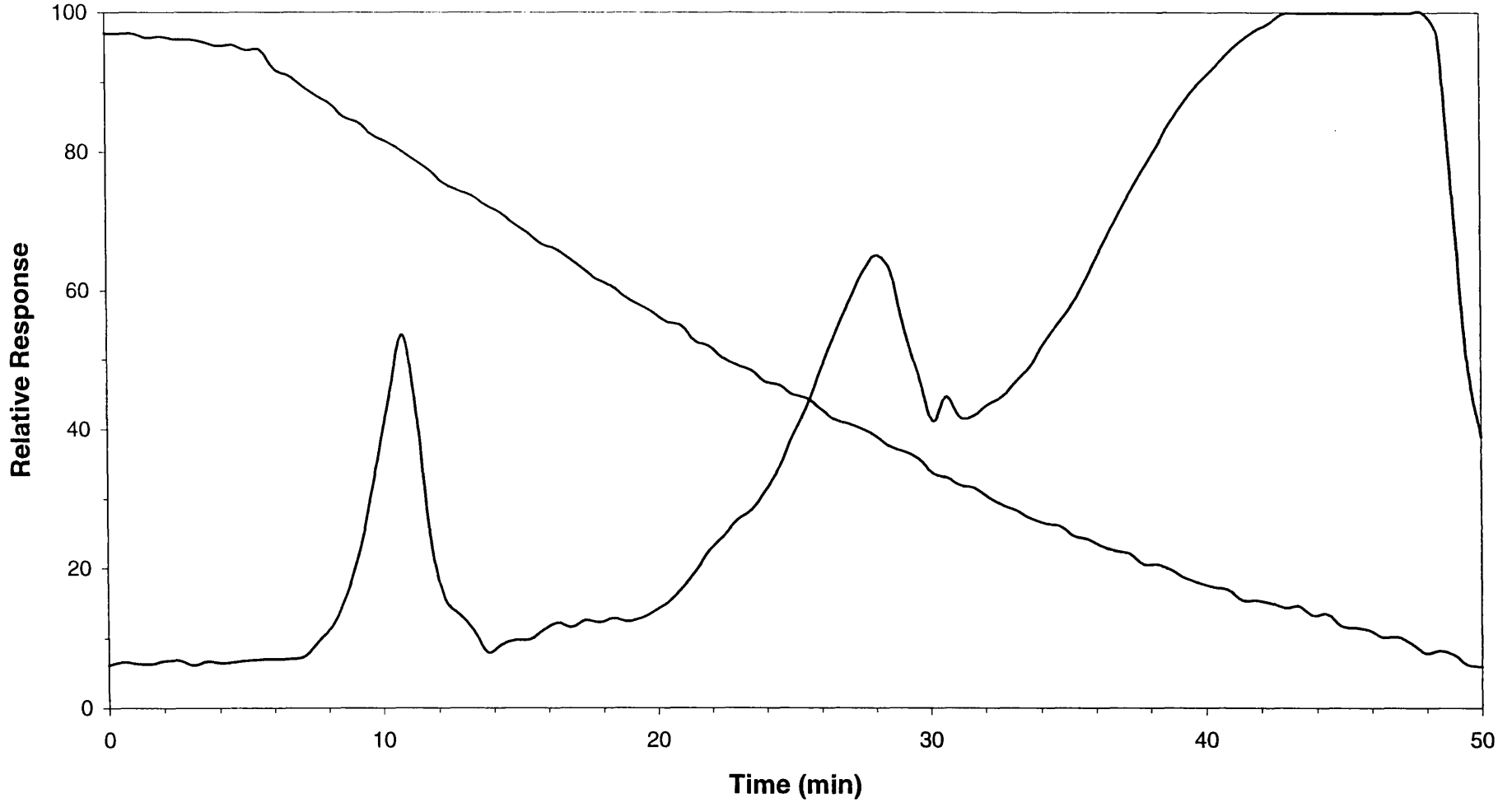

Figure 6.8: SATVA trace from the degradation of Savinyl Yellow 2RLS under dynamic nitrogen

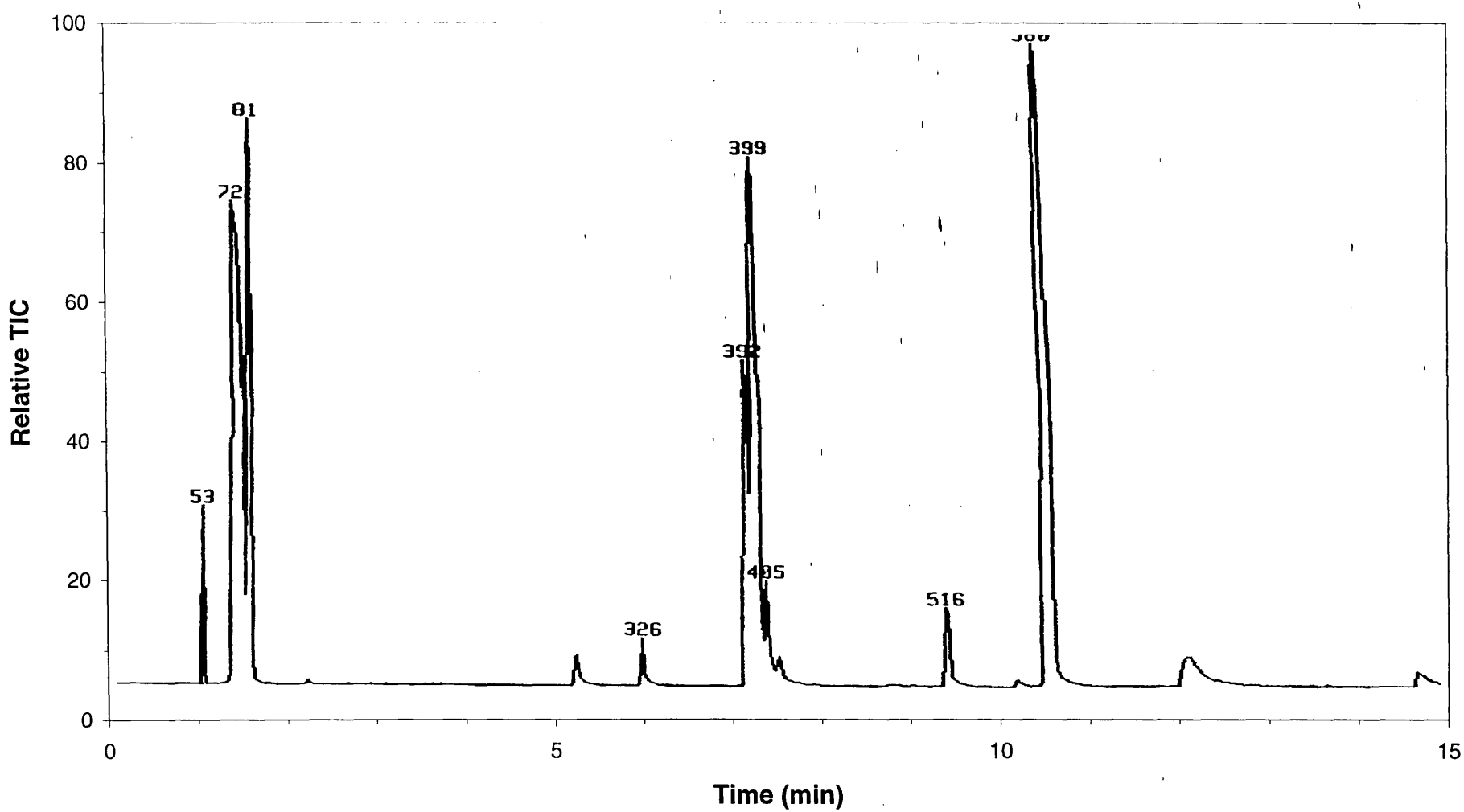

Figure 6.9: TIC trace for the liquid fraction from the SATVA curve in Figure 6.8

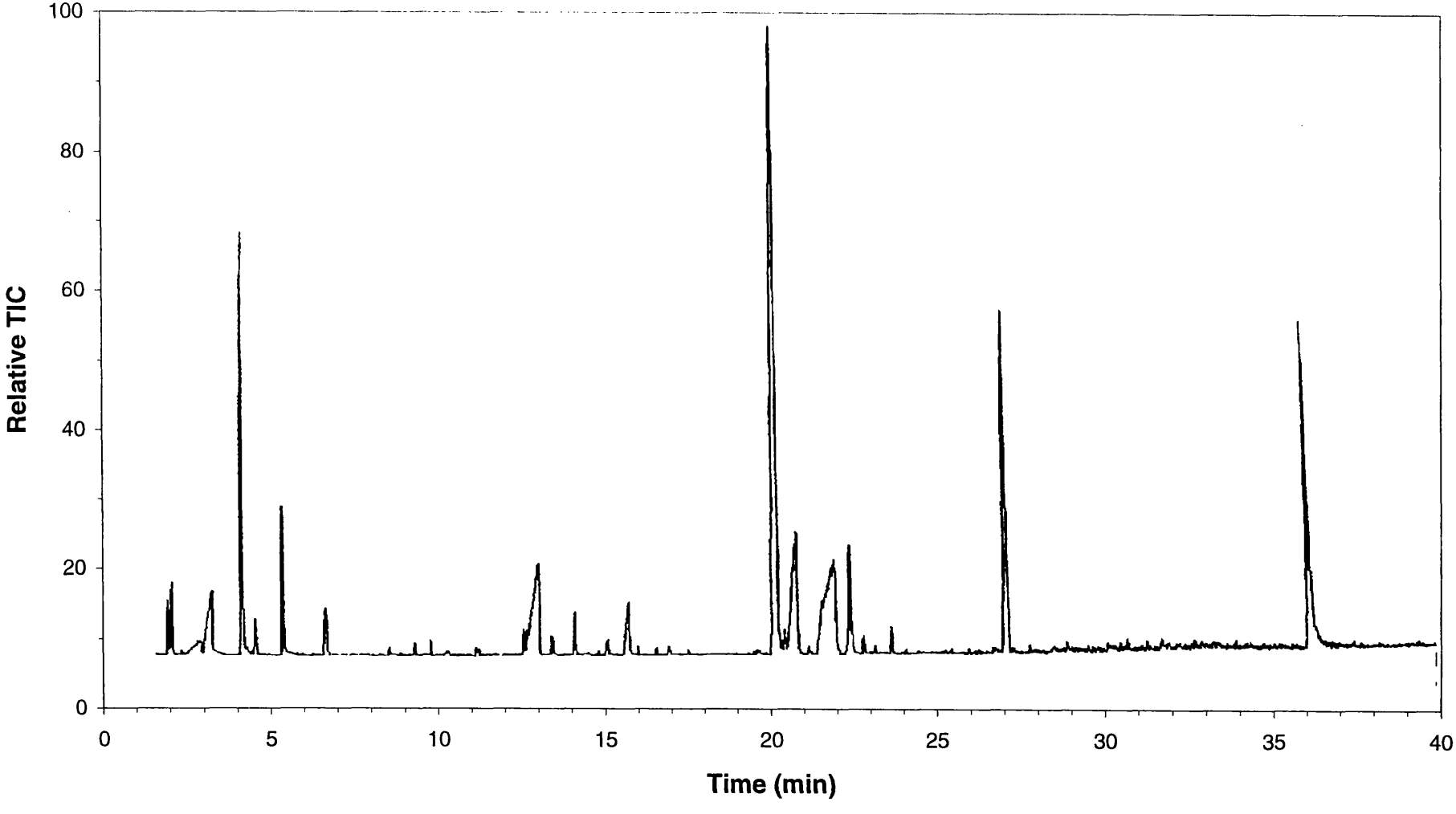

Figure 6.10: TIC trace for the cold ring fraction from the SATVA curve in Figure 6.8

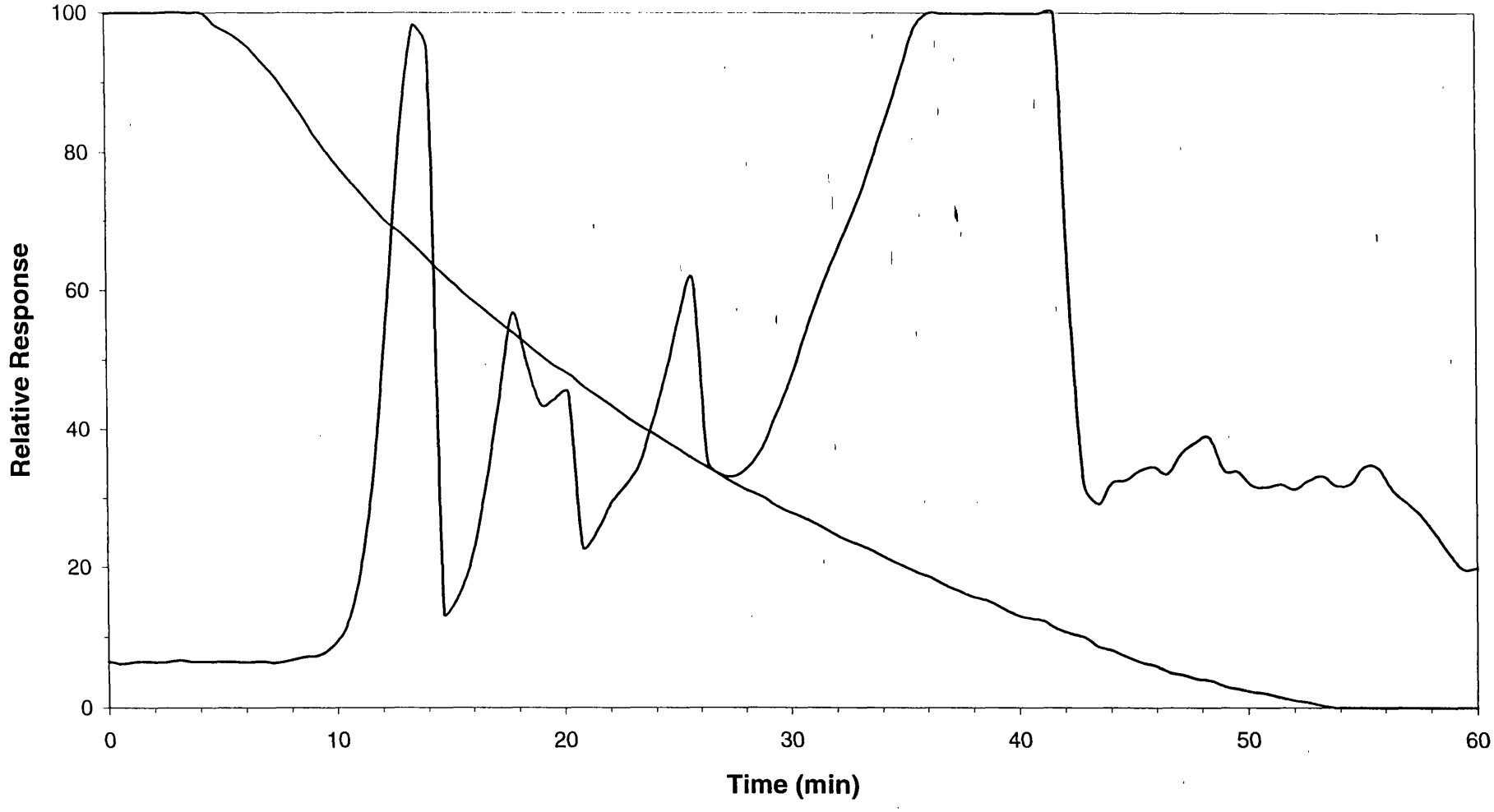

Figure 6.11: SATVA trace from the degradation of Savinyl Yellow 2RLS under dynamic air

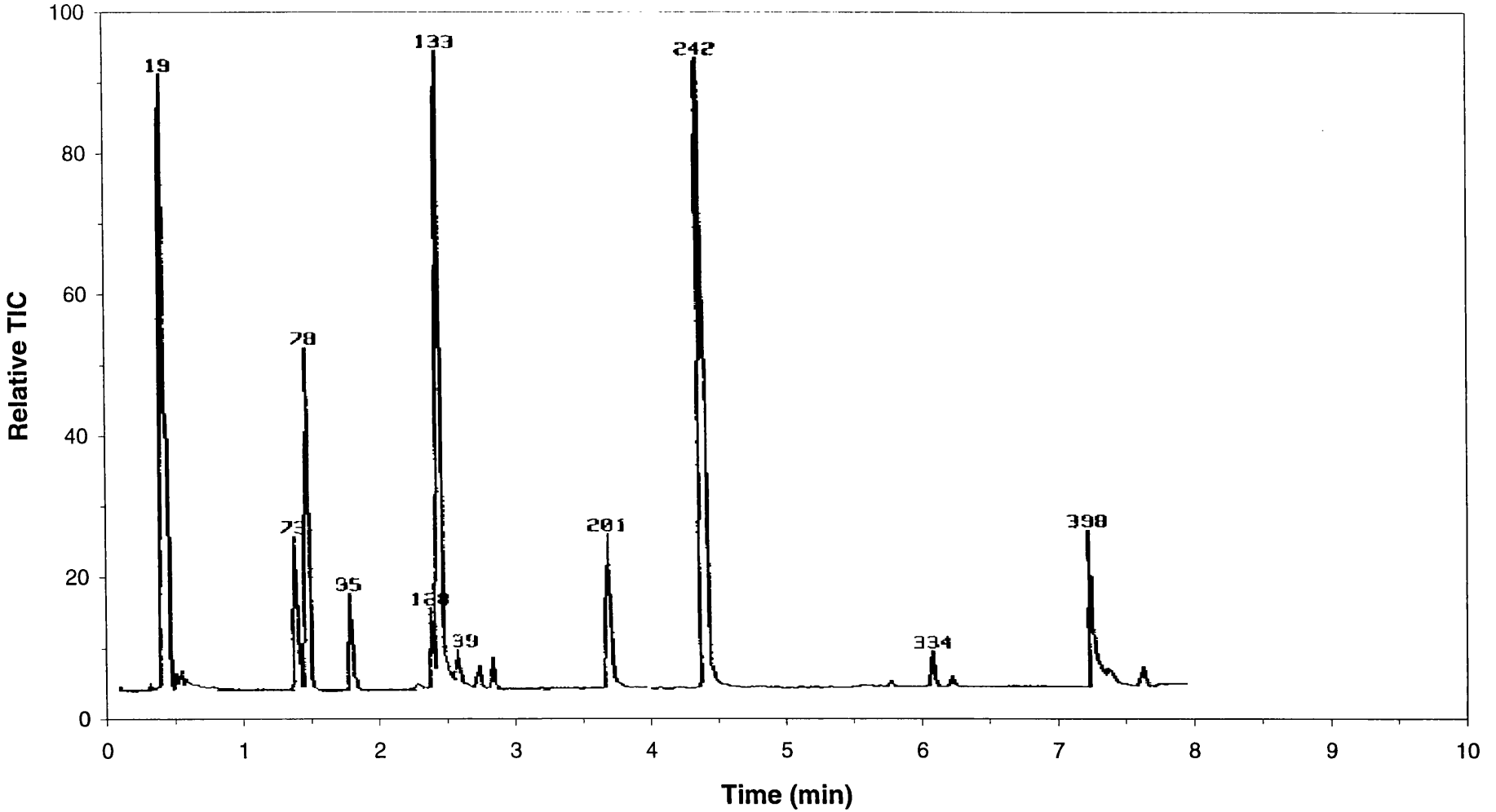

Figure 6.12: TIC trace for the liquid fraction from the SATVA curve in Figure 6.11

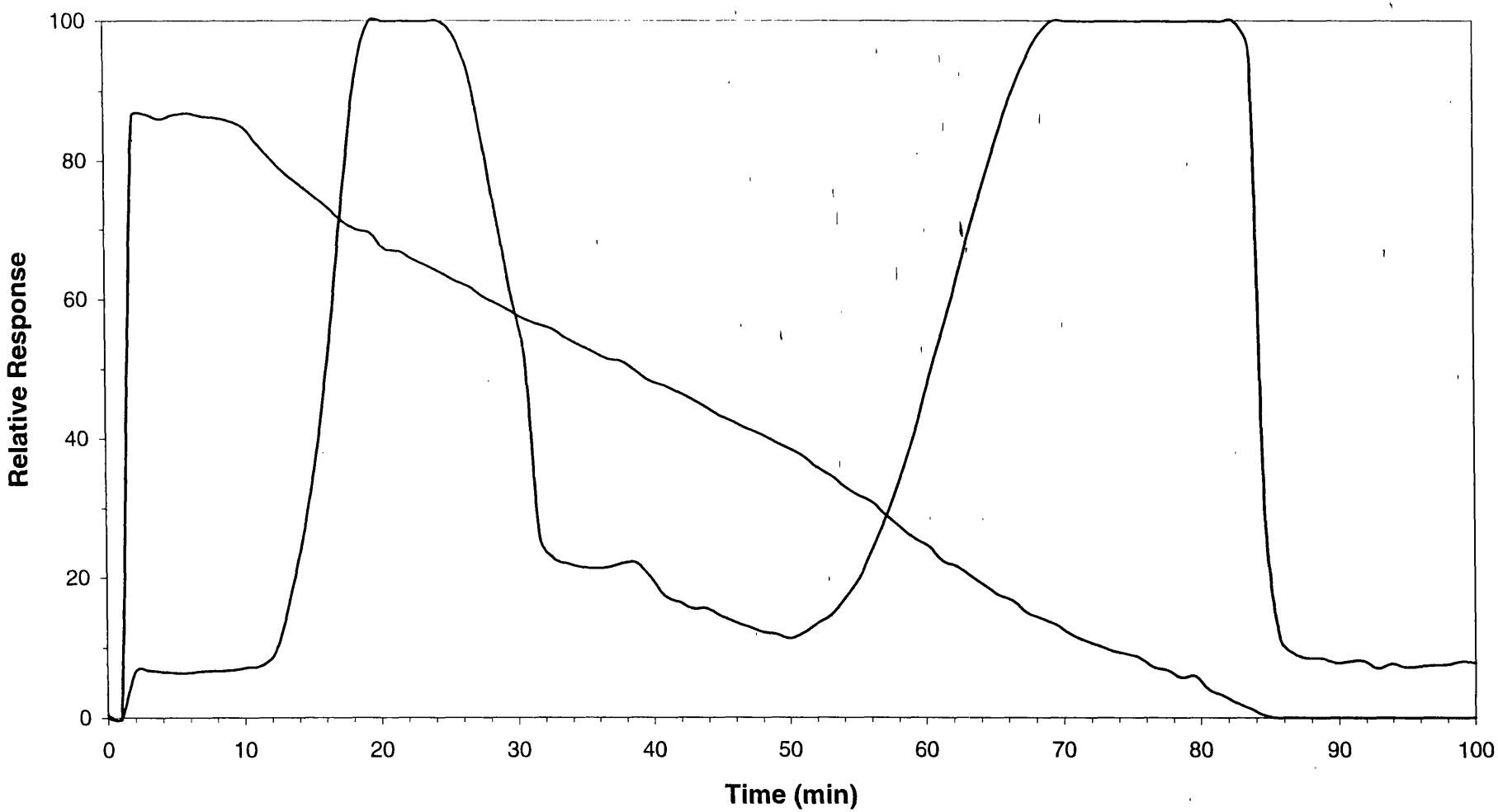

Figure 6.13: SATVA trace from the degradation of Savinyl Yellow 2RLS under flaming conditions

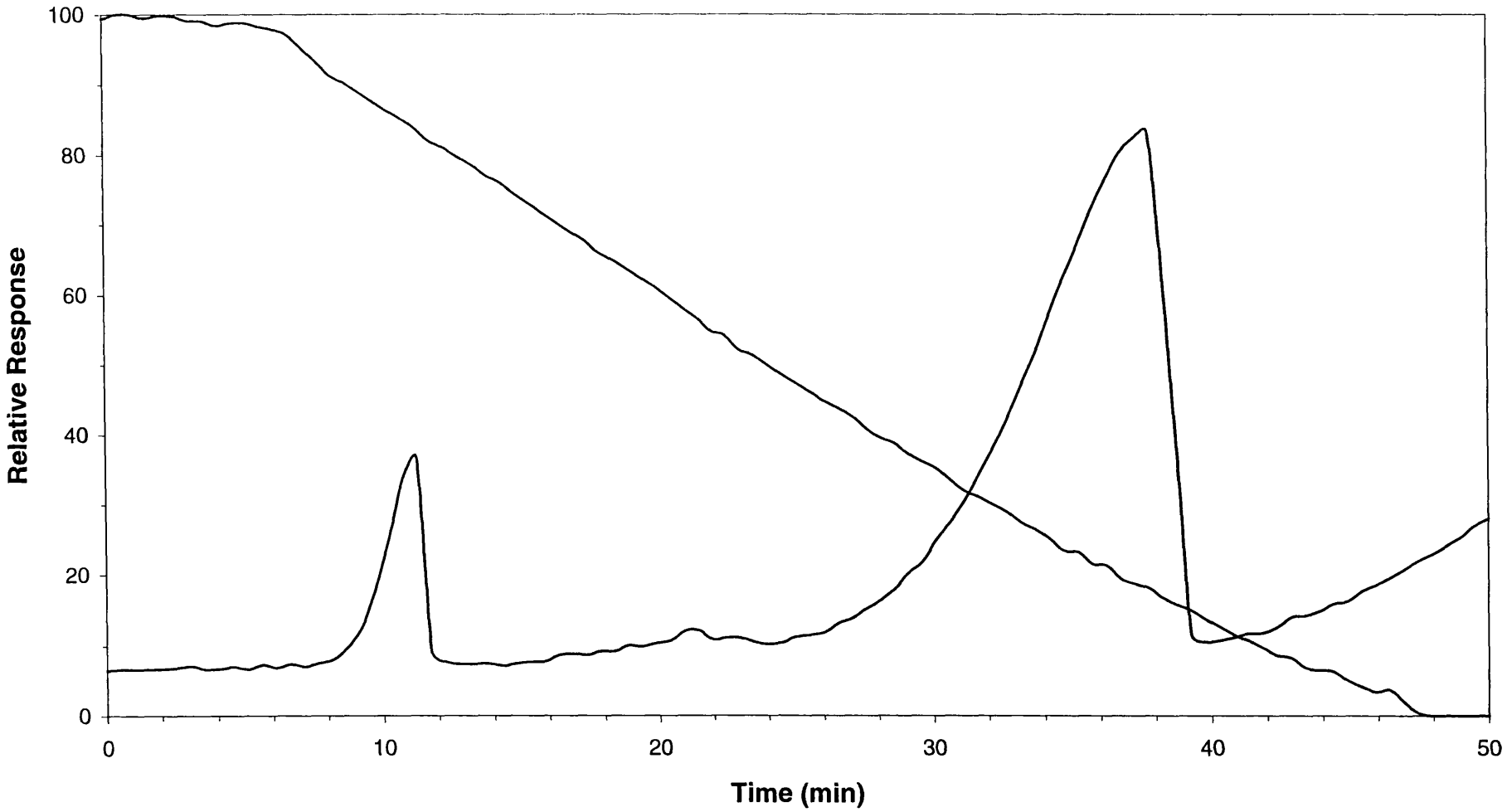

Figure 6.15: SATVA trace from the degradation of Savinyl Orange RLSE up to 300°C under static nitrogen

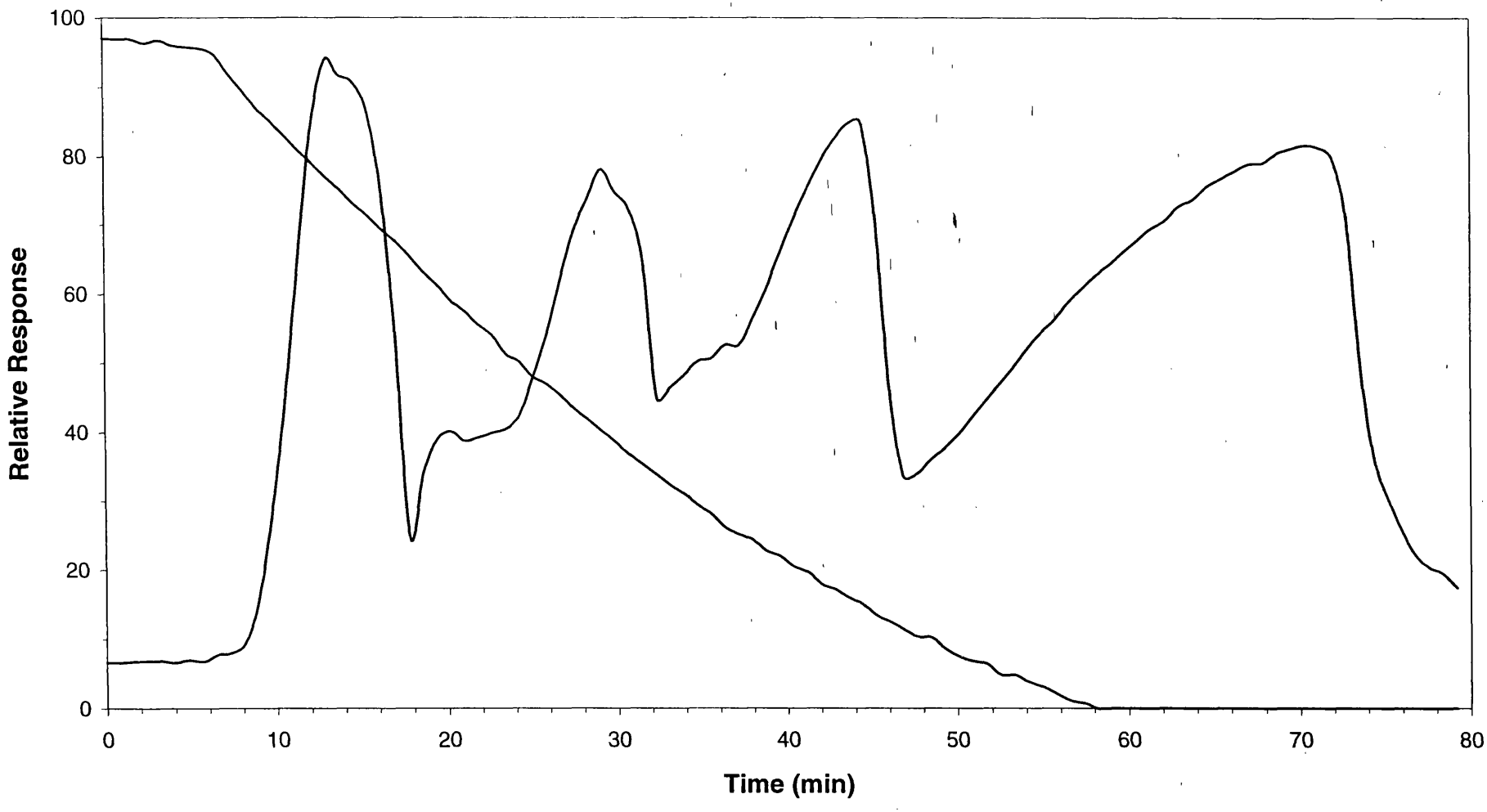

Figure 6.16: SATVA trace from the degradation of Savinyl Orange RLSE up to 500°C under static nitrogen

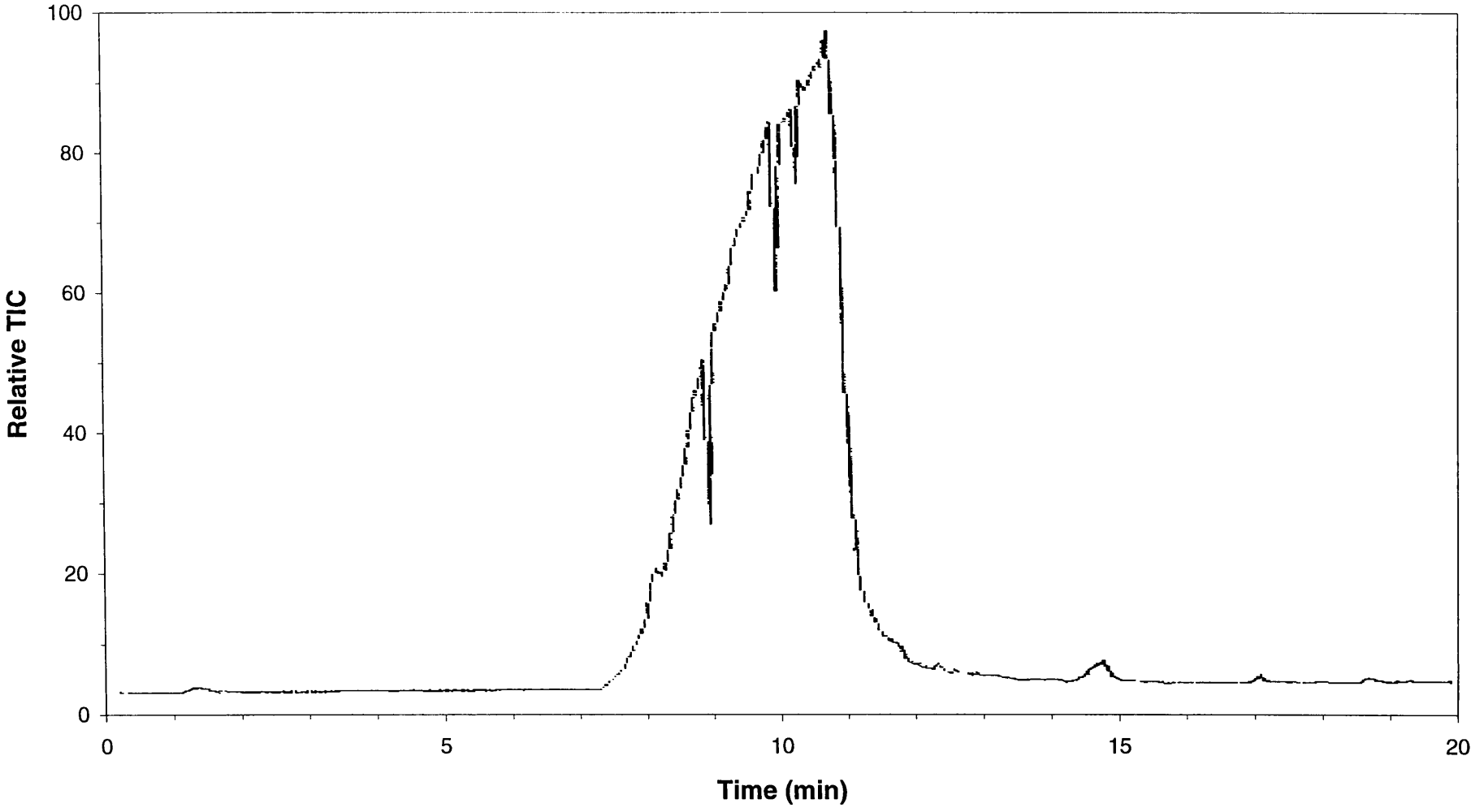

Figure 6.17: TIC trace for the liquid fraction from the SATVA curve in Figure 6.16

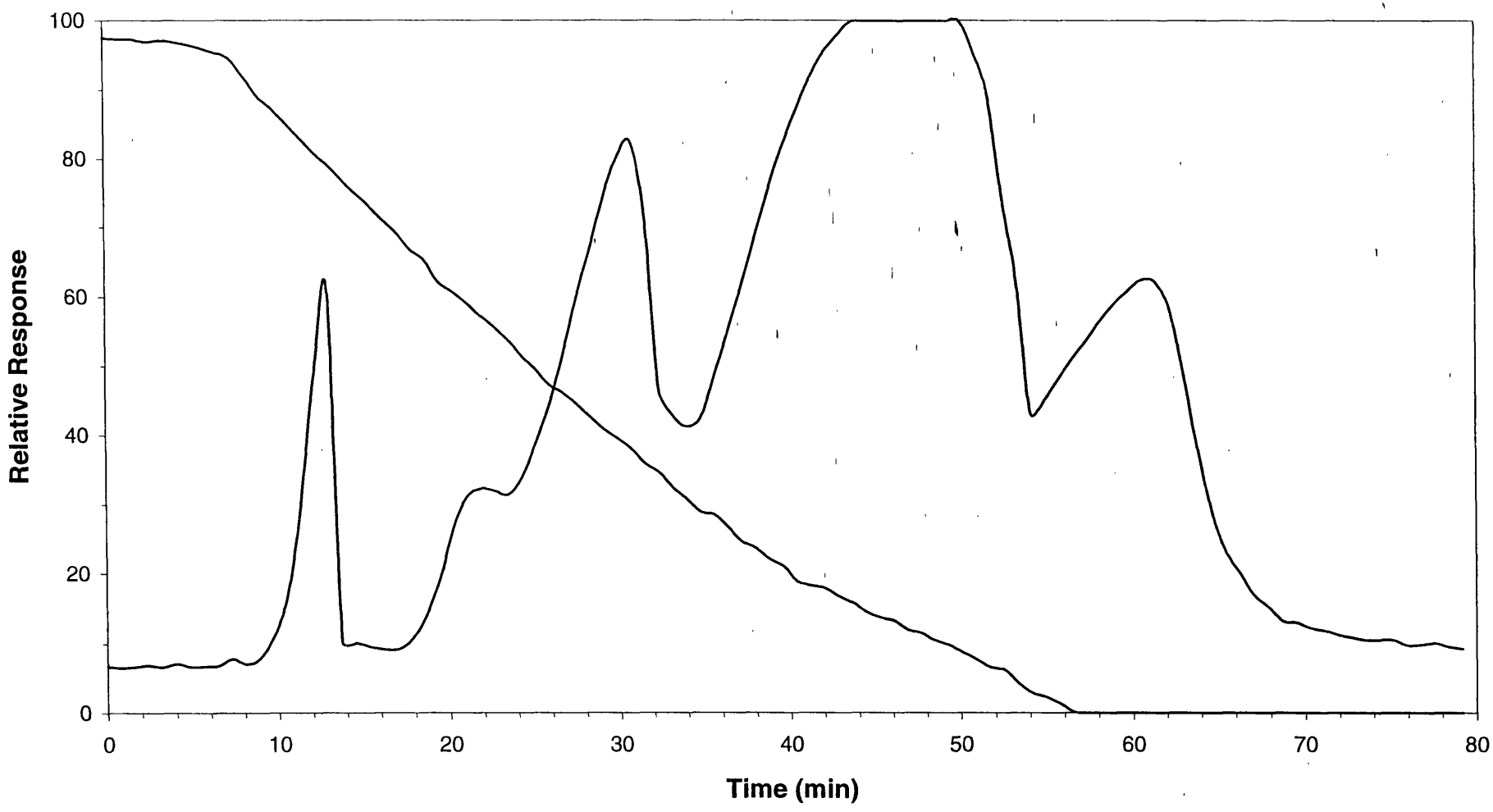

Figure 6.18: SATVA trace from the degradation of Savinyl Orange RLSE under dynamic nitrogen

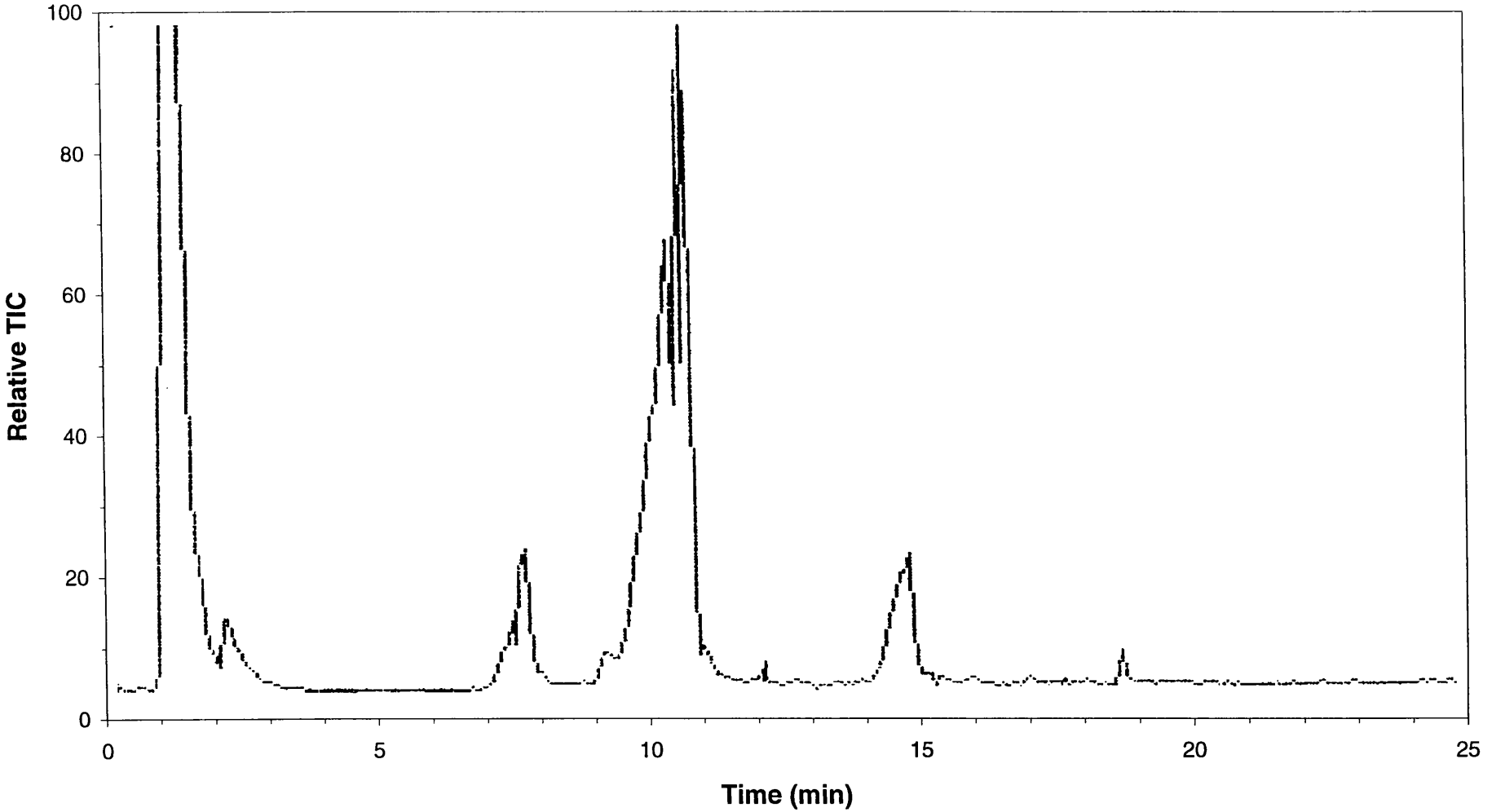

Figure 6.19: TIC trace for the liquid fraction from the SATVA curve in Figure 6.18

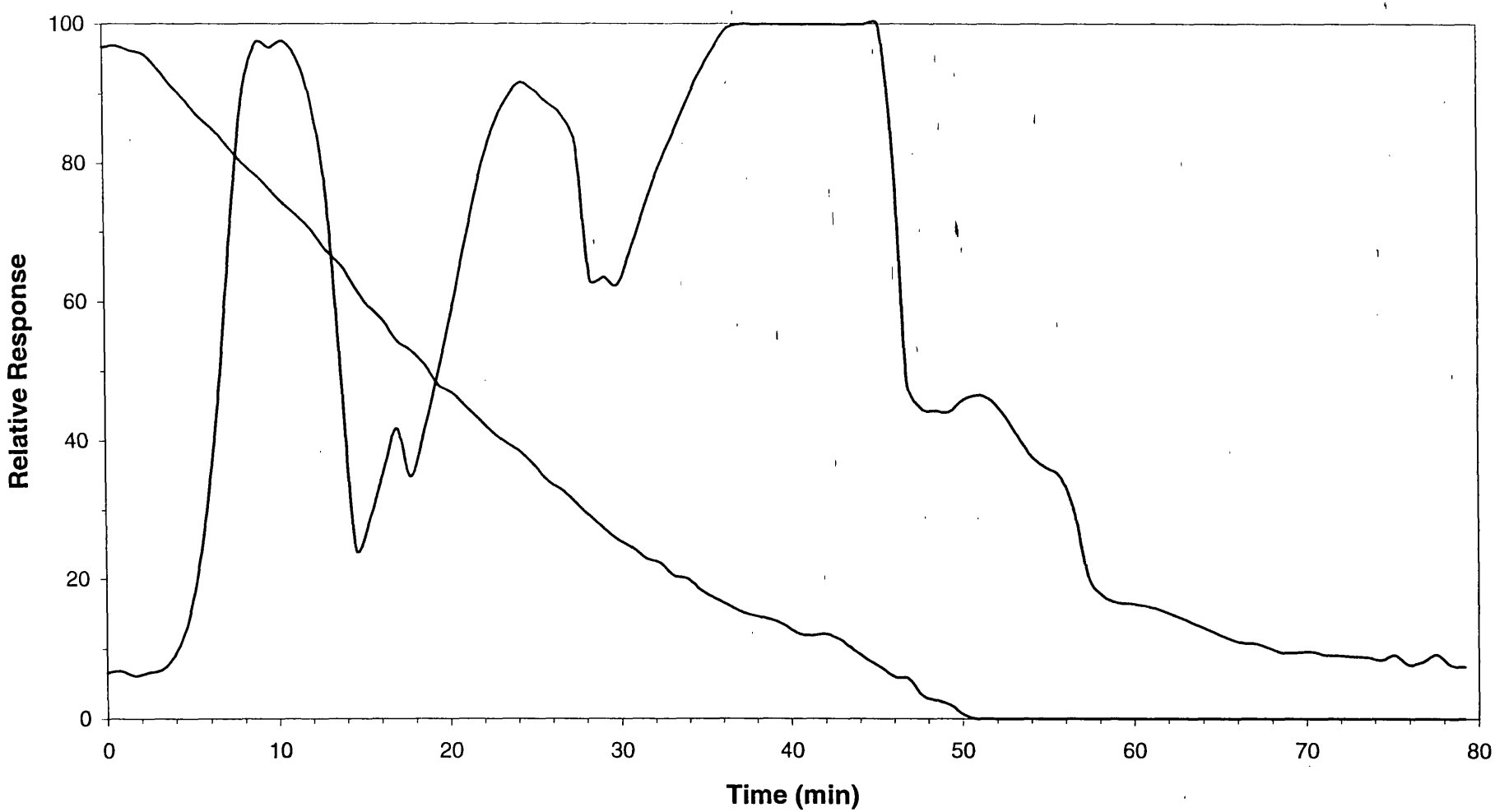

Figure 6.20: SATVA trace from the degradation of Savinyl Orange RLSE under dynamic air

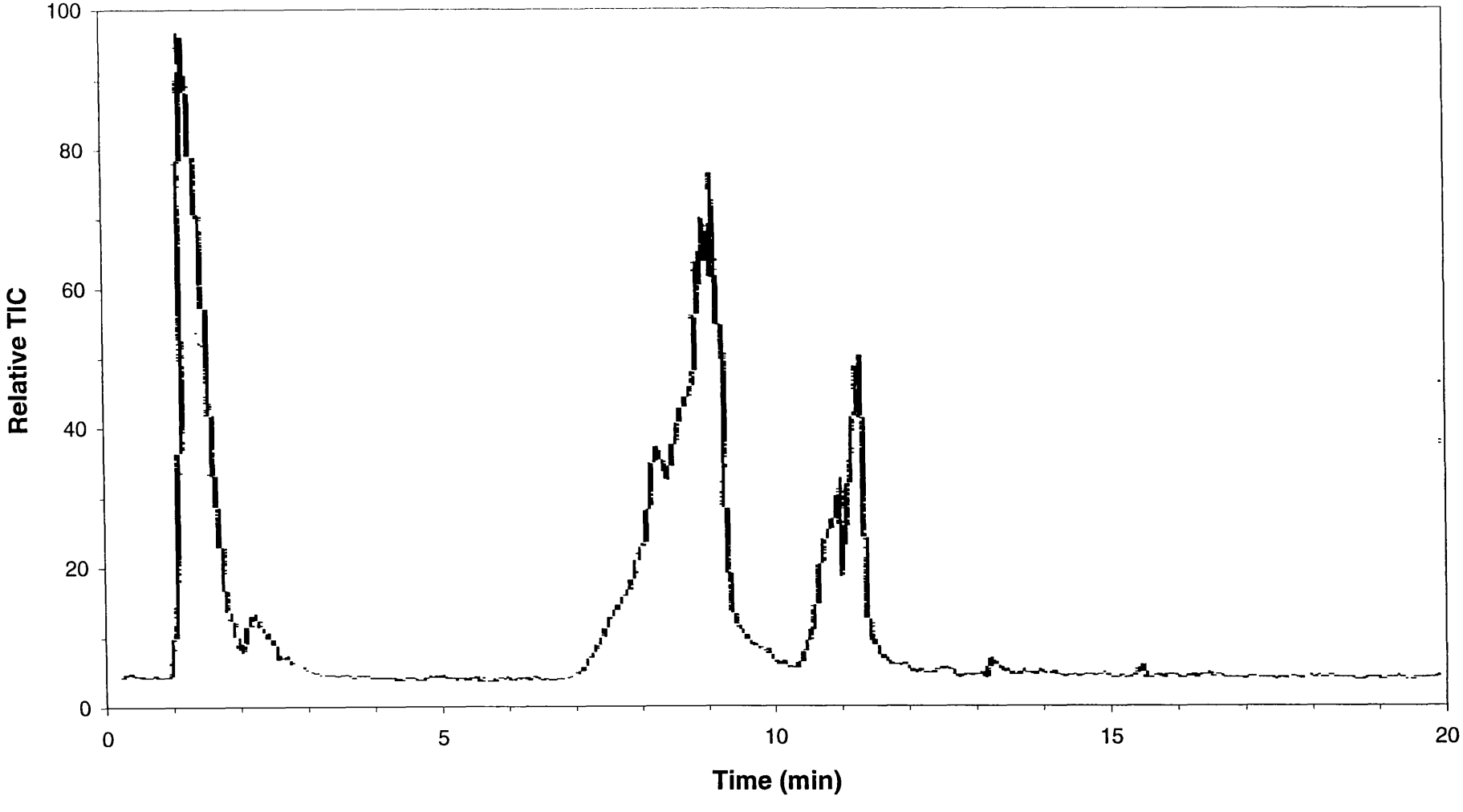

Figure 6.21: TIC trace for the liquid fraction from the SATVA curve in Figure 6.20

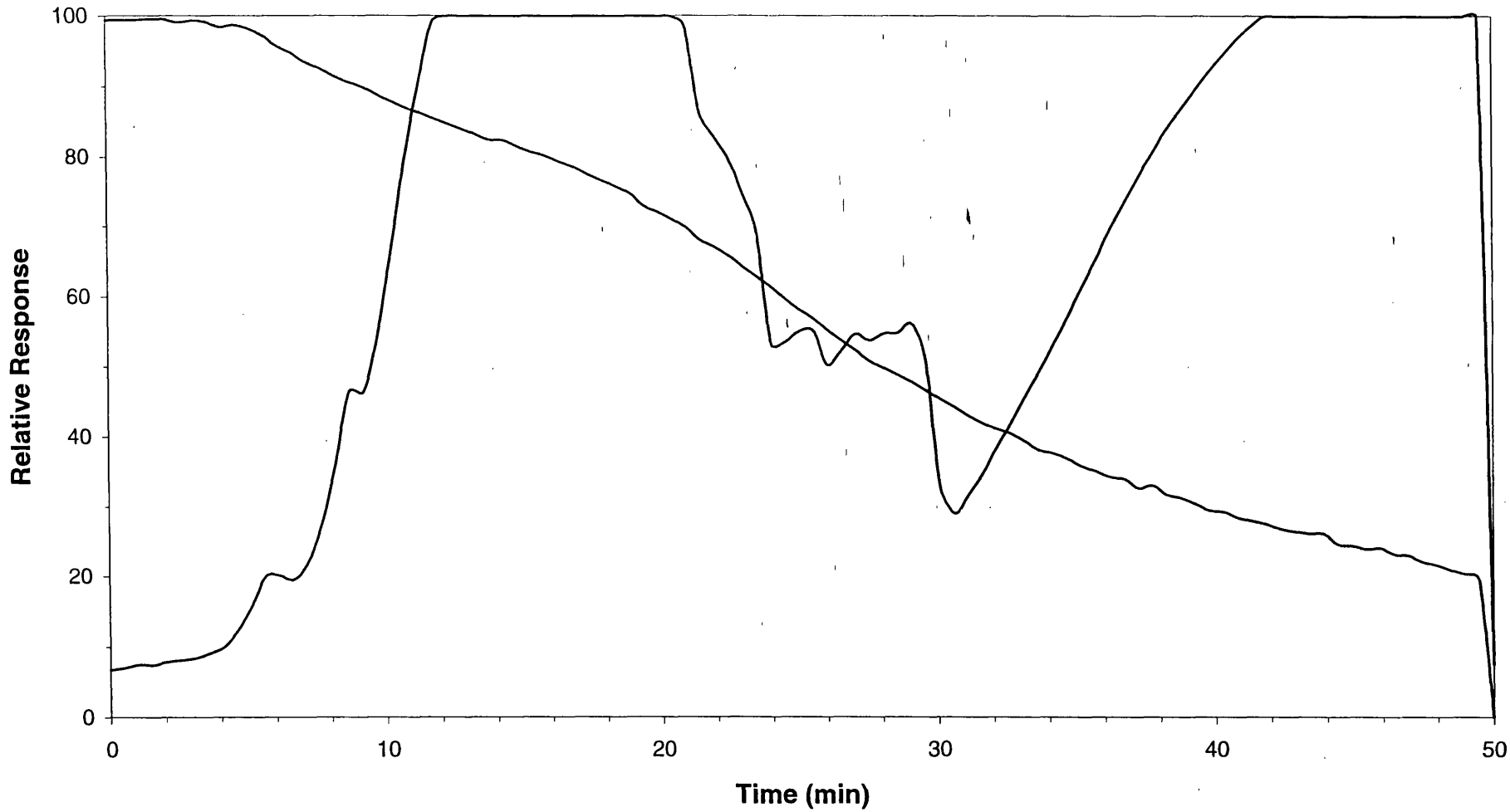

Figure 6.22: SATVA trace from the degradation of Savinyl Orange RLSE under flaming conditions

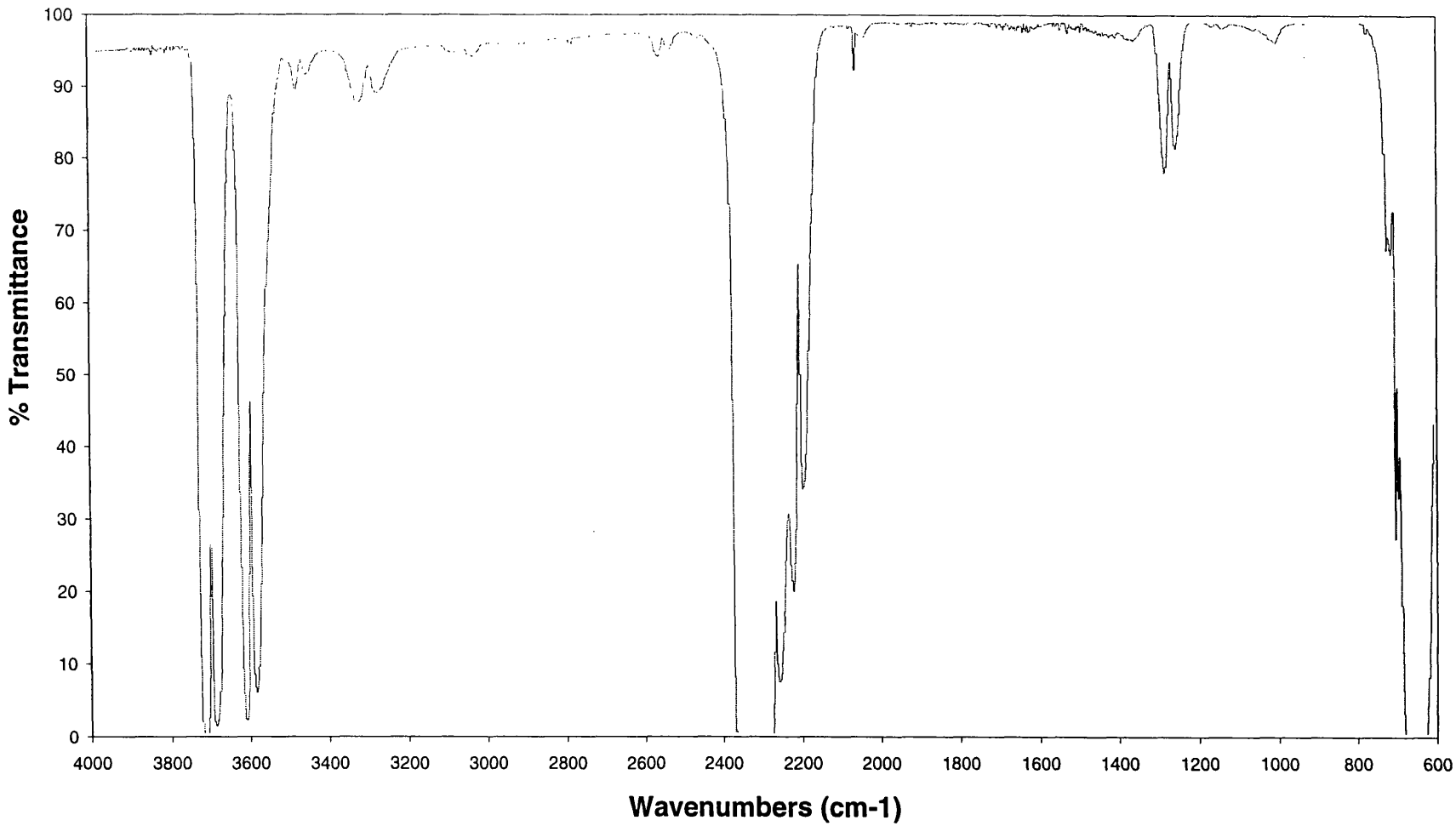

Figure 6.23: IR Spectrum from gas peak from SATVA curve in Figure 6.22

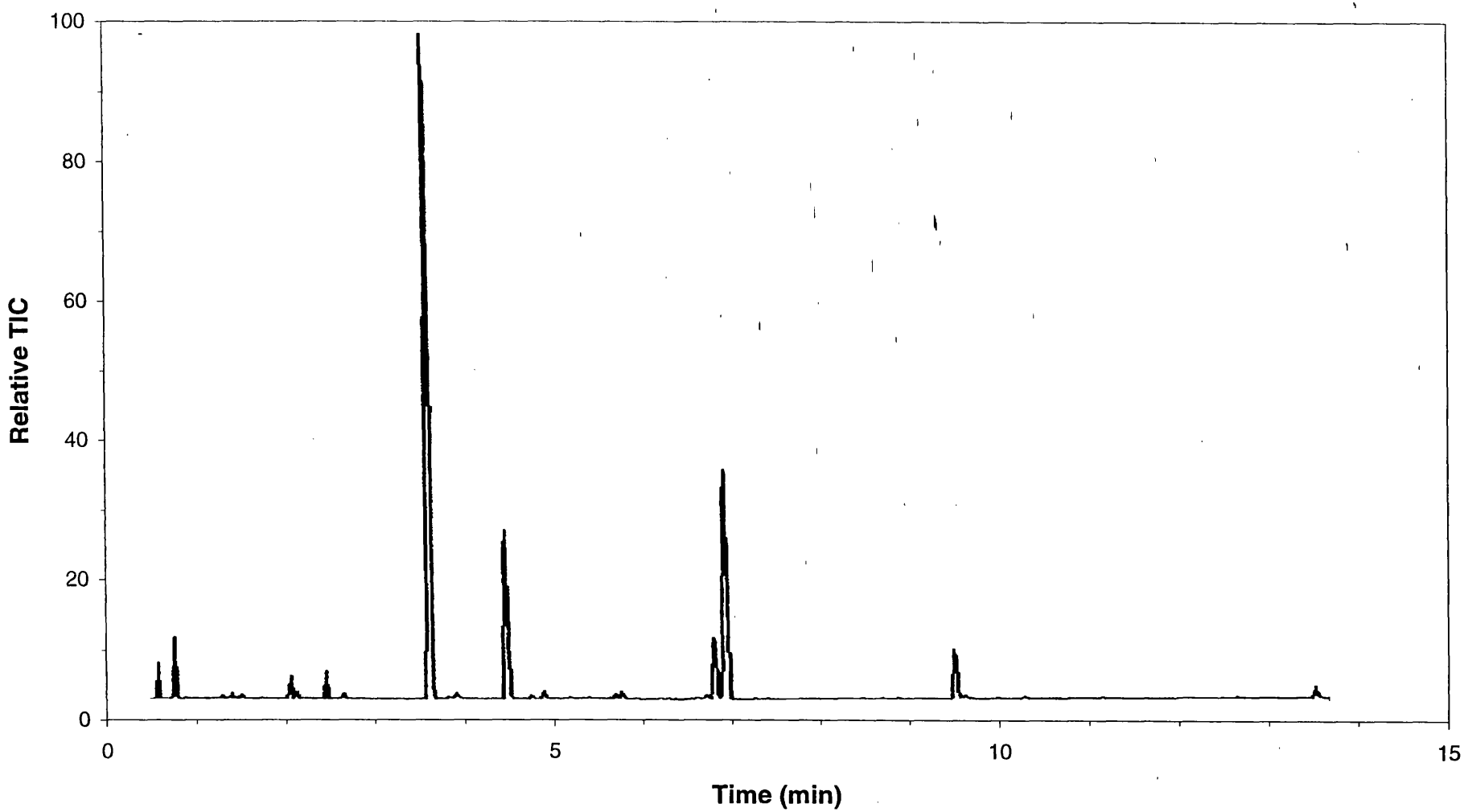

Figure 6.24: TIC trace for the liquid fraction from the SATVA curve in Figure 6.22

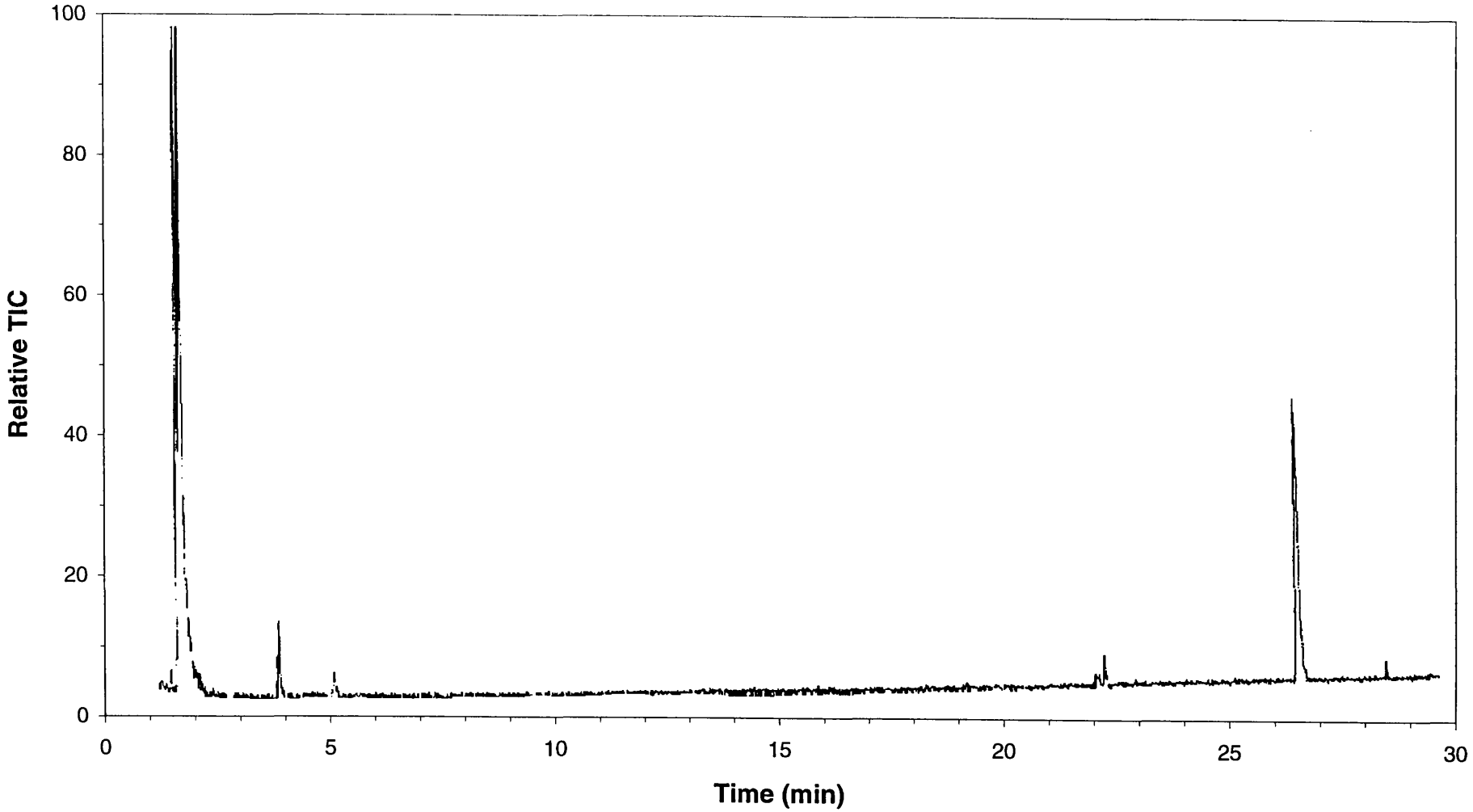

Figure 6.25: TIC trace for the CRF from the SATVA curve in Figure 6.22

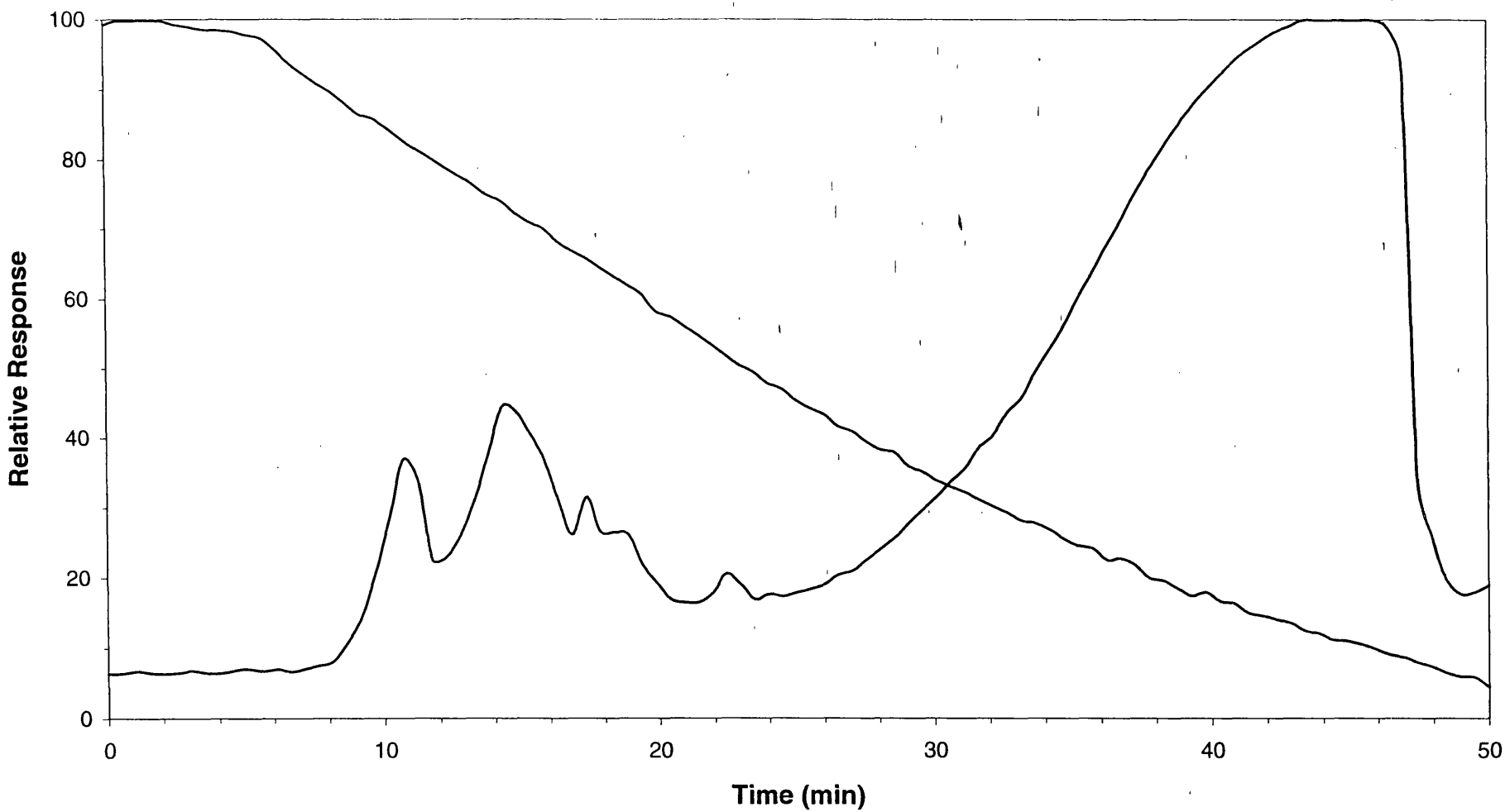

Figure 6.27: SATVA trace from the degradation of Savinyl Black RLS under dynamic nitrogen

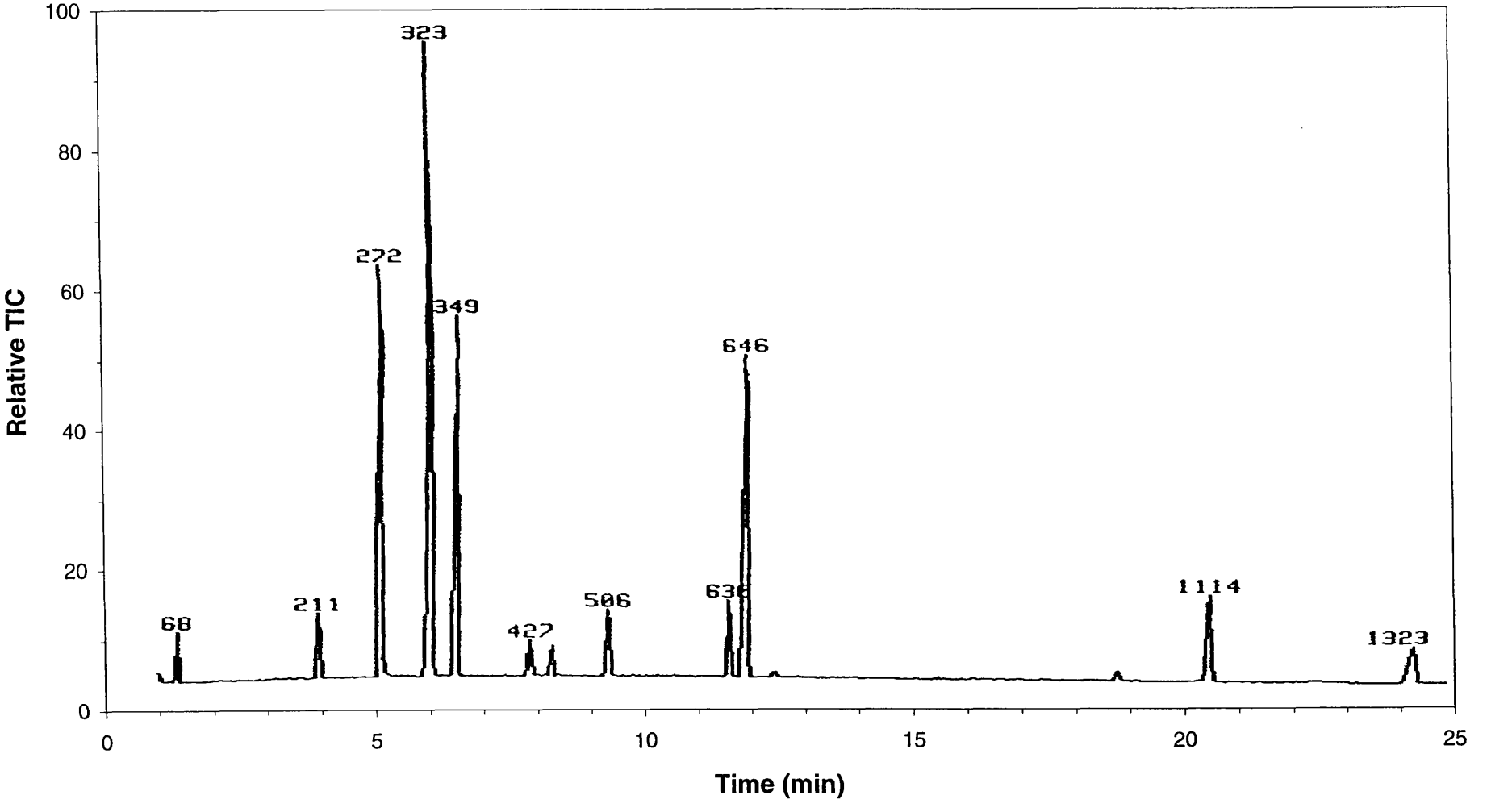

Figure 6.28: TIC trace for the liquid fraction from the SATVA curve in Figure 6.27

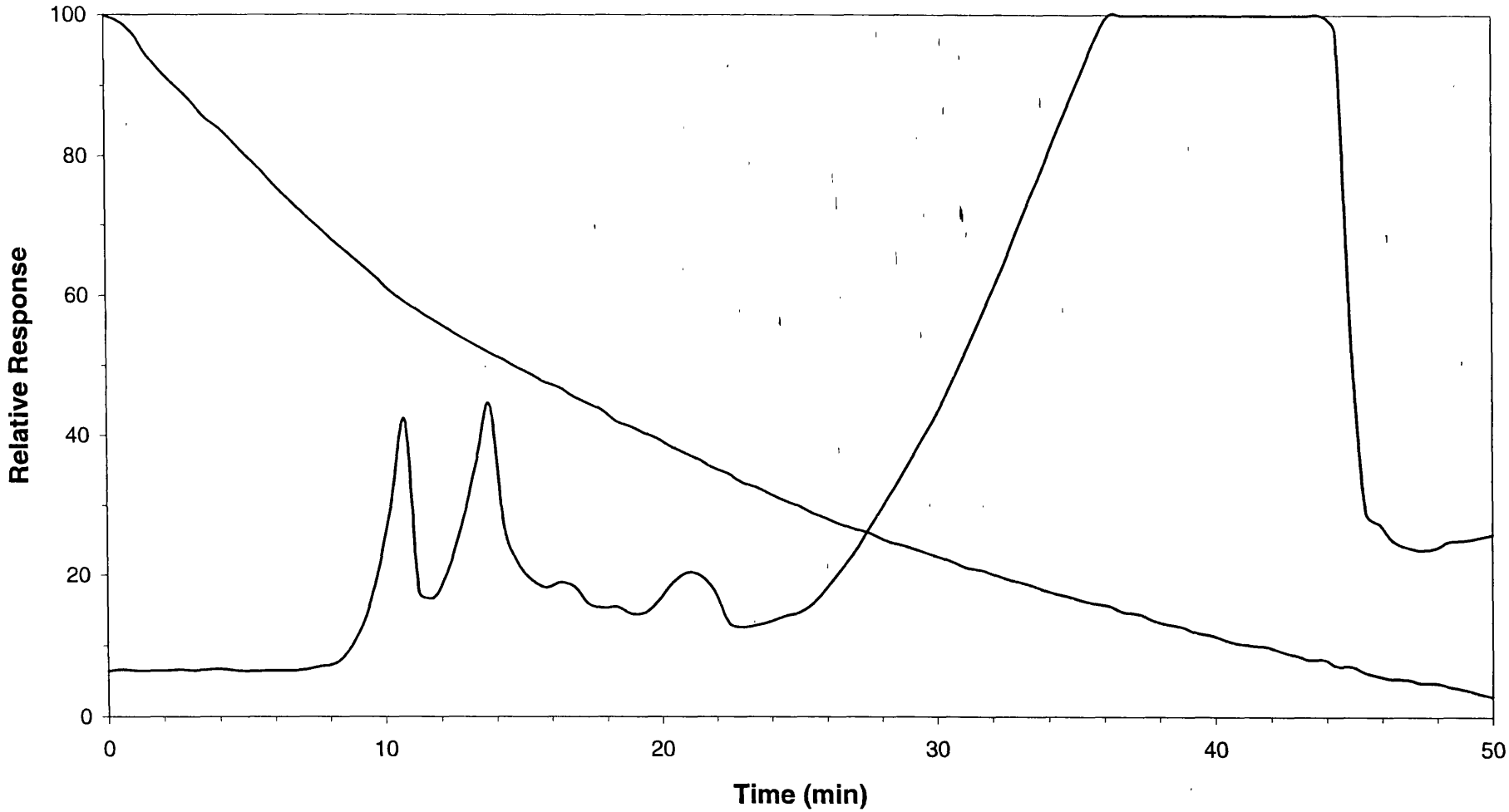

Figure 6.29: SATVA trace from the degradation of Savinyl Black RLS under dynamic air

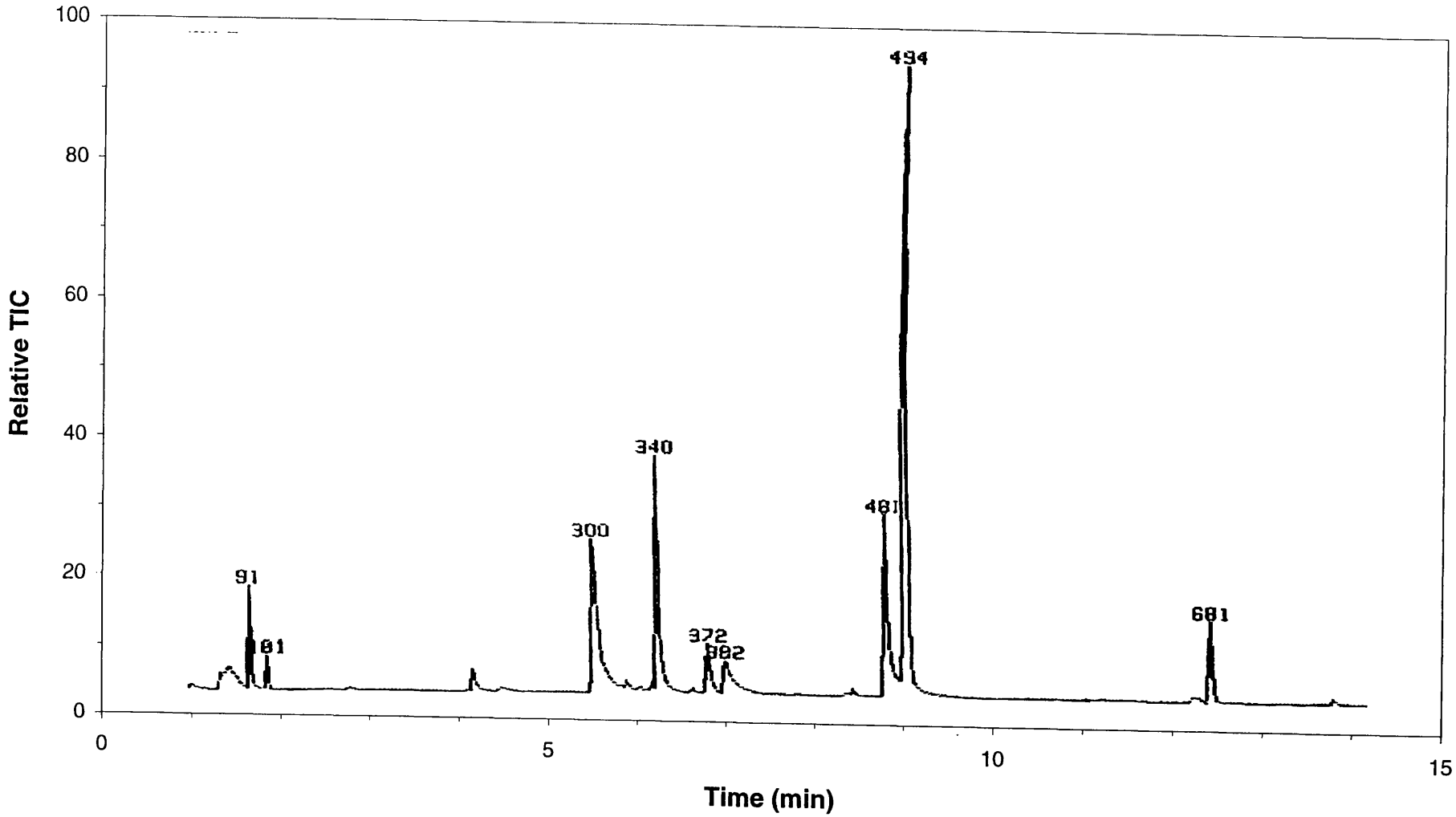

Figure 6.30: TIC trace for the liquid fraction from the SATVA curve in Figure 6.29

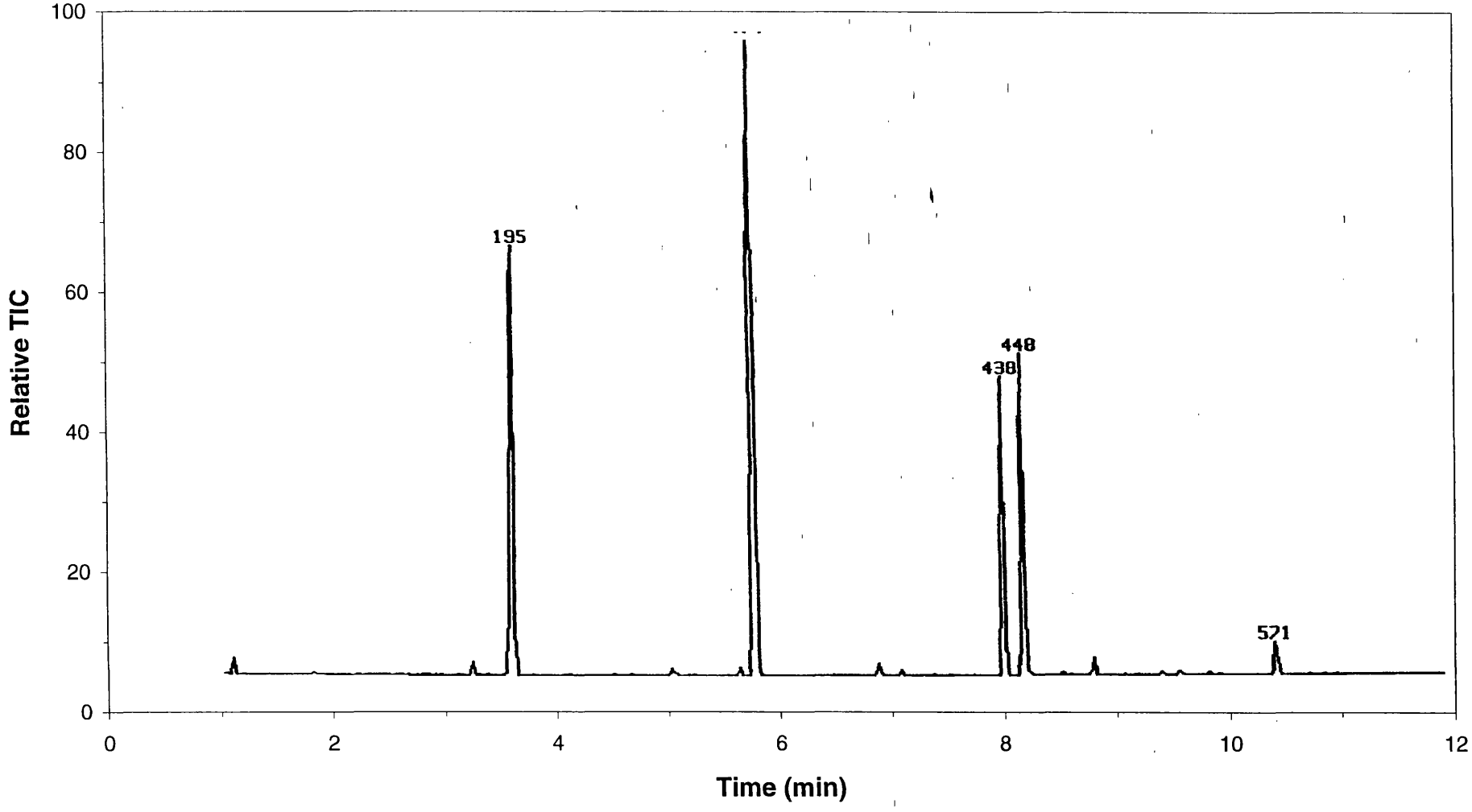

Figure 6.31: TIC trace for the liquid fraction from the degradation of Savinyl Black RLS under flaming conditions

CHAPTER 7

REMAINING METAL CONTAINING COLOURANTS

7.1 INTRODUCTION TO DYES IN THIS SECTION

These colourants were grouped together as they did not fit into any of the other categories[14-17]. The first of these, Graphtol Fire Red 3RL, contains one azo linkage and is dibasic neutralised with a Sr^{2+}. The second, Sandorin Red Violet 3RL, contains nickel and multiply chlorinated aromatics. As will be explained, a quick glance at the structure leaves the impression that this material will produce some hazardous products on degradation. This observation was confirmed during the studies.

7.2 CHEMISTRY OF THE DYES

The first colourant studied in this chapter may relate more to the samples studied in chapter 4 than in the previous chapter. It may be seen from the illustration in Figure 7.2 that this is an azo dye, with two negative ions. The charge is balanced with a Sr^{2+} ion. It is possible that the azo-hydrazone tautomerism described in section 4.2 applies to this sample.

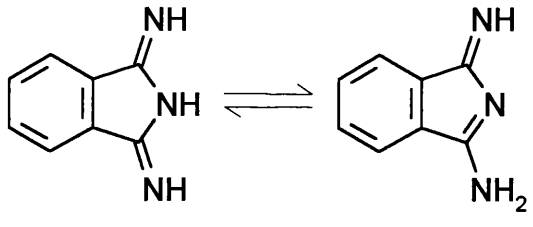

Figure 7.1: Diiminoisoindoline tautomerism

Classification of the second colourant proved difficult. There was a structural analogue in the form of phthalogen dyes. This is a dying process using the precursor diiminoindoline (Figure 7.1) in organic solvents.

There is a textile printing process involving a paste containing the precursor, solvents and a copper or nickel salt.

7.3 STRUCTURES

The first sample studied in this chapter is Graphtol Fire Red 3RL, and the second Sandorin Red Violet 3RL. It is quite apparent from the structures, as seen in Figure 7.2, that the latter only has passing similarities to the materials described in the preceding section. Regrettably, there was some difficulty in finding colourants of similar structure.

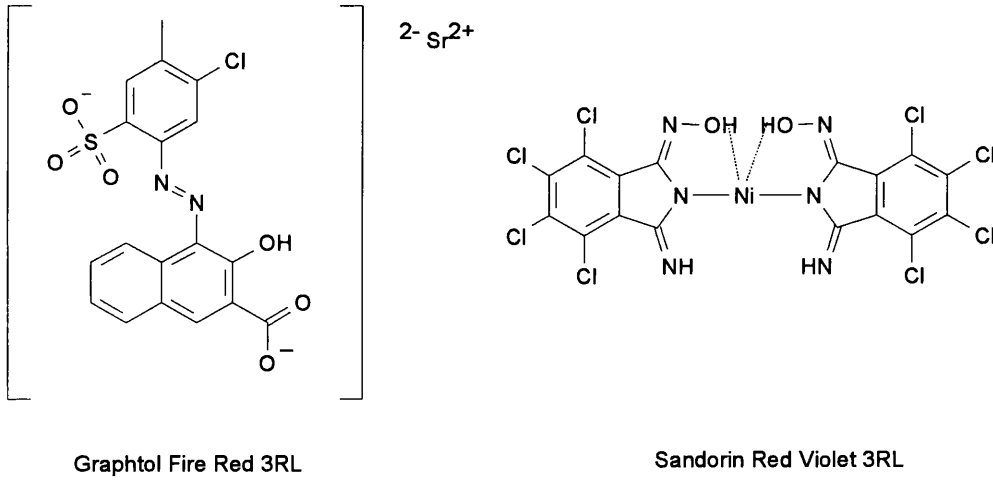

Graphtol Fire Red 3RL

Sandorin Red Violet 3RL

Figure 7.2: Colourants studied in this chapter

7.4 THERMAL DEGRADATION OF GRAPHTOL FIRE RED 3RL

This sample has been presented first as it had more similarities to the colourants already studied. The main complication anticipated in the analysis of the degradation products was the presence of the sulphur group, as experienced in the studies of Graphtol Fast Red 2GLD.

7.4.1 Thermogravimetric Analysis

The TG plots for dynamic nitrogen and air are given in Figure 7.3. The significant temperatures are summarised in the following table:

Table 7.1: Key temperatures from thermogravimetry of Graphtol Fire Red

Conditions	$T_{thresh1}$(°C)	$T_{thresh2}$(°C)	T_{end}(°C)	%Residue
Dynamic Nitrogen	120	320	>1000	/
Dynamic Air	120	340	850	28

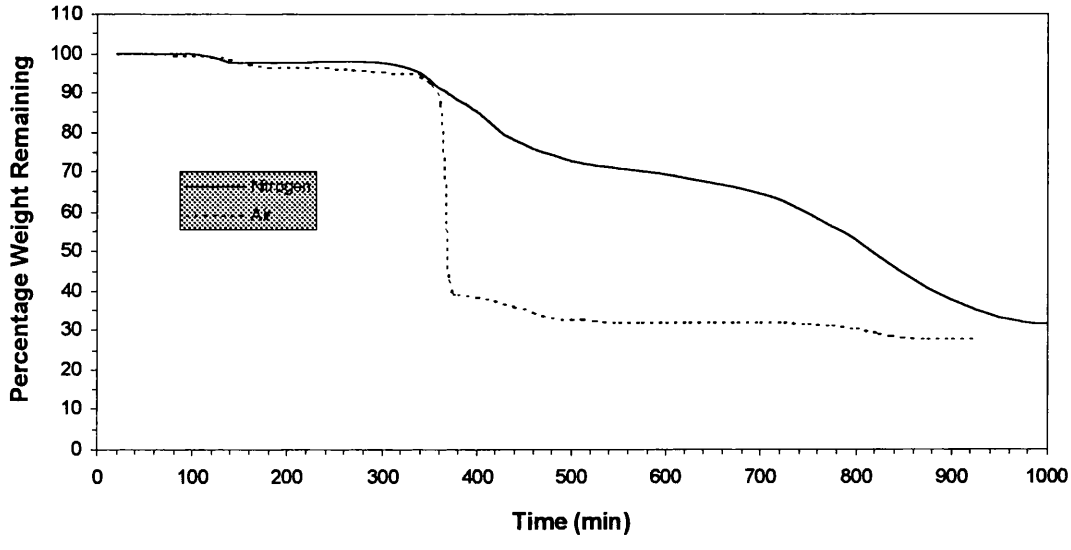

Figure 7.3: Thermogravimetric Analysis traces from Graphtol Fire Red 3RL

There was an initial small weight loss under both conditions at 120°C. This may be due to drying of the sample. It is apparent from the traces that oxidation played a significant role in the decomposition of the sample, with the air trace showing the weight loss almost completed by 380°C. The profile of this weight loss suggests that is

genuine, rather than being due to the sample falling off of the pan. The trace obtained under dynamic nitrogen was not in well defined stages, although the trace appears to show two poorly-resolved stages to the degradation.

7.4.2 Product Analysis - Dynamic Nitrogen

These studies were carried out with a heating rate of 10°C/min up to 900°C. This high temperature was used as TG information was not available to indicate suitable maximum temperatures at the time the degradations were carried out. A typical SATVA trace is presented in Figure 7.4. Peak 1 at 10 minutes was quite small. This was found to be due to CO_2, through the on-line mass spectrometer. The gases evolved as peaks 2 and 3 were collected together for IR analysis, and were monitored during the SATVA by the mass spectrometer. At 16 minutes the predominant mass spectrum was that for HCN. A small amount of H_2S was also observed. HCN remained detectable up to 24 minutes. There was also a weak response for ammonia, but this was partially masked by the water peaks appearing with the start of peak 4. The IR spectrum showed a strong response for HCN and ammonia through the characteristic peaks described in chapter 4. These findings are summarised in the following table:

Table 7.2: SATVA peak assignments from Figure 7.4

Peak	Assignment
1	CO_2
2 and 3	HCN, NH_3 and H_2S. Also possibly a little SO_2.
4	Mainly water. See below for GC-MS of ether extract.

The TIC trace obtained from the GC-MS analysis of the ether extract from peak 4 is presented in Figure 7.5. The interpretation of the MS data is tabulated overleaf:

Table 7.3: GC-MS peak assignments from Figure 7.5

Retention Time	Product	Retention Time	Product
8:38	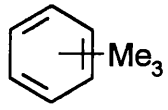 or 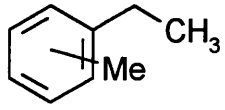 with 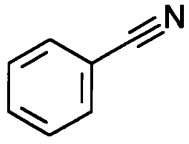	16:45	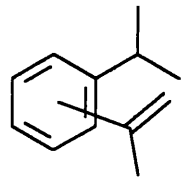 or 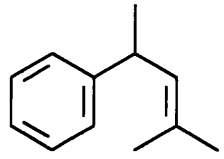
9:00	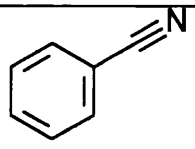 with 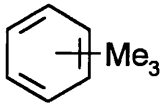 or 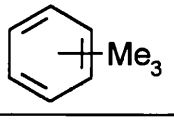	17:22	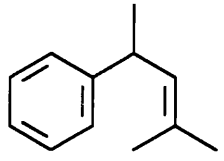 or 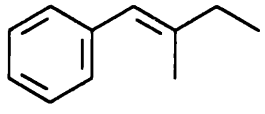 or another isomer
10:56 and 11:12	Silicone contaminant	17:59	Possibly 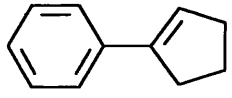
15:47	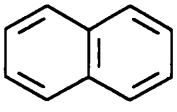	18:41	Isomer of 16:45
16:08	Silicone contaminant	18:51	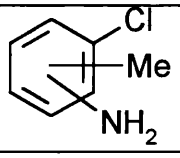

The peaks at 21:04, 25:22, 25:59 and 29:09 were due to silicone containing contaminants. These probably came from the oil used in the diffusion pump. The other unidentified peaks provided weak or ambiguous spectra. Many of these had the characteristics of aromatics with aliphatic substitutions. This was suggested by a number of strong peaks in the range m/e = 75-200 with losses of 15 units from the molecular ion.

7.4.3 Product Analysis - Dynamic Air

These studies were also carried out with a heating rate of 10°C/min up to 900°C, as once again TG information was not available at the time the degradations were carried out. A typical SATVA trace for the volatilisation of the condensable degradation products is shown in Figure 7.6. The on-line mass spectrometer revealed only CO_2 at 9 minutes, and water from 20 minutes onwards. These were the only products observed through spectroscopy. These observations are summarised below:

Table 7.4: SATVA peak assignments from Figure 7.6

Peak	Assignment
1	CO_2
2	Mainly water. See below for GC-MS of ether extract

The TIC trace obtained from the GC-MS of the diethylether extract from the cold finger is shown in Figure 7.7. The peak assignments are listed in the following table:

Table 7.5: GC-MS peak assignments from Figure 7.7

Retention Time	Product	Retention Time	Product
6:25	Mainly 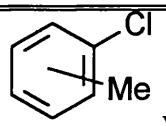 with some 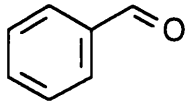	8:50	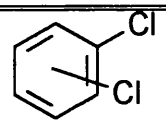
7:15	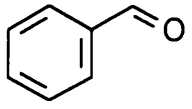	9:13	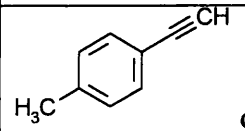 or possibly indene
7:49	Good match with 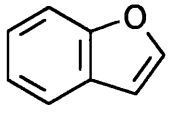	9:35	Unidentified aliphatic hydrocarbon
8:11	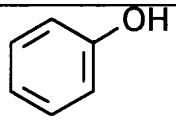		

Table 7.5 (Continued)

Retention Time	Product	Retention Time	Product
9:46	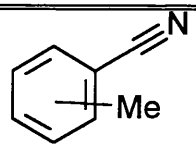 or possibly 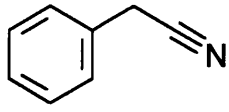	13:18	Spectrum consistent with 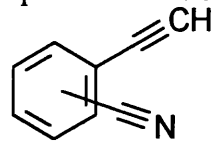 co-eluting 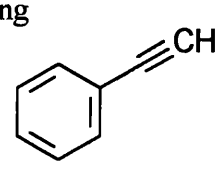 with
11:26	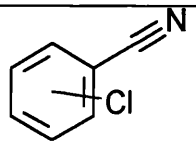	Remaining peaks all gave weak spectra which were consistent with aliphatic hydrocarbons, except:	
11:49	Spectrum too weak. Probably an aliphatic hydrocarbon	18:51	Possibly 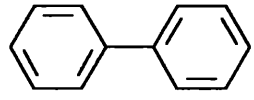
12:33	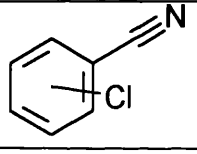		

7.4.4 Product Analysis -Flaming Conditions

The apparatus was arranged as described in Chapter 2. The following observations were made during the degradations:

Table 7.6: Observations from Graphtol Fire Red under flaming conditions

First Run	
Sample Size:	121.7 mg
Time (min)	**Observations:**
1:30	The sample turned black from the centre outwards, and started to smoke.
5:00	Heater switched off.
Comments:	No ignition.

Table 7.6 (continued)

Second Run	
Sample Size:	130.3 mg
Residue:	57.5 mg (44%)
Time (min)	**Observations:**
1:10	Started to discolour.
1:30	Within around 5 seconds the sample went black from the centre outwards, evolving fumes.
1:55	Ashing commenced. There were still some spots of the original red colour present.
5:00	Heater switched off
Comments:	No ignition. The residue was a combination of black powder, ash and some specks of red.

The SATVA trace obtained for the separation of the condensable volatile degradation products is presented in Figure 7.8. This is a fairly typical two peak trace for a flaming conditions study. There was, however, a well defined shoulder following the first peak. The IR spectrum for the non-condensable gases was dominated by peaks for untrapped CO_2, but there were also weak absorptions for CO. The IR spectrum taken for the gases forming the start of peak 1 on the SATVA trace showed the absorptions for CO_2, with a relatively small amount of N_2O. The sample taken for FT-IR analysis at the middle of the peak showed the addition of a small amount of SO_2 through absorptions at around 1374, 1360 and 1348 cm^{-1}. Finally, a sample was taken in the same manner from the tail end of peak 1 to the start of peak 2. This was again dominated by CO_2 with the SO_2 still evident. There was no further detection of N_2O. These observations are summarised in the following table:

Table 7.7: SATVA peak assignments from Figure 7.8

Peak	**Assignment**
Non-condensables	CO
1	Mainly CO_2. N_2O and SO_2 were also present.
2	Mainly water. Only naphthalene and an unidentified aliphatic hydrocarbon were detected through GC-MS from the ether extract.

7.5 THERMAL DEGRADATION OF SANDORIN RED VIOLET 3RL

This sample had few similarities with the other colourants studied. The structure did not contain fragments like any of the other metal containing samples, in the same way that Sandorin Violet BL was quite different to the other all organic colourants. The main interest is the apparent ability to produce toxic degradation products through the multiply chlorinated aromatics, the potential to produce nitriles and the presence of nickel.

7.5.1 Thermogravimetric Analysis

Figure 7.9 shows the thermogravimetric analysis trace obtained under dynamic nitrogen and air with a temperature program of 10°Cmin^{-1}. The key points in the traces are outlined in the following table:

Table 7.8: Key temperatures from thermogravimetry of Sandorin Red Violet

Conditions	$T_{thresh1}$(°C)	$T_{thresh2}$(°C)	T_{end}(°C)	%Residue
Dynamic Nitrogen	285	380	700	13
Dynamic Air	285	380	>1000	/

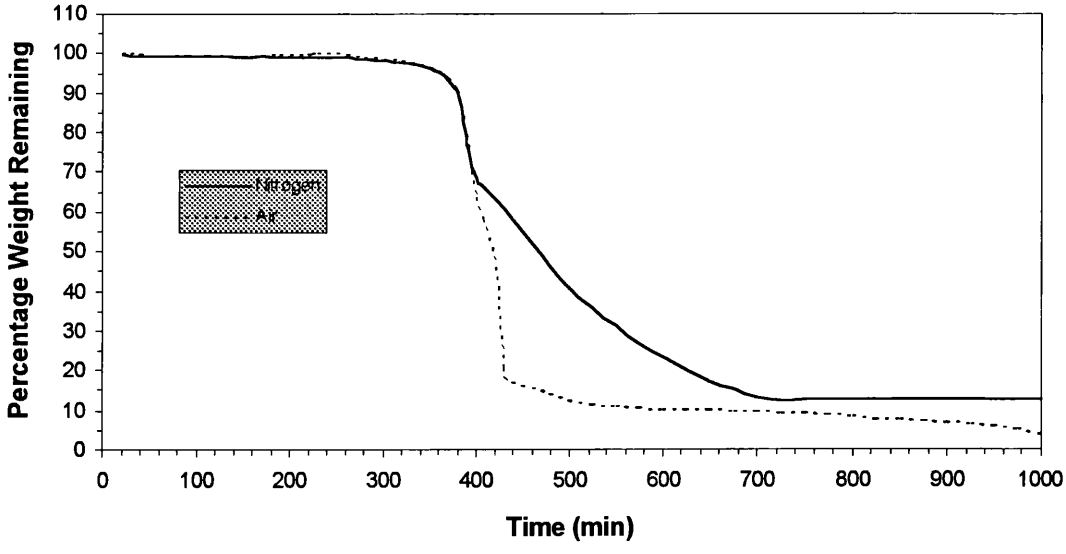

Figure 7.9: Thermogravimetric Analysis traces from Sandorin Red Violet 3RL

The two traces were co-incident to 380°C. There was a slight weight loss before the

listed $T_{thresh1}$, probably due to drying. The nitrogen trace shows only a low rate of weight loss from 380°C onwards. At this temperature it is apparent that oxidation has a significant effect, with the air trace showing only 18% weight remaining by 430°C.

7.5.2 Product Analysis — Dynamic Nitrogen

These studies were carried out with a heating rate of 10°C/min up to 900°C. This was chosen as TG information was not available at the time the degradations were carried out. The comparison between the percentage residue under TG and flow-tube studies is tabulated below:

Table 7.9: Residue percentages from nitrogen degradation of Sandorin Red Violet

	Weight Remaining	
Maximum Temperature	**Thermogravimetry**	**Flow tube**
900°C	12%	28%

This is the more typical result, where there was more residue with the larger flow tube sample. It has previously been suggested in Chapter 2 that side reactions appear to promote the formation of residue.

A typical SATVA trace for the volatilisation of the condensable degradation products is shown in Figure 7.10. The first peak was identified as being due to CO_2 through the usual mass spectrometry peaks. There was too little of this product to provide an IR response. The second peak at 26 minutes was harder to identify, as the FT-IR spectrum did not match any of the spectra in the Aldrich library. There were strong peaks at 2204, 2224, 774 and 790 cm^{-1}. There were also absorptions at 2911, 2930, 2981, 3000 and 2587 cm^{-1}. This spectrum was found to match that of cyanogenchloride (ClCN) reported in the literature[46]. This was confirmed through the mass spectrometer by peaks at m/e = 61, 63, 27. These results repeated perfectly for

the first repeat of the experiment. There was a third degradation performed under the same conditions. This time there was no ClCN detected, but HCl was found. The trap may well have been colder in this case, so it is possible that some HCl was produced on the other runs, but not detected. What is of more interest is the absence of the ClCN. It is possible that the HCl was formed in preference in the final run. This is discussed further in the summaries and mechanistic suggestions at the end of the chapter. These observations are summarised in the following table:

Table 7.10: SATVA peak assignments from Figure 7.10

Peak	Assignment
1	CO_2
2	ClCN
3	Contained water. See below for GC-MS of ether extract.
Note:	HCl was detected and ClCN found absent in a subsequent degradation.

The volatile liquid products forming peak 3 had diethylether added to form an extract for GC-MS analysis. The resulting TIC trace is presented in Figure 7.11, and the peak assignments are presented in the ensuing table:

Table 7.11: GC-MS peak assignments from Figure 7.11

Retention Time	Product	Retention Time	Product
5:55	Mainly 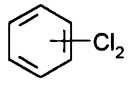 with 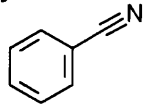 some	11:43	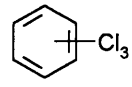
6:44	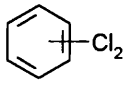	15:11	Possibly styrene, but with 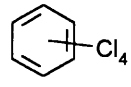 some
9:29	Unidentified aliphatic hydrocarbon	16:24	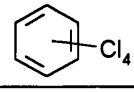
10:48	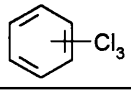	18:08	Unidentified aliphatic hydrocarbon

The CRF was collected as a solid. There was difficulty dissolving it in the solvents normally favoured, however CCl_4 was found to be suitable. The TIC trace from the GC-MS analysis of this sample is presented in Figure 7.12. The sample was also separated through HPLC. The same number of peaks were detected on the trace, which suggest that none of these relatively involatile materials were permanently retained on the GC column. The peak assignments are tabulated below:

Table 7.12: GC-MS peak assignments from Figure 7.12

Retention Time	Product
5.90	No NIST. C_7HNCl_4 from accurate mass study, e.g. 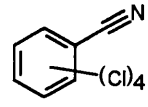
6.38	Possibly trichloronaphthalene by NIST. No reference for 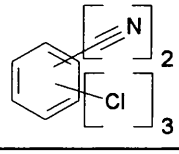 , which is implied by a 109 peak in the mass spectrum.
6.64	An aliphatic hydrocarbon
6.82	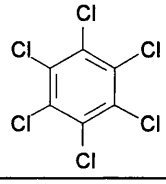
7.18	Pentachlorobenzonitrile, 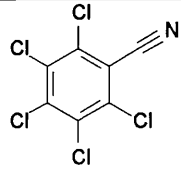
7.67	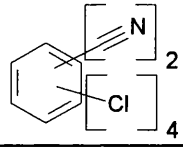
9.01	Probably contaminant, dibutyl phthalate

Table 7.12 (continued)

Retention Time	Product
11.97	$C_8HO_2NCl_4$ from accurate mass. Cl = 4 and probably aromatic from GC-MS. Losses of 71, 44 and 43 with no Cl loss in MS. Group at mass 212 will be due to C_6Cl_4 fragment. The 71 loss accounts for the C_2HO_2N remainder. COOH acid and CN substituents were considered a possibility, but these were ruled out as they would give strong losses of 17 and 45, as was verified by reference spectra. Likewise, 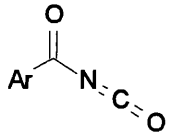 gave 42 and 70, and 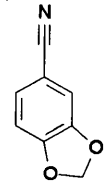 showed a loss of 1 with the remaining spectrum very weak. The correct losses were however consistent with 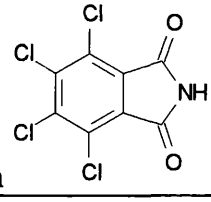
19.00	Unknown

7.5.3 Product Analysis — Dynamic Air

These studies were carried out with a heating rate of 10°C/min up to 900°C, again because TG information was not available at the time of these studies. The comparison between the percentage residue under TG and flow-tube studies is tabulated below:

Table 7.13: Residue percentages from air degradation of Sandorin Red Violet

	Weight Remaining	
Maximum Temperature	**Thermogravimetry**	**Flow tube**
900°C	7%	7%

A typical SATVA trace for the volatilisation of the condensable degradation products is shown in Figure 7.13. The SATVA trace was nearly identical to that for the dynamic nitrogen study. Similarly, the same gaseous products were present, and were identified by the same method. There was also a small amount of CO_2 present in the FT-IR

spectrum. The spectrum for peaks 1 and 2 is shown in Figure 7.14. There are also some water vapour peaks present. These findings are listed in the following table:

Table 7.14: SATVA peak assignments from Figure 7.13

Peak	Assignment
1	CO_2
2	ClCN
3	Mainly water. See below for GC-MS of ether extract.

Figure 7.15 shows the TIC trace from the GC-MS of the diethylether extract from the liquid fraction. All except two of the peaks were due to contamination from silicon compounds, and these have been removed from the trace. Both non-silicon peaks are assigned below:

Table 7.15: GC-MS peak assignments from Figure 7.15

Retention Time	Scan Number	Product
4:33	248	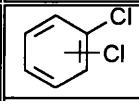
8:08	444	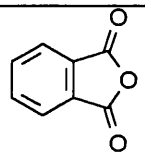 Probably

7.5.4 Product Analysis -Flaming Conditions

The apparatus was assembled as described in Chapter 2. The following observations were made:

Table 7.16: Observations from Sandorin Red Violet under flaming conditions

First Run	
Sample Size:	Weights unreliable.
Time (min)	**Observations:**
1:50	Sample discoloured slightly.
2:50	Started to turn black and ash.
3:05	Some smoking.
3:20	All black and ashing
4:00	Black and white residue (not separable).
6:00	Heater switched off.
Comments:	No ignition.

Table 7.16 (continued)

Second Run	
Sample Size:	170.7 mg
Residue:	22.5 mg (13.2%)
Time (min)	**Observations:**
1:30	Discolouration (blackening) commenced.
1:35	Much smoke evolving. A white solid started to form.
1:50	Sample had developed a white crust on the predominately black residue. There was still some colour on the base of the sample.
2:30	No change since 1:50
4:00	Heater switched off.
Comments:	No ignition. By the end the residue was a mound of the brownish-white crystalline solid on top of a layer of black powder. The white solid blew off of the top when the vacuum was broken after the volatile analysis were collected.

A typical SATVA trace for the volatilisation of condensable degradation products is shown in Figure 7.16. Non-condensable trapping was used, and this gave the normal weak response for CO, along with a very weak pattern for HCl. It is worth remembering that only a small amount of the non-condensable material is trapped through this method, so the response will always be weak, and not provide meaningful quantitative information. The IR spectra taken for the materials producing peak 1 were dominated by the normal CO_2 absorptions. Appreciable amounts of N_2O were also detected. There were also absorptions at 1810 and 1891 cm^{-1} and an unrelated absorption at 1354 cm^{-1} from unidentified materials. The second SATVA peak was found by MS to be mainly due to water. These observations are summarised in the following table:

Table 7.17: SATVA peak assignments from Figure 7.16

Peak	**Assignment**
Non-condensables	CO and HCl
1	Mainly CO_2. N_2O was also present, with some unidentified material.
2	Mainly water. See below for GC-MS of ether extract.

Diethylether was added to the products forming the second peak. The resulting extract was analysed through GC-MS. The TIC trace for this analysis is presented in Figure 7.17, and the peak assignments are tabulated below:

Table 7.18: GC-MS peak assignments from Figure 7.17

Retention Time	Product	Retention Time	Product
1.54	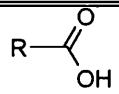	7.24	Probably 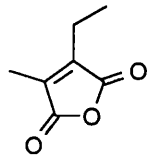 with trace pentachloro-1-propene
1.73	Mainly unidentified aliphatic hydrocarbon with trace 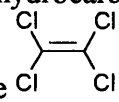	7.96	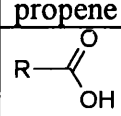
1.88	Siliconecontaminant	8.65	Possibly 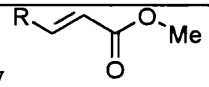
2.15	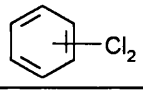	9.40	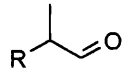
2.42	Unidentified chloroaromatic	9.73	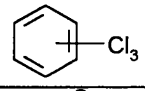
2.68	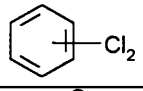	10.55	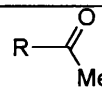
3.10	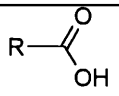	10.61	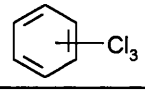
3.92	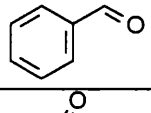	10.75	Siliconecontaminant
4.51	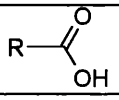	11.18	Siliconecontaminant
5.33	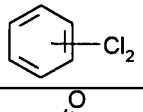	13.39	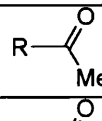
5.51	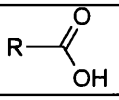	14.82	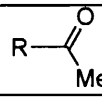
5.87	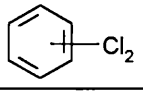	15.60	Siliconecontaminant
6.02 6.16	Siliconecontaminant	16.43	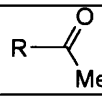

The cold ring fraction was collected by washing the walls of the degradation vessel with acetone. This left the vessel quite clean, so was considered a good enough solvent for this purpose. The dynamic nitrogen study required carbon tetrachloride, perhaps due to the greater amount of product in that method. Here, a large area of thin deposit on the vessel was washed with a relatively large volume of solvent.

The TIC trace from the GC-MS of this sample is displayed in Figure 7.18. The main peaks on the TIC trace are identified first in the following table, followed by a selection of the other products.

Table 7.19: GC-MS peak assignments from Figure 7.18

Retention Time	Product
Up to 5.00	Apparently aliphatic hydrocarbons
5.13	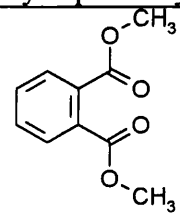 Possibly
5.92	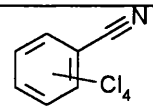 Possibly
6.56	Similar spectrum to peak at 6.40
6.84	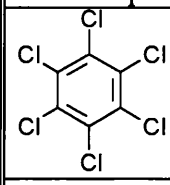
7.76	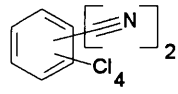 Main Peak
6.40	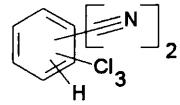 2nd Strongest probably (no NIST)

Table 7.19 (continued)

Retention Time	Product
7.21	3rd strongest, 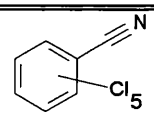
12.10	4th strongest, probably 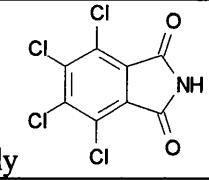

7.6 MAJOR PRODUCT SUMMARIES AND MECHANISMS

The major products for the two materials studied in this chapter are summarised in this section. Some suggestion of the decomposition mechanisms are also offered.

7.6.1 Graphtol Fire Red 3RL

This sample was degraded under dynamic nitrogen and dynamic air under programmed heating to 900°C and under flaming conditions. Cold ring fraction analysis was not performed for this sample.

7.6.1.1 Dynamic Nitrogen

The major gases were NH_3 and HCN with some H_2S and SO_2. A small amount of CO_2 was also detected. There was only a small amount of this final product, so it may be attributed to the background. There was much water, which is also potentially from the background, as these samples tend to be quite hydroscopic and are difficult to dry thoroughly. The water may have been evolved from the sample before the degradation onset temperature was attained, as was implied by the TG curve. Naphthalene was a major component of the liquid fraction. There were also unidentified aromatics with

aliphatic substituents. These materials are difficult to identify, although isomers of

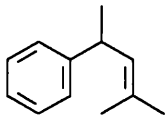

gave good matches with some of the spectra.

The structure of Graphtol Fire Red 3RL is shown in Figure 7.19. Both the azo and the hydrazone forms are shown. Once again, the weakest linkages are marked to highlight the most probable points where degradation can occur.

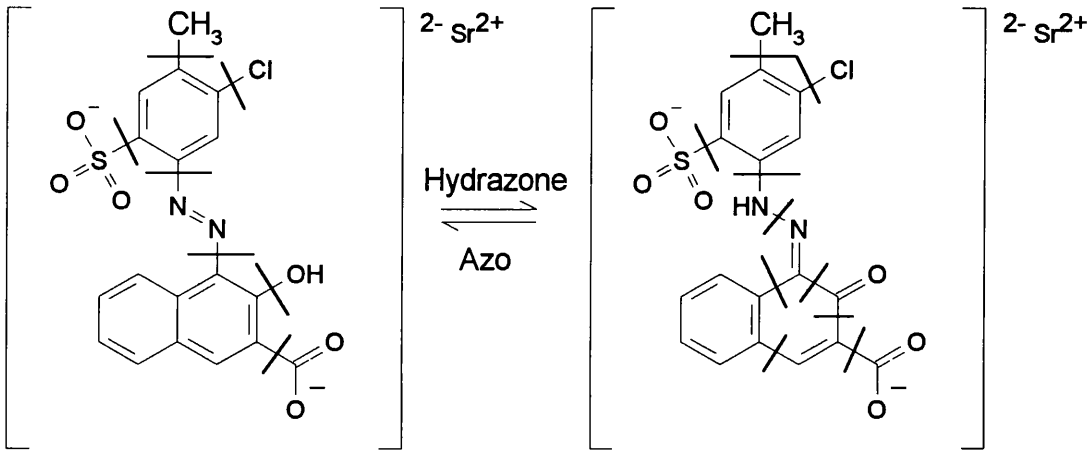

Figure 7.19: Graphtol Fire Red 3RL weak linkages

The naphthalene evolved implies the azo form, but the isomers of 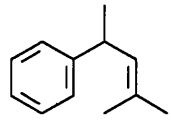 imply the hydrazone tautomer. The hydrazone provides the greatest potential for aliphatic substituents on an aromatic ring, through the loss of conjugation on one of the naphthalene rings. Benzonitrile was also present, although not one of the major products. It was explained in the summaries in chapter 4 that this product probably signals the presence of the hydrazone tautomer. Another minor product of interest was

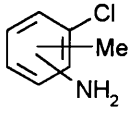

. This was the only chlorinated product identified, and is also evidence for

the hydrazone form, as a —NH_2 free form of this molecule was not found. Furthermore, there were no aromatics detected with sulphur based groups attached. This may be due to the absence of CRF data, or may imply the SO_3 group went elsewhere. The only sulphur detected in the products was as H_2S and a small amount of SO_2. Sulphur dioxide would be the most direct product, yet this was the more minor sulphur material detected. S_8 was found as a product from a sample with an -SO_2- linkage in chapter 5, but was not observed here as CRF data were not available. It may be supposed that the sulphur was evolved as the residue formed. The non-oxidising environment may result in the formation of H_2S from the S_8 in preference to SO_2. The HCN may have been formed from the hydrazone supplying the nitrile, as described in chapter 2. The source of the ammonia is less clear. It has been explained that

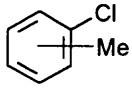

was not detected. This suggests that the —NH— linkage from the aromatic drawn at the top of the structure was not the direct origin. This implies a less direct pathway for the formation. It would be unreasonable to speculate further about the mechanism by which the ammonia is formed.

7.6.1.2 Dynamic Air

The only gas detected was a small amount of CO_2. There was also much water detected in the liquid fraction. There were more compounds detected in this fraction than in the dynamic nitrogen study. Benzaldehyde was the major component. There was also appreciable amounts of phenol, ethynyltoluene or indene, ethynylbenzonitrile and ethynylbenzene. Smaller amounts of chlorobenzonitrile (2 isomers), chlorotoluene, dichlorobenzene (1 isomer) and 2,3-dihydrobenzofuran were also detected.

The change in degradation conditions may not be the reason for the increased number of products. It is also possible that changes in the GC-MS conditions provided by the analysis laboratory may have provided a better sensitivity. The machine used for these runs requires constant attention, resulting in inconsistent sensitivity.

One clear difference between this and the dynamic nitrogen study lies with the major product. There was no naphthalene detected here, and no benzaldehyde detected under nitrogen. It is apparent that the presence of oxygen had a major influence on the degradation of this sample. The level of CO_2 remained low. This is perhaps surprising considering the carboxyl group on the molecule. The source of the benzaldehyde remains something of a mystery. The benzene ring on the sample is already well accounted for with the other products, and has no obvious and direct way of forming the aldehyde. The answer appeared to lie with the naphthalene ring system. The absence of this product under these conditions also implies that this part of the molecule may have been involved. The problem is that the most stable of the aromatic rings is the one drawn to the left in Figure 7.19. If the left ring was connected to a carbon then an oxygen in series then there may have been a clue to the benzaldehyde formation pathway. As there is not, it must be concluded that this product was formed through an indirect process. Any suggestions as to the mechanism of this would be highly speculative.

The ethynylbenzonitrile is almost certainly from the hydrazone tautomer. The source of the nitrile group has already been discussed, and is a common feature of the azo colourants. The —CCH is not a common feature from this class of materials. The origination of this substituent may be due to the cleavage of the carboxyl and the

carbonyl group. If this was the case, then ethynyltoluene may have been formed through a similar pathway.

More curious was the chlorobenzonitrile, especially as there were two isomers. The dichlorobenzene certainly suggests there was some mobility, perhaps through the secondary reactions mentioned in chapter 4, of the chlorine. The creation of the benzonitrile form the naphthalene would leave the *ortho-* site free to pick up such a chlorine. Perhaps the benzonitrile was already formed when it became chlorinated.

7.6.1.3 Flaming Conditions

This sample did not ignite. Water and CO_2 were by far the major products. There was also much N_2O and SO_2 detected. The only organic detected in the liquid fraction was naphthalene.

There is not a great deal of information here, but the products appear to have more in common with the dynamic nitrogen degradation. Sulphur dioxide and naphthalene were not detected in the dynamic air study. It is possible that the ferocity of the flaming environment was such that the sample was not greatly oxidised, but became fragmented by the heat and then oxidation of the product fragments could occur. Although there was no flaming here, the conditions could well result in a stream of radicals leaving the sample to be exposed to the air atmosphere, resulting in rapid oxidation.

7.6.2 Sandorin Red Violet 3RL

These degradations were carried out under dynamic nitrogen and dynamic air under programmed heating at 10°C/min^{-1} up to 900°C. Flaming studies were also performed

under the normal conditions. CRF data were available for the dynamic nitrogen and flaming conditions.

7.6.2.1 Dynamic Nitrogen

Cyanogen chloride was the major gaseous product. There was also a small amount of CO_2, but this was probably from the background. The degradation was repeated three times. These findings were made for two of these studies, but on one occasion HCl was detected and there was no ClCN present. The degradation conditions were identical. The only possible variation was insignificant changes in sample size, or varying degrees of sample drying. It should also be repeated here that HCl was not always detected, as the trap on the degradation apparatus was normally kept at -76°C. Liquid nitrogen was used to keep the dry-ice/acetone trap cool for the duration of the experiment. This sometimes resulted in the trap being cooler. This means that the assumption that HCl was formed as an alternative to ClCN may not be valid.

There was much water in the liquid fraction. The organic extract had one isomer of dichlorobenzene as the major component. There were smaller but roughly equal amounts of the other two dichlorobenzene isomers, benzonitrile, two isomers of trichlorobenzene, styrene and 2 isomers of tetrachlorobenzene. Styrene was a common contaminant in the GC-MS machine used, and should perhaps be disregarded.

The cold-ring fraction structures are re-drawn here for clarity. This was dominated by

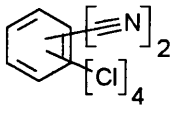
which was by far the major product.
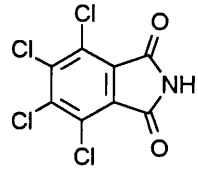
and
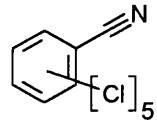
were also detected. There were traces of
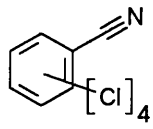
and
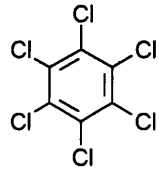
present.

The structure of Sandorin Red Violet 3RL with the weak linkages highlighted is illustrated in Figure 7.20. These are all the non-aromatic single bonds. For clarity the O—H and C—Cl bonds have not been marked, although they are in this category.

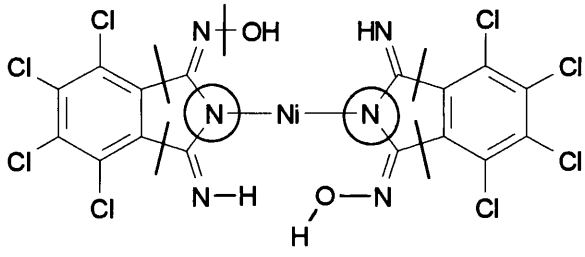

Figure 7.20: Sandorin Red Violet 3RL weak linkages

The source of the major product from the CRF is perhaps the easiest to explain. Loss of the circled nitrogen, the hydroxyl group and the NH hydrogen would result in the correct structure. Any suggestion as to the motion of the electrons would be mere conjecture. Loss of water may be part of the process. Figure 7.20 was drawn with one of the —OH and N—H groups extended to highlight this possibility.

Cyanogen chloride was also a major product, along with dichlorobenzene. Consideration of the structure of the sample reveals that these products must form as an alternative to that described in the previous paragraph. One isomer of

dichlorobenzene was a very major product, compared with the other isomers. The source of the nitrile group is suggested in the above paragraph. It may have been cleaved from the aromatic ring and reacted with a chlorine, perhaps the neighbouring one. This would result in the evolution of one cyanogen chloride and one isomer of dichlorobenzene.

The sample has only a limited supply of hydrogen. This may be why this sample forms cyanogen chloride instead of the hydrogen cyanide normally detected from other samples when nitrile groups are present in the evolved products. The shortage of hydrogen raises the question of where the HCl came from in one of the analyses. One possibility may by that the sample was damp at the start of the degradation when HCl was detected.

The detection of 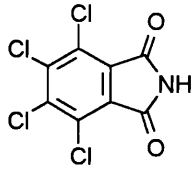

is also hard to explain. There is no obvious mechanism for the formation of this product.

The other materials may be explained by the migration of chlorine, or the preferential loss of one of the nitriles. Perhaps the mechanism for the formation of the first nitrile leads to a small barrier to the formation of the second.

7.6.2.2 Dynamic Air

There were fewer products detected here, although a more sensitive GC-MS was used to analyse the liquid fraction. There was no CRF analysis. Cyanogen chloride was evolved in great quantities. There was only a trace of CO_2. Water dominated the liquid

fraction. Dichlorobenzene was by far the major component of the organic extract of the liquid fraction, and there was also a small amount of 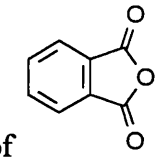 detected.

The explanation for the formation of the cyanogen chloride and the dichlorobenzene is suggested in section 7.6.2.1. Benzonitrile and chlorobenzenes are conspicuously absent from the liquid fraction. It is quite possible that the oxygen has influenced the degradation pathway to cause this change in the products.

7.6.2.3 Flaming Conditions

This sample provided a typical SATVA trace for the volatilisation of the condensable degradation products. There was no ignition. Water and CO_2 were the major products. Also detected were N_2O, CO and HCl. There was no ClCN detected. If present, there was only a very small amount.

Dichlorobenzene (two isomers with less of a third) was the major component of the liquid fraction. There was also reasonable amounts of trichlorobenzene (two isomers) detected. Unusually, various R—CO_2H and R—COMe fragments were found. Trace amounts of tetrachloroethene were present.

The cold ring fraction had similar major products to those found in the dynamic nitrogen degradation. The major product was 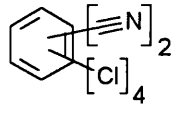 . Following in reducing

intensity were 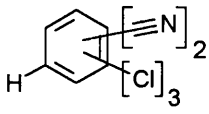

, 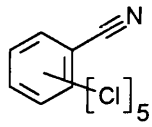

and 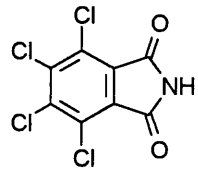

. A small amount of 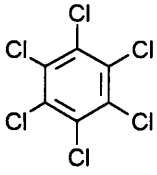

was also detected.

Clearly there are some differences between these products and those obtained under the degradation conditions above. The main points are the absence of cyanogen chloride and the increase in the amount of a second dichlorobenzene isomer. It would appear that there was more migration of the chlorine in this sample. This is confirmed by the traces of tetrachloroethene detected. This must be formed quite indirectly, as all the carbon-carbon bonds in the colourant were in aromatic systems, and there were no examples of two chlorines bonded to a single carbon. This implies the breakdown of the benzene rings — an observation confirmed by the RCOMe and RCO_2H structures found in the liquid fraction.

The nitrile formation has also been hindered. The only nitriles were the chlorinated ones found in the cold-ring fraction, with evidence for cyanogen chloride and benzonitrile failing to appear in the gas and liquid analyses.

The products obtained form this sample included some of relatively high toxicity. Polychlorinated biphenyls (PCBs) were no detected. These should have been detected if present in the studies where CRF analyses were performed. However, if the concentration was low, these materials may not have been observed.

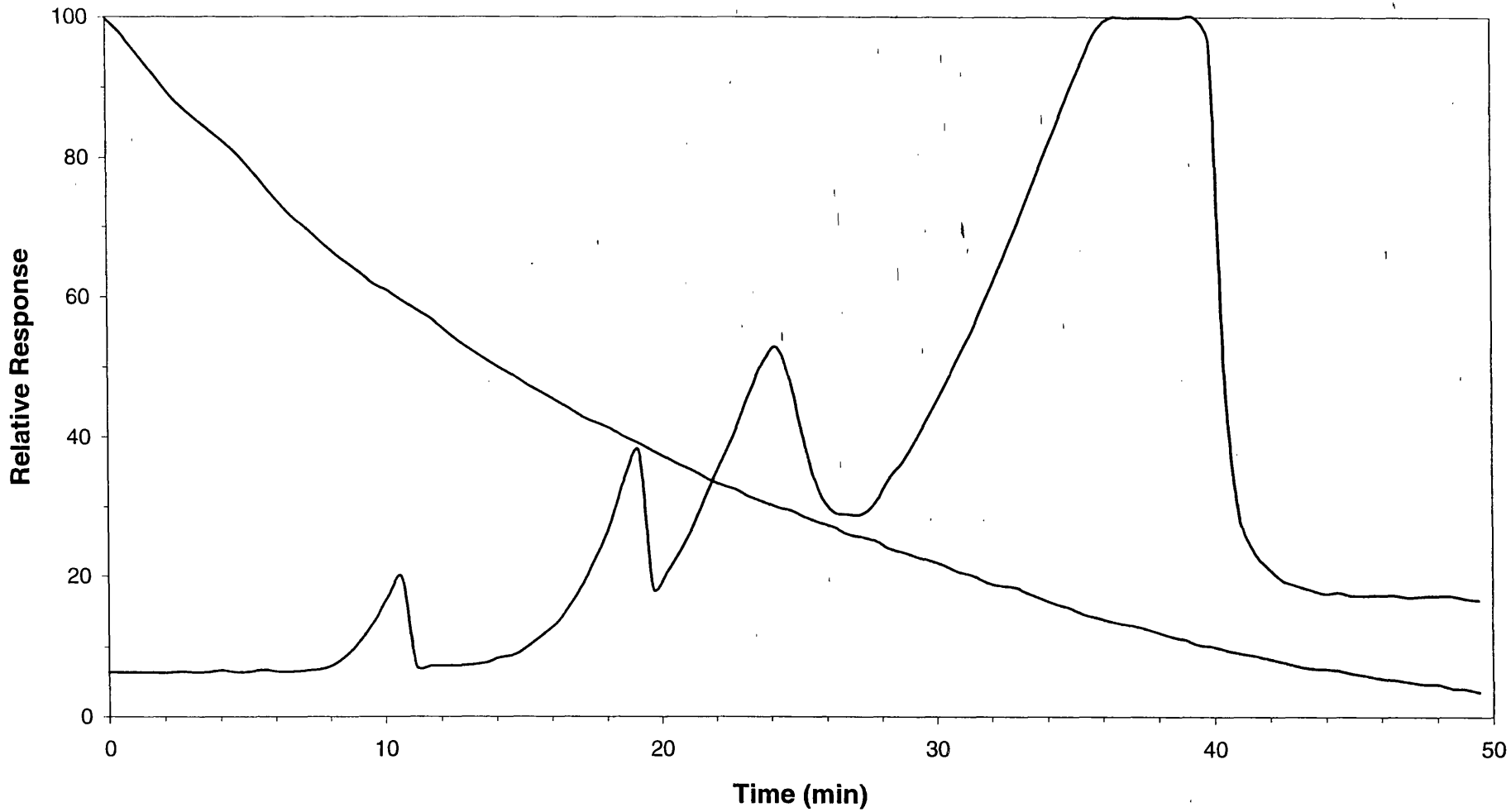

Figure 7.4: SATVA trace from the degradation of Graphtol Fire Red 3RL under dynamic nitrogen

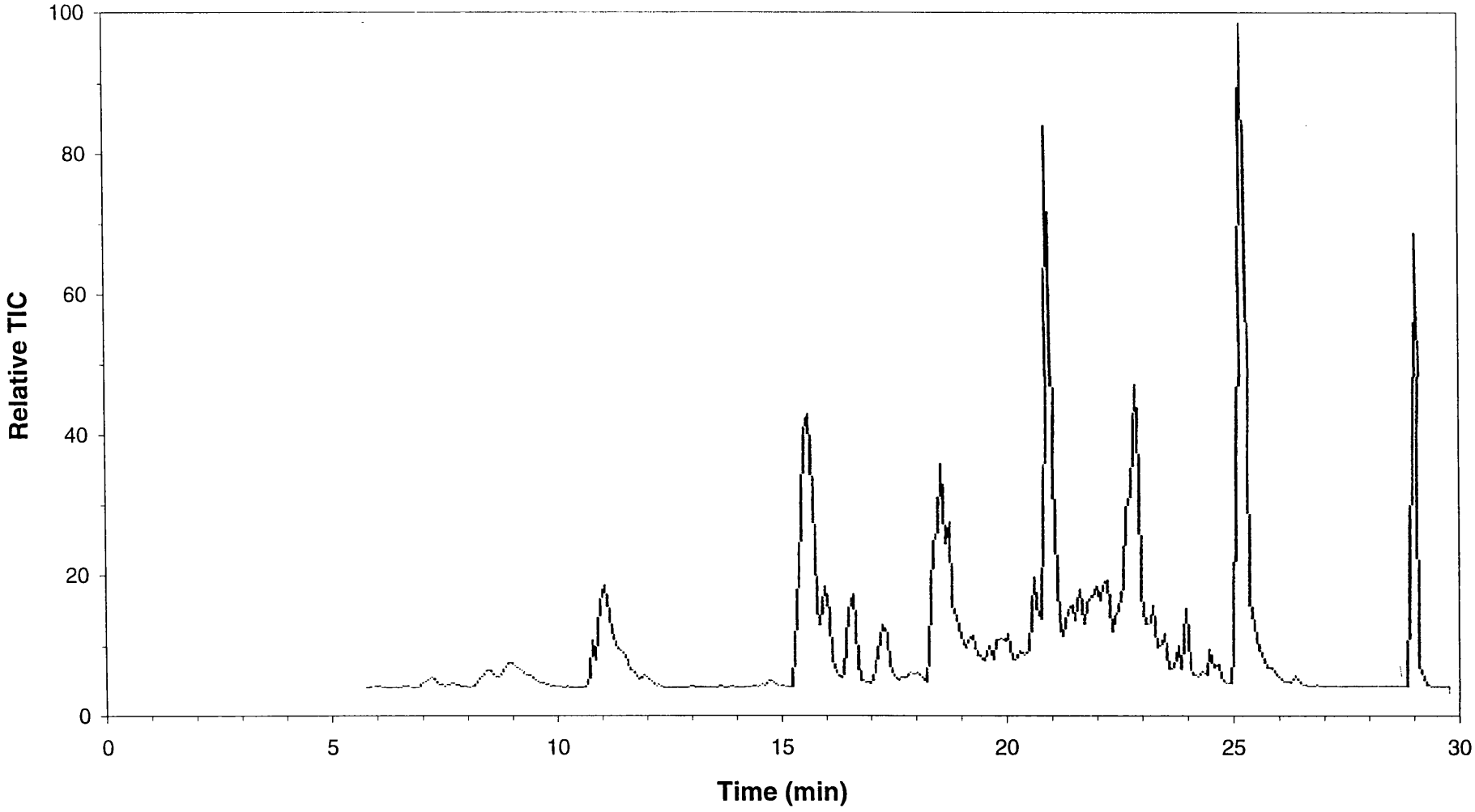

Figure 7.5: TIC trace for the liquid fraction from the SATVA curve in Figure 7.4

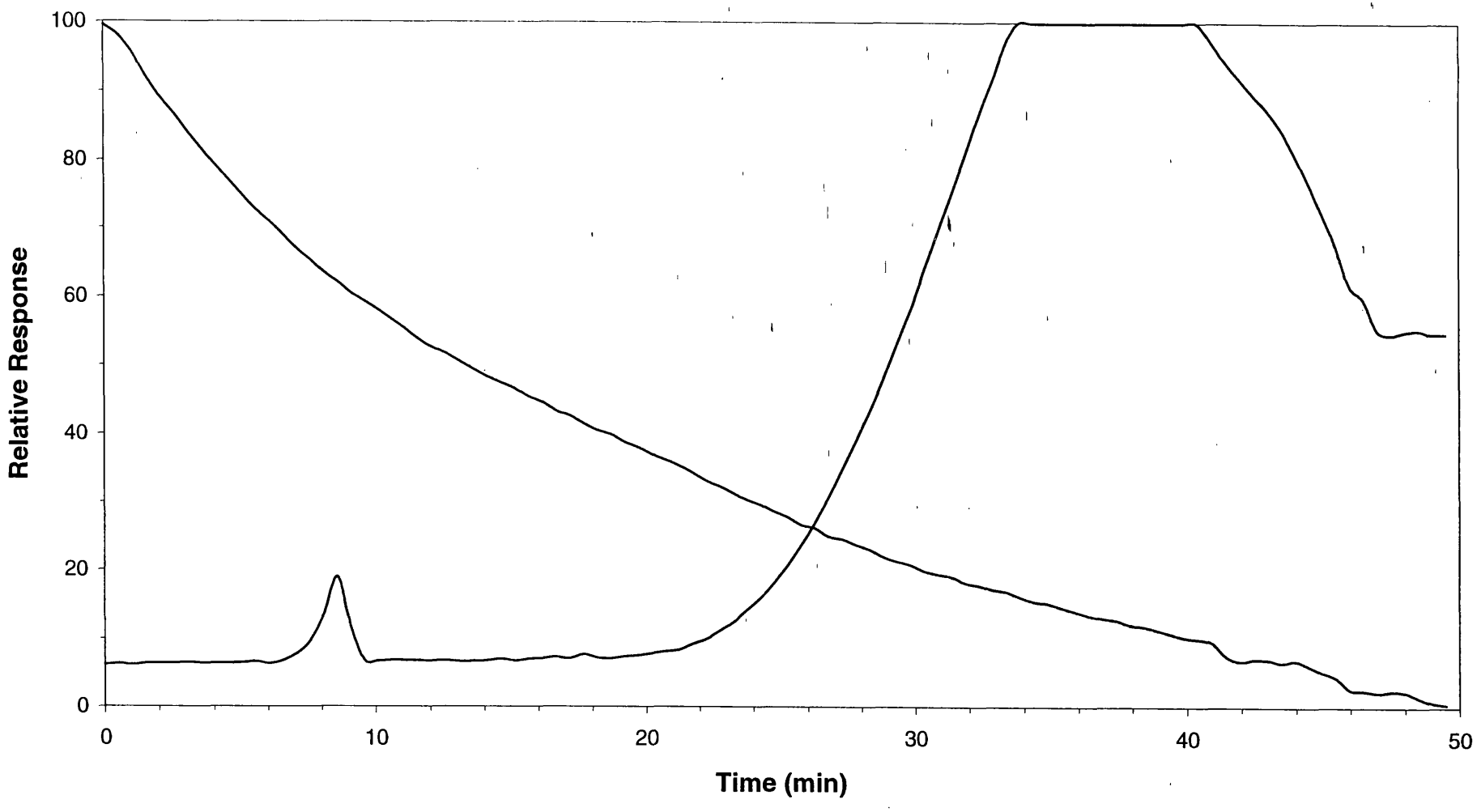

Figure 7.6: SATVA trace from the degradation of Graphtol Fire Red 3RL under dynamic air

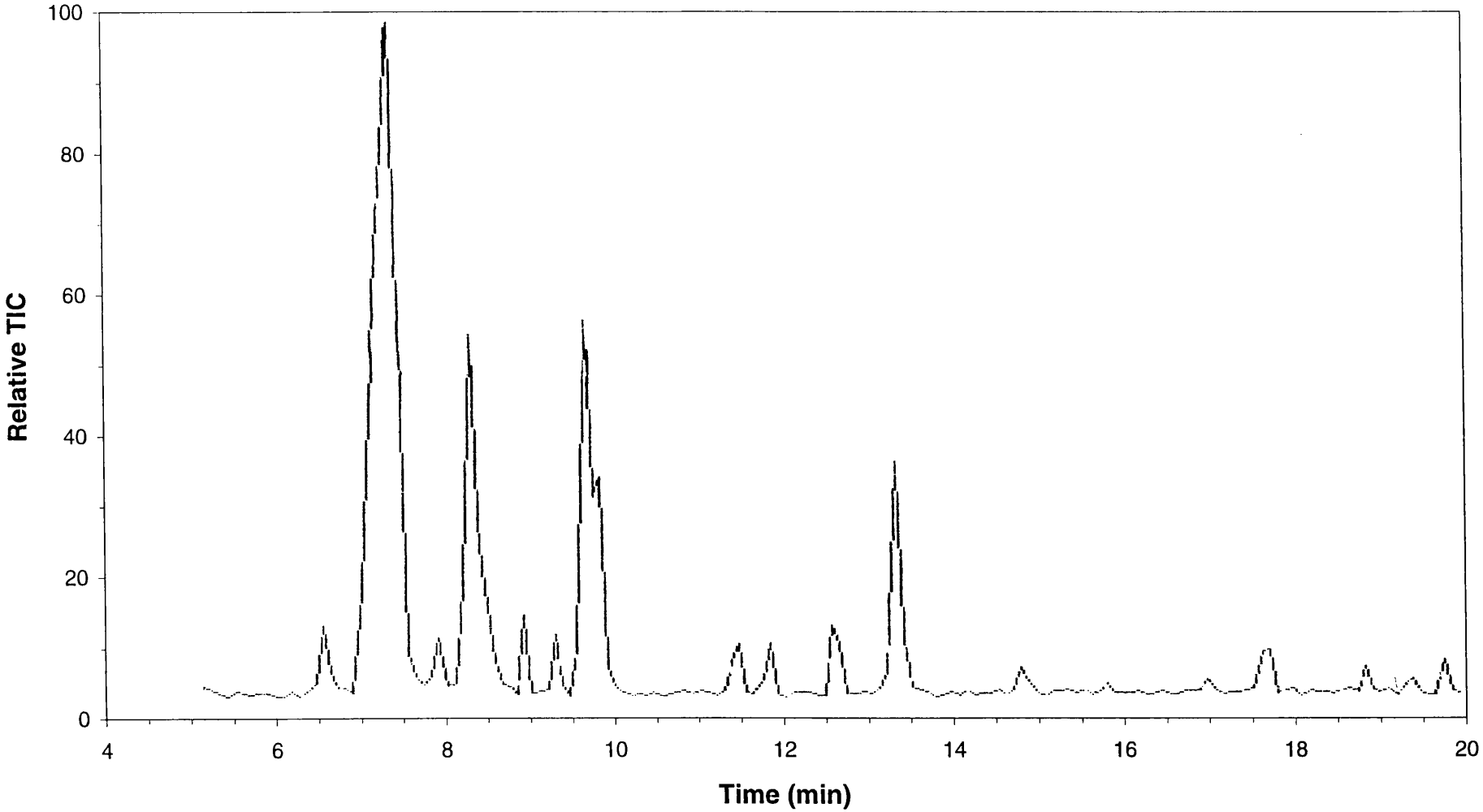

Figure 7.7: TIC trace for the liquid fraction from the SATVA curve in Figure 7.6

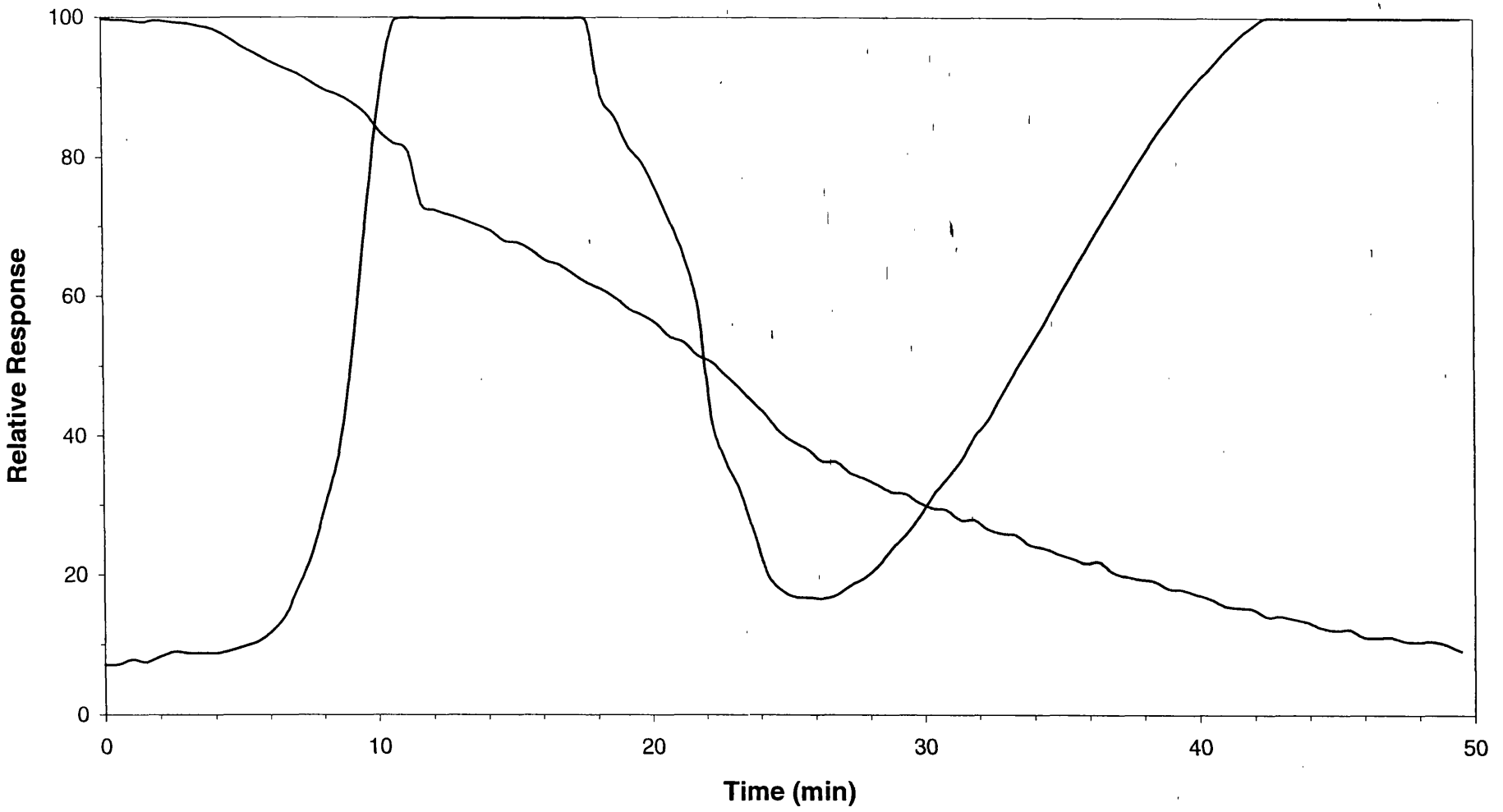

Figure 7.8: SATVA trace from the degradation of Graphtol Fire Red 3RL under flaming conditions

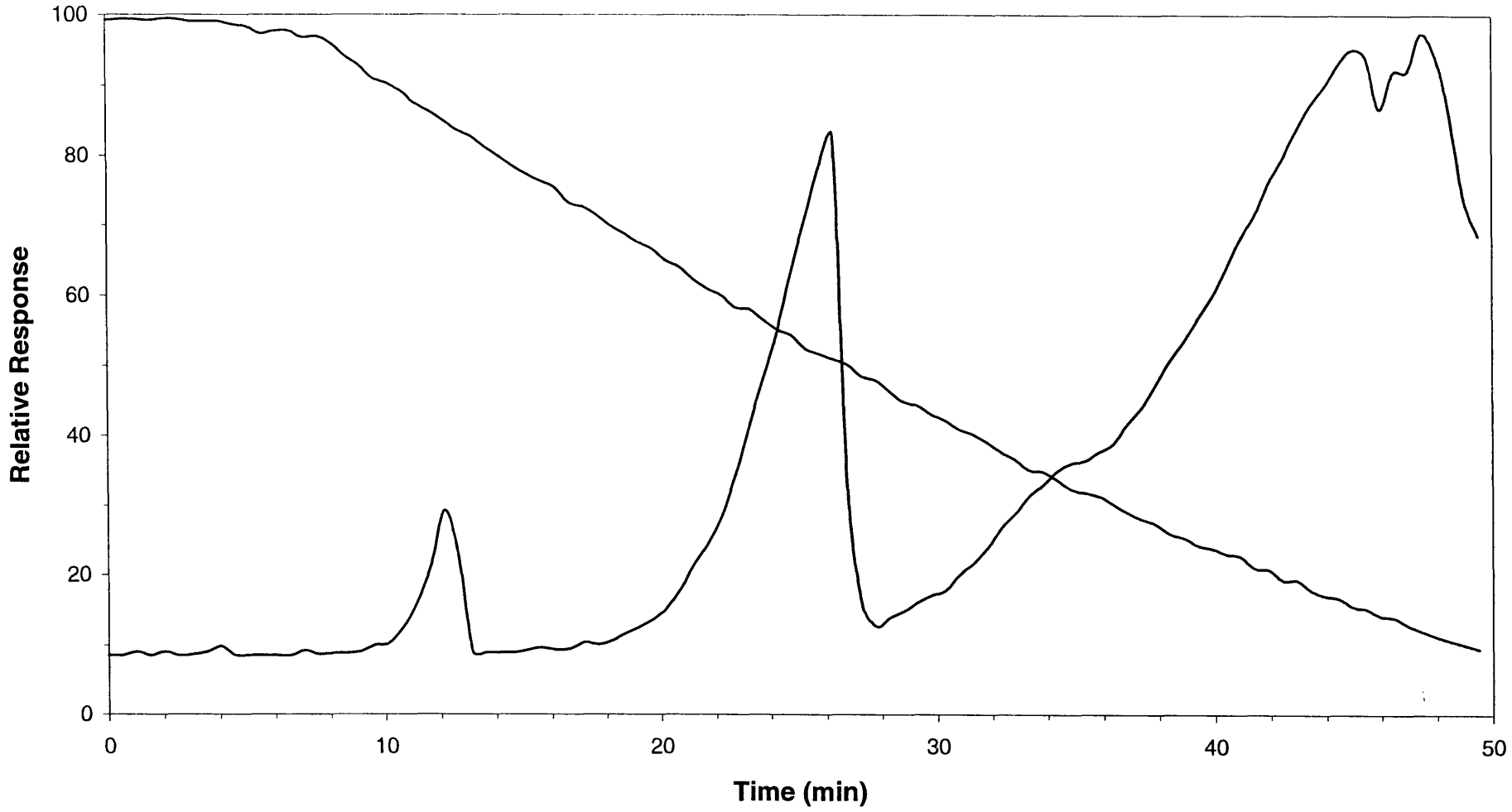

Figure 7.10: SATVA trace from the degradation of Sandorin Red Violet 3RL under dynamic nitrogen

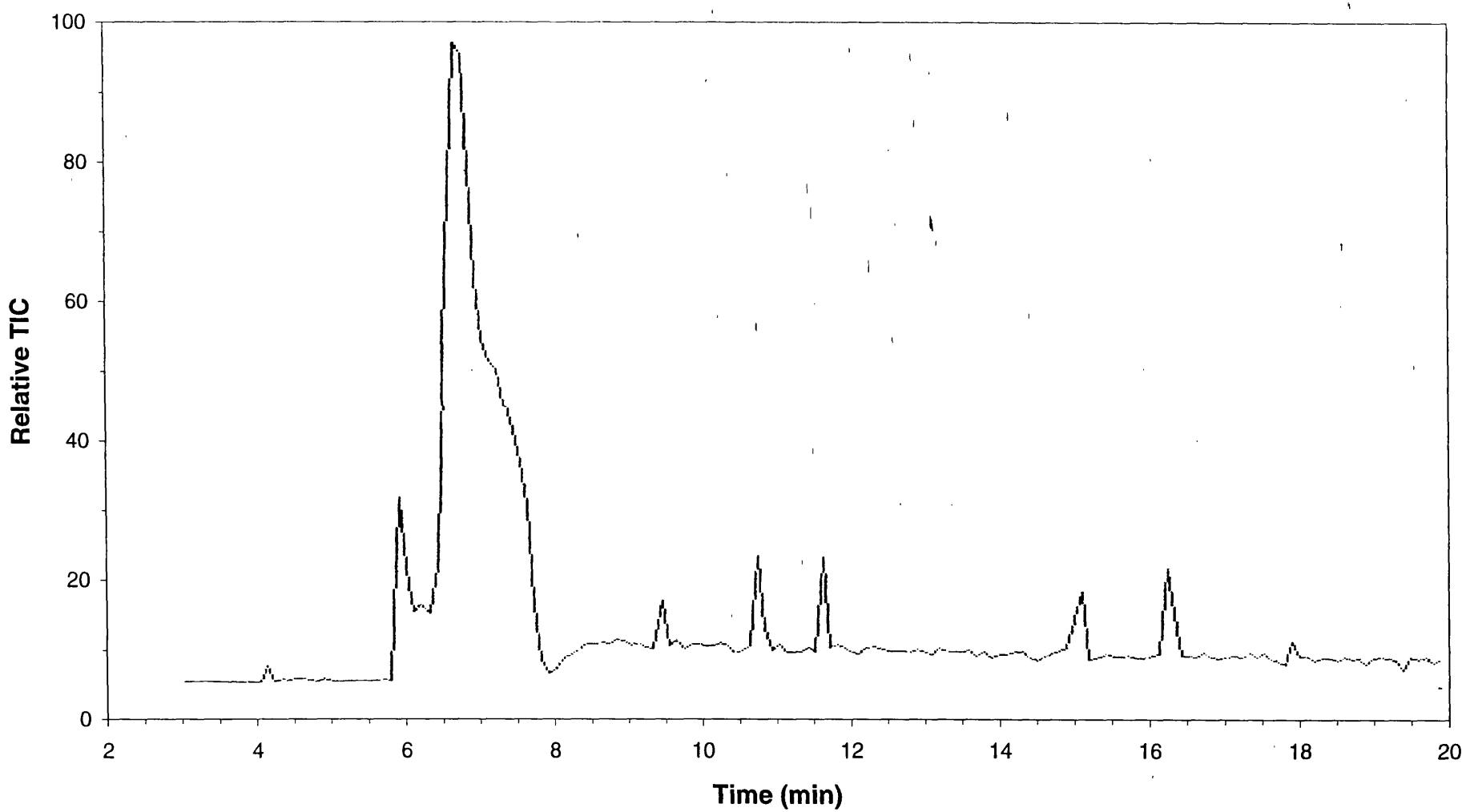

Figure 7.11: TIC trace for the liquid fraction from the SATVA curve in Figure 7.10

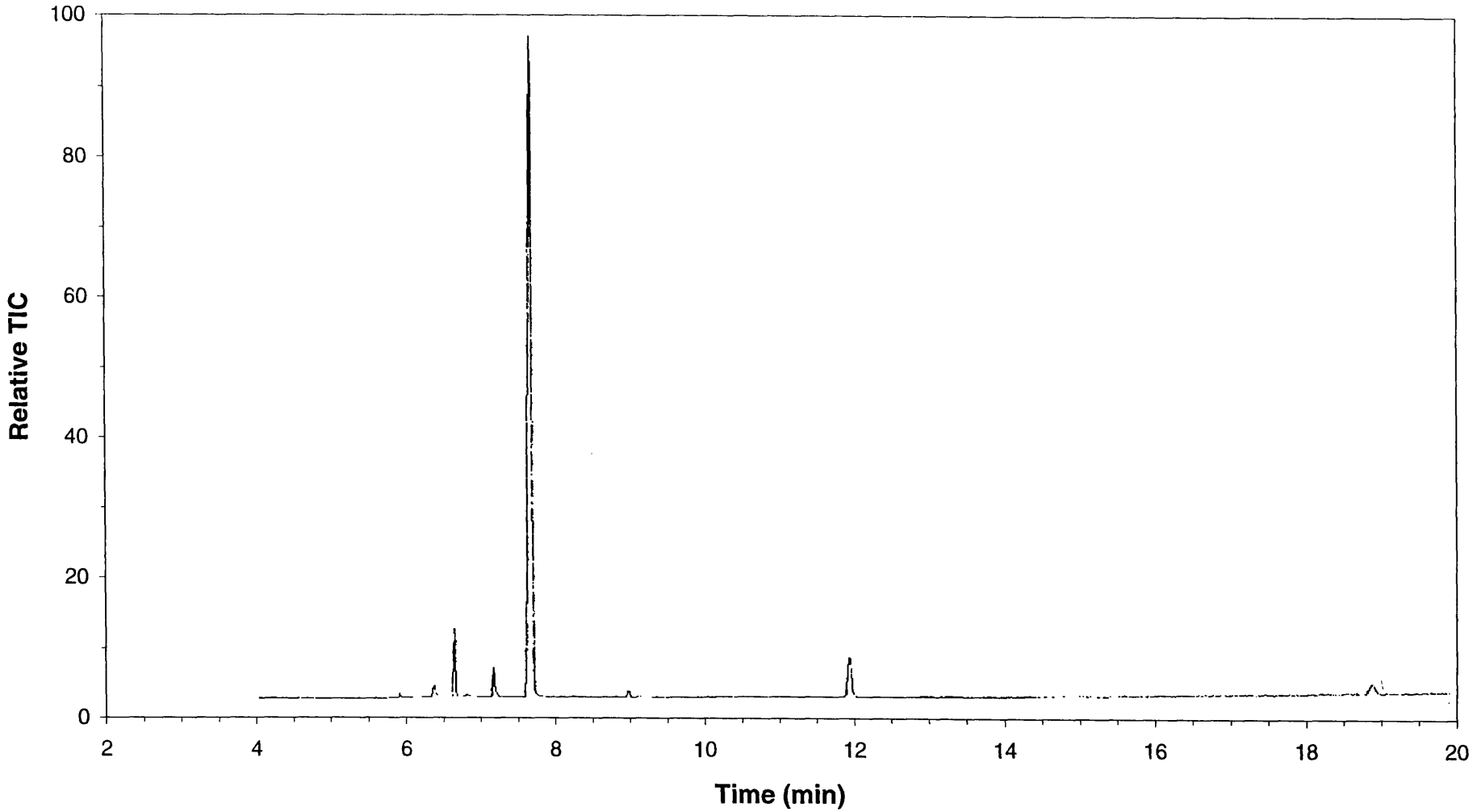

Figure 7.12: TIC trace for the cold ring fraction from the SATVA study in Figure 7.10

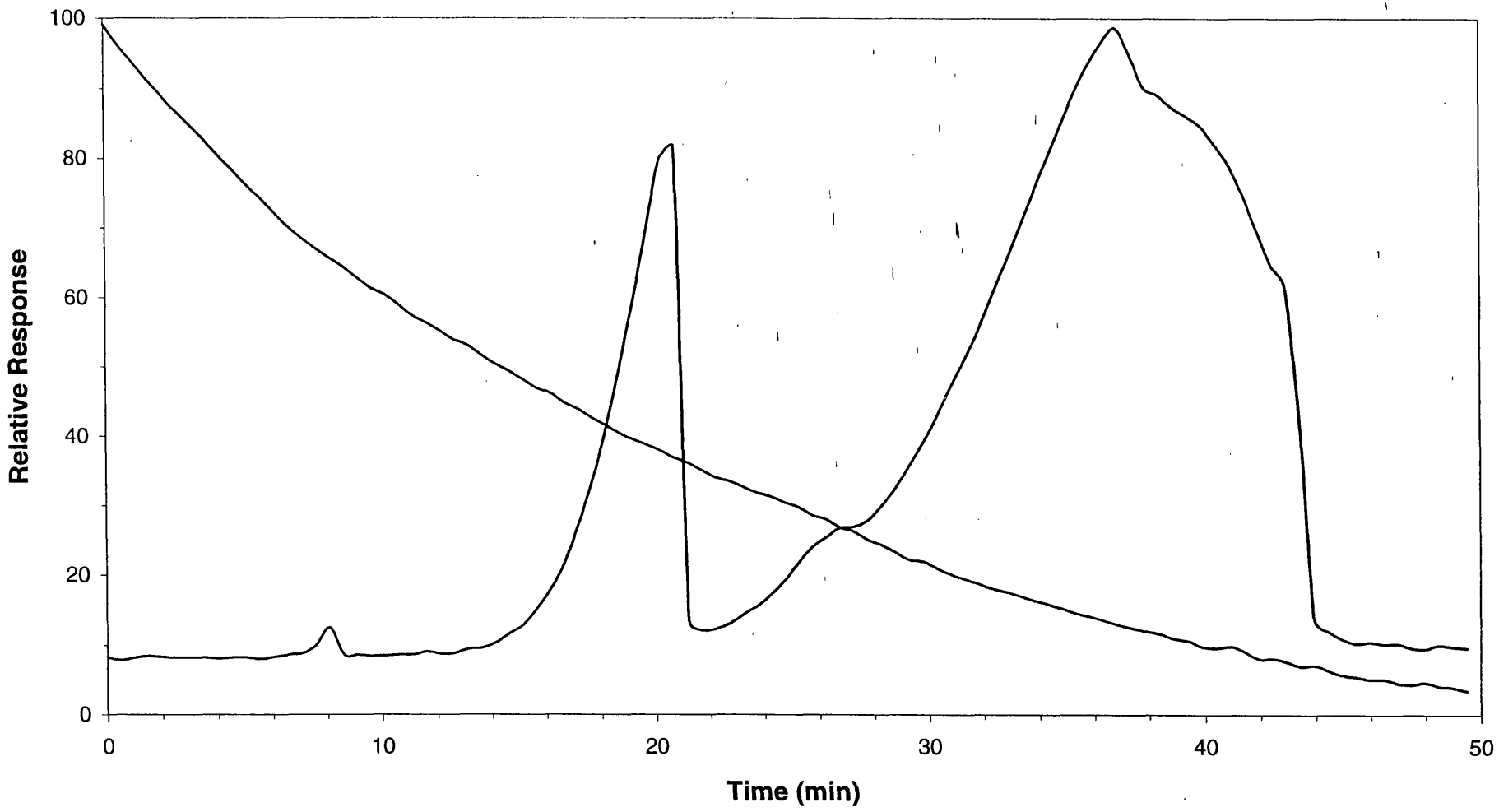

Figure 7.13: SATVA trace from the degradation of Sandorin Red Violet 3RL under dynamic air

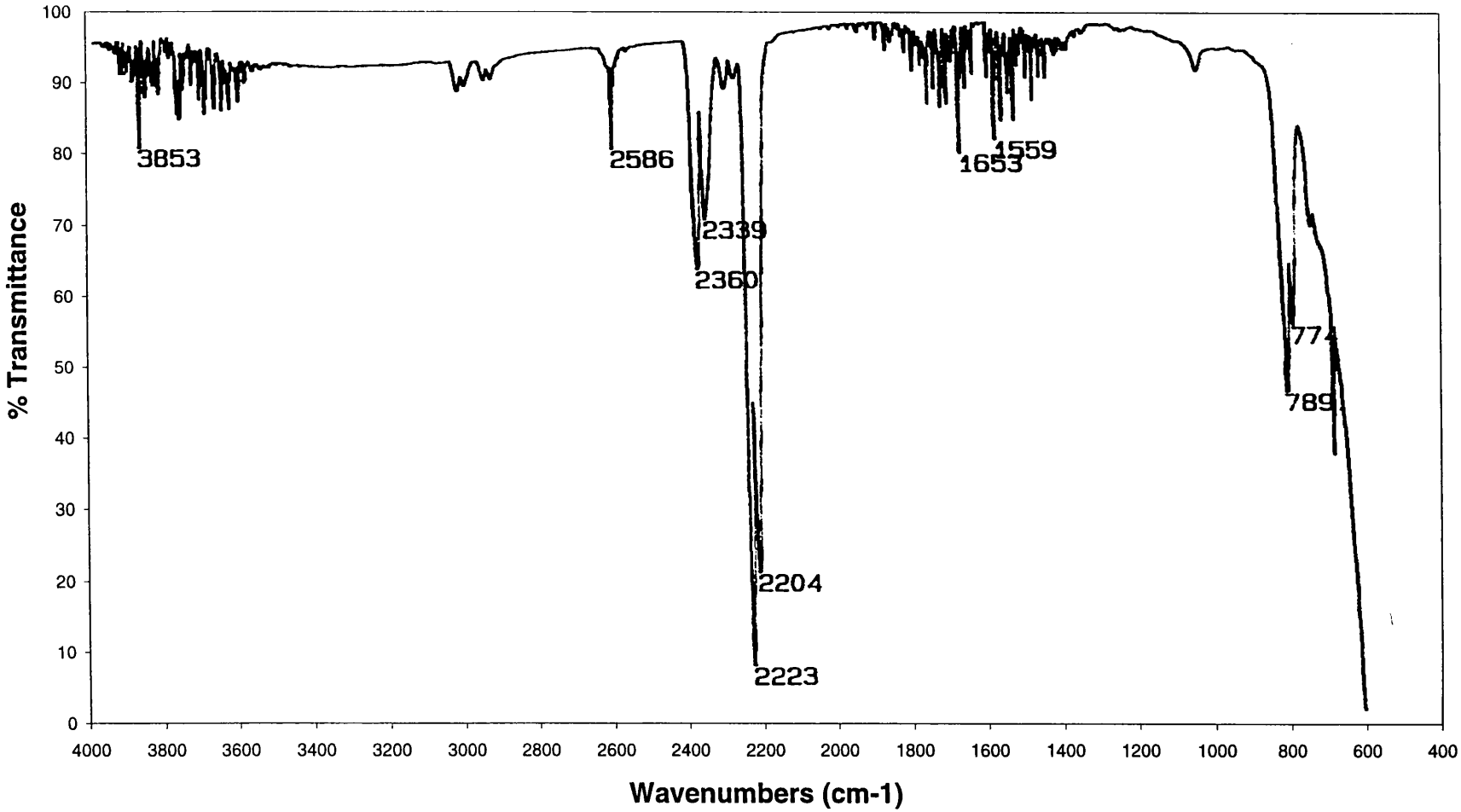

Figure 7.14: IR spectrum from gas peaks 1 and 2 from SATVA curve in Figure 7.13

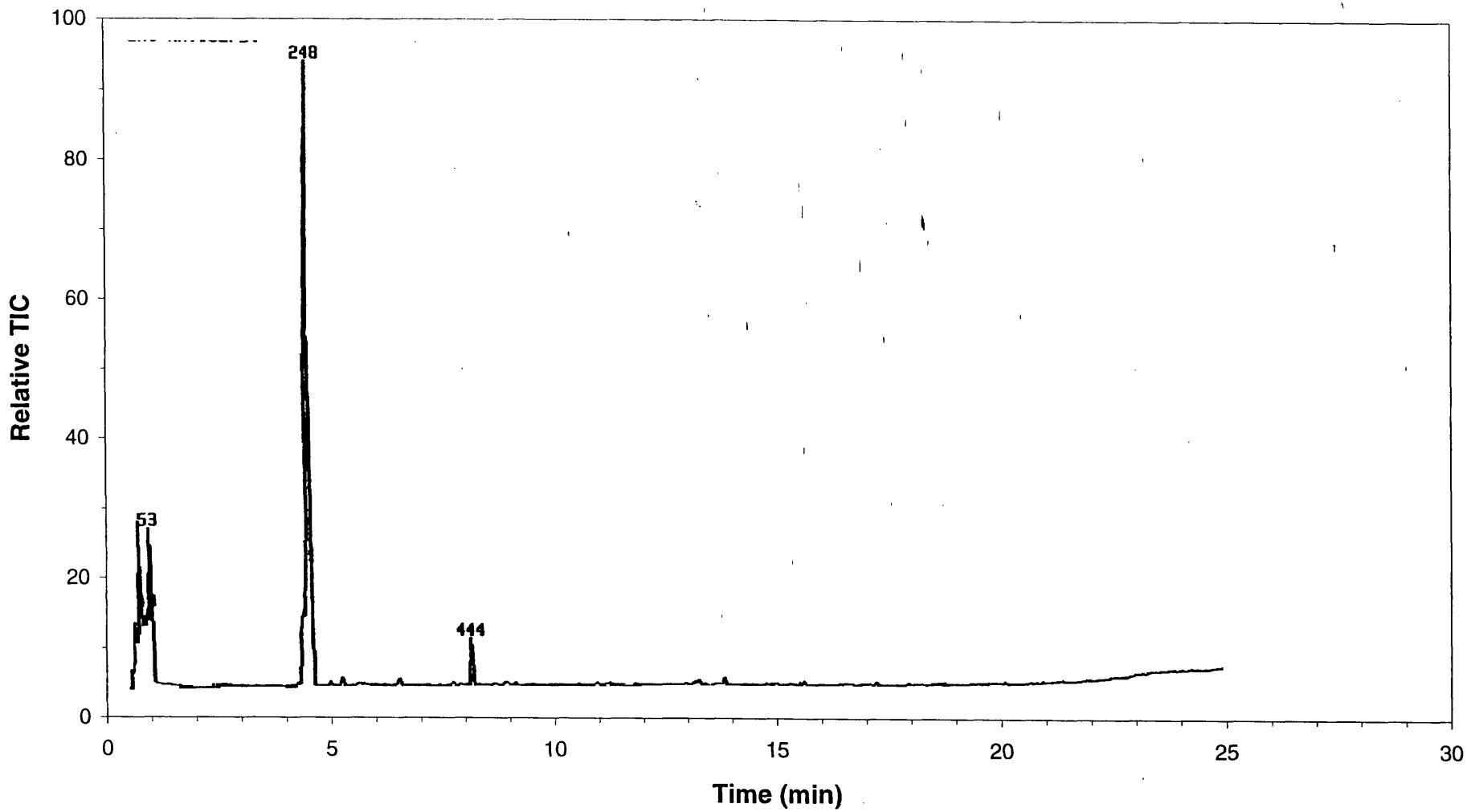

Figure 7.15: TIC trace for the liquid fraction from the SATVA curve in Figure 7.13

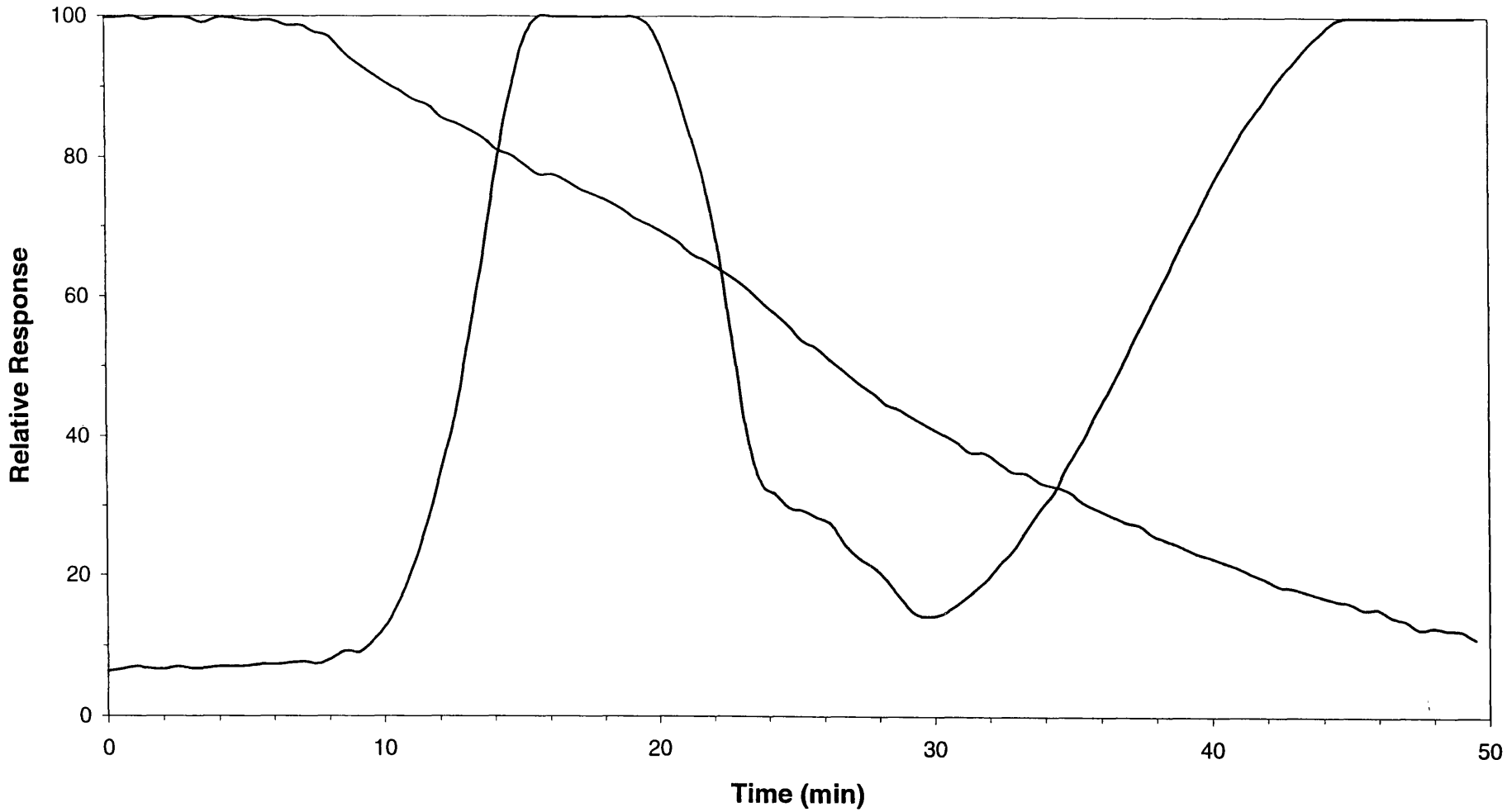

Figure 7.16: SATVA trace from the degradation of Sandorin Red Violet 3RL under flaming conditions

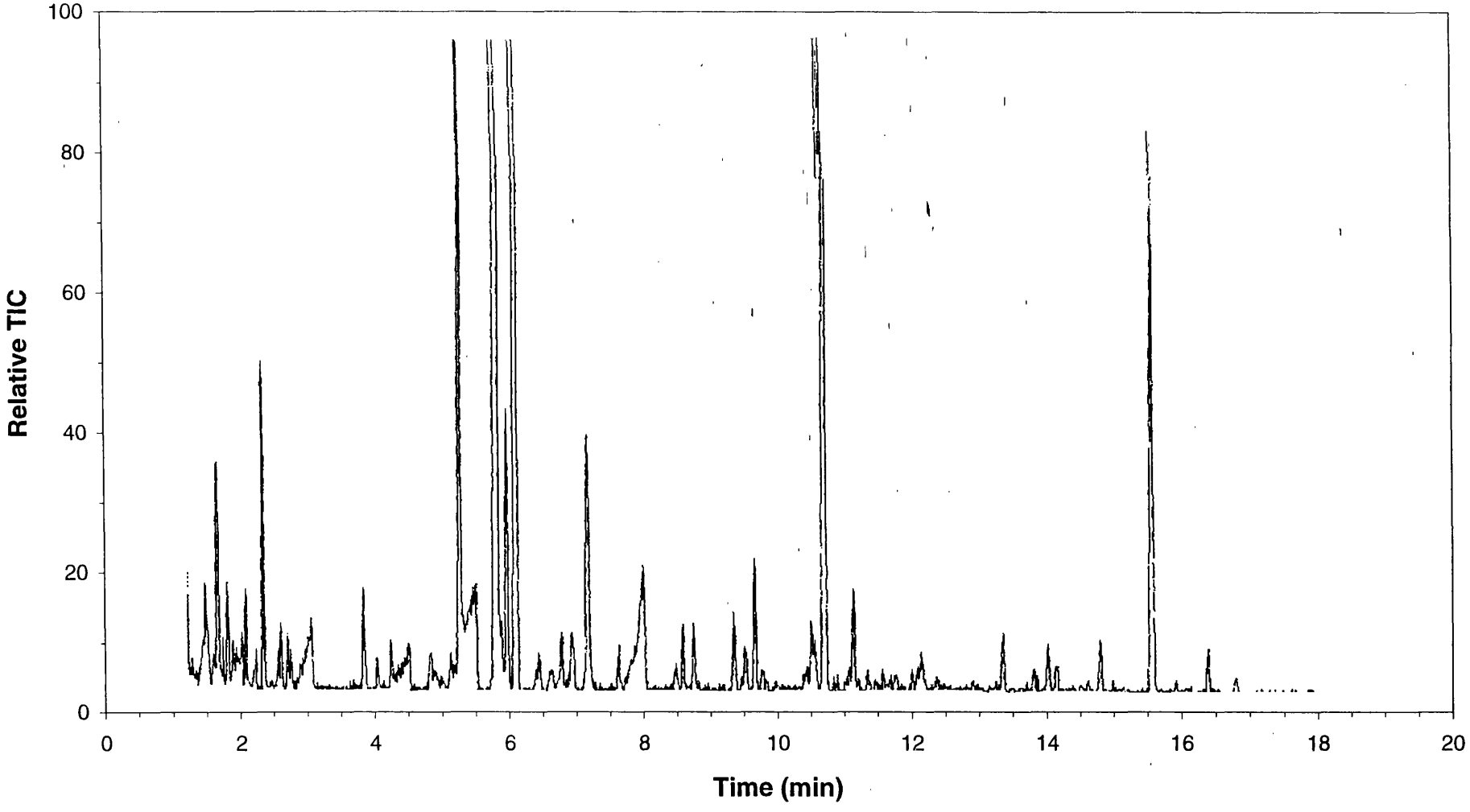

Figure 7.17: TIC trace for the liquid fraction from the SATVA curve in Figure 7.16

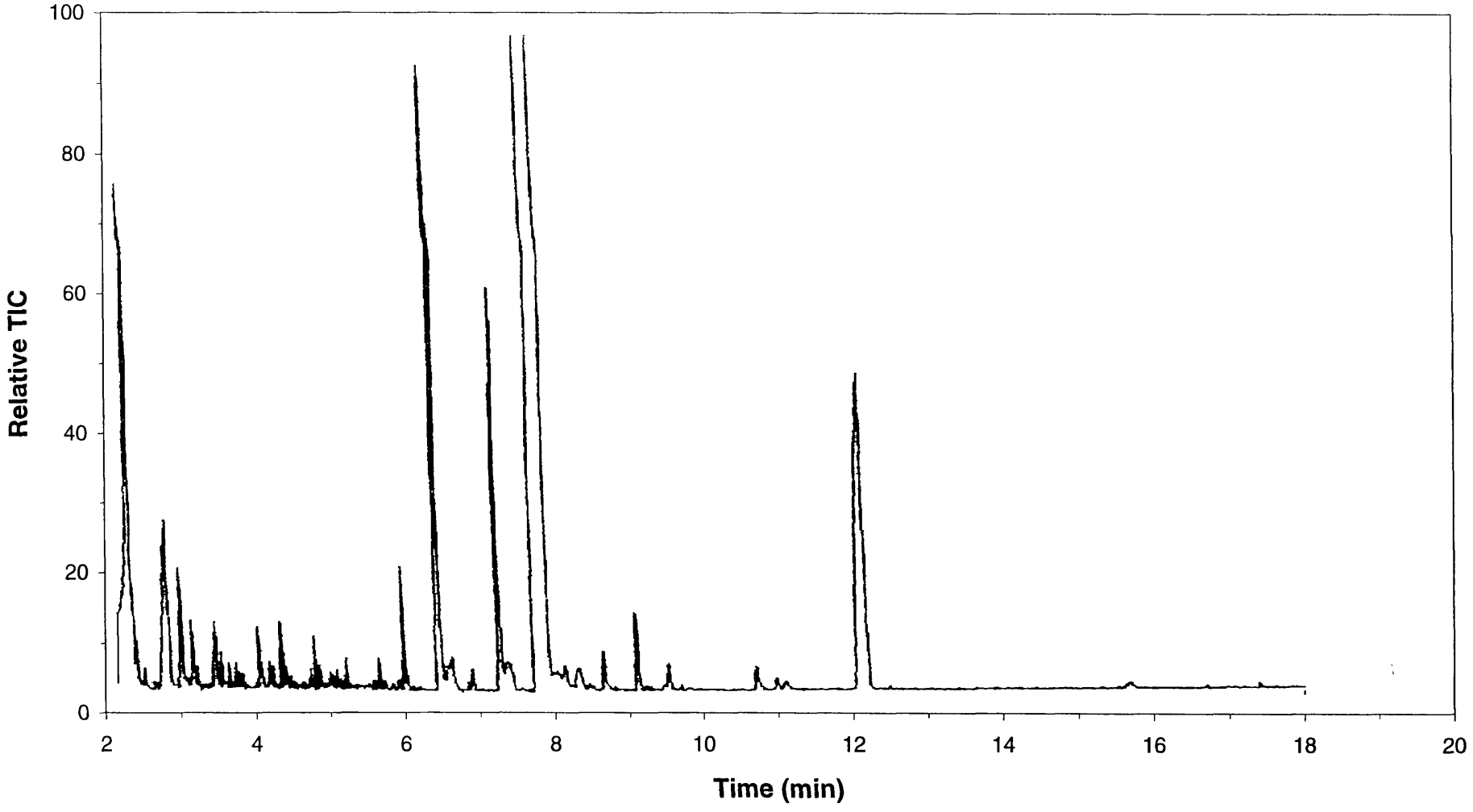

Figure 7.18: TIC trace for the cold ring fraction from the SATVA study in Figure 7.16

CHAPTER 8

PIGMENTED POLYMER SYSTEMS

8.1 INTRODUCTION

This chapter contains the results and interpretations from the degradation of the polymer systems studied. These blends were supplied ready mixed. The behaviour of the individual components when degraded alone has been discussed in previous chapters.

8.2 POLYPROPYLENE SYSTEM

The polypropylene sample was composed of the polypropylene FBF and polypropylene wax discussed in chapter 3. This system also contained the colourant Sandorin Red BN studied in chapter 4. This combination in known as Sanylene Red BN PP. The precise loading of the colourant was not given, although it is believed to be around 25% by weight.

8.3 POLY(BUTYLENETEREPHTHALATE)/ POLY(ETHYLENETEREPHTHALATE) SYSTEM

Here the polymer carrier was the polyester DNOP43 described in chapter 3. This was also provided pre-mixed with the colourant Estofil Blue S-RLS. The degradation of this colourant has been described in chapter 5. The combined system has the designation Estofil Blue MP8.

8.4 THERMAL DEGRADATION OF SANYLENE RED BN

Initial studies were carried out in a breakseal tube. The results from this study have not been presented here as the method was considered inferior to those developed during the course of the project. Some vacuum TVA studies were also performed, but sublimation of the colourant out of the hot zone rendered this method inappropriate. The results given are for the degradation under static nitrogen, dynamic nitrogen, dynamic air and flaming conditions. Thermogravimetric analysis was performed under dynamic nitrogen and dynamic air.

8.4.1 Thermogravimetric Analysis

Figures 8.1 shows the thermogravimetric analysis traces obtained, from which the key temperatures are outlined in the following table:

Table 8.1: Key temperatures from thermogravimetry of Sanylene Red BN

Conditions	$T_{thresh1}$(°C)	$T_{thresh2}$(°C)	T_{end}(°C)	%Residue
Dynamic Nitrogen	245	385	900	2
Dynamic Air	230	410	550	0

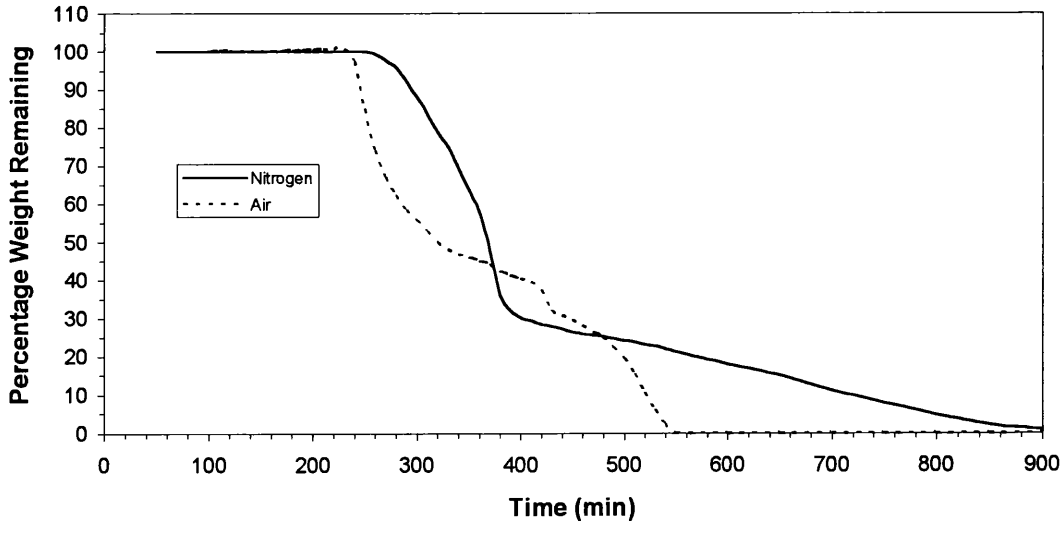

Figure 8.1: Thermogravimetric Analysis traces from Sanylene Red BN

The temperature of onset of weight loss under dynamic nitrogen is lower than that for the Polypropylene FBF or the Sandorin Red BN (Chapters 3 and 4 respectively). It is, however, a little higher than that for the Polypropylene Wax. The shape of the trace from 380°C onwards corresponds with that for the Sandorin Red BN at the higher temperatures. This may indicate that the major component, the Polypropylene FBF, had become completely degraded at a lower temperature than it was when studied alone. The trace under air can be related to the individual components present. The change in rate at just over 400°C roughly corresponds to that observed for the Sandorin Red BN alone. There was also a slight weight gain before the main weight loss commenced, as observed and predicted for the Polypropylene FBF. In this case the onset of the weight loss roughly coincides with that for the Polypropylene FBF. This was to be expected if there was minimal interaction between the components, as the pure colourant had not started to lose weight by this temperature.

8.4.2 Product Analysis — Static Nitrogen

The heating conditions were a programme of 10°C/min up to a maximum of 480°C. This choice of temperature meant that the first stage of degradation from the TG trace was complete, and that the polypropylene would be fully degraded if unaffected by the colourant.

An example of the SATVA trace for the volatilisation of the condensable degradation products is shown in Figure 8.2. The products volatilised to form peak 1 were studied by IR spectroscopy. There were weak absorptions for CO_2. There were also absorptions at 910, 990 cm^{-1} and around 2940, 3080, 1435 and 1655 cm^{-1}. These indicate the presence of propene. The small rise at 15 minutes (peak 2) was too weak

to provide a good spectrum. The product forming peak 3 at 20 minutes was found to be 2-methylpent-1-ene. This was determined through IR absorptions at around 890, 1375, 1460, 2960 (strong) and 3080 cm^{-1}. These findings are summarised in the ensuing table:

Table 8.2: SATVA peak assignments from Figure 8.2

Peak	Assignment
1	Propene with trace CO_2
2	Unidentified trace product.
3	2-methylpent-1-ene.
4	See below for GC-MS investigation of ether extract.

All the products from 25 minutes onwards were collected together and diethylether was added. The TIC trace from the GC-MS investigation of this sample is shown in Figure 8.3. The peak assignments for this trace are presented in the following table:

Table 8.3: GC-MS peak assignments from Figure 8.3

Retention Time	Product	Retention Time	Product
0:46	Solvent (ether)	9:54	Many possibilities, Spectrum mostly similar to that of 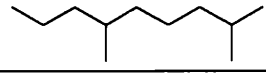
2:04	No perfect match found. The closest spectra were predominated by methyl alkenes such as 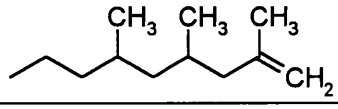	10:05	Isomer of 9:45
3:37	Very good match with 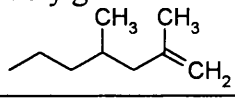	13:11	Many possibilities such as 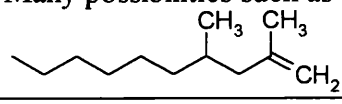
5:05	Probably 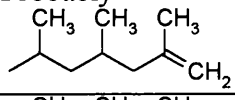	13:21	Isomer of 13:11
8:47	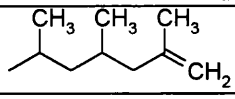	15:31	Spectrum too weak

Table 8.3 (continued)

Retention Time	Product	Retention Time	Product
15:46	Definitely an isomer of $C_7H_5ClF_3N$. References for three were available. Good match with 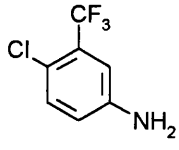 and 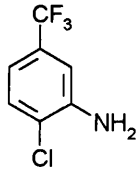 but not 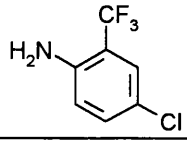	24:08	NIST database gave good matches for mono-unsaturated n-alkenes.
16:33	Weak aliphatic spectrum	24:28	As for 24:08
23:06	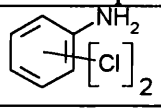	24:49	As for 24:08

There were two isomers of dichlorobenzene detected on a subsequent run. Notice that the order of the evolution of the suggested products does not always correspond to the volatility. Structurally similar materials give near identical mass spectra. What is clear is the general form of the materials, such as the alternating methylation on the chains or the possibility of unsaturation at the chain ends. The length of the chains is less clear.

8.4.3 Product Analysis — Dynamic Nitrogen

These studies were carried out with a heating rate of 10°C/min up to 900°C. This was chosen as TG information was not available at the time the degradations were carried out. The comparison between the percentage residue by TG and from flow-tube studies is tabulated overleaf:

Table 8.4: Residue percentages from nitrogen degradation of Sanylene Red BN

	Weight Remaining	
Maximum Temperature	**Thermogravimetry**	**Flow tube**
900°C	2%	0%

A typical SATVA trace for the volatilisation of the condensable degradation products is shown in Figure 8.4. Some differences can be seen between this trace and that for static nitrogen degradation in Figure 8.2. MS and IR analysis was used to study the gaseous products. Peak 1 at 11 minutes was due to CO_2. Propene was not detected in this case. The lack of propene would explain why this first peak was significantly smaller than that in Figure 8.2. The second peak was very weak. The gases were sampled up to 20 minutes. The evidence was weak and ambiguous, but appeared to indicate 2-methylpropene or 2-methylpentene was present. The remainder of the volatilised materials, collected as a liquid fraction, showed only water on the on line mass spectrometer. These findings are summarised in the following table:

Table 8.5: SATVA peak assignments from Figure 8.4

Peak	Assignment
1	CO_2
2	Includes 2-methyl propene or 2-methylpentene (see text)
3	Due mainly to water. See below for GC-MS investigation of ether extract

The TIC trace from the GC-MS analysis of the extract from the liquid fraction is presented in Figure 8.5. The peak assignments derived from the mass spectra are displayed in the following table:

Table 8.6: GC-MS peak assignments from Figure 8.5

Retention Time	Product	Retention Time	Product
0.40	Silicone contaminant	1.77	Could be better 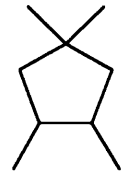 matched. *cis* preferable to *trans*
0.90	Although not quite 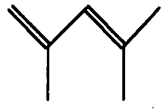 certain, fits best, with 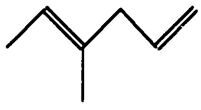 possible	1.98	41 too strong for 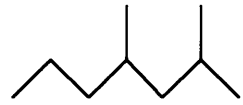 Otherwise a good match
1.24	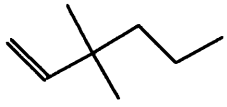 although the m/e = 43 peak was a little strong. Spectrum was also similar to that for (E)-3-undecene	2.05	Probably 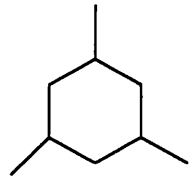 1.alpha,3.alpha,5.beta. Also possibly all alpha, or perhaps 1.alpha,2.beta,4.beta
1.34	No good match.	2.14	Perhaps propyl-cyclohexane, although the sample gives too strong a 69 peak
1.61	GC peak looked like it may have been due to two components. 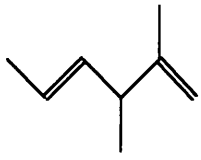 fits the spectra best, although a parent ion of 110 had an accompanying 109	2.25	Major product. 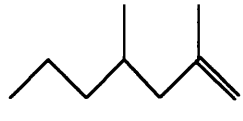 fits best

Table 8.6 (continued)

Retention Time	Product	Retention Time	Product
2.34	No good matches	7.16	3,3-dimethyloctane. Also possibly
2.44	Looks like another trimethylcyclohexane. It is unclear which isomer	7.37	No good matches
2.67	Probably	10.16	Not unlike 1-dodecene, 1-undecene, or less likely 2,4,6-trimethyl-1-nonene
2.84	Spectrum similar to above. Possibly 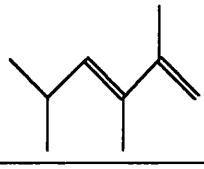	10.38	Nearly identical spectrum to the above
3.23	No Match	12.47	No matches
3.66	No matches. There be two products in this spectrum	12.78	No good matches
5.87	Dichlorobenzene. *Para*- from GC evidence	13.10	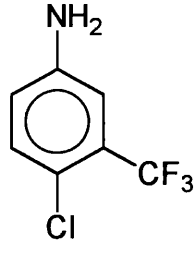 or, perhaps 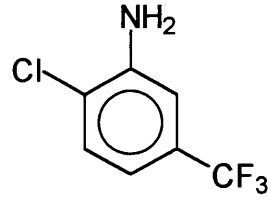
6.33	No good matches. Possibly some co-elution	13.90	Not identified
6.64	Dichlorobenzene. Ortho- from GC evidence	14.07	Not identified
6.97	No good matches		

8.4.4 Product Analysis — Dynamic Air

These studies were carried out with a heating rate of 10°C/min up to 560°C. The TG results implied that the degradation should have been complete by this temperature. The comparison between the percentage residue by TG and from flow-tube studies is tabulated below:

Table 8.7: Residue percentages from air degradation of Sanylene Red BN

	Weight Remaining	
Maximum Temperature	**Thermogravimetry**	**Flow tube**
560°C	0%	~0%

A typical SATVA trace for the volatilisation of condensable degradation products is shown in Figure 8.6. IR evidence showed that peak 1 at 11 minutes was due to the volatilisation of CO_2. The cause of the small rise in the Pirani response at 17 minutes (peak 2) is not clear. There was a peak at 714 cm^{-1} which would denote HCN. One run also provided the IR absorptions associated with propanone. Responses were very weak, so caution must be applied when drawing conclusions from these IR spectra. All the products from 16 minutes onwards were studied with a gas call on one of the repeats of this analysis. The cell was warmed to encourage any liquids to condense on the NaCl plates of the gas cell. This provided the IR spectrum for condensed phase water only. These findings are summarised in the following table:

Table 8.8: SATVA peak assignments from Figure 8.6

Peak	Assignment
1	CO_2
2	Unclear. Possibly propanone with a small amount of HCN
3	Mainly water. See below for GC-MS of ether extract.

The TIC trace from the GC-MS analysis of the liquid fraction is presented in Figure 8.7. The peak assignments are presented in the following table:

Table 8.9: GC-MS peak assignments from Figure 8.7

Retention Time	Product	Retention Time	Product
0.64	Possibly 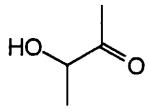	1.33	Various imperfect matches. The following were best: 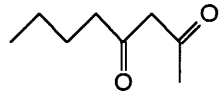 →Needs higher masses 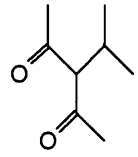 →Needs 101 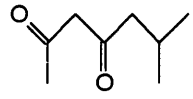 →Needs stronger 57, 58 + higher masses 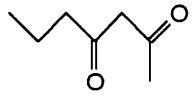 → Needs 113,128 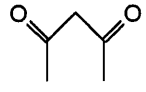 → Very convincing if 85 were stronger
0.73	Unidentified	1.50	Several possibilities. 3-hexen-2-one fits best
0.79	Probably 2-pentanone	1.75	No good matches. 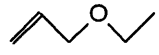 was best, yet quite a poor match
1.06	No match. Heptane was the best, but with significant inconsistencies	1.90	No good matches. 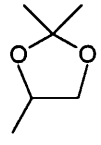 and were best
1.24	Reasonable with 2-heptanol	2.22	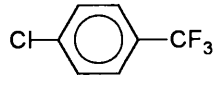 matches well although there were also some alkene peaks present

Table 8.9 (continued)

Retention Time	Product	Retention Time	Product
3.21	Not unlike 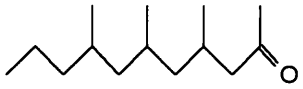 or an analogous compound of different length	5.70	No matches
3.92	Good match with 4-methyl-2-heptanone 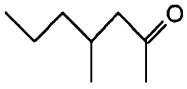 . This was the major peak	5.91	Dichlorobenzene. Para deduced through GC retention, in comparison with references
5.50	No matches	6.66	Dichlorobenzene. Ortho deduced through GC retention time, in comparison with references

8.4.5 Product Analysis — Flaming Conditions

The apparatus was constructed as described in chapter 2. The following observations were made during the degradation:

Table 8.10: Observations from Sanylene Red under flaming conditions

First Run	
Sample Size:	234.8 mg
Residue:	135.4 mg (57.7%)
Time (min)	**Observations:**
1:40	Ignition. Burned smoothly but sootily.
Comments:	Residue was black with a thin red ring around the edge.

Second Run	
Sample Size:	232.2 mg
Residue:	65.9 mg (24.8%)
Time (min)	**Observations:**
1:25	Sample started to smoke.
1:35	Ignition.
2:06	Extinguished.
up to 4:00	The sample continued to smoke but would not re-ignite.
5:00	Heater switched off.
Comments:	Residue all black this time.

A typical SATVA trace for the volatilisation of the condensable degradation products is displayed in Figure 8.8. The non-condensable trap described in chapter 2 was used. This showed a small amount of CO and some untrapped CO_2 by FT-IR analysis. The first major peak on the SATVA trace at around 12 minutes was mainly due to the volatilisation of CO_2. The IR spectrum also provided evidence for N_2O through the absorptions described previously. Ethylene manifested its presence by absorptions at around 2850, 1299 and 1000 cm^{-1}. Small amounts of formaldehyde were indicated by the IR absorptions at around 2850 and 1745 cm^{-1}. The on line mass spectrometer showed only water after 25 minutes of the SATVA separation had elapsed. These findings are summarised in the following table:

Table 8.11: SATVA peak assignments from Figure 8.8

Peak	Assignment
Non-condensables	CO
1	Mainly CO_2.Some N_2O, ethylene and formaldehyde present. Also a small amount of unidentified material.
2	Mostly water. See below for GC-MS analysis of ether extract.

The liquid fraction was analysed by forming a diethylether extract for GC-MS study. The resulting TIC trace is presented in Figure 8.9, and the peak assignments tabulated overleaf:

Table 8.12: GC-MS peak assignments from Figure 8.9

Retention Time	Product	Retention Time	Product
0.72	Not identified. May contain benzene	2.22	Chlorotrifluoromethyl-benzene (any of the three isomers) co-eluting with an alkene such as 2,4-dimethyl-1-heptene or similar of MW 126
0.78	3-methyl-2-butanone	2.47	Xylene (*m*- fits best)
0.99	(E)-3-penten-2-one (not (Z)-)	2.65	Spectrum weak, but similar to 3,3,5,5-tetramethylcyclopentene, or perhaps a alkdiene
1.03	Methylisobutylketone 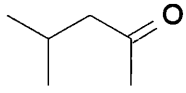	3.16	Unidentified alkene. Spectrum similar in style to (Z)-3-methyl-2-pentene
1.08	4-methyl-4-penten-2-one, 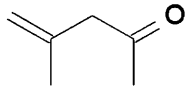	3.26	Probably 2,3,4,5-tetramethyl-1,4-hexadiene, 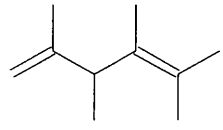
1.26	Probably toluene	3.52	Not identified. Probably an alkdiene
1.45	Not identified	3.70	4-methyl-2-heptanone fits well, 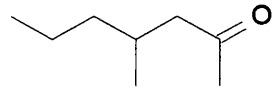
1.82	Probably 2-methyl-3-penten-1-ol co-eluting with a silicone	3.83	Benzaldehyde
2.04	Chlorobenzene	4.23	Benzonitrile. (Spectrum would also fit isocyanobenzene.)
2.14	Probably propylcyclohexane	4.47	1,2,4- or 1,2,3-trimethylbenzene fit best. Methyl-ethyl- or alternative trimethylbenzenes still possible

Table 8.12 (continued)

Retention Time	Product	Retention Time	Product
4.80	Probably phenyl ester of carbamic acid, 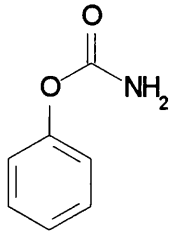 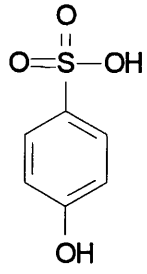 with also possible	9.79	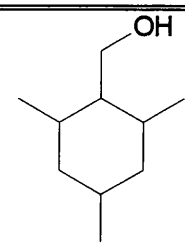 or 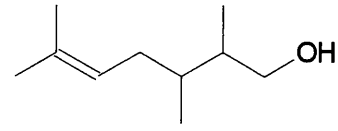
4.94	4,6-dimethyl-2-heptanone fits well	10.63	Silicone contaminant
5.24	Dichlorobenzene	12.00	No matches. Probably an alkene
5.76	Dichlorobenzene	12.15	An isomer of the above
6.06	Contaminant. Probably octamethyl-cyclotetrasiloxane	14.22	Uncertain. Probably a methylated alkane/ene
7.84	Not identified	14.47	Unidentified alkane/ene
7.95	Spectrum similar to 2,4,6-trimethyl-1-nonene	14.67	Unidentified alkane/ene
9.13	Unidentified. Probably another methylated alkene	15.47	Contaminant (dodecamethyl-cyclohexasiloxane)
9.55	Dichlorophenol (probably 2,6-)	16.04	Although unsure, the spectrum is reasonably matched to 2,4,6-trimethyl-, (R,R,R)-11-dodecen-1-ol, 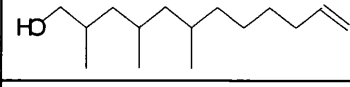
9.63	Trichlorobenzene. Unclear as to which isomer. Small amount of another material co-eluting	16.70	Unidentified alkane/ene
9.72	Naphthalene		

8.5 THERMAL DEGRADATION OF ESTOFIL BLUE MP8

This sample was studied for thermal stability through thermogravimetric analysis. Degradation for product analysis was performed under dynamic nitrogen, dynamic air and flaming conditions.

8.5.1 Thermogravimetric Analysis

Figure 8.10 shows the thermogravimetric analysis traces obtained under dynamic nitrogen and dynamic air. The key temperatures of interest are tabulated below:

Table 8.13: Key temperatures from thermogravimetry of Estofil Blue MP8

Conditions	$T_{thresh1}$(°C)	$T_{thresh2}$(°C)	T_{end}(°C)	%Residue
Dynamic Nitrogen	270	450	>900	<25
Dynamic Air	270	420	560	2

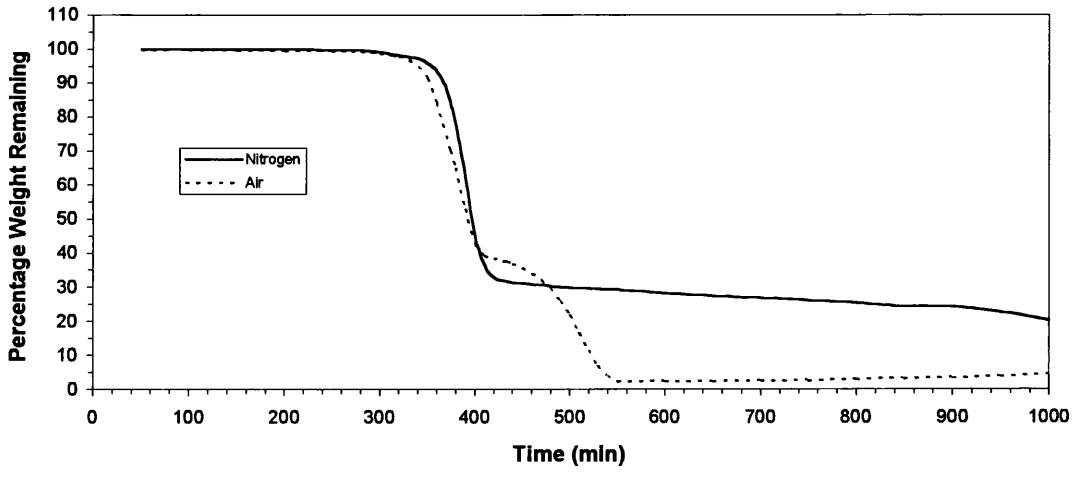

Figure 8.10: Thermogravimetric Analysis traces from Estofil Blue MP8

It can be seen that the onset of weight loss was the same under each condition. The initial weight loss follows a similar profile under both nitrogen and air. There is an unusual difference arising at 420°C on the air trace. It now appears that there is less weight loss from this temperature up to around 480°C. This second stage in the degradation concludes with only a small residue. It may be supposed that there is an

oxidation event, resulting in a heavier residue at 420°C under air than under anaerobic conditions. The residue formed under dynamic nitrogen by 450°C (at 30% of the initial weight) appears to be thermally stable. There was only a slow but constant weight loss from this point to the end of the run, implying that this decomposition of the residue had a rate independent of temperature. Similar profiles have been observed during the previous chapters.

8.5.2 Product Analysis — Dynamic Nitrogen

This degradation was carried out at a heating rate of 10°C/min to a maximum of 450°C. It can be seen from section 8.5.1 that the first and major stage of the degradation was completed by this temperature. The percentage residue under TG and flow tube conditions are compared below. Clearly, these results compare very favourably.

Table 8.14: Residue percentages from nitrogen degradation of Estofil Blue MP8

	Weight Remaining	
Maximum Temperature	**Thermogravimetry**	**Flow tube**
450°C	30%	30%

A sample of the SATVA trace obtained for the volatilisation of the condensable degradation products is shown in Figure 8.11. IR spectroscopy was the only analysis method available at the time for studying the gaseous products. The material(s) forming peak 1 at 9 minutes were not identified. This peak was even weaker in a repeat experiment, although the sample size was doubled from 50 mg to 100 mg. Peak 2 at 13 minutes was due to the evolution of SO_2 and a small amount of an unidentified hydrocarbon. This was deduced from IR absorptions at around 1360 and 1170 cm^{-1} for the SO_2, and at 2920 and 2850 cm^{-1} for the hydrocarbon. The

remaining materials from 18 minutes onwards were collected together for GC-MS analysis. These findings are summarised in the following table:

Table 8.15: SATVA peak assignments from Figure 8.11

Peak	Assignment
1	Unidentified
2	SO_2 and an unidentified hydrocarbon
3 and 4	See below for GC-MS analysis

Diethyl ether was added to the products forming peaks 3 and 4 on the SATVA trace, and it was analysed by GC-MS. The TIC trace for the separation is shown in Figure 8.12. The peak assignments are listed in the following table:

Table 8.16: GC-MS peak assignments from Figure 8.12

Retention Time	Product	Retention Time	Product
1:20 and 1:29	Solvent	5:42	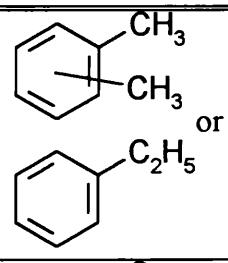
2:12	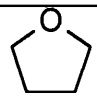	5:47	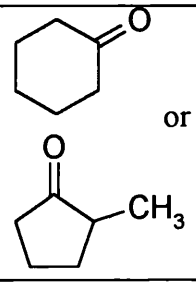
2:40	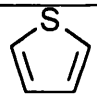	7:20	Probably 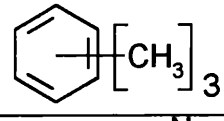
4:02	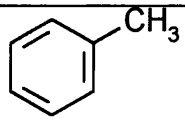	9:15	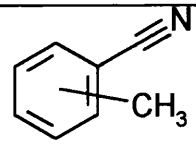 or isomers
4:32		9:45	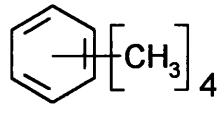 or isomers

8.5.3 Product Analysis — Dynamic Air

This degradation was carried out at a heating rate of 10°C/min to a maximum of 600°C. The thermogravimetric study shows that the both stages of the degradation were completed by this temperature, leaving only a small residue. The percentage residue by TG and from flow tube conditions are compared below. There was slightly more residue found in the flow-tube study.

Table 8.17: Residue percentages from air degradation of Estofil Blue MP8

	Weight Remaining	
Maximum Temperature	**Thermogravimetry**	**Flow tube**
600°C	2%	4.8%

A sample SATVA trace obtained for the volatilisation of the condensable degradation products is shown in Figure 8.13. Both infrared and mass spectroscopy were used to analyse the evolved gases. The best information was provided by the on line mass spectrometer, as this gave information on the order of evolution. The design of the SATVA line only allows separation into four distinct fractions, which is clearly insufficient for this number of products. The first peak at 13 minutes was due to the evolution of CO_2, as was seen through the mass spectrometer peaks at m/e = 44, 28 and 16. The spectrum obtained for the second peak was still dominated by CO_2, but also showed peaks at m/e = 39, 54, 53, 28,27 and 26 indicating 1,3-butadiene. By 18 minutes when peak 3 was produced the mass spectrometer peaks m/e = 64 and 58 signalled the evolution of SO_2. Peak 4 at 20 minutes into the SATVA separation was formed by HCN, as was seen by the mass spectrometer peaks at m/e = 27, 28 and 26. The products evolved to produce peak 4 were harder to identify. The many liquids forming the liquid fraction (the final peak) were now also being evolved, creating a complicated mass spectrum. There were common aliphatic hydrocarbon peaks at

m/e = 41 and 43. There was also some suggestion of benzene and toluene through peaks at m/e = 71 and 72, and m/e = 91 and 92 respectively.

The GC peaks in the GC-MS analysis of the liquid fraction were very weak. Little quantitative information was obtained. The only components identified were THF, tetrahydrothiophene, cyclohexane and styrene.

The above findings are summarised in the following table:

Table 8.18: SATVA peak assignments from Figure 8.13

Peak	Assignment
1	CO_2
2	1,3-Butadiene
3	SO_2
4	HCN
5	Includes benzene and toluene
6	THF, tetrahydrothiophene, cyclohexane and styrene

8.5.4 Product Analysis — Flaming Conditions

The apparatus was arranged in the usual manner. The following observations were made during the degradation.

Table 8.19: Observations from Estofil Blue under flaming conditions

Sample Size:	108.3 mg
Time (min)	**Observations:**
1:45	Sample melted and started to release puffs of gas
4:50	Ignition. Burned for 25 seconds
6:00	No more activity. Heater switched off.

The SATVA trace for the volatilisation of the condensable degradation products was a simple two peak trace. This was a typical CO_2 and water dominated trace for samples degraded under these conditions, so has not been reproduced.

Non-condensable trapping showed that some CO was produced. The gas peak evolved during the SATVA separation was mainly due to CO_2. Some N_2O and SO_2 was also detected. These were identified by FT-IR spectroscopy by the absorptions previously listed for these gases. There was also probably a small amount of methanol present. The mass spectrometer produced a weak response at m/e = 29, 31 and 32. The FT-IR also showed some absorptions in the —CH_3 symmetric and asymmetric stretch region at around 2900 cm^{-1}. There was also the broad absorption at around 3500 cm^{-1} typical of —OH. The on-line MS showed the liquid SATVA peak to be mainly due to water. These findings are summarised in the following table:

Table 8.20: SATVA results from Estofil Blue under flaming conditions

Peak	Assignment
Non-Condensables	CO
1	Mainly CO_2 with some N_2O, SO_2 and methanol.
2	Mainly water. See below for GC-MS analysis of ether extract.

Diethylether was added to the liquid fraction to form an extract for GC-MS analysis. The TIC trace for the separation is provided in Figure 8.14. The peak assignments for this trace are given in the following table:

Table 8.21: GC-MS peak assignments from Figure 8.14

Retention Time	Product	Retention Time	Product
1.59	Probably isopropyl alcohol	2.78	Styrene (or the usual alternatives)
1.85	Silicone contaminant	3.87	Benzaldehyde
2.51	Phenylethyne 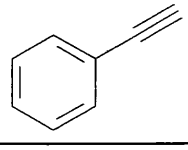	4.26	Benzonitrile (or isocyanobenzene)
2.57	Cyclohexanone	4.79	Phenol

Table 8.21 (continued)

Retention Time	Product	Retention Time	Product
5.22 5.97 6.09	Silicone contaminant	15.08	Probably biphenyl, although 2-ethenylnaphthalene also possible
9.75	Probably naphthalene	15:60	Silicone contaminant
10:50 11.11 13.60	Silicone contaminant	17.56	Silicone contaminant

8.6 MAJOR PRODUCT SUMMARIES AND MECHANISMS

The major products for the two materials studied in this chapter are summarised in this section. Comparisons with the products from the degradation of the individual components are made. Some suggestion of the decomposition mechanisms are also provided.

8.6.1 Sanylene Red BN

This sample was degraded under static nitrogen, dynamic nitrogen, dynamic air and under flaming conditions. Cold ring fraction product analysis was not performed for any of these studies.

8.6.1.1 Static and Dynamic Nitrogen

The static nitrogen degradation was under programmed heating to a maximum of 480°C, and the dynamic nitrogen study to a maximum of 900°C. This discrepancy should not have had too great an influence on the products detected, as the most of the weight loss had occurred by 480°C. Any additional products evolved at the higher temperatures would be due to the decomposition of a carbonaceous residue.

The major gaseous products detected under static nitrogen were propene, 2-methylpent-1-ene and a little CO_2. The CO_2 detected may have been due to leakage from the atmosphere into the vacuum system. 2,4-Dimethylhept-1-ene was by far the major component of the liquid fraction. There were also lesser amounts of other alternatively methylated alk-1-enes. 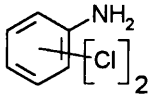 was also present.

Unexpectedly, 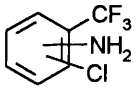 was detected. This product clearly has no relation to the structure of any of the components present. It will be seen in this and following sections that it appears in other studies from this sample, implying that it was present in the sample or was a degradation product of an unlisted component. It was thought that it may have been an additive in the polypropylene used. This theory was disproved, however, when no fluorinated products appeared in any of the polypropylene or polypropylene wax studies. No such products were detected in the Sandorin Red BN degradations. If it had not been otherwise stated, the conclusion that the colourant present was Sandorin Scarlet 4RF would have been made.

The products found under dynamic nitrogen conditions were quite similar. Propene was not present, although methylpropene was detected. 2-Methylpent-1-ene was present once more, and the liquid fraction still had 2,4-dimethylhept-1-ene as the major component. Under these conditions, however, this product was less important. Other alkenes similar to this but of varying lengths were also still present. Some substituted cyclohexanes were also detected. There was a significant quantity of 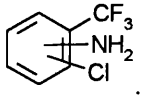 . Dichlorobenzene and dichloroaniline also were present.

The alkenes were all predictable from the degradation of polypropylene[40-43]. The dichlorobenzene and dichloroaniline were all predictable from the degradation of Sandorin Red BN as described in chapter 2. It is perhaps of some interest that the HCl observed under these conditions from the colourant (Sandorin Red BN) alone was not detected here. This is consistent with the presence of Sandorin Scarlet 4RF rather than Sandorin Red BN.

8.6.1.2 Dynamic Air

This degradation was performed to a maximum temperature of 560°C. The major gas produced was CO_2. Evidence for other gases was weak, but propanone and hydrogen cyanide were suspected. Water dominated the liquid fraction. Dichlorobenzene was detected, in a higher ratio to the amount of aliphatic hydrocarbons detected in the dynamic nitrogen study. 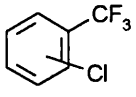

was detected, but 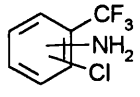

was not. The major aliphatic detected was 4-methyl-2-heptanone. There were also other similar ketones detected. These materials appeared as an alternative to the alk-1-enes found in the nitrogen atmosphere degradations.

The presence of the ketones was predictable due to the degradation mechanism of polypropylene. The oxidation pathway is described in chapter 3. The increase in the amount of aromatic material from the colourant relative to the quantity of aliphatic from the polymer may be due to the ease of oxidation of the polymer. The TG evidence suggested that the colourant was not oxidised until a temperature of 435°C was obtained. The degradation of the polymer was completely different, where the onset of degradation under air was much earlier than that under inert atmosphere. The

polypropylene FBF was fully degraded by 360°C under air, whereas under 10% of the weight was lost by this temperature under dynamic nitrogen. The polymer may have produced more of the CO_2 and water, leaving less aliphatic material in the liquid fraction.

8.6.1.3 Flaming Conditions

This sample ignited very rapidly, within one minute of the blocker being turned to expose the sample to the radiant heat. This time is shorter than that for any of the other materials included in this study. Water and CO_2 dominated the condensable volatile products from this sample. Unusually for degradation under flaming conditions a number of other gases were also detected. These included N_2O, ethylene, acetaldehyde and formaldehyde. The non-aqueous extract of the liquid had dichlorobenzene as the major component, from which one isomer dominated. There was also appreciable amounts of benzonitrile present. The remaining products were various alkenes and ketones.

A trend may be seen in the liquid fractions from this degradation and those under nitrogen and air. There has been a decrease in the relative amount of unsaturated hydrocarbons, while the comparative level of aromatic materials has increased. This is perhaps predictable due to the relative stability of the aromatic ring structure.

The reappearance of the alkenes as seen in inert studies may also have been predicted. It was observed in the dynamic air degradation that the alkenes were not present in the liquid fraction. It may be supposed that the heating caused breaking of the polymer chains in the bulk before the oxidation could occur. These materials will have departed from the bulk of the sample to provide the fuel, as described for the candle model for

the combustion of polymers in chapter 2. The fragments detected were probably evolved before the critical mass flux for combustion was attained, or are a consequence of oxygen depletion.

The gases detected, other than the carbon dioxide, were probably also liberated before the sample was ignited. This may be deduced from the fact that such flammable species are unlikely to survive a flame. An alternative theory is that these products are the result of partial combustion. Some CO was produced, which is known as a product of incomplete combustion of hydrocarbons. If this was the case then larger polymer fragments should also have appeared in the liquid fraction in sufficient quantity to be detected.

8.6.2 Estofil Blue MP8

This sample was degraded under dynamic nitrogen, dynamic air and flaming conditions. The liquid fraction analyses from these degradations revealed fewer products than observed for the degradation of Sanylene Red BN. It would appear that this degradation followed a simpler pathway.

8.6.2.1 Dynamic Nitrogen

This study was performed to a maximum temperature of 450°C, which ensured that the first major stage of the degradation was complete. The thermogravimetric analysis traces from under nitrogen and air experienced the same profile up to around 420°C, with little weight loss from this temperature in the nitrogen case. This implies that oxygenation effects had little or no influence on this first stage. It follows that the products observed under dynamic nitrogen ought also to be present in the dynamic air

study, with the addition of the products evolved in the second stage from 420°C to 560°C. It may be seen in this and the following section that this prediction held true.

Sulphur dioxide was the major gas detected. There was also a peak on the SATVA trace in the position typical of CO_2, but a positive identification was not made. The liquid fraction contained mainly tetrahydrothiophene (THT) and cyclohexanone (or methylcyclopentanone) in roughly equal amounts. Appreciable amounts of tetrahydrofuran (THF) were also present, along with lesser amounts of benzenes with varying numbers of methylations and methylbenzonitrile. It should be noted that there were considerably smaller amounts of all but the first three listed products detected.

The high abundance of sulphur-containing products indicated that the colourant component was the major source of the products. Interestingly, these products did differ from those observed from the colourant alone. This was studied in chapter 5. It was found in that study that H_2S was produced rather than the predicted SO_2. The pathway suggested involved the formation of molecular sulphur. It is hard to see why such a pathway should be followed. A requirement would be that the oxygen go elsewhere, and the sulphur atoms be in sufficient proximity to form molecular sulphur. The sample studied here would have the sulphurs in less close proximity, but this is only of relevance if the SO_2 retains the oxygen. One other difference may be the amount of water, either residual or produced during the degradation. As water is not a predicted degradation product here, then water absorbed by the sample may be of interest. Sulphur dioxide is readily dissolved into water, so if this sample was drier than in the pure colourant then we may have an explanation for the difference. The major reservation for this theory is that the onset of degradation may have been at too high a

temperature for appreciable amounts of water to have remained in the sample. However, there was much water present in the products from the degradation of the pure colourant, yet there was no early weight loss suggesting drying in the thermogravimetric analysis.

The products in the liquid fraction do imply that the degradation mechanism for this sample is very different than that for the constituent components when degraded separately. The other products listed did not arise from the analysis of the pure polymer or colourant. This independence was not predicted from the thermogravimetric data. The coloured polymer system trace displays a profile not dissimilar from the addition of the traces for the polymer and colourant alone. It is apparent that product analysis alone will not yield clear and unambiguous mechanistic information about the degradation pathway.

8.6.2.2 Dynamic Air

This study produced similar products to those found in the preceding section, along with a few additions. This was predicted above, by considering the thermogravimetric analysis results. Carbon dioxide was the major gas, with reasonable quantities of SO_2, Hydrogen cyanide and 1,3-butadiene also detected. Benzene, toluene, THF, THT, cyclohexane and styrene were also present. The cyclohexanone observed in section 8.6.2.1 was not present. The products unique to the dynamic air study were CO_2, benzene, HCN, 1,3-butadiene, cyclohexane and styrene.

The HCN and cyclohexane probably came from the colourant, and the 1,3-butadiene from the polymer. The source of the substituted benzenes is less clear, as aromatics were produced in both the pure polymer and colourant studies. Once again, these

products present few similarities with the materials produced from the degradation of the individual components under dynamic air. Any offer of mechanistic information from these results would be conjecture.

8.6.2.3 Flaming Conditions

This sample ignited at almost 3 minutes after the blocker had been turned. The sample burned for 25 seconds. This was a relatively long burning time.

Water and CO_2 were very much the major condensable volatile degradation products. Some SO_2, N_2O and methanol were detected as gases. The main non-aqueous components of the liquid fraction were naphthalene and benzonitrile.

None of the aliphatic hydrocarbons observed in the previous two sections were detected here. It may be assumed that these products became fuel for the flame. It was expected that some of these materials should have been detected due to the long time to ignition, especially as puffs of gas were released form the sample at 45 seconds after the blocker had been turned.

The observations have been made that

a. Gases were released early into the degradation

b. Ignition was late implying stability

c. Despite b. the sample burned for 25 seconds

This evidence suggests that the gases produced early into the degradation left a more thermally stable yet flammable sample behind. Perhaps the gas was CO_2 from the polymer ester linkages or SO_2 from the colourant. In the case of the CO_2, the weakest point of the polymer was lost, yet the hydrocarbon section remained for fuel for the

later ignition. If this were the case, then perhaps this evolution of flame inhibiting material after a time of heat exposure may be of some relevance for flame retarding with certain colourant additives.

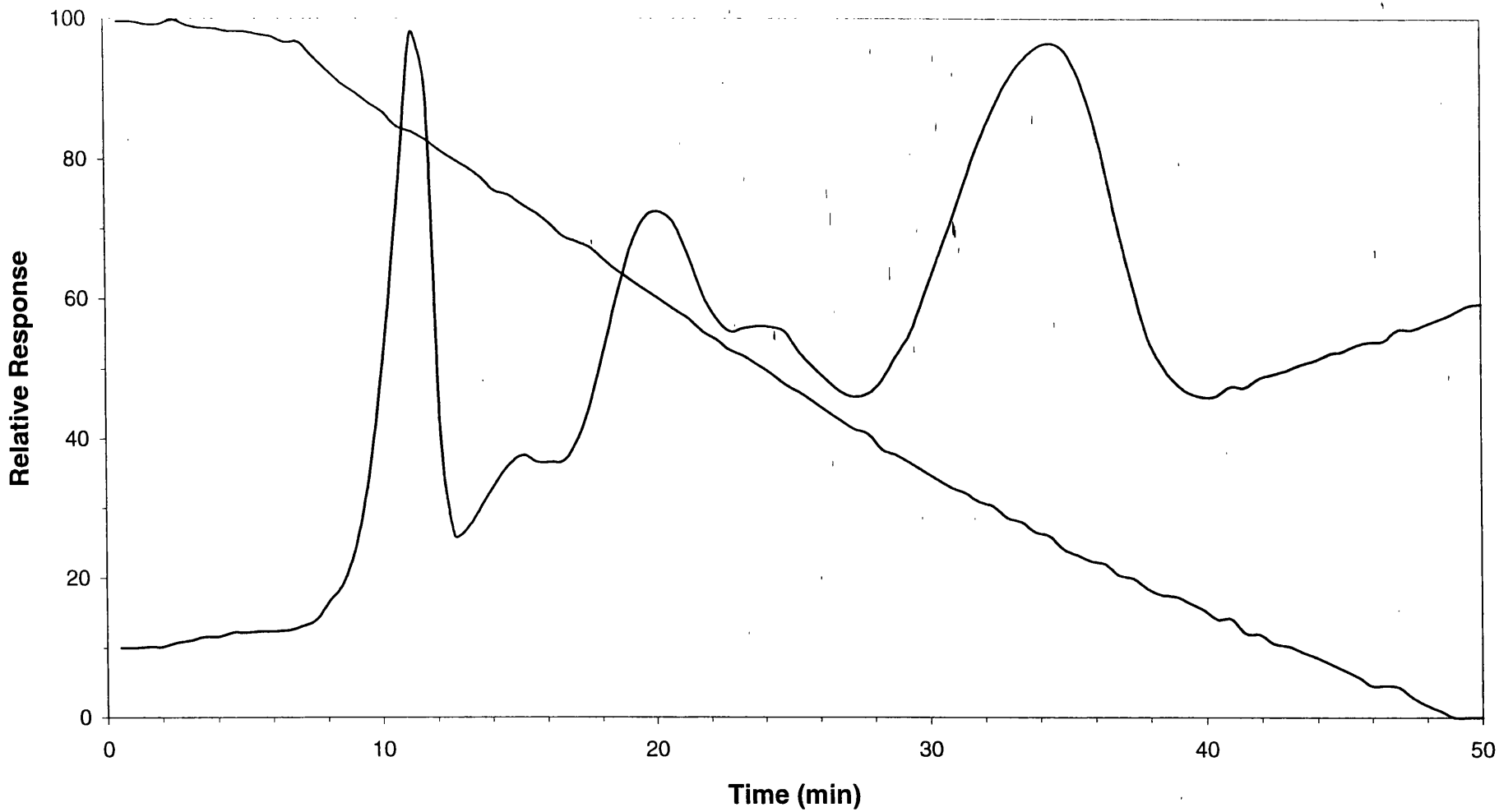

Figure 8.2: SATVA trace from the degradation Sanylene Red BN PP of under static nitrogen

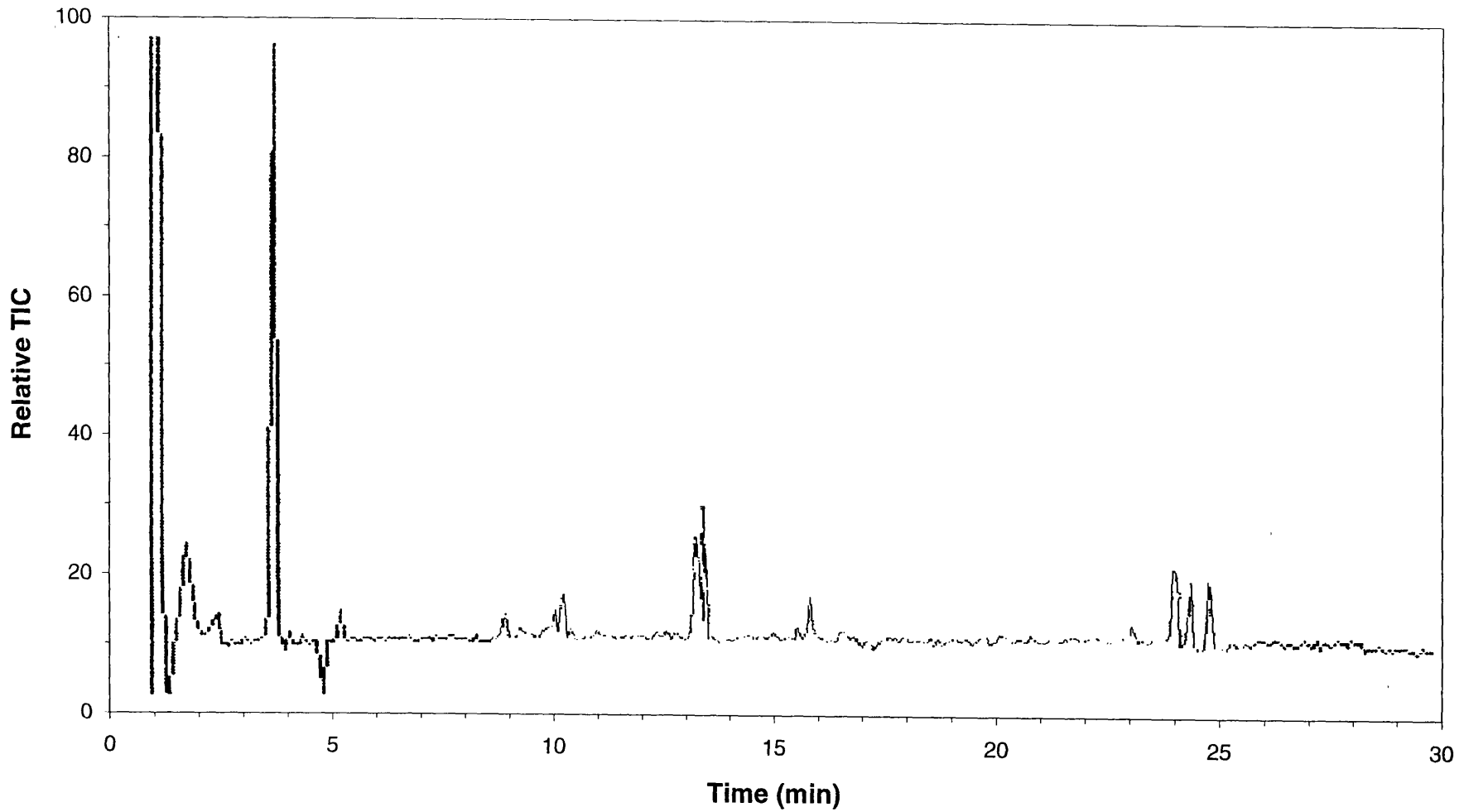

Figure 8.3: TIC trace for the liquid fraction from the SATVA Curve in Figure 8.2

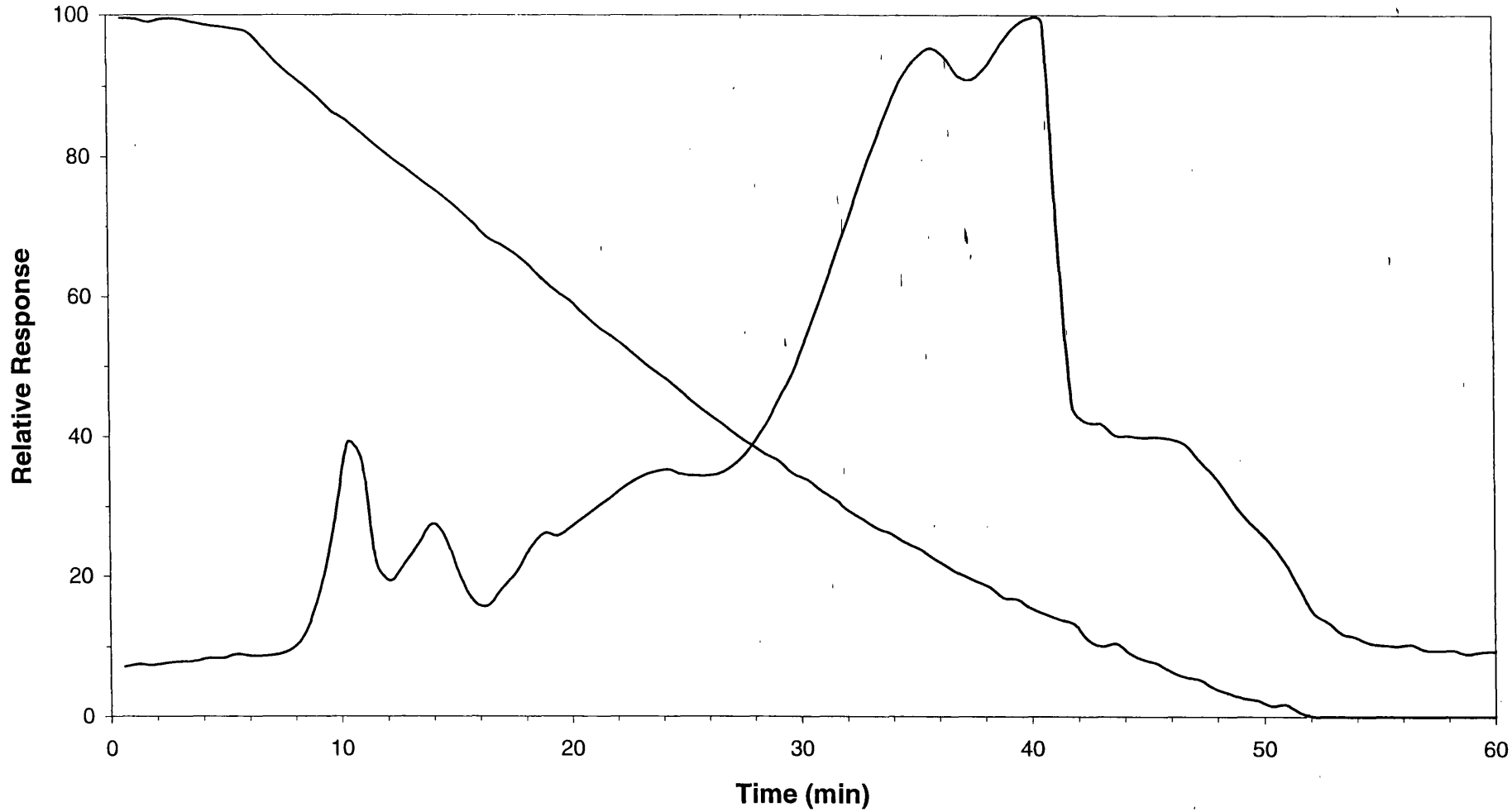

Figure 8.4: SATVA trace from the degradation of Sanylene Red BN PP under dynamic nitrogen

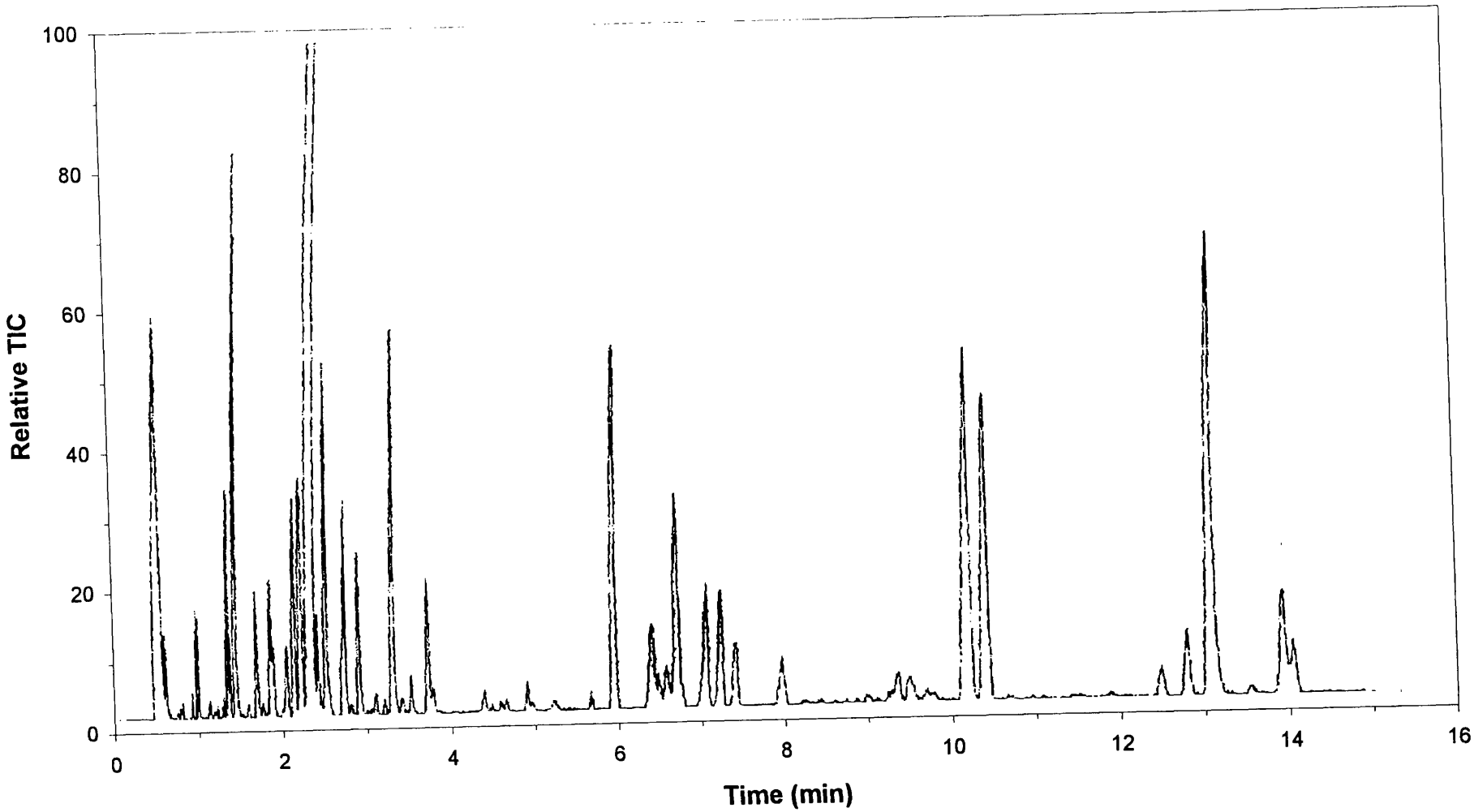

Figure 8.5: TIC trace for the liquid fraction from the SATVA curve in Figure 8.4

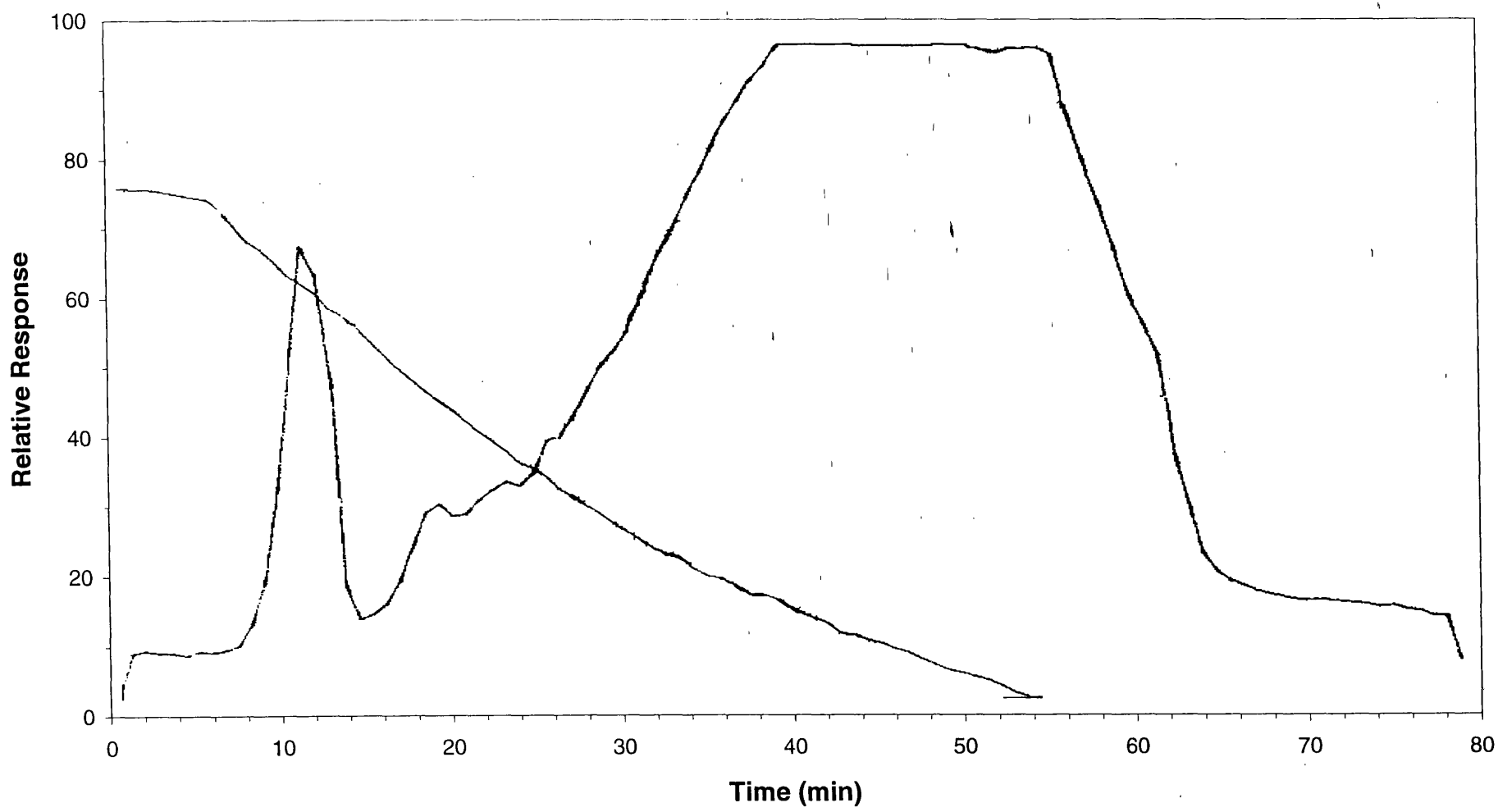

Figure 8.6: SATVA trace from the degradation of Sanylene Red BN under dynamic air

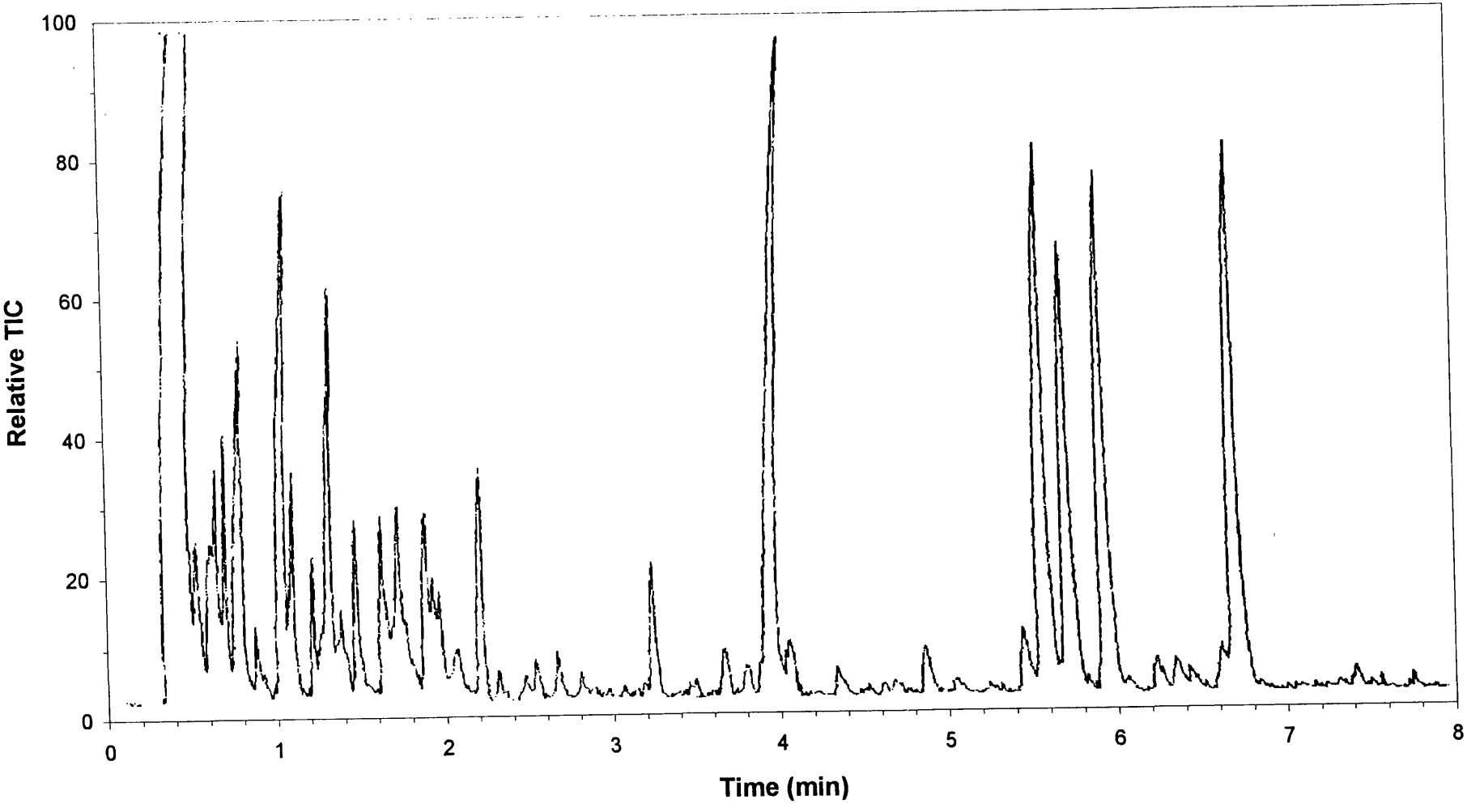

Figure 8.7: TIC trace for the liquid fraction from the SATVA curve in Figure 8.6

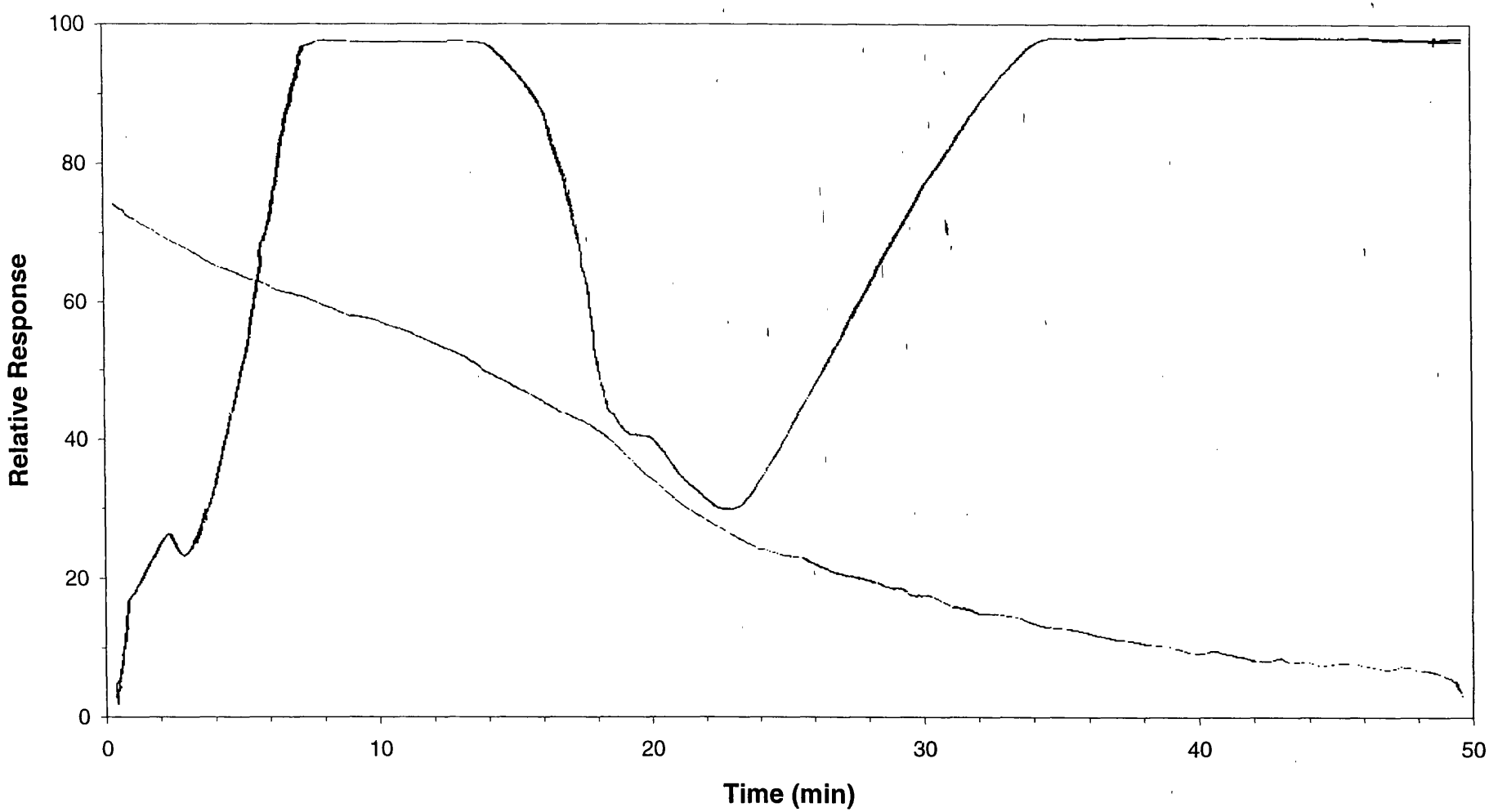

Figure 8.8: SATVA trace from the degradation of Sanylene Red BN under flaming conditions

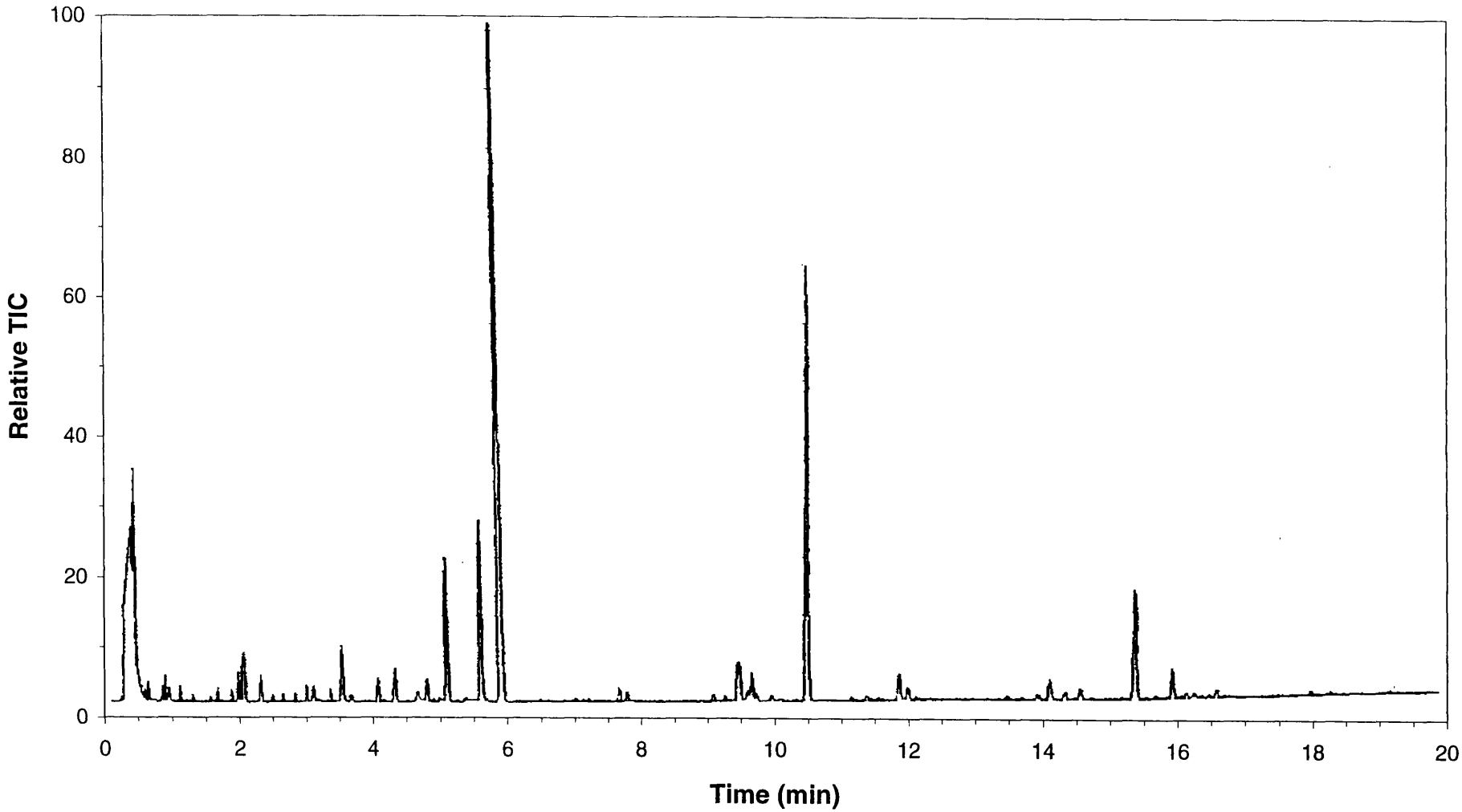

Figure 8.9: TIC trace for the liquid fraction from the SATVA curve in Figure 8.8

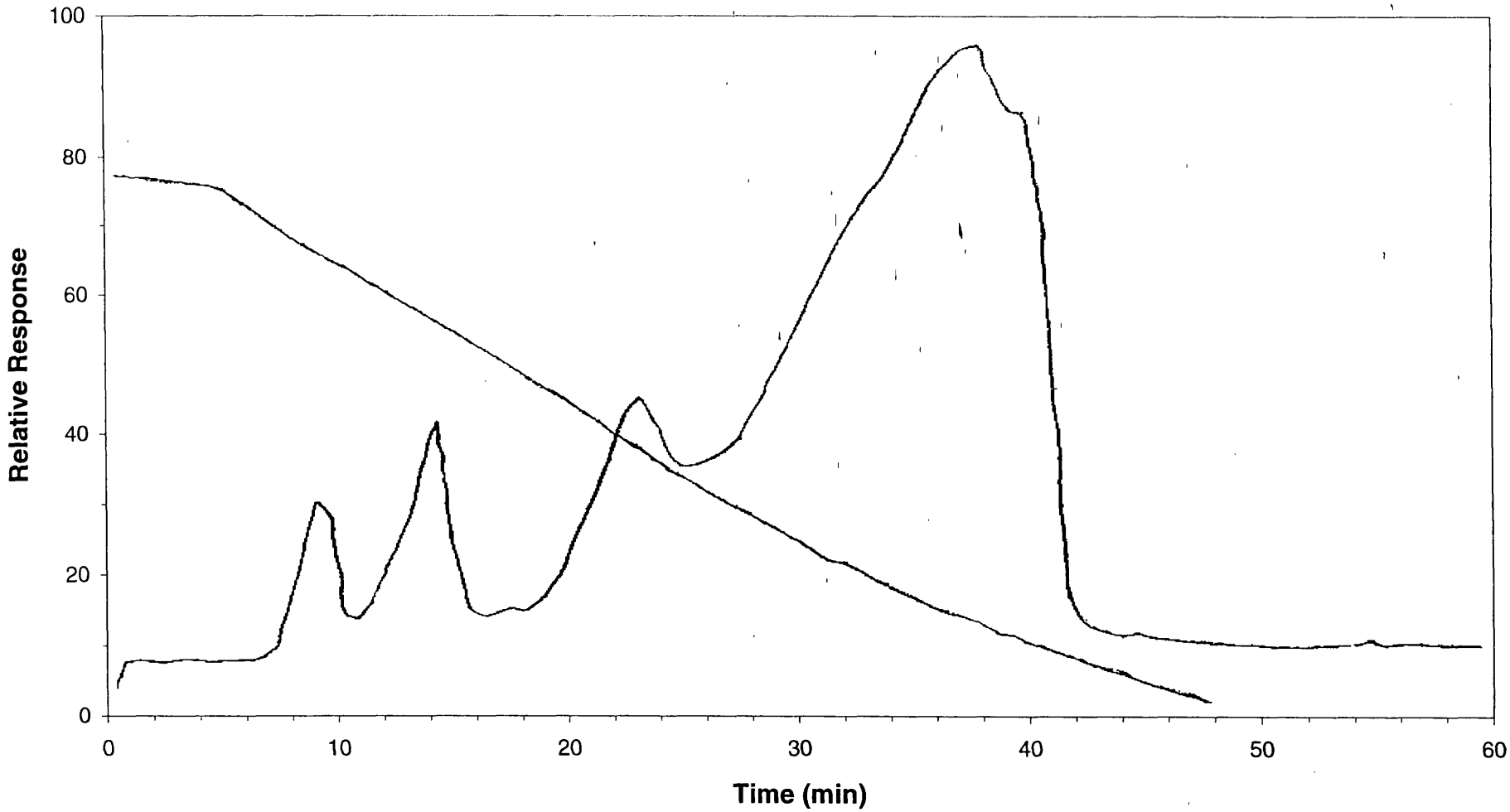

Figure 8.11: SATVA trace from the degradation of Estofil Blue MP8 under dynamic nitrogen

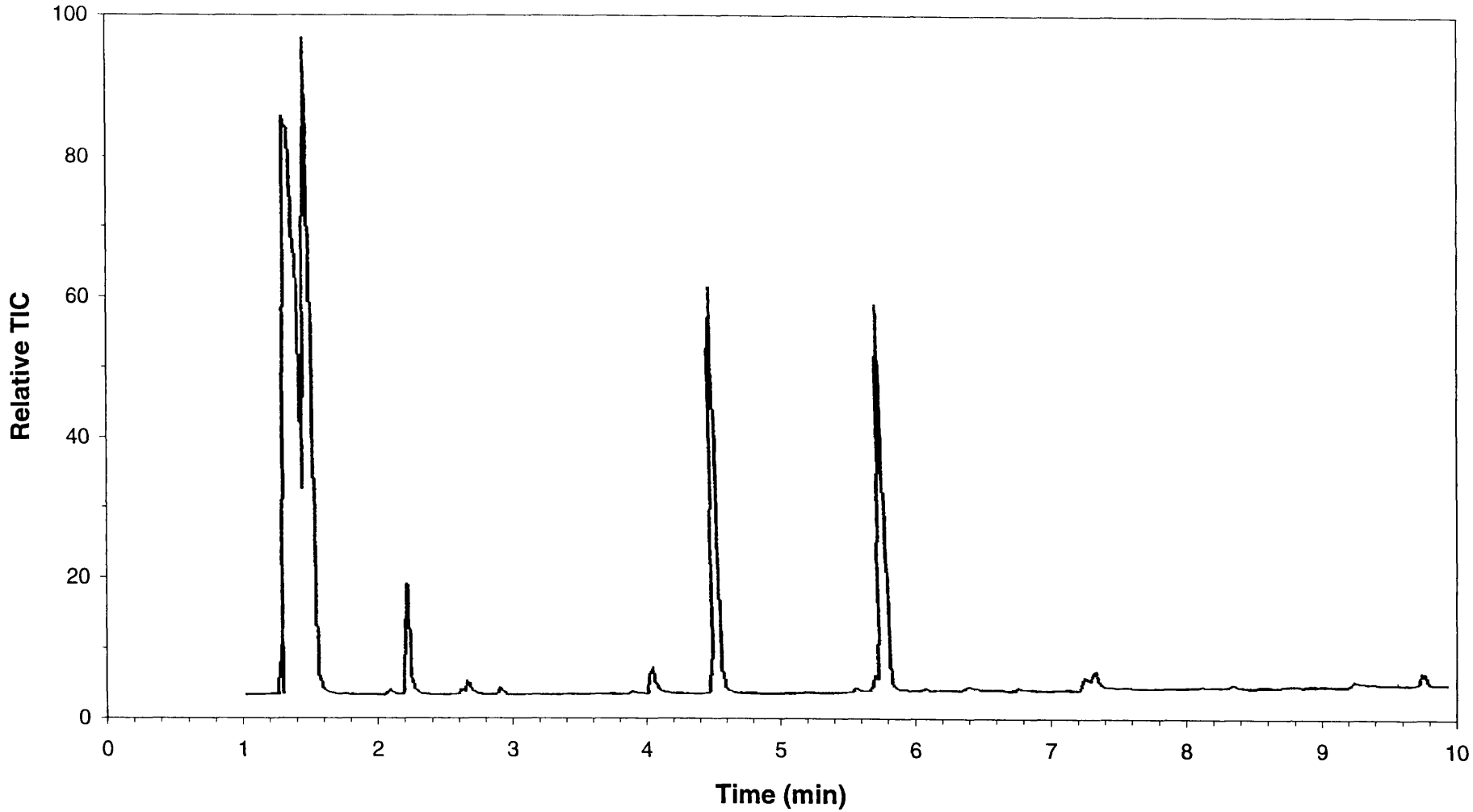

Figure 8.12: TIC trace for the liquid fraction from the SATVA curve in Figure 8.11

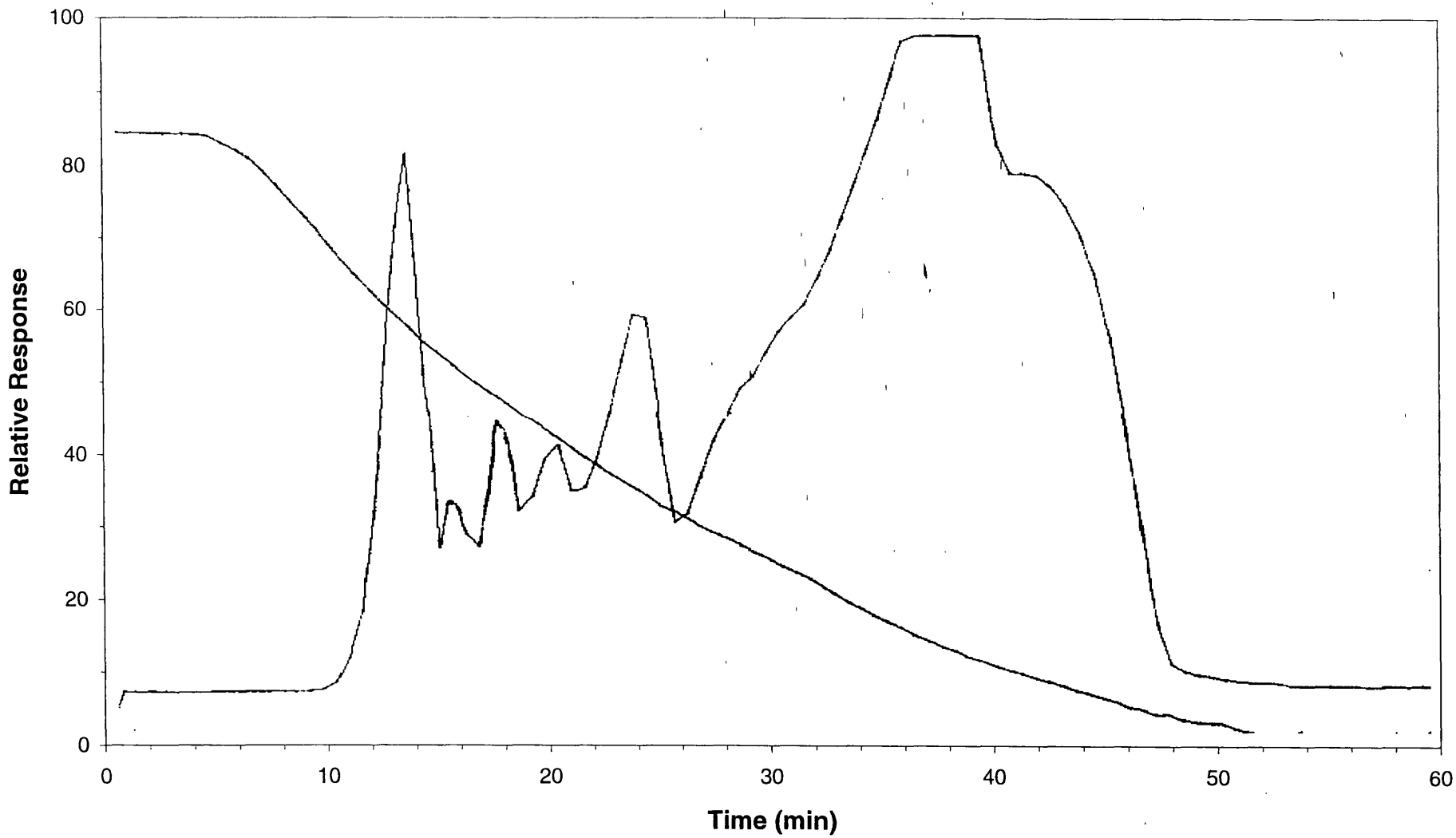

Figure 8.13: SATVA trace from the degradation of Estofil Blue MP8 under dynamic air

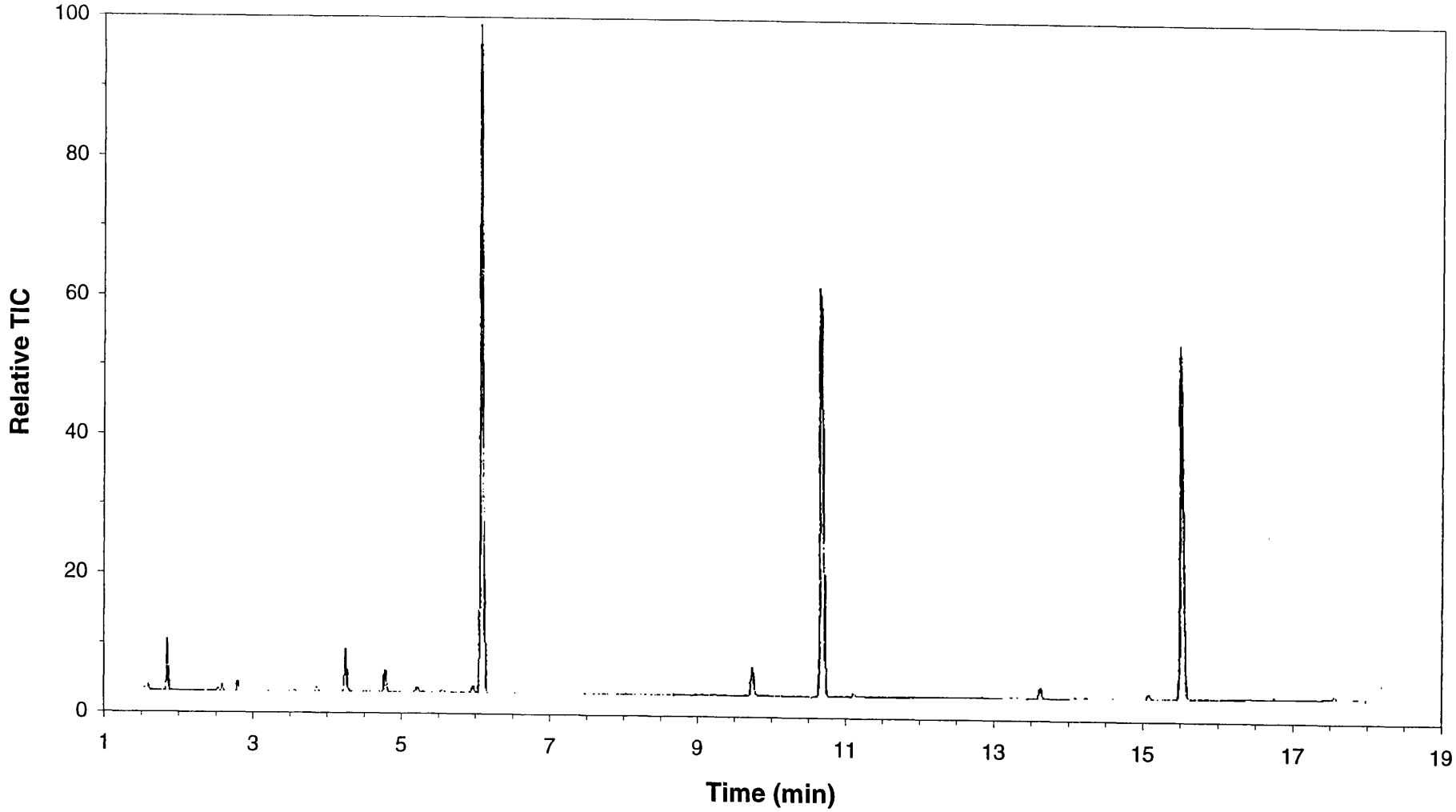

Figure 8.14: TIC trace for the liquid fraction from the degradation in section 8.5.4

CHAPTER 9

CONCLUSIONS

9.1 GENERAL FINDINGS

There exists a discontinuity in the established methods for studying thermal degradation under flaming conditions. There is a growing need to test polymer and additive systems under such conditions to identify hazardous products, ideally on a laboratory scale. This gap between the scope of the polymer degrading chemist and the fire safety engineer has been partially addressed in this work. The project produced a reasonably complete laboratory scale analysis method for studying the degradation of materials under a fire situation.

This task was accomplished through the creation of new techniques largely through the development of established methods. The TVA/ SATVA technique was the initial starting point. Modified degradation environments were developed, with SATVA remaining the basis for the analytical studies. Three main conditions were used. One set of apparatus was applied to the degradations under dynamic nitrogen and dynamic air. A more complicated degradation cell was developed for the study under flaming conditions. This was a miniaturisation of the environment used in the cone calorimeter.

The techniques developed appeared to function satisfactorily. The package of techniques allowed insight into both the degradation mechanisms and the potential products from the fire situation for a range of samples.

The samples where the structure implied flammability burned in the flaming apparatus, and the heavily chlorinated samples did not. This behaviour was consistent with what one may expect.

9.2 EFFECTS OF COLOURANTS ON THE POLYMER SYSTEMS

The candle model for the burning of polymers conforms with the results obtained. The study of the inert and flaming conditions liquid fractions for the Polypropylene/ Sandorin Red BN sample illustrates well the different fuel contribution aliphatics and aromatics provide.

The addition of the chlorinated colourant did not prevent the ignition of the polypropylene sample. The influence of this additive on the flammability performance would have required additional testing. It would appear that the additives had little major effect on the degradation mechanisms.

9.3 TOXICITY OF PRODUCTS

One of the objectives was to develop a method which would test for the potential of materials to evolve hazardous products under the fire situation. The diversity of potential burning environments means that the products evolved from a real fire situation could have more in common with the inert studies than the materials detected under flaming conditions. It is for this reason that the products from all environments tested must be considered as possible products from a fire situation.

It is apparent that some of the products detected do have associated hazards, such as the aromatic amines and chloro-aromatics. Nitriles were also observed in some of the studies. Chlorinated dioxins were not detected. If present, the cold ring fraction (CRF)

analysis work should have detected them. These fractions presented some analytical difficulties, so only selected CRF samples were comprehensively analysed.

9.4 ACHIEVEMENTS

The achievements may be summarised as:

- Methods were determined for product analysis across the range of conditions described by the candle burning model.
- The difficulties of down-scaling fire test conditions were fulfilled
- The methods were applicable to a range of sample forms.
- The problems of analysing additives with vacuum mobility under inert degradation conditions were addressed.
- The methods were validated through a range of samples.
- Some insight into the sample flammability was obtained.
- Screening for specific products could be achieved.

9.5 AREAS FOR FURTHER STUDY

The potential for observing both the products and the fire response in the studies under flaming conditions make the apparatus developed in this study of value for future studies. It is now possible to study the behaviour of relatively small samples in the fire situation. Ease of ignition and burning, along with the weight of and extent of protection from char, may be studied.

The procedures described here could be used to further the understanding of other polymer systems, or in the development of flame retardants. The behaviour of a test

material may be studied under the radiant heating normally associated with a flame. This gives a more realistic model than programmed heating for the study of char formation. The differences in the behaviour of a test material in programmed and radiant heating may be studied in detail. The influence of oxygen on the degradation of the solid of a polymer in the fire situation may also be assessed by applying radiant heating under inert and oxidising atmosphere. It is evident that the package of methods developed and applied in this work have uses outside the scope of this study.

REFERENCES

No	Ref
1	N. Grassie, G.Scott, *Polymer Degradation and Stabilisation*, Cambridge University Press, Cambridge (1985)
2	B.W. Mapperley, P.R. Sewell, *Eur. Poly. J.*, **9**, 1255 (1973)
3	D.W. Skidmore, P.R. Sewell, *Eur. Poly. J.*, **10**, 871 (1974)
4	L.E. Reshetnikove, S.I. Kirsh, Zavodskaya Laboratoriya, **42(8)**, 926 (1976)
5	B. Ceric, E. Simon, *Polymer Degradation and Stability*, **33**, 307 (1991)
6	N.S. Allen, C. Vasiliou, G.P. Marshall, *Polymer Degradation and Stability*, **24**, 17 (1989)
7	G. Camino, L. Costa, *Polymer Degradation and Stability*, **20**, 271 (1988)
8	I.C. McNeill, *Eur. Polym. J.*, **4**, 21 (1968)
9	G. Camino et al., *Polymer Degradation and Stability*, **33**, 131 (1991)
10	Carlos H. Hilado, *Flammability Handbook for Plastics (4th edn.)*, Technomic Publishing Co. Inc., Lancaster, USA (1990)
11	J. Troitzsch, Plastics Flammability Handbook, Hanser (dst. Macmillan Pub. Co. Inc., New York) (1983)
12	Fire-Tests — Reaction to Fire — Ignitability of Building Products, *Int. Standards Org.*, ISO/TC92/SCI/WG2-N54 (1984)
13	D.D. Drysdale, H.E. Thomson, *Fire Safety Journal*, **14**, 179 (1989)
14	E.N. Abrahart, *Dyes and their Intermediates*, Edward Arnold, (1977)

15 Venkataraman, *The Chemistry of Synthetic Dyes vol. VIII*, Academic Press (1978)

16 Gore, Joshi, Sunthankar, Tilak, *Recent Progress in the Chemistry of Natural and Synthetic Colouring Matters and Related Fields*, Academic Press (1962)

17 P.F. Gordon, p. Gregory, *Organic Chemistry in Colour*, Springer-Verlag, (1983)

18 I.C. McNeill, *J. Polymer Sci.*, Part A-1, **4**, 2479 (1966)

19 I.C. McNeill, Eur. *Polymer J.*, **3**, 409 (1967)

20 I.C. McNeill, D. Neil, *Thermal Analysis*, ed. Schwenker and Garn, Academic Press, New York, 353 (1969)

21 C.N. Banwell, Fundamentals of Molecular Spectroscopy (third edition), McGraw-Hill (1983)

22 Dudley H. Williams, Ian Fleming, *Spectroscopic Methods in Organic Chemistry* (fourth edition), McGraw-Hill (1987)

23 H.G. McAdie, *Anal. Chem.*, **35**(12), 1840 (1963)

24 Anthony R. West, *Solid State Chemistry and its Applications*, Wiley (1989)

25 R.O. Gardner, R.F. Browner, *Anal. Chem.*, **52**(8), 1360 (1980)

26 *Pirani Vacuum Gauges*, 07-D021-57-883, Edwards High Vacuum, Crawley, England, 1988

27 *Series 1000 Vacuum Gauges and Controllers*, 07-D386-12-881, Edwards High Vacuum, Crawley, England, 1986

28 Benjamin J. Gudzinowicz, Michael J. Gudzinowicz, Horace F. Martin; *Fundamentals of Integrated GC-MS*, Marcel Dekker, Inc., (1976)

29 David R. Lide (ed.), *Handbook of Chemistry and Physics (73rd edition)*, CRC Press, (1992)

30 C.J. Pouchert (ed.), *The Aldrich Library of Infrared Spectra*, Aldrich Chemical Co., Milwaukee (1981)

31 W.W. Simons (ed.), *The Sadtler Handbook of Infrared Spectra*, Sadtler-Heyden, London (1978)

32 A. Braithwaite, F.J. Smith; *Chromatographic Methods* (Forth Edition), Braithwaite and Smith, (1985).

33 P.G. Jeffery,P.J.Kipping; *Gas Analysis by Gas Chromatography*, Pergamon Press, (1972).

34 L.J. Schmauch, R.A. Dinerstein, *Anal. Chem.*, **32**, 343 (1960)

35 J.H. Beynon, *Mass Spectrometry and its Applications to Organic Chemistry*, **

36 8 peak

37 The NIST/EPA/NIH Mass Spectral Database, ver. 4.0, (1992)

38 Fred W. Billmeyer Jr., *Textbook of Polymer Science*, Wiley, (1984)

39 G. Montaudo, E. Scamporrino, C. Puglusi, D. Vitalini, *J. Appl. Polym. Sci.*, **30**, 1449 (1985)

40 J.K.Y. Kiang, P.C. Uden, J.C.W. Chien, Polymer Degradation and Stability,

2, 113 (1980)

41 J. Van Schooten, J.K. Evenhuis, *Polymer*, **6**, 343, (1965)

42 Y. Tsuchiva, K. Sumi, *J. Poly. Sci.*, A-1, **7**, 1599 (1969)

43 Ian C. McNeill, "Thermal Degradation" from *Comprehensive Polymer Science*, Vol. 6, ** pub? 467, (1989)

44 Sahar Al-Malaika, "Effects of Antioxidants and Stabilizers" from *Comprehensive Polymer Science*, Vol. 6, ** pub? 541, (1989)

45 I.C. McNeill and M. Bounekhel, *Polymer Degradation and Stability*, **34**, 187 (1991)

46 W.O. Freitag, E.R. Nixon, J. of Chem. Phys., **24**, 111 (1956)

GLASGOW UNIVERSITY LIBRARY